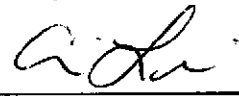


548607

**Sandia National Laboratories
Waste Isolation Pilot Plant**

**Analysis Package for Salado Flow Modeling: 2009
Compliance Recertification Application
Calculation**

Author:	Martin Nemer (6711) Print	 Signature	4/8/08 Date
Author:	Daniel Clayton (6711) Print	 Signature	4/8/08 Date
Technical Review:	Teklu Hadgu (6782) Print	Mario Chavez for Signature	4/9/08 Date
QA Review:	Mario Chavez (6710) Print	Mario Chavez Signature	4/9/08 Date
Management Review:	Moo Lee (6711) Print	 Signature For Moo Lee	4/9/08 Date

WIPP:1.2.5:PA:QA-L:547488

Table of Contents

1	EXECUTIVE SUMMARY	13
2	INTRODUCTION	13
2.1	background.....	13
2.1.1	Compliance Certification Application	14
2.1.2	Technical Baseline Migration.....	14
2.1.3	Analysis Plan 106 (AP106).....	14
2.1.4	2004 Compliance Recertification Application.....	15
2.1.5	CRA-2004 PABC BRAGFLO Analysis.....	15
2.1.6	CRA-2009 PA BRAGFLO Analysis	16
3	CONCEPTUAL APPROACH FOR SALADO FLOW ANALYSIS.....	16
3.1	Model Geometry.....	16
3.2	Initial Conditions	19
3.3	Boundary conditions.....	20
4	SALADO FLOW MODELING METHODOLOGY.....	21
4.1	Salado Flow Modeling Process.....	21
4.1.1	SANTOS	22
4.1.2	Latin Hypercube Sampling	22
4.1.3	GENMESH	22
4.1.4	MATSET.....	23
4.1.5	POSTLHS	23
4.1.6	ICSET 23	
4.1.7	ALGEBRACDB	29
4.1.8	PREBRAG	29
4.1.9	BRAGFLO.....	30
4.1.10	POSTBRAG & ALGEBRACDB (ALG2)	30
4.1.11	SUMMARIZE and SPLAT.....	30
4.1.12	PCCSRC	31
4.1.13	Execution and Run Control.....	31
4.2	Modeling Scenarios	32
5	INFORMATION SPECIFIC TO THE CRA-2009 PA.....	33
5.1	Changes to Input Parameters	33
5.1.1	Emplacement Materials Inventory.....	33
5.1.2	Halite/Disturbed Rock Zone Porosity.....	35
5.1.3	CPR Degradation Rate.....	36
5.2	Changes to Codes used in the BRAGFLO analyses	36
5.2.1	Chemistry Stoichiometric Matrix	37
5.2.2	Wicking and the Effective Saturation	41
5.2.3	Chemical Rate Smoothing and Tapering	43
5.2.4	Solids Production and Consumption.....	43
5.2.5	Implicit and Explicit Reaction Rates	44
5.2.6	Additional Chemistry Parameters	44
5.2.7	Capillary Pressure and Relative Permeability Model in Open Cavities	45
5.2.8	Borehole Reset.....	46
5.2.9	PREBRAG and POSTBRAG	46
6	MODELING RESULTS.....	48

6.1	Exception Vectors.....	48
6.1.1	Replicate R1.....	49
6.1.2	Replicate R2.....	49
6.1.3	Replicate R3.....	50
6.2	Overview of the Salado Flow Analysis	50
6.2.1	Organization.....	50
6.3	Modeling Results for Undisturbed Performance (R1S1).....	51
6.3.1	Sequence of Events	52
6.3.2	Halite Creep	52
6.3.3	Brine Inflow	52
6.3.4	Brine Saturation	53
6.3.5	Gas Generation.....	55
6.3.5.1	Gas Generation by Corrosion.....	56
6.3.5.2	Gas Generation by Microbial Activity.....	57
6.3.5.3	Total Gas Generation	57
6.3.6	Pressure.....	57
6.3.7	Rock Fracturing	58
6.3.8	Brine Outflow	59
6.3.9	Figures for Section 6.3.....	60
6.4	Drilling Disturbance Scenarios.....	97
6.4.1	Sequence of Events	97
6.4.2	Halite Creep	98
6.4.3	Brine Inflow	99
6.4.4	Brine Saturation	99
6.4.5	Gas Generation.....	100
6.4.6	Pressure	101
6.4.7	Rock Fracturing	102
6.4.8	Brine Flow Out of the Repository.....	102
6.4.9	Figures for Subsection 6.4	104
6.5	Comparison of Replicates.....	169
7	SUMMARY AND CONCLUSIONS	173
8	REFERENCES	174
	APPENDIX A: ALGEBRACDB (ALG2) OUTPUT VARIABLES IN STEP 5.....	175

List of Tables

Table 4-1. BRAGFLO model preprocessing steps used for the CRA-2009 PABC	24
Table 4-2. List of sampled material/property pairs with distribution type. Label in parenthesis in MATERIAL column refers to label in Figure 3-1.	26
Table 4-3. BRAGFLO modeling scenarios	32
Table 5-1. Moles of Organic Carbon available for biodegradation.	34
Table 5-2. CRA-2004 PABC CPR Parameters	34
Table 5-3. CPR Parameters Created for the CRA-2009 PA.	35
Table 5-4. Porosity Parameter Values.	35
Table 5-5. Minimum and Maximum values of SMIC_H2 (net amount of gas produced per mole of organic carbon) for the CRA-2004 PABC and the CRA-2009 PA.	38
Table 5-6. Stoichiometric matrix S(I,J) row number I and corresponding reaction	38
Table 5-7. Stoichiometric matrix S(I,J) column number J and corresponding compound	38
Table 5-8. Fe Corrosion Reaction Parameters Created for the CRA-2009 PA.	39
Table 5-9. Microbial Gas Generation Reaction Parameters Created for the CRA-2009 PA.....	39
Table 5-10. Fe(OH) ₂ Sulfidation Reaction Parameters Created for the CRA-2009 PA.....	39
Table 5-11. Metallic Fe Sulfidation Reaction Parameters Created for the CRA-2009 PA.	39
Table 5-12. MgO Hydration Reaction Parameters Created for the CRA-2009 PA.....	40
Table 5-13. Mg(OH) ₂ Carbonation Reaction Parameters Created for the CRA-2009 PA.	40
Table 5-14. MgO Carbonation Reaction Parameters Created for the CRA-2009 PA.	40
Table 5-15. Section of PREBRAG input file used in the CRA-2009 PA that concerns the chemistry stoichiometric matrix. Notice that all the stoichiometric parameters are set to zero, except for reactions I = 1,2 (iron corrosion, biodegradation). The below text was taken from the PREBRAG input file for Scenario 1, BF1_CRA09_S1.INP. This file can be found in CMS in the library LIBCRA09_BF.	41
Table 5-16. Index and corresponding compound in density array DEN	44
Table 5-17. Density Parameters Created for the CRA-2009 PA.	44
Table 5-18. MgO Parameters to be Created for the CRA-2009 PA.	45
Table 5-19. Additional Molecular Weight Parameters to be Created for the CRA-2009 PA.	45
Table 6-1 Exception vectors, CRA-2009 PA Replicate R1	49
Table 6-2 Exception vectors, CRA-2009 PA Replicate R2	50
Table 6-3 Exception vectors, CRA-2009 PA Replicate R3	50
Table 6-4. Statistical comparison of volume averaged porosity in all waste-filled areas at 10,000 years in Replicate R1, Scenario S1 for the CRA-2009 PA and the CRA-2004 PABC.	52
Table 6-5. Statistical comparison of total cumulative brine inflow at 10,000 years for Replicate R1, Scenario S1 for the CRA-2009 PA and the CRA-2004 PAB	53
Table 6-6. Volume-averaged brine saturation at 10,000 years in the waste panel for Replicate R1, Scenario S1 for the CRA-2009 PA, and the CRA-2004 PABC.....	54
Table 6-7. Volume-averaged brine saturation at 10,000 years in different areas of WIPP for Replicate R1, Scenario S1 for the CRA-2009 PA.	54
Table 6-8. Volume-averaged brine saturation at 10,000 years in different areas of WIPP for Replicate R1, Scenario S1 for the CRA-2004 PABC.....	54
Table 6-9. Gas generation statistics at 10,000 years for Replicate R1, Scenario S1 for the CRA-2009 PA and the CRA-2004 PABC.....	56
Table 6-10. Pressure in the waste panel at 10,000 years for Replicate R1, Scenario S1 for the CRA-2009 PA and CRA-2004 PABC.....	58

Table 6-11. Statistics on cumulative brine flow out of the repository at 10,000 years for Replicate R1, Scenario S1 for the CRA-2009 PA and CRA-2004 PABC.....	59
Table 6-12. Statistics on cumulative brine outflow to the LWB for Replicate R1, Scenario S1 for the CRA-2009 and CRA-2004 PABC.	59
Table 6-13. Statistics of porosity at 10,000 years for Replicate R1, Scenarios S2 and S4 for the CRA-2009 PA and CRA-2004 PABC.	98
Table 6-14. Statistics for cumulative brine flow into the repository at 10,000 years Replicate R1, Scenarios S2 and S4 for the CRA-2009 PA and CRA-2004 PABC.....	99
Table 6-15. Brine saturation and cumulative gas generation at 10,000 years averaged over 100 vectors for Replicate R1 for the CRA-2009 and CRA-2004 PABC.....	100
Table 6-16. Statistics on the volume averaged pressure in the waste panel at 10,000 years for Replicate R1 for the CRA-2009 PA and CRA-2004 PABC.....	101
Table 6-17. Statistics on cumulative brine flow out of the repository at 10,000 years for Replicate R1 for CRA-2009 PA and CRA-2004 PABC.....	102
Table 6-18. Statistics on cumulative brine releases to the Culebra, and the LWB at 10,000 years for Replicate R1, for the CRA-2009 PA and CRA-2004 PABC	103
Table 6-19. Statistics on cumulative brine releases to the Magenta and the Dewey Lake at 10,000 years for Replicate R1 of the CRA-2009 PA and the CRA-2009 PABC..	103

List of Figures

Figure 3-1. CRA-2009 BRAGFLO grid (Δx , Δy , and Δz dimensions in meters).....	17
Figure 3-2. Top view of CRA-2009 logical grid showing the radial flaring.....	18
Figure 6-1. Volume averaged porosity (dimensionless) in all waste regions versus time (years) for all 100 vectors in Replicate R1, Scenario S1.....	60
Figure 6-2. Total cumulative inflow of brine (m^3) into the repository versus time (years) for all 100 vectors in Replicate R1, Scenario S1.....	61
Figure 6-3. Total brine volume (m^3) in all waste regions versus time (years) for all 100 vectors in Replicate R1, Scenario S1.....	62
Figure 6-4. Scatter plot of halite porosity (dimensionless) versus cumulative brine inflow (m^3) into the repository for all 100 vectors in Replicate R1, Scenario S1, CRA-2009 PA.....	63
Figure 6-5. Scatter plot of halite porosity (dimensionless) versus cumulative brine inflow (m^3) into the repository for all 100 vectors in Replicate R1, Scenario S1, CRA-2004 PABC.....	64
Figure 6-6. Scatter plot of total cumulative brine flow (m^3) from the marker beds into the DRZ versus cumulative brine flow (m^3) into the repository for all 100 vectors in Replicate R1, Scenario S1, CRA-2009 PA.....	65
Figure 6-7. Scatter plot of total cumulative brine flow (m^3) from the marker beds into the DRZ versus cumulative brine flow (m^3) into the repository for all 100 vectors in Replicate R1, Scenario S1, CRA-2004 PABC.....	66
Figure 6-8. Brine saturation (dimensionless) in the waste panel versus time (years) for all 100 vectors in Replicate R1, Scenario S1.....	67
Figure 6-9. Primary correlations of brine saturation (dimensionless) in the waste panel with input parameters versus time (years), for Replicate R1, Scenario S1, CRA-2009 PA.....	68
Figure 6-10. Primary correlations of brine saturation (dimensionless) in the waste panel with input parameters versus time (years), for Replicate R1, Scenario S1, CRA-2004 PABC.....	69
Figure 6-11. Cumulative gas generation (moles) by iron corrosion versus time (years) for all 100 vectors in Replicate R1, Scenario S1.....	70
Figure 6-12. Fraction of iron (dimensionless) remaining versus time (years) for all 100 vectors in Replicate R1, Scenario S1.....	71
Figure 6-13. Primary correlations (dimensionless) of cumulative gas generation by corrosion with input parameters versus time (years) from the CRA-2009 PA, Replicate R1, Scenario S1.....	72
Figure 6-14. Primary correlations (dimensionless) of cumulative gas generation by corrosion with input parameters versus time (years) from the CRA-2004 PABC, Replicate R1, Scenario S1.....	73
Figure 6-15. Cumulative gas generation (moles) due to microbial activity versus time (years) for all 100 vectors in Replicate R1, Scenario S1.....	74
Figure 6-16. Remaining fraction of cellulose (dimensionless) versus time (years) for all 100 vectors in Replicate R1, Scenario S.....	75
Figure 6-17. Primary correlations (dimensionless) of cumulative microbial gas generation with input parameters versus time (years), from the CRA-2009 PA, Replicate R1, Scenario S1.....	76
Figure 6-18. Primary correlations (dimensionless) of cumulative microbial gas generation with input parameters versus time (years), from the CRA-2004 PABC, Replicate R1, Scenario S1, CRA-2004 PABC.....	77

Figure 6-19. Cumulative gas generation (moles) by all processes versus time (years) for all 100 vectors in Replicate R1, Scenario S1.....	78
Figure 6-20. Primary correlations (dimensionless) of cumulative microbial gas generation with input parameters versus time (years) from the CRA-2009 PA, Replicate R1, Scenario S1.	79
Figure 6-21. Primary correlations (dimensionless) of cumulative microbial gas generation with input parameters versus time (years) from the CRA-2004 PABC, Replicate R1, Scenario S1.	80
Figure 6-22. Cumulative gas generation (moles) by corrosion, by microbial activity and total versus time (years), averaged over 100 vectors from Replicate R1, Scenario S1 of the CRA-2009 PA.	81
Figure 6-23. Cumulative gas generation (moles) by corrosion, by microbial activity and total versus time (years), averaged over 100 vectors from Replicate R1, Scenario S1 of the CRA-2004 PABC.	82
Figure 6-24. Volume averaged pressure (Pa) in the waste area versus time (years) for all 100 vectors in Replicate R1, Scenario S1	83
Figure 6-25. Primary correlations (dimensionless) of volume averaged pressure in the waste area with input parameters versus time (years) from the CRA-2009 PA, Replicate R1, Scenario S1.....	84
Figure 6-26. Primary correlations (dimensionless) of volume averaged pressure in the waste area with input parameters versus time (years) from the CRA-2004 PABC, Replicate R1, Scenario S1.....	85
Figure 6-27. Fracture length (m) in MB138 north of the repository versus time (years) for all 100 vectors in Replicate R1, Scenario S1.....	86
Figure 6-28. Fracture length (m) in MB138 south of the repository versus time (years) for all 100 vectors in Replicate R1, Scenario S1.....	87
Figure 6-29. Fracture length (m) in MB139 north of the repository versus time (years) for all 100 vectors in Replicate R1, Scenario S1.....	88
Figure 6-30. Fracture length (m) in MB139 south of the repository versus time (years) for all 100 vectors in Replicate R1, Scenario S1.....	89
Figure 6-31. Fracture length in Anhydrite A&B (m) north of the repository versus time (years) for all 100 vectors in Replicate R1, Scenario S1.....	90
Figure 6-32. Pressure in Pa in the Experimental area EXP_PRES (left hand axis), and Fracture length in marker bed AB north of the repository FRACXABN (right hand axis), from Vector 53 of the CRA-2009 PA and the CRA-2004 PABC versus time.....	91
Figure 6-33. Fracture length in Anhydrite A and Anhydrite B (m) south of the repository versus time (years) for all 100 vectors in Replicate R1, Scenario S1.....	92
Figure 6-34. Total cumulative brine flow (m ³) away from the repository versus time (years) for all 100 vectors in Replicate R1, Scenario S1.....	93
Figure 6-35. Primary correlations (dimensionless) of cumulative brine outflow from the repository with input parameters versus time (years) from the CRA-2009 PA, Replicate R1, Scenario S1.....	94
Figure 6-36. Primary correlations (dimensionless) of cumulative brine outflow from the repository with input parameters versus time (years) from the CRA-2004 PABC, Replicate R1, Scenario S1.....	95
Figure 6-37. Cumulative brine flow (m ³) to the LWB versus time (years) for all 100 vectors in Replicate R1, Scenario S1.....	96

Figure 6-38. Volume averaged porosity (dimensionless) in all waste regions versus time (years) for all 100 vectors in Replicate R1, Scenario S2..	104
Figure 6-39. Volume averaged porosity (dimensionless) in all waste regions versus time (years) for all 100 vectors in Replicate R1, Scenario S4..	105
Figure 6-40. Total cumulative inflow (m ³) of brine into the repository versus time (years) for all 100 vectors in Replicate R1, Scenario S2..	106
Figure 6-41. Total cumulative inflow of brine (m ³) into the repository versus time (years) for all 100 vectors in Replicate R1, Scenario S4..	107
Figure 6-42. Total volume (m ³) of brine in the repository versus time (years) for all 100 vectors in Replicate R1, Scenario S2..	108
Figure 6-43. Total volume (m ³) of brine in the repository versus time (years) for all 100 vectors in Replicate R1, Scenario S4..	109
Figure 6-44. Brine saturation (dimensionless) in the Waste Panel versus time (years) for all 100 vectors in Replicate R1, Scenario S2..	110
Figure 6-45. Brine saturation (dimensionless) in the waste panel versus time (years) for all 100 vectors in Replicate R1, Scenario S4..	111
Figure 6-46. Primary correlations of brine saturation (dimensionless) in the Waste Panel with input parameters versus time (years) from the CRA-2009 PA, Replicate R1, Scenario S2..	112
Figure 6-47. Primary correlations of brine saturation (dimensionless) in the Waste Panel with input parameters versus time (years) from the CRA-2004 PABC, Replicate R1, Scenario S2..	113
Figure 6-48. Primary correlations of brine saturation (dimensionless) in the waste panel with input parameters versus time (years) from the CRA-2009 PA, Replicate R1, Scenario S4..	114
Figure 6-49. Primary correlations of brine saturation (dimensionless) in the waste panel with input parameters versus time (years) from the CRA-2004 PABC, Replicate R1, Scenario S4..	115
Figure 6-50. Cumulative moles of gas (moles) produced by iron corrosion versus time (years) for all 100 vectors in Replicate R1, Scenario S2..	116
Figure 6-51. Cumulative moles of gas (moles) produced by iron corrosion versus time (years) for all 100 vectors in Replicate R1, Scenario S4..	117
Figure 6-52. Primary correlations of cumulative amount (moles) of gas produced by iron corrosion in the waste panel with input parameters versus time (years) from the CRA-2009 PA, Replicate R1, Scenario S2..	118
Figure 6-53. Primary correlations of cumulative amount (moles) of gas produced by iron corrosion in the waste panel with input parameters versus time (years) from the CRA-2004 PABC, Replicate R1, Scenario S2..	119
Figure 6-54. Primary correlations of cumulative amount (moles) of gas produced by iron corrosion in the waste panel with input parameters versus time (years) from the CRA-2009 PA, Replicate R1, Scenario S4..	120
Figure 6-55. Primary correlations of cumulative amount (moles) of gas produced by iron corrosion in the waste panel with input parameters versus time (years) from the CRA-2004 PABC, Replicate R1, Scenario S4..	121
Figure 6-56. Fraction of iron (dimensionless) remaining versus time (years) for all 100 vectors in Replicate R1, Scenario S2..	122

Figure 6-57. Fraction of iron (dimensionless) remaining versus time (years) for all 100 vectors in Replicate R1, Scenario S4..	123
Figure 6-58. Cumulative amount of gas (moles) produced by microbial gas generation versus time (years) for all 100 vectors in Replicate R1, Scenario S2..	124
Figure 6-59. Cumulative amount of gas (moles) produced by microbial gas generation versus time (years) for all 100 vectors in Replicate R1, Scenario S4..	125
Figure 6-60. Primary correlations of cumulative amount (moles) of gas produced by microbial gas generation in the waste panel with input parameters versus time (years) from the CRA-2009 PA, Replicate R1, Scenario S2.	126
Figure 6-61. Primary correlations of cumulative amount (moles) of gas produced by microbial gas generation in the waste panel with input parameters versus time (years) from the CRA-2004 PABC, Replicate R1, Scenario S2.	127
Figure 6-62. Primary correlations of cumulative amount (moles) of gas produced by microbial gas generation in the Waste Panel with input parameters versus time (years) from the CRA-2009 PA, Replicate R1, Scenario S4.	128
Figure 6-63. Primary correlations of cumulative amount (moles) of gas produced by microbial gas generation in the Waste Panel with input parameters versus time (years) from the CRA-2004 PABC, Replicate R1, Scenario S4.	129
Figure 6-64. Difference in amount of microbial gas produced at 10,000 years from the CRA-2009 PA and the CRA-2004 PABC (normalized by CELL_MOL from the CRA-2004 PABC) versus the difference in the humid gas generation rates from the two analyses (the humid gas generation rates from each analysis are normalized by their respective inundated microbial gas-generation rates).	130
Figure 6-65. Fraction of cellulosics (dimensionless) remaining versus time (years) for all 100 vectors in Replicate R1, Scenario S2. Fraction of cellulosics is either cellulose or CPR depending on the value of WAS_AREA:PROBDEG (see Subsection 5.1.1)..	131
Figure 6-66. Fraction of cellulosics (dimensionless) remaining versus time (years) for all 100 vectors in Replicate R1, Scenario S4. Fraction of cellulosics is either cellulose or CPR depending on the value of WAS_AREA:PROBDEG (see Subsection 5.1.1)..	132
Figure 6-67. Total cumulative amount of gas (moles) generated versus time (years) for all 100 vectors in Replicate R1, Scenario S2..	133
Figure 6-68. Total cumulative amount of gas (moles) generated versus time (years) for all 100 vectors in Replicate R1, Scenario S4..	134
Figure 6-69. Primary correlations of cumulative amount (moles) of gas produced in the waste panel with input parameters, versus time (years) from the CRA-2009 PA Replicate R1, Scenario S2..	135
Figure 6-70. Primary correlations of cumulative amount (moles) of gas produced in the waste panel with input parameters, versus time (years) from the CRA-2004 PABC Replicate R1, Scenario S2..	136
Figure 6-71. Primary correlations of cumulative amount (moles) of gas produced in the Waste Panel with input parameters, versus time (years) from the CRA-2009 PA Replicate R1, Scenario S4..	137
Figure 6-72. Primary correlations of cumulative amount (moles) of gas produced in the Waste Panel with input parameters, versus time (years) from the CRA-2004 PABC Replicate R1, Scenario S4.	138

Figure 6-73. Volume averaged pressure (Pa) in the waste area versus time (years) for all 100 vectors in Replicate R1, Scenario S2.....	139
Figure 6-74. Volume averaged pressure (Pa) in the waste area versus time (years) for all 100 vectors in Replicate R1, Scenario S4.....	140
Figure 6-75. Primary correlations (dimensionless) of volume averaged pressure in the waste panel with input parameters versus time (years) from the CRA-2009 PA Replicate R1, Scenario S2.....	141
Figure 6-76. Primary correlations (dimensionless) of volume averaged pressure in the waste panel with input parameters versus time (years) from the CRA-2004 PABC Replicate R1, Scenario S2.....	142
Figure 6-77. Primary correlations (dimensionless) of volume averaged pressure in the waste panel with input parameters versus time (years) from the CRA-2009 PA Replicate R1, Scenario S4.....	143
Figure 6-78. Primary correlations (dimensionless) of volume averaged pressure in the waste panel with input parameters versus time (years) from the CRA-2004 PABC Replicate R1, Scenario S4.....	144
Figure 6-79. Fracture length (m) in MB138, north of the repository versus time (years) for all 100 vectors in Replicate R1, Scenario S2.....	145
Figure 6-80. Fracture length (m) in MB138, north of the repository versus time (years) for all 100 vectors in Replicate R1, Scenario S4.....	146
Figure 6-81. Fracture length (m) in MB138, south of the repository versus time (years) for all 100 vectors in Replicate R1, Scenario S2.....	147
Figure 6-82. Fracture length (m) in MB138, south of the repository versus time (years) for all 100 vectors in Replicate R1, Scenario S4.....	148
Figure 6-83. Fracture length (m) in MB139, north of the repository versus time (years) for all 100 vectors in Replicate R1, Scenario S2.....	149
Figure 6-84. Fracture length (m) in MB139, north of the repository versus time (years) for all 100 vectors in Replicate R1, Scenario S4.....	150
Figure 6-85. Fracture length (m) in MB139, south of the repository versus time (years) for all 100 vectors in Replicate R1, Scenario S2.....	151
Figure 6-86. Fracture length (m) in MB139, south of the repository versus time (years) for all 100 vectors in Replicate R1, Scenario S4.....	152
Figure 6-87. Fracture length (m) in Anhydrite A&B, north of the repository versus time (years) for all 100 vectors in Replicate R1, Scenario S2.....	153
Figure 6-88. Fracture length (m) in Anhydrite A&B, north of the repository versus time (years) for all 100 vectors in Replicate R1, Scenario S4.....	154
Figure 6-89. Fracture length (m) in Anhydrite A&B, south of the repository versus time (years) for all 100 vectors in Replicate R1, Scenario S2.....	155
Figure 6-90. Fracture length (m) in Anhydrite A&B, south of the repository versus time (years) for all 100 vectors in Replicate R1, Scenario S4.....	156
Figure 6-91. Total cumulative brine flow (m ³) out of the waste panel versus time (years) for all 100 vectors in Replicate R1, Scenario S2.....	157
Figure 6-92. Total cumulative brine flow (m ³) out of the Waste Panel, versus time (years) for all 100 vectors in Replicate R1, Scenario S4.....	158
Figure 6-93. Cumulative brine flow (m ³) out of the repository versus time (years) for all 100 vectors in Replicate R1, Scenario S2.....	159

Figure 6-94. Cumulative brine flow (m ³) out of the repository versus time (years) for all 100 vectors in Replicate R1, Scenario S4.....	160
Figure 6-95. Primary correlations (dimensionless) of brine flow out of the repository with input parameters versus time (years) from the CRA-2009 PA Replicate R1, Scenario S2.	161
Figure 6-96. Primary correlations (dimensionless) of brine flow out of the repository with input parameters versus time (years) from the CRA-2004 PABC Replicate R1, Scenario S2....	162
Figure 6-97. Primary correlations (dimensionless) of brine flow out of the repository with input parameters versus time (years) from the CRA-2009 PA Replicate R1, Scenario S4.	163
Figure 6-98. Primary correlations (dimensionless) of brine flow out of the repository with input parameters versus time (years) from the CRA-2004 PABC Replicate R1, Scenario S4....	164
Figure 6-99. Cumulative brine flow (m ³) to the Culebra formation versus time (years) for all 100 vectors in Replicate R1, Scenario S2.....	165
Figure 6-100. Cumulative brine flow (m ³) to the Culebra formation versus time (years) for all 100 vectors in Replicate R1, Scenario S4.....	166
Figure 6-101. Cumulative brine flow (m ³) to the LWB versus time (years) for all 100 vectors in Replicate R1, Scenario S2.....	167
Figure 6-102. Cumulative brine flow (m ³) to the LWB versus time (years) for all 100 vectors in Replicate R1, Scenario S4.....	168
Figure 6-103. Vector-averaged pressure (Pa) in the waste area versus time (years) from the CRA-2009 PA, Scenario S1, Replicates R1-R3.	170
Figure 6-104. Vector-averaged pressure (Pa) in the waste area versus time (years) from the CRA-2004 PABC, Scenario S1, Replicates R1-R3.	170
Figure 6-105. Vector-averaged brine saturation (dimensionless) in the waste panel versus time (years)) from the CRA-2009 PA, Scenario S1, Replicates R1-R3.	171
Figure 6-106. Vector-averaged brine saturation (dimensionless) in the waste panel versus time (years)) from the CRA-2004 PABC, Scenario S1, Replicates R1-R3.	171
Figure 6-107. Vector-averaged cumulative brine flow (m ³) away from the repository versus time (years) from the CRA-2009 PA, Scenario S1, Replicates R1-R3.....	172
Figure 6-108. Vector-averaged cumulative brine flow (m ³) away from the repository versus time (years) from the CRA-2004 PABC, Scenario S1, Replicates 1-3.	172

Acronyms

AP	Analysis Plan
CCA	Compliance Certification Application
CCDF	Complementary Cumulative Distribution Function
CMS	Code Management System
CDB	Camdat database file
CRA	Compliance Recertification Application
CPR	Cellulose, plastic, and rubber
DCL	Digital Command Language
DOE	U.S. Department of Energy
DRZ	Disturbed Rock Zone
EPA	U.S. Environmental Protection Agency
LHS	Software that performs Latin Hypercube sampling
LWB	Land Withdrawal Boundary
MB	Marker Bed
OC	Organic Carbon
PA	Performance Assessment
PAPDB	Performance Assessment Parameter Database
PAVT	Performance Assessment Verification Test
PCS	Panel Closure System
PRCC	Partial Rank Correlation Coefficient
RoR	Rest of Repository
SNL	Sandia National Laboratories
TBM	Technical Baseline Migration
TRU	Transuranic Waste
WIPP	Waste Isolation Pilot Plant

1 EXECUTIVE SUMMARY

This report describes and compares the results of BRAGFLO calculations for the CRA 2009 PA to results of the CRA-2004 PABC. Significant changes include a new version of BRAGFLO (version 6.0), inclusion of emplacement materials in the cellulose, plastic, and rubber (CPR) inventory used by BRAGFLO, a correction to the porosity in the disturbed rock zone (DRZ), and an updated conditional relationship between the humid and inundated CPR degradation rate.

The changes described above had a minimal effect on the overall results of the CRA-2009 PA. Microbial gas generation was slightly higher in the CRA-2009 PA compared to the CRA-2004 PABC due to the addition of the emplacement materials. Some vectors had a larger fracture length in the CRA-2009 PA compared to the CRA-2004 PABC but the larger fracture length had no effect on brine flows to the Land Withdrawal Boundary.

2 INTRODUCTION

2.1 BACKGROUND

The Waste Isolation Pilot Plant (WIPP) is located in southeastern New Mexico and has been developed by the U.S. Department of Energy (DOE) for the geologic (deep underground) disposal of transuranic (TRU) waste (U. S. DOE 1980; U. S. DOE 1990; U. S. DOE 1993). In 1992, Congress designated the U.S. Environmental Protection Agency (EPA) as WIPP's official certifier, and mandated that once DOE demonstrated to EPA's satisfaction that WIPP complied with Title 40 of the Code of Federal Regulations, Part 191 (U.S. DOE 1996; U.S. EPA 1996), EPA would certify the repository. To show compliance with the regulations the DOE had their scientific advisor, Sandia National Laboratories (SNL) develop a computational modeling system to predict the future performance of the repository for 10,000 years after closure, given the conceptual models of E1/E2 intrusions (see Subsection 6.4.1) being the primary pathways for releases. SNL has developed a system called WIPP Performance Assessment (PA), which examines failure scenarios, quantifies their likelihoods, estimates potential releases to the surface or the site boundary, and evaluates the potential consequences, including uncertainties. The regulation also requires that these models be maintained and updated with new information to be part of a recertification process that occurs at five-year intervals after the first waste is received at the site.

The WIPP PA consists of a suite of software designed to predict conditions in and around the repository over a period of 10,000 years. One of the first models that are run for the PA is the BRAGFLO software (Nemer 2006; Nemer 2006), which simulates brine and gas flow in and around the repository. BRAGFLO includes the effects of processes such as gas generation and creep closure. Outputs from the BRAGFLO simulations describe the conditions (pressure, brine saturation, porosity) and flow patterns (brine flow up an intrusion borehole and out anhydrite marker beds to the accessible environment) that are used by other software to predict radionuclide releases.

This report documents the BRAGFLO simulations and results that support the baseline PA calculations for the second recertification of the repository as described below.

2.1.1 Compliance Certification Application

In October 1996, DOE submitted the Compliance Certification Application (CCA) to the EPA, which included the results of the WIPP PA system. During the review of the CCA, EPA mandated an additional Performance Assessment Verification Test (PAVT), which revised selected CCA inputs to the PA (SNL 1997). The PAVT analysis ran the full suite of WIPP PA software and confirmed the conclusions of the CCA analysis that the repository design met the regulations. Following the receipt of the PAVT analysis, EPA ruled in May 1997 that WIPP had met the regulations for permanent disposal of transuranic waste. Several lawsuits in opposition to the EPA's ruling were filed in court and were eventually dismissed. The first shipment of radioactive waste from the nation's nuclear weapons complex arrived at the WIPP site in late March 1999, starting the five-year clock for the site's required recertification. The results of CCA PA analyses were subsequently summarized in an SNL report (Helton, Bean et al. 1998).

2.1.2 Technical Baseline Migration

The Technical Baseline Migration (TBM) was an effort begun in 2001 to merge the CCA (U.S. DOE 1996) and PAVT (SNL 1997) PA baselines while at the same time implementing conceptual model changes being reviewed by the Salado Flow Peer Review in preparation for the first Compliance Recertification Application PA. The TBM analysis eventually consisted of a full PA calculation which implemented several changes from the PAVT PA baseline. As part of this migration, a new BRAGFLO numerical grid (mesh) was developed and is described in Hansen et al. (2002). The new TBM BRAGFLO grid replaced the CCA/PAVT BRAGFLO grid. The most important changes with respect to the TBM BRAGFLO grid were the implementation of the Option D panel closure design, which was mandated by the EPA as a condition to their final rule, and the removal of an explicit representation of the shaft seal system in the grid. Additional grid refinements were implemented to increase numerical accuracy and computational efficiency and to reduce numerical dispersion in transport simulations that used the same grid as BRAGFLO.

In May, 2002, the Salado Flow Peer Review panel met in Carlsbad to evaluate the proposed changes to conceptual models for the TBM. A set of PA calculations was run to demonstrate the effects of these changes on BRAGFLO results. The peer review panel judged the changes to be "generally sound in their structure, reasonableness, and relationship to the original models". However the panel required that a total systems PA be run and complementary cumulative distribution functions (CCDFs) be generated before they would agree to the changes (Caporuscio, Gibbons et al. 2002).

2.1.3 Analysis Plan 106 (AP106)

After the first meeting of the Salado Flow Peer Review, the conceptual models were revised to address new concerns of the EPA and to incorporate new technical information from laboratory and field investigations (Stein and Zelinski 2003). The Salado Flow Peer Review Panel held a

second and final meeting in Carlsbad in February 2003 to consider the results of the total systems PA using the new revised BRAGFLO grid and modeling assumptions. The panel approved the proposed conceptual model changes (Caporuscio, Gibbons et al. 2003) permitting the start of PA analyses for the 2004 Compliance Recertification Application (CRA-2004) beginning with the Salado Flow Analysis of gas and brine flow in the vicinity of the repository.

2.1.4 2004 Compliance Recertification Application

The first compliance recertification application (CRA-2004) was submitted to the EPA by the DOE in March 2004 (U.S. DOE 2004). During its review of CRA-2004, the EPA raised several questions regarding its completeness and technical adequacy (Cotsworth 2004; Cotsworth 2004; Cotsworth 2004; Cotsworth 2004), (Gitlin 2005). The DOE and SNL responded to EPA questions in writing (Detwiler 2004; Detwiler 2004; Detwiler 2004; Detwiler 2004; Detwiler 2004; Detwiler 2004; Piper 2004; U.S. DOE 2004; Patterson 2005; Triay 2005) and by engaging in technical meetings with EPA staff. The result of these technical interactions was that the EPA required SNL to revise the CRA-2004 PA analysis and run a new PA analysis, which became the new PA baseline following recertification.

2.1.5 CRA-2004 PABC BRAGFLO Analysis

The EPA required that DOE revise the CRA-2004 analysis and present results before EPA would judge the CRA-2004 complete (Cotsworth 2005). The EPA noted a number of technical changes and corrections to the CRA-2004 PA that it deemed necessary. Additionally, the EPA stated that a number of modeling assumptions used in CRA-2004 were not sufficiently justified and that alternative modeling assumptions must be used. The issues and changes mandated by the EPA that effect the BRAGFLO portion of WIPP PA included the following:

- 1) Inventory information was updated.
- 2) Changes to the parameter describing the probability of microbial gas generation in the repository were made.
- 3) Methanogenesis was no longer assumed to be the primary microbial gas generation reaction.

Minor corrections were also made in the CRA-2004 PABC to the LHS's parameter sampling step to correct an error that was discovered after completion of the CRA-2004 (Vugrin, Kirchner et al. 2005).

The CRA-2004 PABC was performed under AP-122 (Kanney and Leigh 2005). The PABC was completed in October of 2005 (Leigh, Kanney et al. 2005) and was submitted to EPA shortly thereafter. In September of 2005, EPA determined that the CRA application was complete (EPA 2005). In March of 2006 the EPA officially certified the CRA (EPA 2006). The BRAGFLO results of the CRA-2004 PABC are documented in Nemer et al. (2005) and Leigh et al. (2005).

2.1.6 CRA-2009 PA BRAGFLO Analysis

As part of the 2009 Compliance Recertification Application (CRA-2009), a performance assessment was run. This report, BRAGFLO analysis, is one part of the CRA-2009 PA. The CRA-2009 PA was run under AP-137, *Analysis Plan for the Performance Assessment for the 2009 Compliance Recertification Application, Revision 1* (Clayton 2008).

3 CONCEPTUAL APPROACH FOR SALADO FLOW ANALYSIS

The conceptual models implemented in the BRAGFLO simulations for the CRA-2009 PA are unchanged from those used in the CRA-2004 PABC. However several numerical enhancements have been added to a new version of BRAGFLO, version 6.00 (Nemer 2006; Nemer 2006). These are discussed further in Subsection 5.2.

3.1 MODEL GEOMETRY

The BRAGFLO grid used for CRA-2009 PA BRAGFLO calculations is the same as that used for the CRA-2004 PABC (Nemer and Stein 2005). This grid is shown as a logical grid with dimensions in Figure 3-1 and it is shown from the top, displaying its radial flaring in Figure 3-2.

CRA-2004 and CRA-2004 PABC BRAGFLO Grid

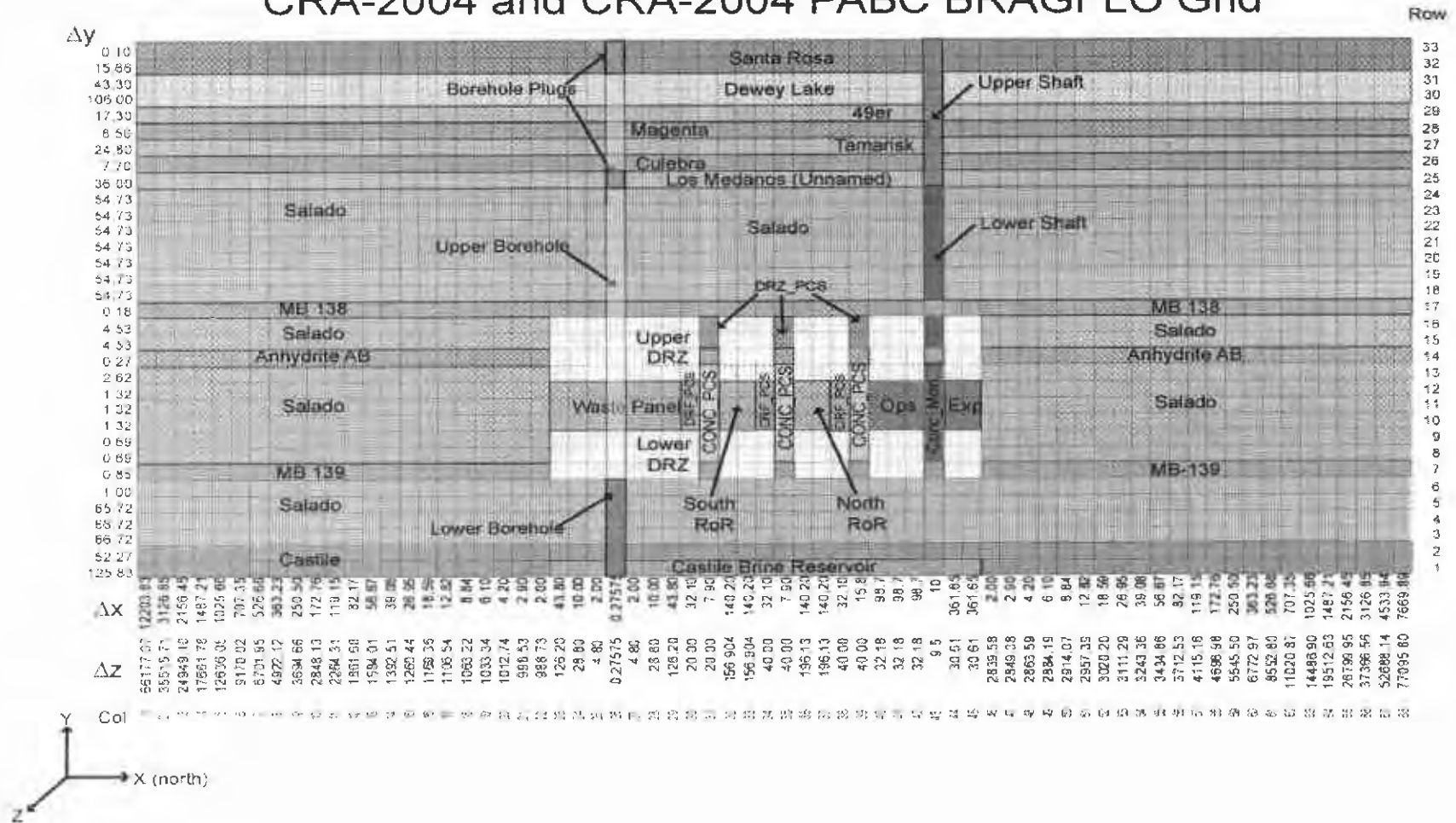


Figure 3-1. CRA-2009 BRAGFLO grid (Δx , Δy , and Δz dimensions in meters). Note that “north of the repository” is to the right of the Exp area on the above graph and “south of the repository” is to the left of the Panel area.

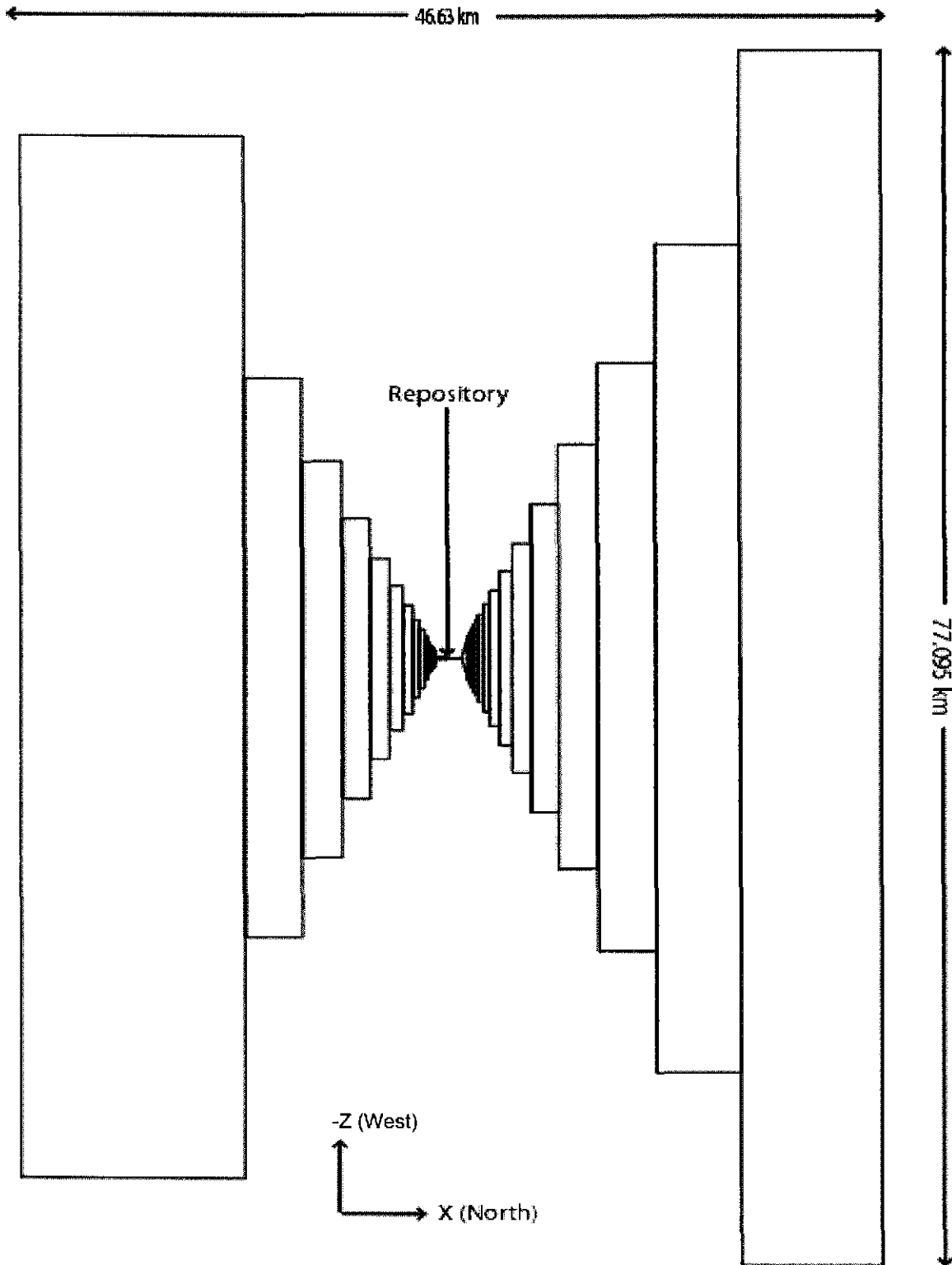


Figure 3-2. Top view of CRA-2009 logical grid showing the radial flaring.

The primary objective in creating the modeling grid for BRAGFLO is to capture the effects of known and significant hydrologic features in and around the repository. This is accomplished by using a vertical, two-dimensional grid, oriented south to north through the repository and surrounding strata (Figure 3-1). The lengths (Δx), the widths (Δz), and the heights (Δy) of each grid cell are indicated in Figure 3-1. The wide variation in grid cell dimensions captures a relatively large amount of detail with a relatively small number of grid cells.

The two dimensional BRAGFLO grid captures three-dimensional flow effects by employing the technique of “radial flaring.” This flaring is visible when looking down on the grid from the top as shown in Figure 3-2. In this figure, the width of each grid cell to the north and south of the repository increases with distance away from the center of the waste filled region. The flaring simulates convergent or divergent flow to the north and south centered on the repository, and laterally away from the repository. The flaring methodology used to create the grid is discussed in a separate memorandum (Stein 2002). This general methodology was tested in WIPP PA (SNL 1996) and shown to adequately represent fluid releases when compared to an alternative three dimensional approach, which is more computationally expensive.

The Salado flow grid incorporates the repository, the Castile brine reservoir, the Salado Formation, bedded units above the Salado, the shaft, panel seals, and an intrusion borehole, used for disturbed scenarios. The analysis report for CRA-2004 (Stein and Zelinski 2003) provides a detailed explanation of all the stratigraphic and other materials used to represent the repository and surrounding units.

3.2 INITIAL CONDITIONS

BRAGFLO simulation of brine and gas flow in the vicinity of the WIPP site requires the assignment of initial conditions including brine pressure, brine saturation, and concentrations of iron and biodegradable material. These initial conditions are provided to BRAGFLO through various pre-processing steps during which values are extracted or sampled from the WIPP PA Performance Assessment Parameter Database (WIPP PAPDB).

At the beginning of each BRAGFLO run (scenario-vector combination), the model simulates a short period of time representing disposal operations. This portion of the run is called the initialization period and lasts for 5 years (from $t = -5$ to 0 years), corresponding to the time a typical waste panel is expected to be open during disposal operations. All grid blocks require initial pressure and saturation at the beginning of the run ($t = -5$ years). At the beginning of the regulatory period (0 to 10,000 years), BRAGFLO resets initial conditions within the excavated regions and in the shaft.

The initial conditions at -5 years for BRAGFLO modeling are listed below:

- Brine pressure in all non-excavated regions is equal to lithostatic pressure (sampled at one location and assumed hydrostatic at all other locations).
- Pressure within the open cavities (CAVITY_1 through CAVITY_4) is set to 1.01325×10^5 Pa at -5 years

- Pressure in the excavated waste regions at time = 0 is set to $1.28039 \times 10^5 \text{ Pa} = (1.01325 \times 10^5 \text{ Pa} + 0.26714 \times 10^5 \text{ Pa})$, which is greater than one atmosphere ($1.01325 \times 10^5 \text{ Pa}$) due to the pre-charging of the repository with microbial gas produced at short times ($0.26714 \times 10^5 \text{ Pa}$) (see Subsection 4.2.1 of Nemer, Stein et al. 2005).
- Brine saturation within the non-excavated regions is set to 1.0.
- Brine saturation within the open cavities (CAVITY_1 through CAVITY_4) is set to 0 at - 5 years.
- Brine saturation in the excavated regions at time 0:
 - 0.015 for the excavated waste regions, which was chosen to be conservative with respect to the WIPP Waste Acceptance Criteria which allows waste to come to WIPP with no more than 1 % liquids by volume (see Subsection 3.4.1 of DOE 2007)
 - 0.0 for the operations and experimental areas
 - 0.99999990 for the shaft, concrete monolith and panel closures and the panel-closure drifts

During the initialization period brine tends to flow into the excavated areas and the shaft, resulting in decreased pressure and saturation in the rock immediately adjacent to the excavations. At time $t = 0$ the pressure and saturation in all the excavations is reset to initial conditions for the materials used to represent these regions for the regulatory period. This practice is intended to capture the effect of evaporation of brine inflow during the operational period and the transport of this brine up the shaft ventilation system, as well as the depressurization of the surrounding rock formations due to excavation.

3.3 BOUNDARY CONDITIONS

The boundary conditions assigned for the BRAGFLO calculations in the CRA-2009 PA are slightly different from the CRA-2004 PABC and are as follows:

- Constant pressure at the north and south ends of the Culebra and Magenta Dolomites.
- Constant pressure ($1.01325 \times 10^5 \text{ Pa}$) and saturation (0.08363 dimensionless see Vaughn1996) conditions at the land surface boundary of the grid, except at the shaft cell on the land surface boundary (new for the CRA-2009). In the CRA-2009 the saturation constraint has been removed from the shaft cell that lies at the land surface because at $t = 0$, the saturation in this cell is reset along with the rest of the shaft to the initial saturation in the WIPP parameter database (SAT_IBRN) for each of the respective shaft materials. The combination of a fixed saturation boundary condition equal to 0.08363 and simultaneously being reset at $t = 0$ to 0.796 (SHFTU:SAT_IBRN) had the potential to create numerical difficulties.
- No flow conditions at all other grid boundaries.

4 SALADO FLOW MODELING METHODOLOGY

The BRAGFLO software calculates the flow of brine and gas in the vicinity of the WIPP repository over a 10,000-year regulatory compliance period. The results of these calculations are used by other software to calculate potential radionuclide releases to the accessible environment. Some of the specific processes included in the BRAGFLO calculations include:

- Brine and gas flow.
- Creep closure of the waste filled regions within the repository.
- Gas generation due to corrosion of steel and degradation of biodegradable materials (cellulosics, plastics, and rubbers).
- Physical changes (e.g. permeability and porosity) in the modeling domain over time.
- The consequences of rock fracturing due to high pressure.

There is a significant amount of uncertainty associated with characterizing the physical properties of geologic materials that influence these processes. WIPP PA deals with these uncertainties in two ways. Properties such as permeability and porosity are usually measured indirectly and vary significantly depending upon location. This uncertainty in the appropriate value to assign to certain physical properties is called subjective uncertainty. Subjective uncertainty (epistemic) can, in theory, be reduced by further study of the system. Subjective uncertainty in uncertain parameters, including spatially uncertain parameters, is dealt with in the Salado Flow Modeling by running multiple realizations in which the values of uncertain parameters are varied. For spatially uncertain parameters such as the permeability of the DRZ, the entire material is assigned a single permeability which varies by realization. To reduce the number of realizations required and to ensure that low probability (and possibly high consequence) combinations are represented, Latin Hypercube sampling (LHS) is used to create the realizations. For the WIPP PA, the LHS software (Vugrin 2005) is used to create a “replicate” of 100 distinct parameter sets (“vectors”) that span the full range of parameter uncertainty. To ensure that the Latin Hypercube replicates are representative, a total of three replicates are run for a total of 300 separate vectors.

Another type of uncertainty faced by WIPP PA is what is called “stochastic” uncertainty (aleatory), or the uncertainty in what will happen in the future. Unlike subjective uncertainty, stochastic uncertainty cannot be reduced by further study. To deal with this type of uncertainty, WIPP PA employs a Monte Carlo method of sampling on random “futures”. A future is defined as one possible sequence of events. In the context of the BRAGFLO calculations, stochastic uncertainty is included by defining a set of six scenarios for which brine and gas flow is calculated for each of the vectors generated by the LHS software. Another software (CCDFGF) run after BRAGFLO and other PA software use the results of these scenarios to construct the individual futures. The total number of BRAGFLO simulations that have to be run for a WIPP PA calculation is 300 vectors times 6 scenarios, or 1,800 BRAGFLO simulations.

4.1 SALADO FLOW MODELING PROCESS

To run each of these 1,800 separate BRAGFLO simulations requires a series of preprocessing steps to be performed:

- A numerical modeling grid must be defined.
- Material types need to be assigned to regions
- Physical properties for all material types must be defined
- Other parameters required by BRAGFLO (e.g. gas generation rates, etc ...) must be defined.

These tasks are accomplished in five discrete computer-modeling steps, which are summarized in Table 4-1. This table also includes the software names and version numbers used for the CRA-2009 BRAGFLO analysis. Additional information can be found in Long (2008).

4.1.1 SANTOS

Creep closure calculations (SANTOS see Stone 1995) are performed before BRAGFLO is run. SANTOS produces an ASCII input file that contains information about the porosity surface(s) to be used in the BRAGFLO calculation. The ASCII file used for the CRA-2009 PA is named BF2_CRA1BC_CLOSURE.DAT and is located in the Code Management System (CMS) library: LIBCRA1BC_BF (not LIBCRA09_BF). This file is identical to the one used for the CRA-2004 PABC calculations, and therefore was not placed into the CRA-2009 library. The porosity surface data contained in the file is identical to that used for the 1996 CCA and 1997 PAVT PA calculations as well.

4.1.2 Latin Hypercube Sampling

The Latin Hypercube Sampling (LHS see Vugrin 2005) software is run before BRAGFLO calculations begin. The LHS software obtains information from the WIPP PAPDB via the preprocessing software PRELHS (Gilkey 2002). From an input files, PRELHS reads the names of parameters to be retrieved from the WIPP PA database, the number of vectors to produce, the random seed to use, and the correlations to enforce between sampled parameters. PRELHS then finds in the database the parameters that describe the probability distributions used in the WIPP PA analysis, and creates an ASCII output file, which is used as input to the LHS software, which does the actual parameter sampling. There are three ASCII input files read by PRELHS (one for each replicate) for the CRA-2009. These files are named: LHS1_CRA09_R1.INP, LHS1_CRA09_R2.INP, and LHS1_CRA09_R3.INP. They are stored in the CMS library: LIBCRA09_LHS.

4.1.3 GENMESH

The first step in the BRAGFLO modeling process (Step 1 in Table 4-1) is the definition of the modeling grid using the software, GENMESH (Shuldberg 1995). The parameters required to define the mesh include grid cell dimensions and region definitions. The analyst supplies these parameters in an ASCII input file. The CRA-2009 PA uses the file: GM_BF_CRA09.INP located in CMS library: LIBCRA09_BF. This file is identical to the file used in the CRA-2004 PABC, with a change in the header section.

4.1.4 MATSET

Details of the functionality of MATSET are discussed in the MATSET Users Manual (Gilkey 2001). MATSET is the first step for assigning the material property values needed by BRAGFLO (Step 1 in Table 4-1). The GENMESH binary output file, which is required as input for the MATSET software, provides the initial material map. All materials and properties that are used in BRAGFLO modeling should be specified in this modeling step, although the values may be changed in subsequent steps. For example, the parameters that are assigned sampled values by the LHS software in modeling Steps 3 through 5, must be assigned initial values by MATSET so that they can be reassigned in later steps.

Each property assignment requires specification of both the material (e.g. Salado halite) and the property (e.g. bulk compressibility) to be associated with that material. For PA analyses, MATSET extracts the information from the WIPP PAPDB according to instructions in the user-supplied input control file. If the database contains information defining a distribution of values for a material/property pair, MATSET retrieves the median value. For parameters that are constants, no distribution, MATSET retrieves the constant value. The MATSET input file used for the CRA-2009 PA is MS_BF_CRA09.INP and is located in the CMS library: LIBCRA09_BF.

4.1.5 POSTLHS

Modeling Step 2 (Table 4-1) employs the software, POSTLHS (Vugrin 2005), which takes the binary output from MATSET and creates 100 copies of this file replacing median values with the sampled values from the LHS software for every sampled parameter in each vector. Table 4-2 summarizes the parameters that are assigned sampled values by the LHS software. The independent variable name in the right hand column of the table is used in the analysis of BRAGFLO and is simply an alternative single-word name for each sampled MATERIAL/PROPERTY pair. These “independent variable” names are used in the sensitivity analysis described in section 4.1.12. POSTLHS requires that a dummy ASCII file be specified, which is not used in the calculations. The dummy file used for the CRA-2009 PA is LHS3_DUMMY.INP and is located in CMS library: LIBCRA09_BF. This file is identical to the file used in the CRA-2004 PABC.

4.1.6 ICSET

Initial conditions required by BRAGFLO include pressure, saturation, and steel and biodegradable material concentrations in all grid cells. Modeling Step 3 (Table 4-1) uses the application, ICSET to define some of these initial conditions. The functionality of ICSET is described in the Users Manual (Rath 1995). The software requires a user-supplied input control file defining how initial conditions are to be set and the POSTLHS binary (.CDB) file from Step 2. ICSET updates the input CDB file with the user supplied initial conditions creating a new output CDB file. The ICSET input file used for the CRA-2009 PA is IC_BF_CRA09.INP and is stored in the CMS library: LIBCRA09_BF.

Table 4-1. BRAGFLO model preprocessing steps used for the CRA-2009 PABC

Modeling Step	Software	Version	WIPP Prefix	Function	Interaction
0	SANTOS	2.1.7		Run prior to BRAGFLO analyses to provide porosity in waste-filled areas as a function of pressure and time. The porosity surface has not changed from the CCA.	
0	PRELHS	2.30	LHS1	Beginning with the CRA-2004 PABC, this software is run for all PA analyses software once (prior to BRAGFLO analysis). Identifies correlated properties. Retrieves property distribution data from WIPP database. User identifies properties to be sampled. Accepts user specified "seed" number that is used by LHS2 to randomly select values of sampled variables.	User Input Control File & Input from MATSET
0	LHS	2.42	LHS2	Beginning with the CRA-2004 PABC, this software is run for all PA analyses software once, prior to BRAGFLO analysis. Latin hypercube sampling is performed creating 100 "vectors" of sampled data. Each vector is defined by a set of randomly generated values for sampled variable based upon the distribution information retrieved by LHS1 from the WIPP database.	No direct user interaction. Input from LHS1.
1	GENMESH	6.08	GM	Generates the modeling grid and defines groups of cells as regions that are stored as material "blocks" in the output file.	User Input Control File
1	MATSET	9.10	MS	Defines additional material blocks and extracts properties from the WIPP database and assigns material-property values.	User Input Control File & Input from GENMESH
2	POSTLHS	4.07A	LHS3	Generates 100 CAMDAT output files (one for each vector).	No direct user interaction. Input from LHS2 and MATSET.
3	ICSET	2.22	IC	Sets selected initial conditions such as initial brine saturation, and initial pressure in the Culebra and Magenta units at the edge of the grid. Other initial conditions are set in the next step.	User Input Control File & Input from LHS3

Table 4-1. BRAGFLO model preprocessing steps used for the CRA-2009 PABC (continued)

Modeling Step	Software	Version	WIPP Prefix	Function	Interaction
3	ALGEGRACDB	2.35	ALG1	User can use ALGEGRACDB to calculate values for specified material properties from other input information (e.g. log permeability to permeability, bulk compressibility to pore compressibility, etc.). Calculations defining initial pressures, steel and biodegradable concentrations, gas generation rates, etc. are made.	User Input Control File & Input from ICSET
4	PREBRAG	8.00	BF1	User specifies temporal parameters for BRAGFLO including drilling location and time and changes in material properties over time. This is the step where each scenario is defined.	User Input Control File & Input from ALG1
5	BRAGFLO	6.0	BF2	Performs calculations for gas generations and gas/brine flow in a porous medium.	No direct user interaction. Input from BF1.
5	POSTBRAG	4.00A	BF3	Converts BF2 binary output file into the binary WIPP database format.	No direct user interaction. Input from BF2.
5	ALGEBRACDB	2.35	ALG2	User defines time-integrated output variables used in the analysis of results (e.g. volume averaged pressures and saturations).	User Input Control File & Input from BF3.
	SUMMARIZE	3.01	SUM	Generates ASCII tables of output variables.	User Input Control File & Input from ALG2
	SPLAT	1.02		Creates plots of output variables for each vector (usually 100)	User Input control File & Input from SUMMARIZE
	PCCSRC	2.21		Performs correlation and regression analyses	User Input control File & Input from SUMMARIZE & LHS

Steps with user interaction are indicated with bold italics lettering

Table 4-2. List of sampled material/property pairs with distribution type. Label in parenthesis in MATERIAL column refers to label in Figure 3-1.

INDEPENDENT VARIABLE	MATERIAL	PROPERTY	DISTRIBUTION	DESCRIPTION
Unchanged From CRA-2004 PABC				
ANHBCEXP	S_MB139 (MB-138, MB-139, Anhydrite AB)	PORE_DIS	Student's T	Brooks-Corey pore distribution parameter for anhydrite (dimensionless).
ANHBCVGP	S_MB139 (MB-138, MB-139, Anhydrite AB)	RELP_MOD	Cumulative	Pointer variable for selection of relative permeability model for use in anhydrite (dimensionless).
ANHPRM	S_MB139 (MB-138, MB-139, Anhydrite AB)	PRMX_LOG	Student's T	Logarithm of intrinsic anhydrite permeability, x-direction (m^2).
ANRBR SAT	S_MB139 (MB-138, MB-139, Anhydrite AB)	SAT_RBRN	Student's T	Residual brine saturation in anhydrite (dimensionless).
BHPERM	BH_SAND (Borehole)	PRMX_LOG	Uniform	Logarithm of intrinsic borehole permeability, x-direction (m^2).
BPCOMP ¹	CASTILER (Castile Brine Reservoir)	COMP_RCK	Triangular	Logarithm of bulk compressibility of brine pocket (Pa^{-1}).
BPINTPRS	CASTILER (Castile Brine Reservoir)	PRESSURE	Triangular	Initial pressure in brine pocket (Pa).
BPPRM ¹	CASTILER (Castile Brine Reservoir)	PRMX_LOG	Triangular	Logarithm of intrinsic brine pocket permeability, x-direction (m^2).
CONBCEXP	CONC_PCS (CONC_PCS)	PORE_DIS	Cumulative	Brooks-Corey pore distribution parameter for the concrete portion of Panel Closure System (PCS) (dimensionless).
CONBR SAT	CONC_PCS (CONC_PCS)	SAT_RBRN	Cumulative	Residual brine saturation in the concrete portion of PCS (dimensionless).

¹ BPPRM and BPCOMP are assumed to be correlated with a correlation coefficient equal to -0.75

Table 4-2. List of sampled material/property pairs with distribution type. (continued)

INDEPENDENT VARIABLE	MATERIAL	PROPERTY	DISTRIBUTION	DESCRIPTION
CONGSSAT	CONC_PCS (CONC_PCS)	SAT_RGAS	Uniform	Residual gas saturation in the concrete portion of PCS (dimensionless).
CONPRM	CONC_PCS (CONC_PCS)	PRMX_LOG	Triangular	Logarithm of concrete permeability, x-direction, in concrete portion of the PCS (m ²).
DRZPCPRM	DRZ_PCS (DRZ_PCS)	PRMX_LOG	Triangular	Logarithm of concrete permeability, x-direction, in the DRZ above the PCS (m ²).
DRZPRM	DRZ_1 (Upper DRZ, Lower DRZ)	PRMX_LOG	Uniform	Logarithm of DRZ permeability, x-direction (m ²).
HALCOMP ²	S_HALITE (Salado)	COMP_RCK	Uniform	Bulk compressibility of halite (Pa ⁻¹).
HALPOR	S_HALITE (Salado)	POROSITY	Cumulative	Halite porosity (dimensionless).
HALPRM ²	S_HALITE (Salado)	PRMX_LOG	Uniform	Logarithm of halite permeability, x-direction (m ²).
PLGPRM	CONC_PLG (Conc_Mon)	PRMX_LOG	Uniform	Logarithm of concrete plug permeability, x-direction (m ²).
SALPRES	S_HALITE (Salado)	PRESSURE	Uniform	Initial brine pressure, without the repository being present, at a reference point located in the center of the combined shafts at the elevation of the midpoint of Marker Bed (MB) 139 (Pa).
SHLPRM2	SHFTL_T1 (SHFTL_T1)	PRMX_LOG	Cumulative	Logarithm of intrinsic permeability of the lower portion of the simplified shaft (0-200 years)(m ²).
SHLPRM3	SHFTL_T2 (SHFTL_T2)	PRMX_LOG	Cumulative	Logarithm of intrinsic permeability of the lower portion of the simplified shaft (after 200 years)(m ²).
SHUPRM	SHFTU (SHFTU)	PRMX_LOG	Cumulative	Logarithm of intrinsic permeability of the upper portion of the simplified shaft (m ²).
SHURBRN	SHFTU (SHFTU)	SAT_RBRN	Cumulative	Residual brine saturation of the upper portion of the simplified shaft (dimensionless)
SHURGAS	SHFTU (SHFTU)	SAT_RGAS	Uniform	Residual gas saturation of the upper portion of the simplified shaft (dimensionless)
WASTWICK	WAS_AREA (Panel)	SAT_WICK	Uniform	Increase in brine saturation of waste due to capillary forces (dimensionless).

² HALPRM and HALCOMP are assumed to be correlated with a correlation coefficient equal to -0.99

Table 4-2. List of sampled material/property pairs with distribution type. (continued)

INDEPENDENT VARIABLE	MATERIAL	PROPERTY	DISTRIBUTION	DESCRIPTION
WFBETCEL	CELLULS	FBETA	Uniform	Scale factor used in definition of stoichiometric coefficient for microbial gas generation (dimensionless).
WGRCOR	STEEL	CORRMCO2	Uniform	Corrosion rate for steel under inundated conditions in the absence of CO ₂ (m/s).
WGRMICH	WAS_AREA (Panel)	GRATMICH	Uniform	Microbial degradation rate for cellulose under humid conditions (mol/kg·s).
WGRMICI	WAS_AREA (Panel)	GRATMICI	Uniform	Microbial degradation rate for cellulose under inundated conditions (mol/kg·s).
WMICDFLG	WAS_AREA (Panel)	PROBDEG	Cumulative	Categorical variable for microbial degradation of cellulose (dimensionless).
WRBRNSAT	WAS_AREA (Panel)	SAT_RBRN	Uniform	Residual brine saturation in waste (dimensionless).
WRGSSAT	WAS_AREA (Panel)	SAT_RGAS	Uniform	Residual gas saturation in waste (dimensionless).
BIOGENFC	WAS_AREA (Panel)	BIOGENFC	Added for CRA-2004 PABC	Probability of attaining sampled microbial gas generation rate (dimensionless) (Nemer, Stein et al. 2005).

4.1.7 ALGEBRACDB

Modeling Step 3 (Table 4-1) employs the ALGEBRACDB software, which is used to manipulate data from the binary (.CDB) output file from ICSET. ALGEBRACDB is capable of performing most common algebraic manipulations and evaluating most common transcendental functions (trigonometric, logarithmic, exponential, etc.). Its functionality is discussed in the Users Manual (Gilkey 1996).

ALGEBRACDB reads its instructions from a user-supplied ASCII input file that employs an algebraic syntax that is similar in appearance to FORTRAN syntax. It then executes the mathematical instructions to modify input data from ICSET and to calculate new parameters needed by the BRAGFLO software. The results are written to a new binary (.CDB) output file. Files associated with this step are designated with ALG1 in the filename, because ALGEBRACDB is also used in post-BRAGFLO processing (see Subsection 4.1.10).

Calculations performed in this step include:

- Calculation of total amount of steel and biodegradable organic materials from densities reported in the inventory.
- Conversion between units stored in the WIPP PAPDB and units required by BRAGFLO.
- Assignment of parameters sampled for one material to another material (e.g. hydraulic properties are sampled for anhydrite marker bed 139 and assigned to the other marker bed materials in the model).
- Assignment of gas generation parameters including initial concentration, humid and inundated gas generation rates that depend on inventory and sampled parameters.
- Calculation and application of the 1° stratigraphic dip of the Salado Formation.

The ALGEBRACDB input file used for this step of the CRA-2009 PA is ALG1_BF_CRA09.INP and is located in CMS library: LIBCRA09_BF.

4.1.8 PREBRAG

The final pre-processing step for BRAGFLO modeling (Step 4 in Table 4-1) employs the software, PREBRAG, which accepts the binary (.CDB) output file from ALGEBRACDB (ALG1) and creates the ASCII file used as input to the BRAGFLO software. The functionality of PREBRAG is discussed in the User's Manual (Gilkey and Rudeen 2007). The user supplies instructions to PREBRAG in an ASCII input file to specify changes in modeling conditions at different times and to identify what information should be calculated and written by BRAGFLO to the output files. This is the modeling step in which scenarios are defined by specifying changes in materials and properties at different times (e.g. "create" a borehole at 350 or 1000 years by redefining the material map at that time in the simulation). The PREBRAG input files the CRA-2009 PA are BF1_CRA09_Ss.INP, where s = 1, ...6, and are located in CMS library: LIBCRA09_BF

4.1.9 BRAGFLO

The final step in the BRAGFLO analysis (Step 5 in Table 4-1) is to run the BRAGFLO software for each vector / scenario / replicate combination (1800 model runs). The functionality and the theory on which BRAGFLO is based are discussed in the Users Manual (Nemer 2006). The results of BRAGFLO include calculated values for variables such as pressure, brine saturation, porosity, and fluid flow at times and grid locations that are specified in the PREBRAG input control file. The output data is written to ASCII and binary output files. Only the binary files are used for Salado Flow analysis and for input to subsequent WIPP PA activities (e.g. NUTS, CUTTINGS_S, etc.). The ASCII input files used for the CRA-2009 PA runs are named BF2_CRA09_R#_S#_V###.INP, where R# is R1, R2, or R3, depending on the replicate, S# is S1-S6, depending on the scenario, and V### is V001 to V100, depending on the vector. These files are stored in 18 separate CMS libraries with the naming convention: LIBCRA09_BFR#S#, where R# and S# are described above.

4.1.10 POSTBRAG & ALGEBRACDB (ALG2)

The post-BRAGFLO processing application, POSTBRAG (Nemer 2007), is used to convert the BRAGFLO binary output file (.BIN) into the CAMDAT (Rechard, Gilkey et al. 1990) database file (.CDB) that is used by other WIPP PA software (Step 5 in Table 4-1). The software ALGEBRACDB is again used to calculate cumulative and/or volume-averaged values for specific regions in the grid. The output is written to a binary (.CDB) file (modeling Step 5 in Table 4-1). Files associated with post-BRAGFLO processing using ALGEBRACDB are identified with ALG2 in their names. The ALGEBRACDB input file used for this post-processing step of the CRA-2009 PA is ALG2_BF_CRA09.INP and is located in CMS library: LIBCRA09_BF.

4.1.11 SUMMARIZE and SPLAT

The software, SUMMARIZE (see Table 4-1) is used to extract data from the binary output files (.CDB) from POSTBRAG or ALGEBRACDB (ALG2) to produce ASCII tables organized according to analytical needs. One common use of SUMMARIZE is to create a table of output variables with values for all 100 vectors reported at specified time intervals. In this case, SUMMARIZE will linearly interpolate output values at specific times from the nearest times included in the binary file. This interpolation is necessary because BRAGFLO uses a variable time-step and thus vectors do not have output at exactly the same times. SUMMARIZE can take input from each vector and combine it into a single table file.

Tables from SUMMARIZE are used to make plots that show the values of output variables for each of the 100 vectors in a scenario over time (usually the full 10,000 year regulatory period). These plots are generated using the software, SPLAT (Gilkey 1996) (see Table 4-1).

4.1.12 PCCSRC

Several approaches are used in this analysis to evaluate the effects of sampled input parameters on BRAGFLO results. The simplest method is to use scatter plots to visually evaluate relationships of an output variable with a single input parameter (or another output variable).

Excel is used to calculate Pearson sample correlation coefficients for pairings of variables and input parameters. Pearson correlation coefficients were calculated to determine the relative importance of various input parameters to annualized brine outflow rates during this stage. The Pearson correlation coefficient, r , for two arrays, X and Y containing n elements is:

$$r = \frac{n(\sum XY) - (\sum X)(\sum Y)}{\sqrt{[n\sum X^2 - (\sum X)^2][n\sum Y^2 - (\sum Y)^2]}} \quad (1)$$

Pearson correlation coefficients vary from -1.0 to 1.0 and indicate the extent of a linear relationship between the two arrays.

The application, PCCSRC is a systematic approach to identifying the most important input parameters that explain the variability in model outputs (Gilkey 1995) (see Table 4-1). PCCSRC produces plots of correlation statistics for selected output variables (dependent variables) relative to sampled input parameters (independent variables). Partial rank correlation coefficients (PRCC's) are used in the Salado Flow Analysis, because some relationships may be non-linear over the full range of conditions represented in 100 vectors. These correlation calculations are performed on the ranks of the variables rather than their values, which reduces numerical-computation problems due to large differences in the magnitudes of input parameters. Each PRCC explains how much of the ranking for the output variable can be explained by the ranking of the input variable with the linear effects of the other variables removed (Helton, Bean et al. 1998).

PRCC's are calculated at selected times to produce plots of PRCC's over an extended period of time. Only the input parameters with the top five PRCC's are plotted, and any variable with a PRCC below 0.25 is disregarded. The correlations may be positive or negative, and the absolute value of the PRCC indicates the relative importance of each input parameter to the uncertainty in the output variable.

4.1.13 Execution and Run Control

Digital Command Language (DCL) scripts, referred to here as EVAL run scripts, are used to implement and document the running of all software. These scripts, which are the basis for the WIPP PA run control system, are stored in the LIBCRA09_EVAL library. All inputs are fetched at run time by the scripts, and outputs and run logs are automatically stored by the scripts in class CRA09-0 of the CMS libraries.

4.2 MODELING SCENARIOS

A total of six scenarios (S1-S6) are considered in the BRAGFLO modeling for the WIPP PA. These scenarios are unchanged from those used for the 1996 CCA, the 1997 PAVT, and CRA-2004 PABC. The scenarios include one undisturbed scenario (S1), four scenarios that include a single inadvertent future drilling intrusion into the repository in 10,000 years, and one scenario that investigates the effect of two intrusions into a single waste panel. Two types of intrusions are considered. An E1 intrusion assumes the borehole passes through a waste-filled panel and into a pressurized brine pocket that may exist under the repository in the Castile formation. An E2 intrusion assumes that the borehole passes through the repository but does not encounter a brine pocket. Scenarios S2 and S3 model the effect of an E1 intrusion occurring at 350 years and 1000 years, respectively, after the repository is closed. Scenarios S4 and S5 model the effect of an E2 intrusion at 350 and 1000 years. Scenario S6 models an E2 intrusion occurring at 1000 years, followed by an E1 into the same panel at 2000 years. Table 4-3 summarizes the six scenarios used in this analysis.

Table 4-3. BRAGFLO modeling scenarios

Scenario	Description
S1	Undisturbed Repository
S2	E1 intrusion at 350 years
S3	E1 intrusion at 1,000 years
S4	E2 intrusion at 350 years
S5	E2 intrusion at 1,000 years
S6	E2 intrusion at 1,000 years; E1 intrusion at 2,000 years.

E1: Borehole penetrates through the repository and into a hypothetical pressurized brine reservoir in the Castile Formation.

E2: Borehole penetrates the repository, but does not encounter brine in the Castile Formation.

5 INFORMATION SPECIFIC TO THE CRA-2009 PA

This section describes changes to the BRAGFLO modeling made for the CRA-2009 PABC calculation. In this report, changes are divided into two groups: changes or corrections to input parameters (Subsection 5.1), and code changes implemented in the CRA-2009 PA (Subsection 5.2).

5.1 CHANGES TO INPUT PARAMETERS

In the CRA-2009 the following changes were made to parameters upstream of the BRAGFLO code:

- 1) Inventory information was updated to include emplacement CPR materials in the CPR densities used by BRAGFLO.
- 2) Correction to the halite and DRZ porosity values.
- 3) Updated conditional relationship between the humid and inundated CPR degradation rate.

Each of these changes and their supporting references are discussed below in Subsections 5.1.1 - 5.1.3.

5.1.1 Emplacement Materials Inventory

The CRA-2004 PABC included CPR materials in the waste and container (packaging) materials (Table 5-2), but the CPR contents in emplacement materials were erroneously omitted from the CRA-2004 PABC (Nemer 2007). To correct this omission, six new parameters representing the density of CPR materials in emplacement materials were created and used in the CRA-2009 PA. Many of these parameters were added for book-keeping purposes and are currently equal to zero, i.e. RH waste has no CPR in the emplacement materials, and CH waste has no rubber in the emplacement materials. Four additional parameters representing the density of CPR in container packaging were created and used in the CRA-2009 PA. Table 5-3 lists the names and descriptions of those ten additional parameters. The addition of these four additional parameters was also done solely for book-keeping purposes since packaging materials do not contain cellulose or rubber materials, as seen by the zero values in Table 5-3. The CRA-2009 PA used the parameters in Table 5-2 and Table 5-3.

Based on the parameters in Table 5-2 and Table 5-3, ALGEBRA in the ALG1 step calculates the total moles of organic carbon available for degradation in the case where only cellulose can degrade (WAS_AREA:PROBDEG = 1) and in the case where cellulose, plastic and rubber can degrade (WAS_AREA:PROBDEG = 2 see Subsection 5.4 of Nemer and Stein 2005). These values are shown below in Table 5-1.

Table 5-1. Moles of Organic Carbon available for biodegradation.

WAS_AREA:PROBDEG	Total mass of organic carbon available (kg)¹	Total Moles of organic carbon available (moles)²
1 (Cellulose only)	1.04 x 10 ⁷	3.9 x 10 ⁸
2 (CPR)	3.25 x 10 ⁷	1.2 x 10 ⁹

1. Three digits are kept here for comparison to BRAGFLO input and output files. Only two digits are significant because many of the CPR parameters in Table 5-2 have only two significant digits.

2. Mass of organic carbon was converted to moles of organic carbon using the formula

$$mol\ C = kg\ cellulose \times \frac{1000\ mol\ cellulose}{162\ kg\ cellulose} \times \frac{6\ mol\ C}{mol\ cellulose}, \quad (2)$$

where 162/1000 is the molecular weight of cellulose in mol/kg and there are 6 mol of organic carbon in 1 mol of cellulose (C₆H₁₀O₅).

Table 5-2. CRA-2004 PABC CPR Parameters.

Name	Description	Value (kg/m³)
WAS_AREA: DCELLCHW	Average density of cellulosics in CH waste materials	60.0
WAS_AREA: DCELLRHW	Average density of cellulosics in RH waste materials	9.3
WAS_AREA: DPLASCHW	Average density of plastic in CH waste materials	43.0
WAS_AREA: DPLASRHW	Average density of plastic in RH waste materials	8.0
WAS_AREA: DPLSCCHW	Average density of plastic in CH waste container (packaging) materials	17.0
WAS_AREA: DPLSCRHW	Average density of plastic in RH waste container (packaging) materials	3.1
WAS_AREA: DRUBBCHW	Average density of rubber in CH waste materials	13.0
WAS_AREA: DRUBBRHW	Average density of rubber in RH waste materials	6.7

Table 5-3. CPR Parameters Created for the CRA-2009 PA.

Name	Description	Value (kg/m ³)
WAS_AREA:DCELECHW	Average density of cellulose in CH waste emplacement materials	1.22
WAS_AREA:DCELERHW	Average density of cellulose in RH waste emplacement materials	0.0
WAS_AREA: DCELCCHW	Average density of cellulose in CH waste container materials	0.0
WAS_AREA: DCELCRHW	Average density of cellulose in RH waste container materials	0.0
WAS_AREA:DPLSECHW	Average density of plastic in CH waste emplacement materials	8.76
WAS_AREA:DPLSERHW	Average density of plastic in RH waste emplacement materials	0.0
WAS_AREA:DRUBECHW	Average density of rubber in CH waste emplacement materials	0.0
WAS_AREA:DRUBERHW	Average density of rubber in RH waste emplacement materials	0.0
WAS_AREA: DRUBCCHW	Average density of rubber in CH waste container materials	0.0
WAS_AREA: DRUBCRHW	Average density of rubber in RH waste container materials	0.0

5.1.2 Halite/Disturbed Rock Zone Porosity

An error in the determination of the intact halite porosity variable, S_HALITE:POROSITY, was discovered and reported in Parameter Problem Report 2007-002 (Ismail 2007). The maximum of the range was taken from data reported in weight fraction without the conversion to volume fraction. Converting the maximum value from a weight fraction to a volume fraction changed the value from 0.03 to 0.0519 (Ismail 2007). The minimum and mode values of the distribution were not affected. Furthermore, current WIPP PA practice for determining the disturbed rock zone (DRZ) porosity is to increase the S_HALITE:POROSITY value by 0.0029. Therefore, the maximum value of the range for the DRZ_0:POROSITY, DRZ_1:POROSITY and DRZ_PCS:POROSITY increased from 0.0329 to 0.0548. The CRA-2009 PA used the corrected porosity ranges as listed in Table 5-4. This parameter is used in BRAGFLO calculations.

Table 5-4. Porosity Parameter Values.

Name	Description	Analysis	Min	Mode	Max
S_HALITE:POROSITY	Halite porosity	CRA-2004 PABC	0.001	0.01	0.03
		CRA-2009 PA	0.001	0.01	0.0519
DRZ_0:POROSITY	DRZ porosity -5 to 0 yrs	CRA-2004 PABC	0.0039	0.0129	0.0329
		CRA-2009 PA	0.0039	0.0129	0.0548
DRZ_1:POROSITY	DRZ porosity 0 to 10,000 yrs	CRA-2004 PABC	0.0039	0.0129	0.0329
		CRA-2009 PA	0.0039	0.0129	0.0548
DRZ_PCS:POROSITY	DRZ above panel closure porosity -5 to 10,000 yrs	CRA-2004 PABC	0.0039	0.0129	0.0329
		CRA-2009 PA	0.0039	0.0129	0.0548

5.1.3 CPR Degradation Rate

The WIPP PA brine and gas flow model includes gas generation from the microbial degradation of CPR materials. The model assumes that the gas generation occurs at a given zero'th order rate, for which the possible range was determined from laboratory experiments. The inundated microbial degradation rate for cellulose, WAS_AREA:GRATMICI, is represented by a uniform distribution between $3.08269\text{e-}11$ and $5.56921\text{e-}10$ moles/kg/s, while the humid microbial degradation rate for cellulose, WAS_AREA:GRATMICH, is represented by a uniform distribution between 0 and $1.02717\text{e-}09$ moles/kg/s. The experimental data for the gas generation experiments run under humid conditions indicate that the long-term maximum humid microbial gas-generation rate is greater than the long-term inundated rate. The DOE believes this is due to the sparsity of data for the humid rate and physically unrealistic. Given the lack of water under humid experimental conditions, DOE expects the humid rate to be much less than the case where the microbes are inundated with brine.

In previous analyses, no upstream correlation was imposed between the inundated and humid microbial cellulose degradation rate, and so it is possible that the Latin Hypercube Sampling code, LHS, may sample a humid rate that is higher than the inundated rate for a single vector. In the CRA-2004 PABC, if the sampled humid rate was higher than the inundated rate in a given single vector, the humid rate was set to be equal to the inundated rate in the ALG1 preprocessing step for the BRAGFLO calculations,

$$R_{mh} = \min(R_{mi}, R_{mh}), \quad (3)$$

where R_{mh} is the sampled humid microbial-gas-generation rate and R_{mi} is the sampled inundated microbial-gas-generation rate.

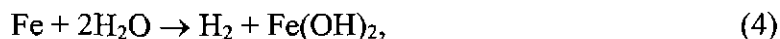
For the CRA-2009 PA, a conditional relationship was applied such that the sampled inundated rate was used as the maximum for sampling the humid rate. For each vector the inundated rate was first sampled according to the uniform distribution in the WIPP PABP. Next, for the same vector, the humid rate was sampled from zero up to the sampled inundated rate (already obtained for this vector) using a uniform distribution. This conditional relationship was applied during the LHS process, instead of in the ALG1 step as was done previously. We refer the reader to Kirchner (2008) for the full details of this process. This change from the CRA-2004 PABC is an improvement because sensitivity to the humid rate can now be calculated using the LHS output file and the BRAGFLO results using the PCCSRC code (see Subsection 4.1.12).

5.2 CHANGES TO CODES USED IN THE BRAGFLO ANALYSES

Herein the new version of BRAGFLO, version 6.00, is discussed in the context of the CRA-2009. Changes to the code that were employed in the CRA-2009 are discussed here, unused changes will not be discussed in great detail but can be found in the BRAGFLO user's manual (Nemer 2006).

5.2.1 Chemistry Stoichiometric Matrix

As discussed in Subsection 4.13.2 of the BRAGFLO Version 6.00 user's manual (Nemer 2006), in BRAGFLO Version 6.0 the stoichiometric coefficients for the chemical reactions have been reorganized into a single matrix $S(I,J)$; stoichiometric coefficients are dimensionless. A stoichiometric coefficient is defined as the moles of reactant (or product) consumed (or produced) relative to the other reactants and products in a given reaction. For example, in the anoxic corrosion reaction of iron to form iron hydroxide,



the stoichiometric coefficient for hydrogen (H_2) is 1 (positive, indicating that it is produced) and that of iron (Fe) is -1 (negative, indicating that it is consumed). The stoichiometric coefficient for water in reaction (4) is -2.

In BRAGFLO, The stoichiometric matrix is organized as follows: I represents the reaction index and J represents the individual compound index. These indices are listed below in Table 5-6 and Table 5-7. All of the stoichiometric coefficients are parameters in the WIPP PAPDB. The values of these parameters in the database are given below in Table 5-8 through Table 5-14. A positive value of $S(I,J)$ represents production, and negative represents consumption. Note that although the MgO hydration and iron sulfidation stoichiometric parameters have non-zero values in the WIPP PA database, they have been overwritten and set equal to zero in the PREBRAG input file, as shown below in Table 5-15.

In Table 5-9, the stoichiometric coefficient for the amount of hydrogen gas produced per mole of organic carbon is set to zero. This does not mean, however, that microbial CPR degradation produces no gas in the CRA-2009 PA. The amount of gas produced per mole of organic carbon was input through the variable SMIC_H2, which was previously named STOIMIC in the CRA-2004 PABC. This additional variable was added primarily for future capabilities, as it allows for different types of waste in different waste areas (i.e WAS_AREA, NRR, SRR). For the CRA-2009 PA, it does not matter whether the amount of gas produced by microbial CPR degradation is entered through $S(2,1)$ or SMIC_H2 because in the CRA-2009 PA all of the waste areas are treated the same. The value of SMIC_H2 is ~ 0.5 and corresponds to the gas remaining from microbial CPR degradation after all CO_2 is consumed by MgO. This is fully explained in Subsections 4.1 – 4.4 of Nemer and Zelinski (2005). The actual values of SMIC_H2 are given below in Table 5-5 for the CRA-2004 PABC and the CRA-2009 PA. This parameter is calculated in the ALGEBRA1 step. Details of this calculation can be found by viewing the ALGEBRA1 input file: ALG1_BF_CRA09.INP, which is located in CMS in library LIBCRA09_BF.

Table 5-5. Minimum and Maximum values of SMIC_H2 (net amount of gas produced per mole of organic carbon) for the CRA-2004 PABC and the CRA-2009 PA.

PA Calculation	SMIC_H2 <i>min</i>	SMIC_H2 <i>max</i>
CRA-2004 PABC	0.486	0.497
CRA-2009 PA	0.450	0.496

Table 5-6. Stoichiometric matrix S(I,J) row number I and corresponding reaction

Index (I)	Reaction
1	Anoxic corrosion of iron
2	Microbial gas generation
3	Iron hydroxide sulfidation
4	Metallic iron sulfidation
5	MgO hydration
6	Magnesium hydroxide (brucite) carbonation
7	MgO carbonation

Table 5-7. Stoichiometric matrix S(I,J) column number J and corresponding compound

Index (J)	Compound
1	H ₂
2	H ₂ O
3	Fe
4	Cellulosics
5	Fe(OH) ₂
6	FeS
7	MgO
8	Mg(OH) ₂
9	MgCO ₃

Table 5-8. Fe Corrosion Reaction Parameters Created for the CRA-2009 PA.

Name	Description	Value
REFCON:STCO_11	Fe Corrosion:H2 Stoichiometric Coefficient	1
REFCON:STCO_12	Fe Corrosion:H2O Stoichiometric Coefficient	-2
REFCON:STCO_13	Fe Corrosion:Fe Stoichiometric Coefficient	-1
REFCON:STCO_14	Fe Corrosion:Cellulosics Stoichiometric Coefficient	0
REFCON:STCO_15	Fe Corrosion:FeOH2 Stoichiometric Coefficient	1
REFCON:STCO_16	Fe Corrosion:FeS Stoichiometric Coefficient	0
REFCON:STCO_17	Fe Corrosion:MgO Stoichiometric Coefficient	0
REFCON:STCO_18	Fe Corrosion:MgOH2 Stoichiometric Coefficient	0
REFCON:STCO_19	Fe Corrosion:MgCO3 Stoichiometric Coefficient	0

Table 5-9. Microbial Gas Generation Reaction Parameters Created for the CRA-2009 PA.

Name	Description	Value
REFCON:STCO_21	Microbial Gas Generation:H2 Stoichiometric Coefficient	0
REFCON:STCO_22	Microbial Gas Generation:H2O Stoichiometric Coefficient	0
REFCON:STCO_23	Microbial Gas Generation:Fe Stoichiometric Coefficient	0
REFCON:STCO_24	Microbial Gas Generation:Cellulosics Stoichiometric Coefficient	-1
REFCON:STCO_25	Microbial Gas Generation:FeOH2 Stoichiometric Coefficient	0
REFCON:STCO_26	Microbial Gas Generation:FeS Stoichiometric Coefficient	0
REFCON:STCO_27	Microbial Gas Generation:MgO Stoichiometric Coefficient	0
REFCON:STCO_28	Microbial Gas Generation:MgOH2 Stoichiometric Coefficient	0
REFCON:STCO_29	Microbial Gas Generation:MgCO3 Stoichiometric Coefficient	0

Table 5-10. Fe(OH)₂ Sulfidation Reaction Parameters Created for the CRA-2009 PA.

Name	Description	Value
REFCON:STCO_31	FeOH2 Sulfidation:H2 Stoichiometric Coefficient	-1
REFCON:STCO_32	FeOH2 Sulfidation:H2O Stoichiometric Coefficient	2
REFCON:STCO_33	FeOH2 Sulfidation:Fe Stoichiometric Coefficient	0
REFCON:STCO_34	FeOH2 Sulfidation:Cellulosics Stoichiometric Coefficient	0
REFCON:STCO_35	FeOH2 Sulfidation:FeOH2 Stoichiometric Coefficient	-1
REFCON:STCO_36	FeOH2 Sulfidation:FeS Stoichiometric Coefficient	0
REFCON:STCO_37	FeOH2 Sulfidation:MgO Stoichiometric Coefficient	0
REFCON:STCO_38	FeOH2 Sulfidation:MgOH2 Stoichiometric Coefficient	0
REFCON:STCO_39	FeOH2 Sulfidation:MgCO3 Stoichiometric Coefficient	0

Table 5-11. Metallic Fe Sulfidation Reaction Parameters Created for the CRA-2009 PA.

Name	Description	Value
REFCON:STCO_41	Metallic Fe Sulfidation:H2 Stoichiometric Coefficient	0
REFCON:STCO_42	Metallic Fe Sulfidation:H2O Stoichiometric Coefficient	0
REFCON:STCO_43	Metallic Fe Sulfidation:Fe Stoichiometric Coefficient	-1
REFCON:STCO_44	Metallic Fe Sulfidation:Cellulosics Stoichiometric Coefficient	0
REFCON:STCO_45	Metallic Fe Sulfidation:FeOH2 Stoichiometric Coefficient	0
REFCON:STCO_46	Metallic Fe Sulfidation:FeS Stoichiometric Coefficient	1
REFCON:STCO_47	Metallic Fe Sulfidation:MgO Stoichiometric Coefficient	0
REFCON:STCO_48	Metallic Fe Sulfidation:MgOH2 Stoichiometric Coefficient	0
REFCON:STCO_49	Metallic Fe Sulfidation:MgCO3 Stoichiometric Coefficient	0

Table 5-12. MgO Hydration Reaction Parameters Created for the CRA-2009 PA.

Name	Description	Value
REFCON:STCO 51	MgO Hydration:H2 Stoichiometric Coefficient	0
REFCON:STCO 52	MgO Hydration:H2O Stoichiometric Coefficient	-1
REFCON:STCO 53	MgO Hydration:Fe Stoichiometric Coefficient	0
REFCON:STCO 54	MgO Hydration:Cellulosics Stoichiometric Coefficient	0
REFCON:STCO 55	MgO Hydration:FeOH2 Stoichiometric Coefficient	0
REFCON:STCO 56	MgO Hydration:FeS Stoichiometric Coefficient	0
REFCON:STCO 57	MgO Hydration:MgO Stoichiometric Coefficient	-1
REFCON:STCO 58	MgO Hydration:MgOH2 Stoichiometric Coefficient	1
REFCON:STCO 59	MgO Hydration:MgCO3 Stoichiometric Coefficient	0

Table 5-13. Mg(OH)₂ Carbonation Reaction Parameters Created for the CRA-2009 PA.

Name	Description	Value
REFCON:STCO 61	MgOH2 Carbonation:H2 Stoichiometric Coefficient	0
REFCON:STCO 62	MgOH2 Carbonation:H2O Stoichiometric Coefficient	1
REFCON:STCO 63	MgOH2 Carbonation:Fe Stoichiometric Coefficient	0
REFCON:STCO 64	MgOH2 Carbonation:Cellulosics Stoichiometric Coefficient	0
REFCON:STCO 65	MgOH2 Carbonation:FeOH2 Stoichiometric Coefficient	0
REFCON:STCO 66	MgOH2 Carbonation:FeS Stoichiometric Coefficient	0
REFCON:STCO 67	MgOH2 Carbonation:MgO Stoichiometric Coefficient	0
REFCON:STCO 68	MgOH2 Carbonation:MgOH2 Stoichiometric Coefficient	-1
REFCON:STCO 69	MgOH2 Carbonation:MgCO3 Stoichiometric Coefficient	1

Table 5-14. MgO Carbonation Reaction Parameters Created for the CRA-2009 PA.

Name	Description	Value
REFCON:STCO 71	MgO Carbonation:H2 Stoichiometric Coefficient	0
REFCON:STCO 72	MgO Carbonation:H2O Stoichiometric Coefficient	0
REFCON:STCO 73	MgO Carbonation:Fe Stoichiometric Coefficient	0
REFCON:STCO 74	MgO Carbonation:Cellulosics Stoichiometric Coefficient	0
REFCON:STCO 75	MgO Carbonation:FeOH2 Stoichiometric Coefficient	0
REFCON:STCO 76	MgO Carbonation:FeS Stoichiometric Coefficient	0
REFCON:STCO 77	MgO Carbonation:MgO Stoichiometric Coefficient	-1
REFCON:STCO 78	MgO Carbonation:MgOH2 Stoichiometric Coefficient	0
REFCON:STCO 79	MgO Carbonation:MgCO3 Stoichiometric Coefficient	1

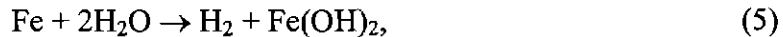
Table 5-15. Section of PREBRAG input file used in the CRA-2009 PA that concerns the chemistry stoichiometric matrix. Notice that all the stoichiometric parameters are set to zero (val= 0.0), except for reactions I = 1,2 (iron corrosion, biodegradation), which are the top two lines (val = STCO_11,...). The text shown below was taken from the PREBRAG input file for Scenario 1, BF1_CRA09_S1.INP. This file can be found in CMS in the library LIBCRA09_BF.

```

SCOEFF, MAT= REFCON, TYPE= COR, VAL= STCO_11 STCO_12 STCO_13 STCO_14
STCO_15 STCO_16 STCO_17 STCO_18 STCO_19
SCOEFF, MAT= REFCON, TYPE= MIC, VAL= STCO_21 STCO_22 STCO_23 STCO_24
STCO_25 STCO_26 STCO_27 STCO_28 STCO_29
SCOEFF, MAT= REFCON, TYPE= FEOH2SR, VAL= 0.0 0.0 0.0 0.0
0.0 0.0 0.0 0.0 0.0
SCOEFF, MAT= REFCON, TYPE= FESR, VAL= 0.0 0.0 0.0 0.0
0.0 0.0 0.0 0.0 0.0
SCOEFF, MAT= REFCON, TYPE= MGOHR, VAL= 0.0 0.0 0.0 0.0
0.0 0.0 0.0 0.0 0.0
SCOEFF, MAT= REFCON, TYPE= MGOH2CR, VAL= 0.0 0.0 0.0 0.0
0.0 0.0 0.0 0.0 0.0
SCOEFF, MAT= REFCON, TYPE= MGOCR, VAL= 0.0 0.0 0.0 0.0
0.0 0.0 0.0 0.0 0.0

```

In the CRA-2009 PA the only reactions that are active are anoxic iron corrosion (reaction I = 1)



and microbial gas generation (reactions I = 2)



which is consistent with the CRA-2004 PABC. Here SMIC_H₂ is the moles of gas (BRAGFLO treats all gas as hydrogen for the purpose of calculating pressure through the Redlich-Kwong-Soave equation of state) produced per mole of organic carbon after CO₂ is sequestered by MgO carbonation, as was discussed above.

Although MgO carbonation and iron sulfidation are implicitly included in BRAGFLO calculations (all CO₂ is assumed to be sequestered by MgO and all H₂S is assumed to be converted to H₂, see Subsection 4.1 of Nemer and Zelinski 2005), they have not been explicitly modeled in BRAGFLO. BRAGFLO version 6.0 includes the ability to explicitly model iron sulfidation, MgO carbonation, and hydration, albeit simplified. Since these reactions were turned off for the CRA-2009 PA they are not discussed further here. More information can be found in Subsection 4.13.3 and 4.13.5 of the BRAGFLO version 6.0 user's manual (Nemer 2006). Note that although the MgO hydration and iron sulfidation stoichiometric parameters have non-zero values in the WIPP PA database, they have been overwritten and set equal to zero in the PREBRAG input file, as shown above in Table 5-15.

5.2.2 Wicking and the Effective Saturation

Brine-consuming reactions such as anoxic iron corrosion tend to dry out the waste-filled regions of the repository. The BRAGFLO code and the underlying models (being a two-phase porous

media flow code) cannot simulate completely dry ($S_w = 0$) cells. Furthermore there is no reason to believe that anoxic iron corrosion hydration will stop at the residual brine saturation. To accommodate brine-consuming reactions and allow the code to run, in BRAGFLO Version 6.0 we have introduced a lower cut off in saturation S_{min} in the waste filled areas that we consider “numerically” dry. This cut off is meant to be chosen small enough such that the amount of water in the waste filled areas at the cut off is small, but large enough to prevent numerical difficulties. Below this saturation biodegradation, and iron corrosion cease. The parameter S_{min} shows up in the BRAGFLO subroutines PROPS and PROPS1, which calculate the properties of the grid or a single cell, respectively. In these routines an effective saturation S_{eff} is calculated and sent to each of the chemistry routines which calculate the rates of reactions, based on the effective saturation (rather than the actual saturation). The effective saturation includes the effects of wicking, which is unchanged from the CRA-2004 PABC. In BRAGFLO Version 5.0 (in the subroutines PROPS and PROPS1) the effective saturation is calculated from

$$S_{eff} = S_w + S_{wick} (1 - e^{\alpha S_w}), \quad (7)$$

where α is a large negative number (ALPHARXN in the PREBRAG input files), and S_{wick} is the wicking parameter (SATWICK in the PREBRAG input files). The wicking parameter is multiplied by the $(1 - e^{\alpha S_w})$ term so that the effective saturation smoothly approaches zero as S_w approaches zero.

In BRAGFLO Version 6.0, equation (7) has been replaced with,

$$S_{eff} = S_w - S_{min} + S_{wick} (1 - \text{Exp}(200\alpha(\text{Max}(S_w - S_{min}, 0))^2)). \quad (8)$$

Equation (8) mimics equation (7) except that S_{eff} now goes to zero as S_w approaches S_{min} . The factor of 200 in the exponential function was chosen to make the difference between equation (7) and equation (8) small away from $S_{eff} = 0$. The term $(\text{Max}(S_w - S_{min}, 0))^2$ insures that the value and first derivative of S_{eff} are continuous around $S_{eff} = 0$. The parameter S_{min} enters BRAGFLO through the input file and, for now, is hard coded in the PREBRAG input files = 0.015 (1.5 % saturation) as that is the initial waste-area saturation,

SOCMIN=1.5000E-02,

which can be seen in the *REACTION_CHEMISTRY section of the PREBRAG input files. The smoothing of the wicking term is turned on in the PREBRAG input files,

NUMERICS, SMOOTH=ON

as can be seen in the *REACTION_CHEMISTRY section of the PREBRAG input files titled BF1_CRA09_Sx.inp, where x = 1,...,6. These files can be found in the CMS library LIBCRA09_BF.

5.2.3 Chemical Rate Smoothing and Tapering

As described in Subsection 4.13.6 of the BRAGFLO Version 6.0 user's manual (Nemer 2006), and in BRAGFLO Version 6.0 smoothing is performed on the total (inundated+hydrated) rates of all chemical reactions,

$$K_{smoothed} = K [1 - Exp(\alpha C / C_i)], \quad (9)$$

where K is the unsmoothed rate of a reaction described in Subsections 4.13.3 - 4.13.5 of the BRAGFLO user's manual (Nemer 2006), C is the concentration of the species being produced (or destroyed) by the reactions described above in Subsection 5.2.1, C_i is an initial concentration of a relevant compound, and α is a large negative number as described in Subsection 5.2.2. For all iron reactions the initial concentration of iron is used for C_i . For all biodegradation reactions the initial concentration of cellulose is used for C_i . This smoothing prevents a discontinuity in the first derivative of the rates when a reaction runs out of a reactant (other than water which is handled by equation (8)). The concentration based smoothing is turned on in the PREBRAG input files,

```
NUMERICS, CONC_SMOOTH=ON
```

as can be seen in the *REACTION_CHEMISTRY section of the PREBRAG input files titled BF1_CRA09_Sx.inp, where $x = 1, \dots, 6$. These files can be found in the CMS library LIBCRA09_BF.

5.2.4 Solids Production and Consumption

In BRAGFLO Version 6.0 the volume of solids produced (or consumed) from the chemical reactions are calculated. In Version 6.0 and the CRA-2009 PA this quantity is used only for post processing and does not affect the results in any way. The total volume of solids produced (or consumed) normalized by cell volume is calculated from the concentrations of species 3 through 9 in

Table 5-7 minus the initial concentrations, and the concentration of salt produced by dehydrating brine,

$$\Delta V = \sum_{i=1}^9 \Delta V_i, \quad (10)$$

where

$$\Delta V_i = (C_{i,t} - C_{0,i}) / DEN(i), \quad (11)$$

$C_{i,t}$ is the concentration of species i at time t (kg/m^3), $C_{0,i}$ is the initial concentration of species i , and $DEN(i)$ the density of species i (kg/m^3). The index and identity of the species in this subroutine is given in Table 5-16. These densities are parameters in the WIPP PA Parameter database and are given below in Table 5-17.

Table 5-16. Index and corresponding compound in density array DEN

Index	Compound
1	Fe
2	Fe(OH) ₂
3	FeS
4	cellulosics
5	MgO
6	Mg(OH) ₂
7	MgCO ₃
8	Salts

Table 5-17. Density Parameters Created for the CRA-2009 PA.

Name	Description	Value (kg/m ³)
REFCON:DN_FE	Density of Iron	7,870
REFCON:DN_FEOH2	Density of Iron Hydroxide	3,400
REFCON:DN_FES	Density of Iron Sulfide	4,700
REFCON:DN_CELL	Density of Cellulosics Materials for BRAGFLO	1,100
REFCON:DN_MGO	Density of Magnesium Oxide	3,600
REFCON:DN_MGOH2	Density of Magnesium Hydroxide	2,370
REFCON:DN_MGCO3	Density of Magnesium Carbonate	3,050
REFCON:DN_SALT	Density of Salts for BRAGFLO	2,180

5.2.5 Implicit and Explicit Reaction Rates

In BRAGFLO Version 5.0, the chemical reaction rates were based on the total initial mass of reactants present in the entire repository, they were not calculated on a cell by cell initial mass basis. The code was written this way because concentrations of reactants were spread evenly throughout the waste-filled regions of the repository. In BRAGFLO Version 6.0, we have added the capability of having cell by cell initial concentrations, and rates that correspond to cell by cell initial concentrations. This is controlled by the following PREBRAG input line,

```
INTRINSIC=INTRIN, &
```

which is under the *REACTION_CHEMISTRY section of the input file. The above value indicates that we are not using this feature, i.e. the way in which BRAGFLO calculates rates is unchanged from BRAGFLO Version 5.0 and the CRA-2004 PABC.

5.2.6 Additional Chemistry Parameters

The inclusion of the MgO hydration reaction required parameters to calculate the amount of MgO present, and the rate of the MgO hydration reaction which are shown in Table 5-18. Furthermore, the additional species from the additional reactions also require supplementary molecular weights, as shown in Table 5-19. Given that for the CRA-2009 PA, the additional reactions are deactivated, the parameters in Table 5-18 and Table 5-19 had no impact on the results. The amount of MgO remaining at 10,000 years (ALGEBRA2 variable MGO_REM) in all vectors, all scenarios, all replicates was equal to 1.

These additional reactions may be used in future calculations if deemed appropriate, but is mentioned here only to comprehensively describe the changes implemented in BRAGFLO version 6.0.

Table 5-18. MgO Parameters to be Created for the CRA-2009 PA.

Name	Description	Value
WAS_AREA:MGO_EF	MgO Excess Factor: ratio of MgO to organic carbon in CPR	1.2
WAS_AREA:BRUCITEH	MgO humid hydration rate	8.9860E-02 (mol/kg/s)
WAS_AREA:BRUCITEC	MgO inundated hydration rate in ERDA-6 brine	8.7911E-02 (mol/kg/s)
WAS_AREA:BRUCITES	MgO inundated hydration rate in GWB brine	8.4314E-02 (mol/kg/s)

Table 5-19. Additional Molecular Weight Parameters to be Created for the CRA-2009 PA.

Name	Description	Value (kg/mol)
REFCON:MW_FEOH2	Molecular Weight of Iron Hydroxide	8.9860E-02
REFCON:MW_FES	Molecular Weight of Iron Sulfide	8.7911E-02
REFCON:MW_MGO	Molecular Weight of Magnesium Oxide	4.0304E-02
REFCON:MW_MGOH2	Molecular Weight of Magnesium Hydroxide	5.8320E-02
REFCON:MW_MGCO3	Molecular Wight of Magnesium Carbonate	8.4314E-02

5.2.7 Capillary Pressure and Relative Permeability Model in Open Cavities

As discussed in Subsection 4.9 of the BRAGFLO Version 6.0 user's manual (Nemer 2006), in BRAGFLO Version 5.00 an inconsistency occurred during the -5 to 0 year operational period during which BRAGFLO is run. During this period the operational areas were modeled as open-completely-saturated ($S_w = 1$) cavities with porosity equal to 1. In the CRA-2004 PABC the model used (RELP_MOD=4) had zero capillary pressure, but still included capillary pressure effects on the relative permeability model. It's clear that the now-open areas of the WIPP repository are not completely saturated and do not have significant capillary pressure effects on pressure or permeability. A modified model for the relative permeabilities has been added with (RELP_MOD = 11) to remove capillary-pressure effects from the relative permeabilities for open cavities. In this model the relative permeabilites decrease from 1 to zero linearly between the residual saturations (brine and gas) and the residual saturation plus a tolerance,

$$k_{rel} = 0 \quad \text{for } S < S_r, \quad (12)$$

$$k_{rel} = \frac{(S - S_r)}{tol} \quad \text{for } S_r \leq S \leq S_r + tol, \quad (13)$$

$$k_{rel} = 1 \quad \text{for } S > S_r + tol, \quad (14)$$

where k_{rel} is the relative permeability, S is saturation (brine or gas), S_r is the residual saturation (brine or gas) and tol is a tolerance over which the relative permeability changes linearly from zero to 1. For now, tol is hard coded in the PREBRAG input files (BF1_CRA09_Sx.INP, where $x = 1, \dots, 6$, see LIBCRA09_BF in CMS) equal to 10^{-2} , i.e.

PERM, TOL=1.0E-2,

in the *PROPERTIES block of the input file.

Because of numerical difficulties, capillary pressure has been turned off in the waste-filled areas of the BRAGFLO grid for $t = 0$ to 10,000 years since the CCA. Thus for $t > 0$, modified models have no impact on the results of the CRA-2009 PA.

5.2.8 Borehole Reset

In BRAGFLO Version 6.0, a new subroutine RESETMID has been added which resets the saturation, pressure, and concentrations in a material at the time of a material change. This routine was designed for the Borehole material at the time of an intrusion but can be used on other materials as well. The input parameters for this subroutine are set in the PREBRAG input file (BF1_CRA09_Sx.INP, $x = 1, \dots, 6$). For example in BF1_CRA09_S2.INP (PREBRAG input file for scenario 2), under the *RESET section the input file contains the following lines,

```
BORERESET, NTIME=4, NUM=2, MATERIAL=BH_OPEN, CONC_PLG, &  
PRES_BRIN=-1.0, SAT_BRIN=-1.0, ICHEM=1
```

which means that the borehole and the concrete plug are to be reset at material change number 4 (550 years in Scenario 2, see Subsection 6.4.1) pressure and saturation are unchanged, but concentrations of Fe and CPR in those cells are set to zero. The above PREBRAG lines were added for code development purposes, they have little impact on the results. The only impact is that the Fe and CPR are removed from the borehole at 550 years. The time at which the Fe and CPR were removed from the borehole (550 years), is incorrect. It should be 350 years, which is the time of intrusion. We expect that this error had no impact on the results because the amount of CPR and Fe in the borehole is small and because the difference in time (200 years) is small compared to the 10,000 year regulatory period. In future PA's the Fe and CPR will be removed from the borehole at 350 years.

5.2.9 PREBRAG and POSTBRAG

The code PREBRAG has changed substantially in order to accommodate the new features in BRAGFLO version 6.0. These changes are primarily in receiving new parameters and outputting them to the BRAGFLO input file, which is discussed fully in the PREBRAG Version 8.00 user's manual (Gilkey and Rudeen 2007). However two more substantial changes have been made and are discussed in the following two paragraphs.

In PREBRAG Version 7.00, the saturations, iron concentrations, and CPR concentrations were uniformly applied to all waste cells from a master set of input parameters. That is, the cell by cell initial values of these parameters set in the ICSET code were ignored. This is acceptable if all waste areas have the same initial conditions, but doesn't allow cell-by-cell initial conditions. PREBRAG Version 8.00 now respects the initial values for saturations, iron and CPR concentrations obtained from the cell by cell values in the CDB file, set by ICSET.

In PREBRAG Version 7.00 chemical rates were modified in PREBRAG to obtain units suitable for BRAGFLO, which added an additional less-transparent step to the calculation process. In PREBRAG Version 8.00, the rates RKCOR and RKBIO that are placed in the CDB file from the ALGEBRA1 step are what go into the BRAGFLO input file, without additional calculations. In this manner all calculation steps are now documented in the ALGEBRA1 input file, ALG1_BF_CRA09_Rx.INP, x = 1,...,3 for Replicates R1 to R3.

In building BRAGFLO Version 6.0, a bug was discovered in POSTBRAG 4.00. The bug was in the sizing of dynamic memory arrays which affected output when the number of variables output grew large. This bug is discussed in Software Problem Report SPR 07-001 (Nemer 2007). The repaired version of POSTBRAG is 4.00A (Nemer 2007).

6 MODELING RESULTS

The parameter values (distributions for sampled parameters) used for the Salado Flow Analysis are stored in the WIPP PAPDB, which is accessible on line. The results of Salado Flow Analysis are stored in binary (.CDB) files that reside in CMS library LIBCRA09_BFRrSs, where $r = 1,2,3$, and $s = 1,2,\dots,6$. The CMS class for these files is CRA09-0. These results include detailed and summarized information about:

- Creep closure of the excavated areas of the repository
- Gas generation by corrosion of metal and microbial consumption of organic material
- Pressure
- Fracturing of rock due to high pressure
- Permeability
- Brine and gas saturation
- Brine and gas flow

Other output may be selected by the user, but this may require adjustments to pre-processing steps. The Salado Flow output data are preserved for all cells and areas of the grid at incremental times between 0 and 10,000 years.

The application, ALGEBRACDB, is used to post-process numerical output from BRAGFLO resulting in data that are useful for analysis. This is performed in the ALG2 step. The output variables from ALGEBRACDB are listed in Appendix B. Graphics are used extensively to demonstrate observations, relationships, and dependencies. Plots using the application SPLAT, plot values of individual variables for all vectors in a scenario as a function of time for the entire 10,000-year regulatory compliance period. These plots are an effective method for demonstrating the potential range and behavior of results. “Composite” plots display the statistics for a replicate over time (e.g. median, mean, maximum and minimum over 100 vectors in a scenario at selected times). These plots are used to collectively view results for comparison purposes (e.g. comparing trends for two different output variables). The application PCCSRC is used to correlate output variables with sampled input parameters and to generate plots displaying the most prominent partial ranked correlation coefficients (PRCC) over time.

In the following subsections, results from the CRA-2009 PA are often compared to results from the CRA-2004 PABC. The results of the CRA-2004 PABC Salado Flow Analysis are stored in binary (.CDB) files that reside in CMS library LIBCRA1BC_BFRrSs, where $r = 1,2,3$, and $s = 1,2,\dots,6$. The CMS class for these files is CRA1BC-0. File names can be found in Long and Kanney (2005).

6.1 EXCEPTION VECTORS

The ASCII input control file to BRAGFLO includes a series of input numerical control parameters that influence the way BRAGFLO performs calculations. The standard settings optimize calculations under most circumstances, but occasionally certain BRAGFLO vectors do not run to completion in the maximum number of timesteps (10,000) or encounter a fatal error.

These “exception vectors” must be rerun with modified inputs so that they will complete the 10,000 year simulation. Exception vectors usually result from the combination of extreme conditions of coincident sampled variables and/or very small grid cells (e.g., the intersection of the borehole or shaft with a marker bed). These circumstances can lead to extreme spatial or temporal gradients within the model that exceed the default tolerances specified in the input control file. These conditions cause BRAGFLO to shorten its time step. For most vectors this is sufficient to solve the short-lived numerical problem, however for some exception vectors it is necessary to relax, tighten, or otherwise adjust BRAGFLO input numerical control parameters in order to complete the calculations. In BRAGFLO Version 6.00, the effective saturation cut off described in Subsection 5.2.2 has eliminated many of the exception vectors that occurred when the repository became dry (see Subsection 6.1 of Nemer and Stein 2005) . However, in BRAGFLO Version 6.0 we did not add any smoothing to extremes in pressure which would help with many of the remaining exception vectors. This is a task for future versions of BRAGFLO.

The capability to make such adjustments is a normal part of any numerical modeling study including the BRAGFLO modeling process. The input control parameters are included in BRAGFLO software to permit the analyst to make adjustments for circumstances that fall outside of the typical range of modeling conditions and allow a difficult calculation to complete. Description of adjustments to input control parameters for exception vectors are included in the discussion of results for each replicate/scenario. Descriptions of the actual control parameters that were changed are discussed fully in the BRAGFLO user’s manual (see Subsection 7.27 in Nemer 2006). Briefly FTOLNORM(1) is the relative gas-saturation residual in the mass-balance equation; EPSNORM(1) is the number of digits to which the change in gas saturation is converged in the obtained solution to the mass-balance equation; ICONVTEST is a flag which decides whether the acceptable solution has both FTOLNORM and EPSNORM satisfied or whether it is acceptable to have a solution that satisfies either FTOLNORM or EPSNORM.

6.1.1 Replicate R1

In Replicate 1, BRAGFLO calculations for 15 simulations did not run to completion using standard input control values. The vectors and the changes made to their numerical parameters are listed in Table 6-1. The changes required for a successful run are indexed 1,...,3 in increasing severity, i.e. vector 46 required the greatest change and presumably has the greatest uncertainty. The meaning of this index is discussed below Table 6-1.

Table 6-1 Exception vectors, CRA-2009 PA Replicate R1

Vector	S1	S2	S3	S4	S5	S6
22			1	1		1
28	1	2	2	2	2	2
46	3	3	3	1	1	3

1 (in table) ftolnorm(1) changed from 10^{-2} to 10^{-1}

2 (in table) ftolnorm(1) changed from 10^{-2} to 10^{-1} and epsnorm(1) changed from 3 to 2

3 (in table) ICONVTEST changed from "1" to "0"

6.1.2 Replicate R2

Three simulations were rerun with modified input control parameters in order to have BRAGFLO complete the calculations. The vectors and the changes made to their

numerical parameters are listed in Table 6-2. The changes required for a successful run are indexed 1, ..., 3 in increasing severity, i.e. vector 95 required the greatest change and presumably has the greatest uncertainty. The meaning of this index is discussed below Table 6-2.

Table 6-2 Exception vectors, CRA-2009 PA Replicate R2

Vector	S1	S2	S3	S4	S5	S6
95		3				
99	1			1		

- 1 (in table) ftolnorm(1) changed from 10^{-2} to 10^{-1}
- 2 (in table) ftolnorm(1) changed from 10^{-2} to 10^{-1} and epsnorm(1) changed from 3 to 2
- 3 (in table) ICONVTEST changed from "1" to "0"

6.1.3 Replicate R3

Seven simulations were rerun with modified input control parameters in order to have BRAGFLO complete the calculations. The vectors and the changes made to their numerical parameters are listed in Table 6-3. The changes required for a successful run are indexed 1, ..., 3 in increasing severity, i.e. vector 71 required the greatest change and presumably has the greatest uncertainty. The meaning of this index is discussed below Table 6-3.

Table 6-3 Exception vectors, CRA-2009 PA Replicate R3

Vector	S1	S2	S3	S4	S5	S6
32	1	1				
35			2	2		2
71		3				
75			2			

- 1 (in table) ftolnorm(1) changed from 10^{-2} to 10^{-1}
- 2 (in table) epsnorm(1) changed from 3 to 2
- 3 (in table) ftolnorm(1) changed from 10^{-2} to 10^{-1} and epsnorm(1) changed from 3 to 2

6.2 OVERVIEW OF THE SALADO FLOW ANALYSIS

Repository behavior is characterized by interactions among creep closure, gas generation, and fluid and gas flow. The Salado Flow Analysis is divided into three replicates (R1, R2, R3), and each is comprised of the same six modeling scenarios. Replicate R1 is the primary subject for analysis, and the other two are used to confirm the results for the most important output variables and to demonstrate statistical confidence in the results. Each scenario consists of 100 vectors that are defined by a unique set of sampled input values.

6.2.1 Organization

The discussion of results is organized by scenario or pair of scenarios as follows:

- Subsection 6.3: Undisturbed (Scenario S1)

- Subsection 6.4: E2 drilling intrusion at 350 years (Scenario S2), E1 drilling intrusion at 350 years (Scenario S4).
- Subsection 6.5: Comparison of pressure, saturation, and brine flow away from the waste panel for all the Replicates, Scenario S1.

Subsections 6.3 and 6.4 include an analysis of the following:

- *Halite Creep*. Plastic flow of salt will cause the pore volume of the repository to decrease over time by gradually compressing the waste-filled rooms and filling the empty space.
- *Brine Inflow*. Availability of brine is required for gas generation and for fluid flow away from the repository.
- *Brine Saturation*. This affects the rate of corrosion of steel. This is also a primary output variable to subsequent PA analyses.
- *Gas Generation*. In some scenarios, gas generation results in high pressures within the repository.
- *Pressure*. High pressure within the repository can increase permeability of wall rock by causing hydro fracturing. This is a primary output variable to subsequent PA analyses.
- *Rock Fracturing*. Caused by high gas pressure. Rock fracturing can increase the porosity and permeability of the wall rock in the DRZ and of anhydrite in the marker beds providing a conduit for local brine migration (e.g., around the panel closures and into the shaft).
- *Brine Outflow*. Brine outflow through the Salado to the accessible environment is a potential pathway for radionuclide transport. Brine flow is a BRAGFLO output variable that is used as input to analyses of radionuclide flow and transport in the Salado and Culebra.

6.3 MODELING RESULTS FOR UNDISTURBED PERFORMANCE (R1S1)

Previous analyses (U.S. DOE 1996; SNL 1997; Helton, Bean et al. 1998; Hansen and Leigh 2002) have identified two potential pathways for brine flow and radionuclide transport away from the repository in the undisturbed scenario. In the first pathway, brine may migrate through the panel seals and drifts or through the disturbed rock zone (DRZ) surrounding the repository to the shaft and then upwards towards the Culebra Dolomite Member of the Rustler Formation. The quantity of brine reaching the Culebra is important, because transport then may occur laterally towards the subsurface land withdrawal boundary. In the second pathway, brine may migrate from the repository through the DRZ and laterally towards the subsurface land withdrawal boundary through the anhydrite interbeds of the Salado formation.

In addition, pressure and brine saturation in the undisturbed scenario are important variables because conditions in this scenario are used as input for other software used to calculate direct releases from the first intrusion into the repository. Subsequent intrusions look to conditions in the other disturbed scenarios.

6.3.1 Sequence of Events

In scenario 1, there is a change in lower shaft material at 200 years after closure. This change primarily represents the consolidation and recrystallization of the crushed salt portion of the shaft seal system that is expected during this time.

6.3.2 Halite Creep

Creep closure of the excavated regions begins immediately because of excavated-induced loading. As rooms close, waste consolidation will occur and continue until back stresses imposed by compressed waste resist further closure or until fluid pressures become sufficiently high due to gas generation. Room closure causes the pore volume (void space), of the waste filled regions of the repository to decrease over time.

BRAGFLO calculates the porosity of materials that undergo creep closure by interpolating over a “porosity surface.” The porosity surface gives porosity as a function of time and pressure, and was obtained by modeling deformation of a waste-filled room using the software SANTOS (Stone 1995; Park and Hansen 2003). Porosity is calculated by dividing the pore volume by total volume, and it can be expressed as a fraction or as pore volume percent of total volume.

The output variable, W_R_POR, is the volume-averaged porosity for all waste areas. Figure 6-1 compares plots of volume-averaged porosity in all waste-filled areas (W_R_POR) for the CRA-2009 and the CRA-2004 PABC. The statistics are quite similar, and are summarized in Table 6-4.

Table 6-4. Statistical comparison of volume averaged porosity in all waste-filled areas at 10,000 years in Replicate R1, Scenario S1 for the CRA-2009 PA and the CRA-2004 PABC. W_R_POR is a variable calculated in the ALG2 post-processing step (see Table 4-1 and Appendix B).

W_R_POR (dimensionless)	CRA-2009 PA	CRA-2004 PABC
Minimum	1.07E-01	1.12E-01
Average	1.64E-01	1.64E-01
Maximum	2.41E-01	2.24E-01

6.3.3 Brine Inflow

The ALG2 (see Table 4-1, Appendix B) output variable, BRNREPTC, includes all brine that flows into the repository. Figure 6-2 compares plots of BRNREPTC from the CRA-2009 PA and the CRA-2004 PABC. Figure 6-3 shows plots of brine volume in the waste areas versus time from the CRA-2009 PA and the CRA-2004 PABC. The average and maximum brine inflow are larger in the CRA-2009 PA compared to the CRA-2004 PABC. This is because of the

increased porosity in the DRZ (as discussed in Subsection 5.1.2), which is assumed to be completely saturated. The increase in brine inflow follows the increase in DRZ porosity.

Table 6-5. Statistical comparison of total cumulative brine inflow at 10,000 years for Replicate R1, Scenario S1 for the CRA-2009 PA and the CRA-2004 PABC. BRNREPTC is an output variable calculated in the ALG2 post-processing step (see Table 4-1 and Appendix B).

BRNREPTC (m ³)	CRA-2009 PA	CRA-2004 PABC
Minimum	367	346
Average	16403	10050
Maximum	73344	45063

In the undisturbed scenario, S1, brine can only come in contact with the waste by flowing through or from the DRZ. The only significant potential external source of brine to the DRZ is from the anhydrite marker beds or from in situ brine within the DRZ. The permeability of undisturbed halite is too low to permit significant migration of brine. The CRA-2009 PA analysis described in the following two paragraphs corroborates the results of the CRA-2009 PA that brine inflow comes primarily from the DRZ.

The sampled input parameter halite porosity, HALPOR (see Table 4-2), determines how much brine is available in the DRZ for each vector. A scatter plot of HALPOR versus BRNREPTC at 10,000 years, Figure 6-4 and Figure 6-5, shows that vectors with high brine inflow have high HALPOR values for the CRA-2009 PA and the CRA-2004 PABC respectively. Permeability also influences brine inflow, but there are no vectors with high brine inflow that do not have relatively high HALPOR values.

The ALG2 (see Table 4-1) output variable, BRAALIC, is the cumulative total brine inflow from all marker beds into the DRZ. A scatter plot of BRAALIC versus BRNREPTC at 10,000 years shown in Figure 6-6 and Figure 6-7 for the CRA-2009 PA and the CRA-2004 PABC indicates no significant relationship between the two brine flows. In fact, brine flow from the marker beds into the DRZ (BRAALIC) appears to be about the same regardless of whether brine flow into the repository (BRNREPTC) is relatively high or low. This means that brine outside of the DRZ is not a major contributor to brine flow into the repository, which is coming almost entirely from the DRZ. Brine flow from the marker beds is not a significant contributor to brine in the repository.

6.3.4 Brine Saturation

Brine saturation is an important result of the BRAGFLO model, because (1) gas generation processes require the availability of brine to proceed and (2) Direct Brine Releases, which are modeled in another PA activity, depend on the brine saturation in the waste regions calculated by BRAGFLO. Figure 6-8 compares plots of brine saturation in the waste panel for the CRA-2009 PA and the CRA-2004 PABC. The patterns are similar, but the CRA-2009 PA has more vectors with saturation greater than 60 %, which is due to the increased DRZ porosity. Table 6-6 contains a statistical comparison of brine saturation in the waste panel (ALG2 output variable WAS_SATB) at 10,000 years for the CRA-2009 PA, the CRA-2004 PABC. The average and maximum values are similar. The minimum is greater in the CRA-2009 PA due to the effective

saturation cut off which prevents chemical reactions from completely drying out the repository (see Subsection 5.2.2).

Table 6-6. Volume-averaged brine saturation at 10,000 years in the waste panel for Replicate R1, Scenario S1 for the CRA-2009 PA, and the CRA-2004 PABC. WAS_SATB is calculated in the ALG2 post-processing step (see Table 4-1 and Appendix B).

WAS_SATB (dimensionless)	CRA-2009 PA	CRA-2004 PABC
Minimum	1.39E-02	1.01E-06
Average	1.21E-01	8.13E-02
Maximum	9.59E-01	9.59E-01

Statistics for volume-averaged brine saturation in different regions of the repository are summarized in Table 6-7 - Table 6-8, for the CRA-2009 PA and the CRA-2004 PABC. The Waste Panel has the widest range of volume-averaged brine saturation at 10,000 years (Figure 6-8) ranging from a low of 0.014 to a high of 0.96 (Table 6-7). Higher brine saturation in the Waste Panel than the RoR areas is due to the direct proximity of the Waste Panel to the markerbeds and the isolation of the RoR areas by the Option D panel closures. Many vectors show a sharp increase in brine saturation during the first 500 years followed by slowly declining brine saturation to 10,000 years (Figure 6-8).

Table 6-7. Volume-averaged brine saturation at 10,000 years in different areas of WIPP for Replicate R1, Scenario S1 for the CRA-2009 PA. These brine saturations were calculated in the ALG2 post processing step (see Table 4-1 and Appendix B).

	Brine saturation (dimensionless)	Min	Avg	Max
Waste Panel	WAS_SATB	1.39E-02	1.21E-01	9.59E-01
RoR South	SRR_SATB	1.26E-02	5.87E-02	4.31E-01
RoR North	NRR_SATB	1.26E-02	5.90E-02	4.26E-01
Operations Area	OPS_SATB	4.59E-02	6.42E-01	1.00E+00
Experimental Area	EXP_SATB	0.00E+00	8.00E-02	8.14E-01

Table 6-8. Volume-averaged brine saturation at 10,000 years in different areas of WIPP for Replicate R1, Scenario S1 for the CRA-2004 PABC. These brine saturations were calculated in the ALG2 post processing step (see Table 4-1 and Appendix B).

	Brine saturation (dimensionless)	Min	Avg	Max
Waste Panel	WAS_SATB	1.01E-06	8.13E-02	9.59E-01
RoR South	SRR_SATB	1.19E-07	1.80E-02	2.56E-01
RoR North	NRR_SATB	5.96E-08	1.83E-02	2.59E-01
Operations Area	OPS_SATB	1.91E-02	4.34E-01	1.00E+00
Experimental Area	EXP_SATB	9.97E-03	9.53E-02	8.02E-01

The Operations area (OPS_SATB) has the highest average brine saturations according to Table 6-7 and Table 6-8. The waste-filled and non-waste areas are separated by Option D panel closures, which impede the transfer of brine.

Sensitivity analysis for BRAGFLO is complicated by the coupled, non-linear processes that are modeled. Generally the results of sensitivity analysis indicate which input parameters are most important for average performance, but often they will not explain anomalous modeling results. For example, the relationship between brine saturation and pressure changes as a function of pressure. At low pressures, which occur dominantly in early years of the model, there is a positive correlation between brine saturation and pressure, because increases in saturation accelerate the rate of gas generation, which results in increasing pressure. However, at higher pressures, which develop as a consequence of gas generation, the correlation decreases and becomes negative, because increasing pressure tends to impede brine inflow and eventually, high pressure drives brine out of the repository thereby reducing brine saturation.

When all 100 vectors are used to evaluate Waste Area brine saturation dependencies on sampled input parameters, the PRCC's plotted in Figure 6-9 and Figure 6-10 for the CRA-2009 PA and the CRA-2004 PABC reflect a mixture of results from high and low pressure regimes. At 10,000 years, the high-pressure regime dominates. Consequently, Waste Area brine saturation has prominent PRCC's with the gas generation factors (e.g. DRZPRM, WGRCOR, HALPOR, and WASTWICK, see Table 4-2 for a description of these parameters).

Brine saturation in the Waste Panel has a high positive PRCC with the permeability of the DRZ, DRZPRM, and with the porosity of halite, HALPOR (see Table 4-2), because together these two input parameters determine how much brine can enter the repository at relatively low pressure. At high pressure DRZPRM determines how much brine can be forced out of the repository. Higher values of halite porosity result in more water being available in the DRZ for release to the repository, and higher permeability in the DRZ provides less resistance for brine flow into the repository. There is a moderate positive correlation with ANHPRM, especially at long times, indicating that some brine does enter the repository from the marker beds. There are moderate negative correlations to the gas generation factors for the corrosion rate of steel WGRCOR (see Table 4-2), because corrosion generates gas and consumes brine. The weaker negative correlation with the wicking input parameter WASTWICK (see Table 4-2), the increase in effective brine saturation of waste due to capillary forces, is due to the increase in pressure associated with higher wicking factors. As discussed above, brine is forced out of the repository at higher pressures.

6.3.5 Gas Generation

Gas generation and brine/gas flow are coupled processes. Because moisture is required for both corrosion and microbial gas generation processes (and it is consumed by the corrosion of steel), the rate of brine inflow into the repository affects the total rate of gas generation. Brine inflow decreases as pressure increases, and brine may eventually be expelled from the repository if pressure exceeds brine pressure in the surrounding formation. This may result in the slowing or even stopping of gas generation in some vectors. Gas may flow away from the waste into areas with lower pressure, which may include the northern experimental and operations areas, the DRZ, the anhydrite interbeds and the shaft. Gas flow into intact halite is not significant because of the high threshold pressure of halite.

There are two potential sources for gas generation in the Salado Flow Model.

The corrosion of steel, in the presence of brine, generates hydrogen gas in the model, and microbial degradation of organic material in the waste, including cellulose, plastic, and rubber may yield N₂, H₂S, and CO₂. However, all gas is assumed to have hydrogen properties in BRAGFLO, which maximizes the pressure per mole of gas generated (i.e. hydrogen is nearly an ideal gas at standard temperature and pressure). The carbon dioxide produced by microbial degradation is assumed to be sequestered by MgO and is thus not released into the repository (See Subsections 4.1 – 4.4 of Nemer and Zelinski 2005).

6.3.5.1 Gas Generation by Corrosion

Gas generation by corrosion (Figure 6-11) continues until all steel or all brine is consumed (Figure 6-12). Gas generation by corrosion declines rapidly after a few thousand years, but it continues at a relatively slow rate in many vectors to the end of 10,000 years (Figure 6-11). Cumulative gas generated by corrosion is not generally limited by the availability of steel (Figure 6-12) since at least 4% of the steel remains in all vectors at 10,000 years. However, steel inventory in certain grid cells may be depleted before 10,000 years. Brine availability is the limiting factor for gas generation by corrosion for many vectors (Figure 6-13 - Figure 6-14).

Statistics of gas generation for the CRA-2009 PA and the CRA-2004 PABC are given below in Table 6-9. The differences between the two analyses are modest. The minimum moles of gas in the CRA-2009 PA is lower than the CRA-2004 PABC. This is due to the effective-saturation cut off, as discussed in Subsection 5.2.2. The remaining statistics are higher in the CRA-2009 than the CRA-2004 PABC due to the increased DRZ porosity (Subsection 5.1.2) and the emplacement CPR materials (Subsection 5.1.1).

Table 6-9. Gas generation statistics at 10,000 years for Replicate R1, Scenario S1 for the CRA-2009 PA and the CRA-2004 PABC. The values in the table were calculated in the ALG2 post processing step (see Table 4-1 and Appendix B).

	CRA-2009 PA	CRA-2004 PABC
FE_MOLE^{1,4} (moles)		
Minimum	3.28E+07	3.40E+07
Average	3.37E+08	2.99E+08
Maximum	8.87E+08	8.16E+08
CELL_MOL^{2,4} (moles)		
Minimum	1.45E+05	2.34E+05
Average	1.15E+08	1.14E+08
Maximum	5.23E+08	4.93E+08
GAS_MOLE^{3,4} (moles)		
Minimum	1.41E+08	1.58E+08
Average	4.52E+08	4.13E+08
Maximum	1.34E+09	1.06E+09

1. Here FE_MOLE is the amount of gas (moles) produced by iron corrosion.
2. CELL_MOL is the amount of gas (moles) produced by microbial gas generation.
3. GAS_MOLE is the total amount of gas (moles) produced.
4. Note that the average GAS_MOLE is the sum of the average FE_MOLE and CELL_MOL, but the minimum and maximum typically correspond to different vectors and thus for different quantities and thus don't sum to the respective GAS_MOLE maximum or minimum.

As shown in Figure 6-13 - Figure 6-14, the porosity of halite HALPOR is the most important input parameter influencing corrosion. As discussed in Subsection 6.3.3, higher values of HALPOR means that more brine is available to flow into the repository from the DRZ.

6.3.5.2 Gas Generation by Microbial Activity

Figure 6-15 shows the cumulative amount (in moles) of gas generated by microbial consumption of cellulose or CPR (depending on the value of WAS_AREA:PROBDEG, see Subsection 5.4 of Nemer and Stein 2005) versus time. Microbial gas generation requires the presence of some brine, and it continues at the humid rate at very low brine-saturation values. However microbial gas generation ceases completely when brine saturation reaches the effective-saturation cut off (see Subsection 5.2.2). As shown in Figure 6-16, several vectors in Scenario 1 show that microbial degradation has all but stopped before all decomposable organic material (which we call cellulosics) is consumed. This occurs because brine saturation has dropped to levels at the effective-saturation cut off. Consumable organic material survives to the end of the 10,000-year regulatory period for these vectors.

Figure 6-17 - Figure 6-18 show the five most prominent correlations of microbial gas generation to sampled input parameters for the CRA-2009 PA and the CRA-2004 PABC. The greatest positive correlation is with W BIOGENF (WAS_AREA:BIOGENFC) which is the scaling factor that is multiplied by the sampled gas-generation rates. In the CRA-2009 PA the second largest correlation is with WMICDLF (WAS_AREA:PROBDEG) which influences the amount of CPR that is available and thus the rate of CO₂ production (see Nemer et al.2005). This is in contrast to the CRA-2004 PABC where the second largest positive correlation was with WGRMICI (WAS_AREA:GRATMICI), which is the inundated gas-generation rate. This change is most probably a result of the changes to the way in which the humid rate is sampled (see Subsection 5.1.3).

6.3.5.3 Total Gas Generation

Figure 6-19 shows the total cumulative gas generation obtained by combining gas generation due to corrosion and gas generation due to microbial degradation. Figure 6-22 - Figure 6-23 show the cumulative amount of gas generated versus time averaged over 100 vectors for corrosion, microbial, and total, for the CRA-2009 PA and the CRA-2004 PABC. On average, iron corrosion generates ~ 3 times as much gas as microbial gas generation.

Figure 6-20 - Figure 6-21 present the most prominent PRCC's for total cumulative gas generation with sampled input parameters for the CRA-2009 PA and the CRA-2004 PABC. Notable is HALPOR which, as described in Subsection 6.3.3 controls brine availability.

6.3.6 Pressure

Pressure within the repository is particularly important to WIPP PA because the release mechanisms Spallings and DBR are quite sensitive to this variable. In addition, pressure strongly influences the extent to which contaminated brine can migrate from the repository into

the marker beds or up the shaft to the Culebra. As shown in Figure 6-24, and Table 6-10 pressures are similar in the CRA-2009 PA and the CRA-2004 PABC.

Table 6-10. Pressure in the waste panel at 10,000 years for Replicate R1, Scenario S1 for the CRA-2009 PA and CRA-2004 PABC. The output variable WAS_PRES is calculated in the ALG2 post processing step (see Table 4-1 and Appendix B).

WAS_PRES (Pa)	CRA-2009 PA	CRA-2004 PABC
Minimum	5.85E+06	6.18E+06
Average	1.01E+07	9.95E+06
Maximum	1.63E+07	1.55E+07

PCCR's for volume averaged pressure in the Waste Area are shown in Figure 6-25 - Figure 6-26, for the CRA-2009 PA and the CRA-2004 PABC. The strongest positive correlation after around two thousand years is with HALPOR (halite permeability). Brine is consumed by corrosion and is required for microbial gas generation.

6.3.7 Rock Fracturing

If pressures in the DRZ or in the anhydrite marker beds exceed the initial pressure in these materials by 0.2 MPa, BRAGFLO treats the material as being fractured and increases the porosity and permeability of the material according to the fracture model described in the BRAGFLO users manual (See Subsection 4.10 in Nemer 2006). Figure 6-27 through Figure 6-33 show fracture length in the anhydrite marker beds versus time. Fracture length is arbitrarily defined in this analysis as the length of marker bed from the repository to the exterior edge of the furthest grid cell where the permeability has doubled from its initial value. Significant fracturing does not occur in all vectors. Looking at Figure 6-27 through Figure 6-33, the fracturing length is generally higher in the CRA-2009 PA compared to the CRA-2004 PABC. The CRA-2009 PA fracture lengths are similar to those from the CRA-2004 PABC.

Vector 53 of S1 has a particularly large but transient fracture length that begins around 2000 years, shown in Figure 6-31. This occurred because the initial anhydrite permeability in this vector was the largest of all vectors in this scenario and replicate and because the pressure in this vector was higher than vectors with similar anhydrite permeabilities in the CRA-2004. When looking at Figure 6-31, one should remember that the fracture model in BRAGFLO allows fractures to propagate indefinitely, as if the marker beds were perfectly laminar sheets, and that fracture length was arbitrarily defined as the distance over which permeability increased by a factor of 2. Figure 6-32 shows the fracture length in marker bed AB north of the repository for vector 53 along with pressure in the experimental area, for the CRA-2009 PA and the CRA-2004 PABC. The main difference between the two analyses is the total pressure, which is ~ 1 % higher in the CRA-2009 PA than the CRA-2004 PABC. Clearly the current BRAGFLO fracture model is sensitive to exceedingly small changes in pressure. Regardless of the larger fracture length, the net brine flow to the Land Withdrawal Boundary did not change significantly, as shown in Subsection 6.3.8. This is because the large fractures are primarily driven by gas flows, and not brine.

The intact permeability enters the equation for the fractured permeability

$$k = k_i \left[\frac{\phi}{\phi_i} \right]^n, \quad (15)$$

where k is the fractured permeability, k_i is the intact permeability, ϕ is the porosity of the fractured material and ϕ_i is the porosity of the intact material at the fracture initiation pressure (See Subsection 4.10 in Nemer 2006).

6.3.8 Brine Outflow

Figure 6-34 shows total cumulative brine flow out of repository areas for the CRA-2009 PA and the CRA-2004 PABC. The amount of brine outflow is larger in the CRA-2009 PA than in the CRA-2004 PABC. Table 6-11 gives statistics for the CRA-2009 PA and the CRA-2004 PABC for cumulative brine outflow at 10,000 years.

Table 6-11. Statistics on cumulative brine flow out of the repository at 10,000 years for Replicate R1, Scenario S1 for the CRA-2009 PA and CRA-2004 PABC. BRNREPOC is an output variable calculated in the ALG2 post processing step (see Table 4-1 and Appendix B).

BRNREPOC (m ³)	CRA-2009 PA	CRA-2004 PABC
Minimum	1.39E+00	1.49E+00
Average	1.97E+03	7.16E+02
Maximum	3.17E+04	2.11E+04

Correlations of total cumulative brine flow away from the repository, BRNREPOC (an ALG2 output variable, see Table 4-1), are shown in Figure 6-35 - Figure 6-36. The strongest positive correlation is with the permeability of the DRZ. The second strongest positive correlation is with CONPRM, the permeability for concrete (see Table 4-2). The positive PRCC indicates that increased flow through concrete corresponds to increased outflow from the repository, because the brine can pass more quickly through internal barriers within the repository.

Figure 6-37 shows the cumulative brine flow to the Land Withdrawal Boundary (LWB); releases to the Culebra are negligible for scenario S1. In both the CRA-2009 PA and the CRA-2004 PABC only a few vectors had significant brine flow to the LWB. Table 6-12 gives statistics for cumulative brine flow at 10,000 years to the LWB, the results are similar.

Table 6-12. Statistics on cumulative brine flow to the LWB for Replicate R1, Scenario S1 for the CRA-2009 and CRA-2004 PABC. BRAALLWC is an output variable calculated in the ALG2 post processing step (see Table 4-1 and Appendix B).

BRAALLWC (m ³)	CRA-2009 PA	CRA-2004 PABC
Minimum	4.79E-05	4.96E-05
Average	1.79E+01	1.21E+01
Maximum	1.60E+03	1.21E+03

6.3.9 Figures for Section 6.3

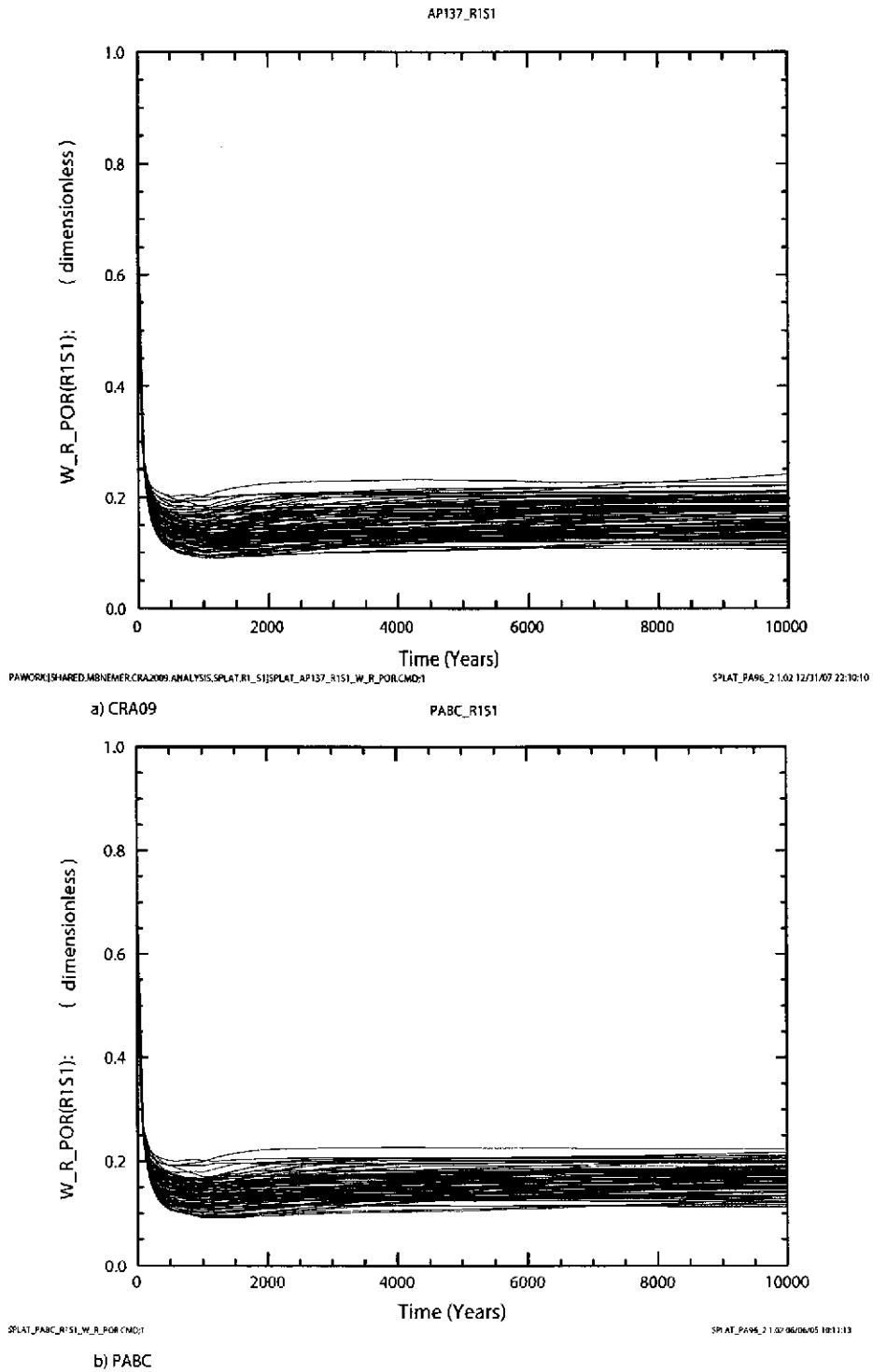
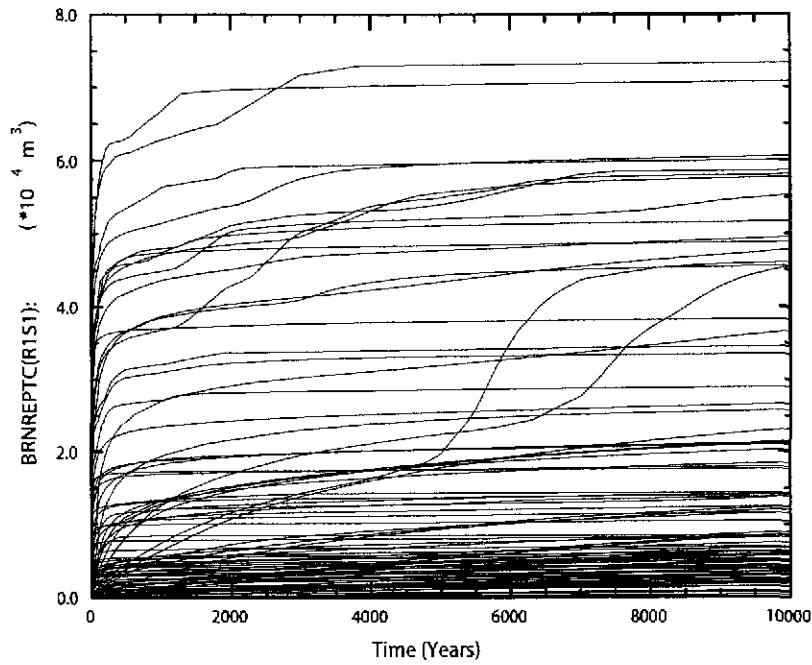


Figure 6-1. Volume averaged porosity (dimensionless) in all waste regions versus time (years) for all 100 vectors in Replicate R1, Scenario S1. Figure a) shows results from the CRA-2009 PA, figure b) shows results from the CRA-2004 PABC.

AP137_R151

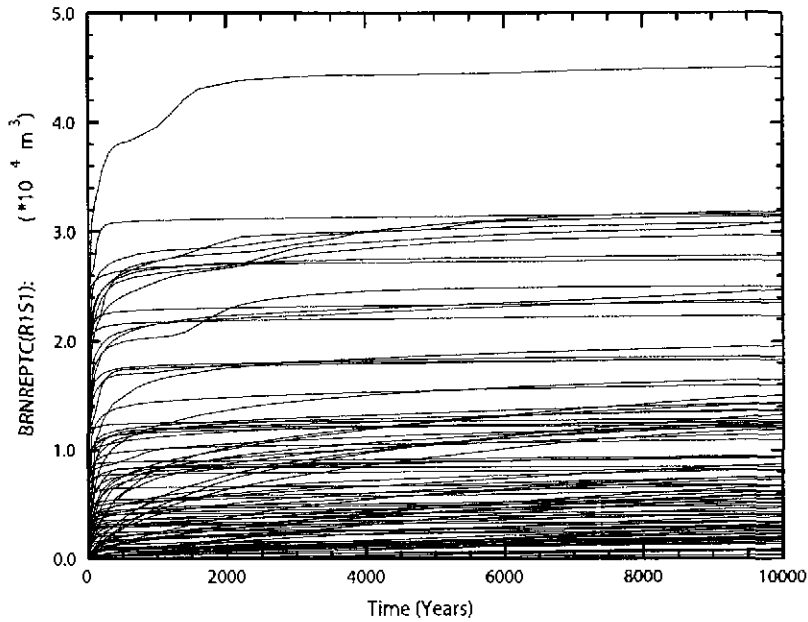


PAYDIR:\S1\ARC\EMERGENCY\ANALYSIS\SP1\AT_R1_S1\SP1AT_AP137_R151_BRNREPTC.D21

SP1AT_PAGE_2 1/2 1/201/07 23:31:50

a) CRA-09

PABC_R151

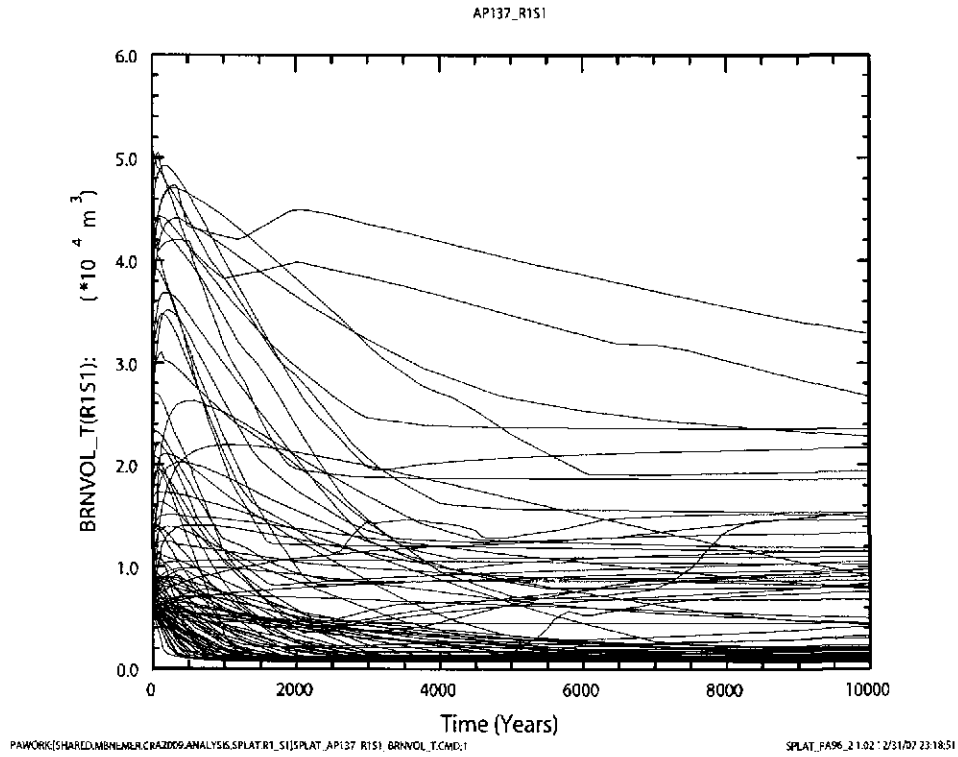


SP1AT_PABC_R151_BRNREPTC.D21

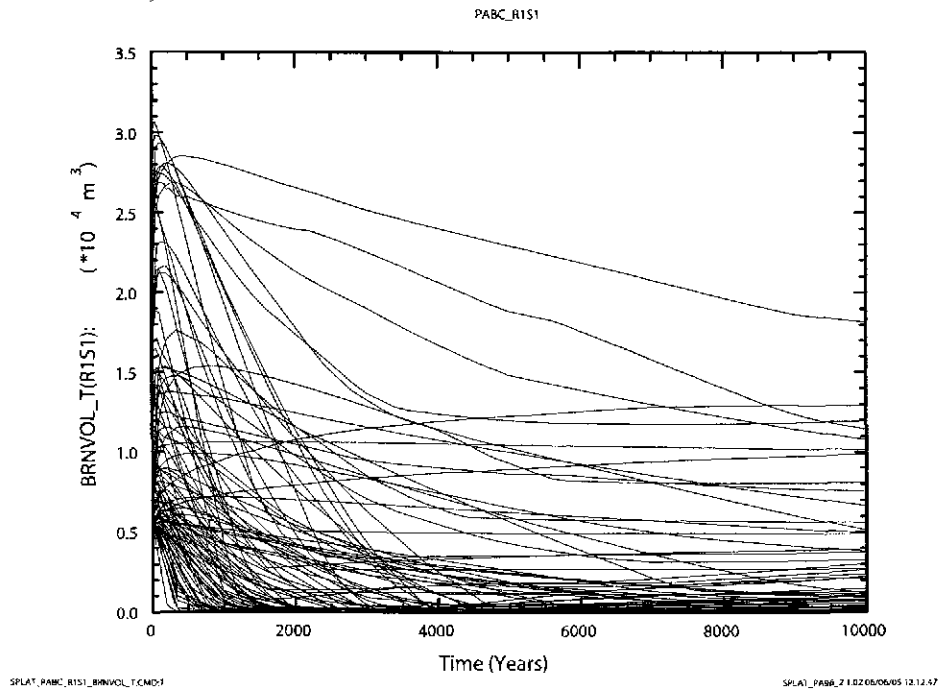
SP1AT_PAGE_2 1/2 06/26/05 12:19:38

b) PABC

Figure 6-2. Total cumulative inflow of brine (m³) into the repository versus time (years) for all 100 vectors in Replicate R1, Scenario S1. Figure a) shows results from the CRA-2009 PA Figure b) shows results from the CRA-2004 PABC.



a) CRA-09



b) PABC

Figure 6-3. Total brine volume (m^3) in all waste regions versus time (years) for all 100 vectors in Replicate R1, Scenario S1. Figure a) shows results from the CRA-2009 PA. Figure b) shows results from the CRA-2004 PABC.

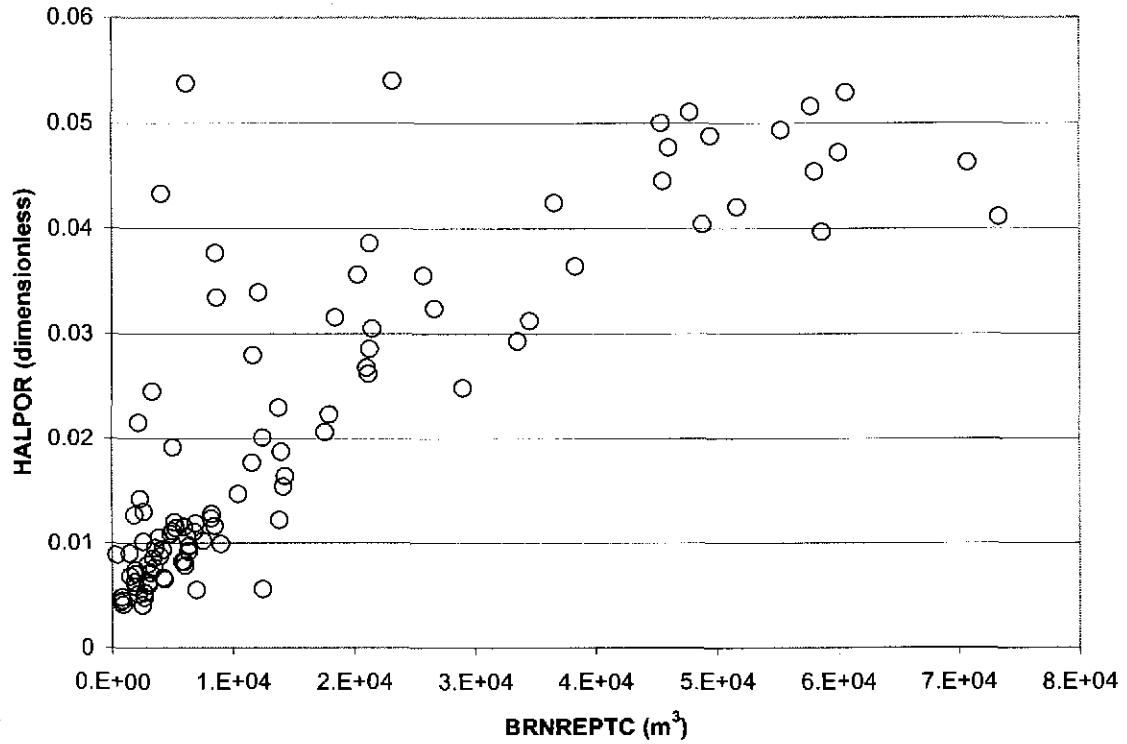


Figure 6-4. Scatter plot of halite porosity (dimensionless) versus cumulative brine inflow (m³) into the repository for all 100 vectors in Replicate R1, Scenario S1, CRA-2009 PA.

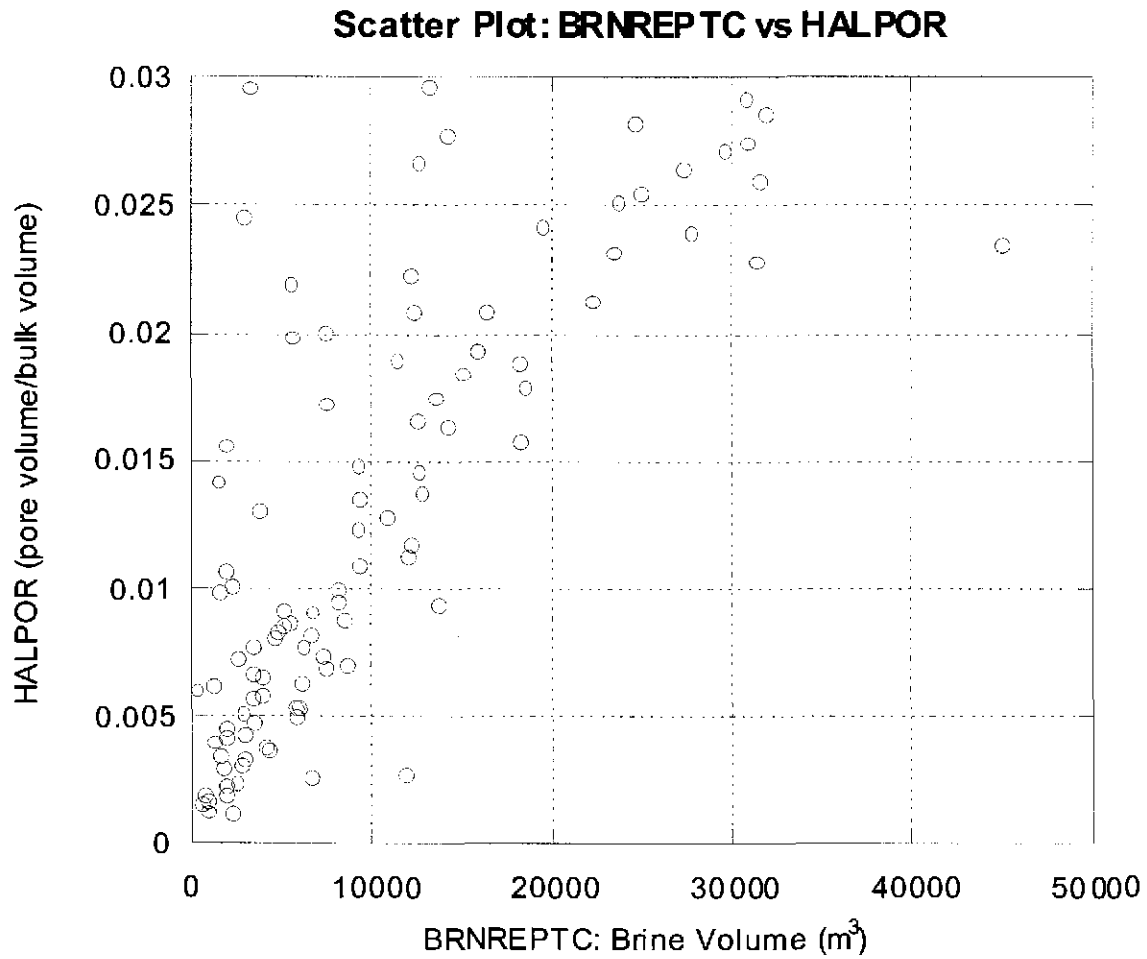


Figure 6-5. Scatter plot of halite porosity (dimensionless) versus cumulative brine inflow (m³) into the repository for all 100 vectors in Replicate R1, Scenario S1, CRA-2004 PABC.

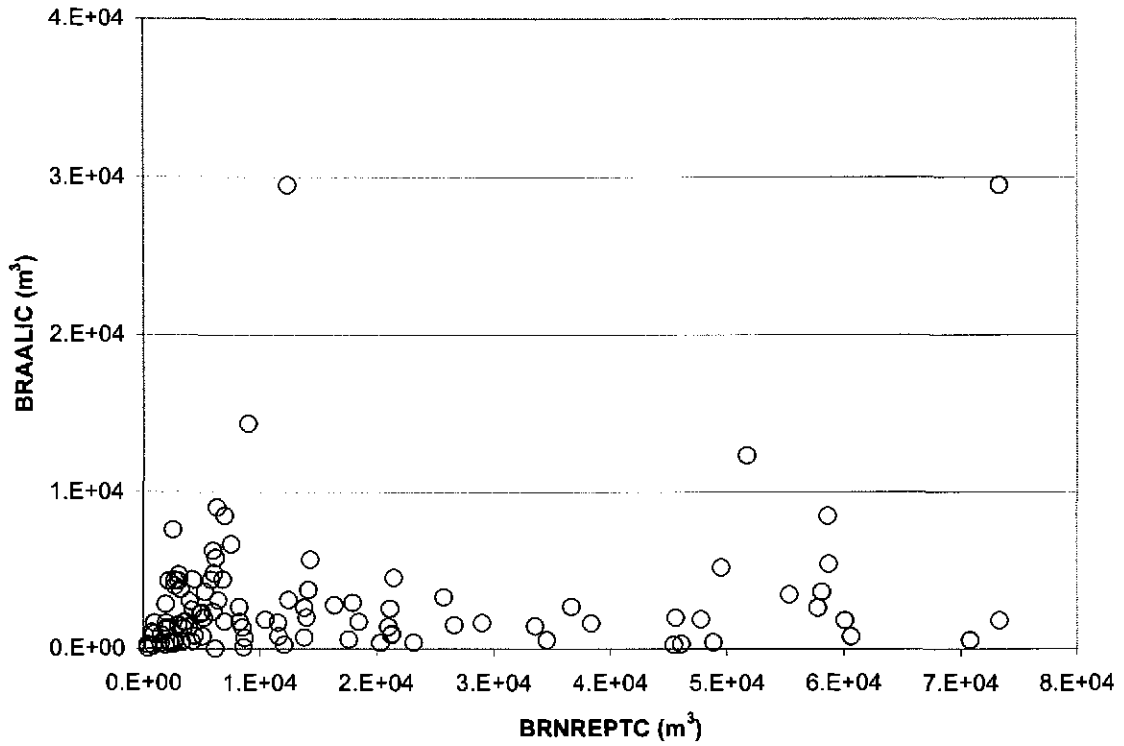


Figure 6-6. Scatter plot of total cumulative brine flow (m³) from the marker beds into the DRZ versus cumulative brine flow (m³) into the repository for all 100 vectors in Replicate R1, Scenario S1, CRA-2009 PA.

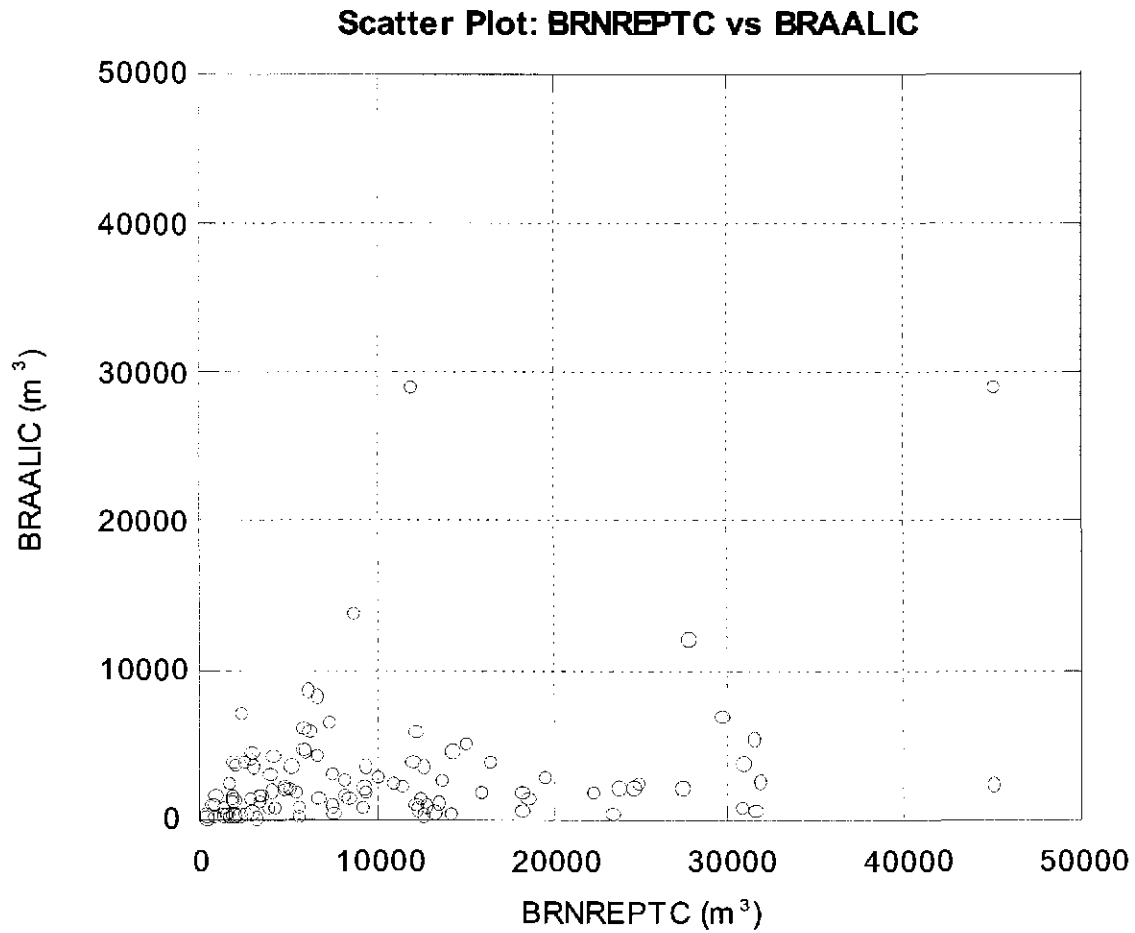
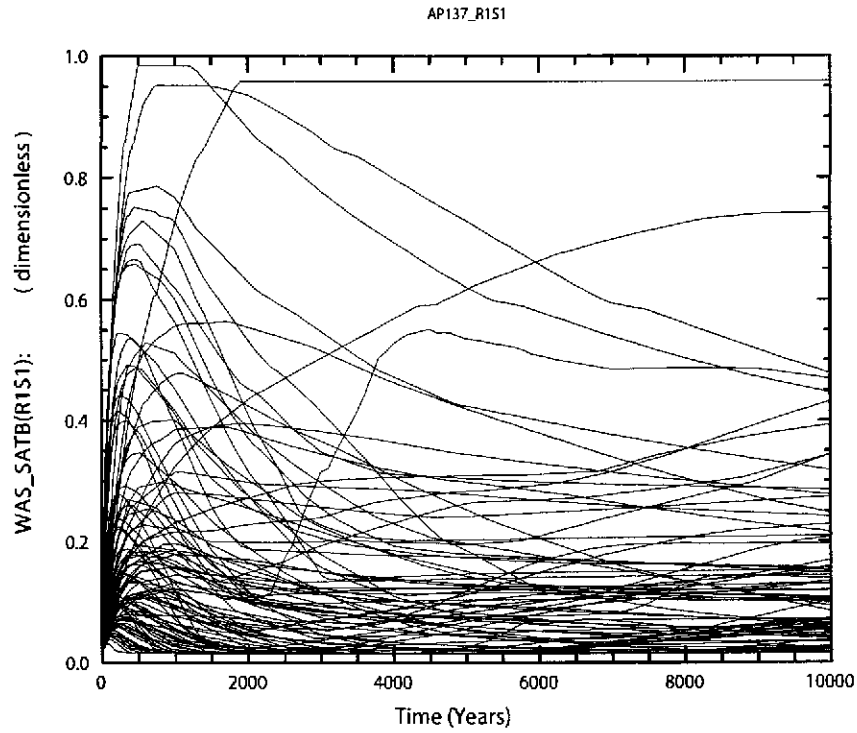
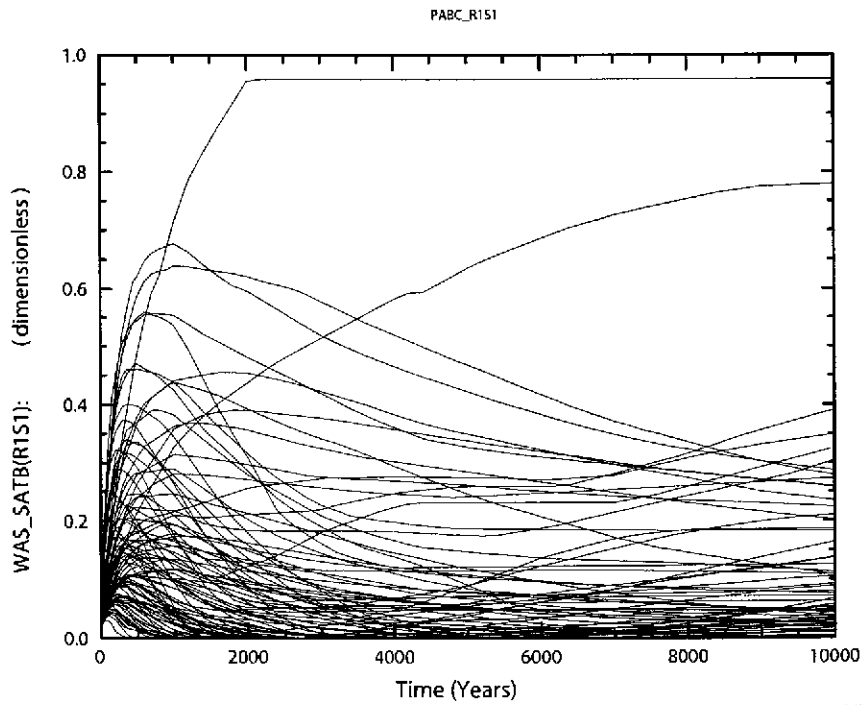


Figure 6-7. Scatter plot of total cumulative brine flow (m³) from the marker beds into the DRZ versus cumulative brine flow (m³) into the repository for all 100 vectors in Replicate R1, Scenario S1, CRA-2004 PABC.



a) CRA-09



b) PABC

Figure 6-8. Brine saturation (dimensionless) in the waste panel versus time (years) for all 100 vectors in Replicate R1, Scenario S1. Figure a) shows results from the CRA-2009 PA. Figure b) shows results from the CRA-2004 PABC.

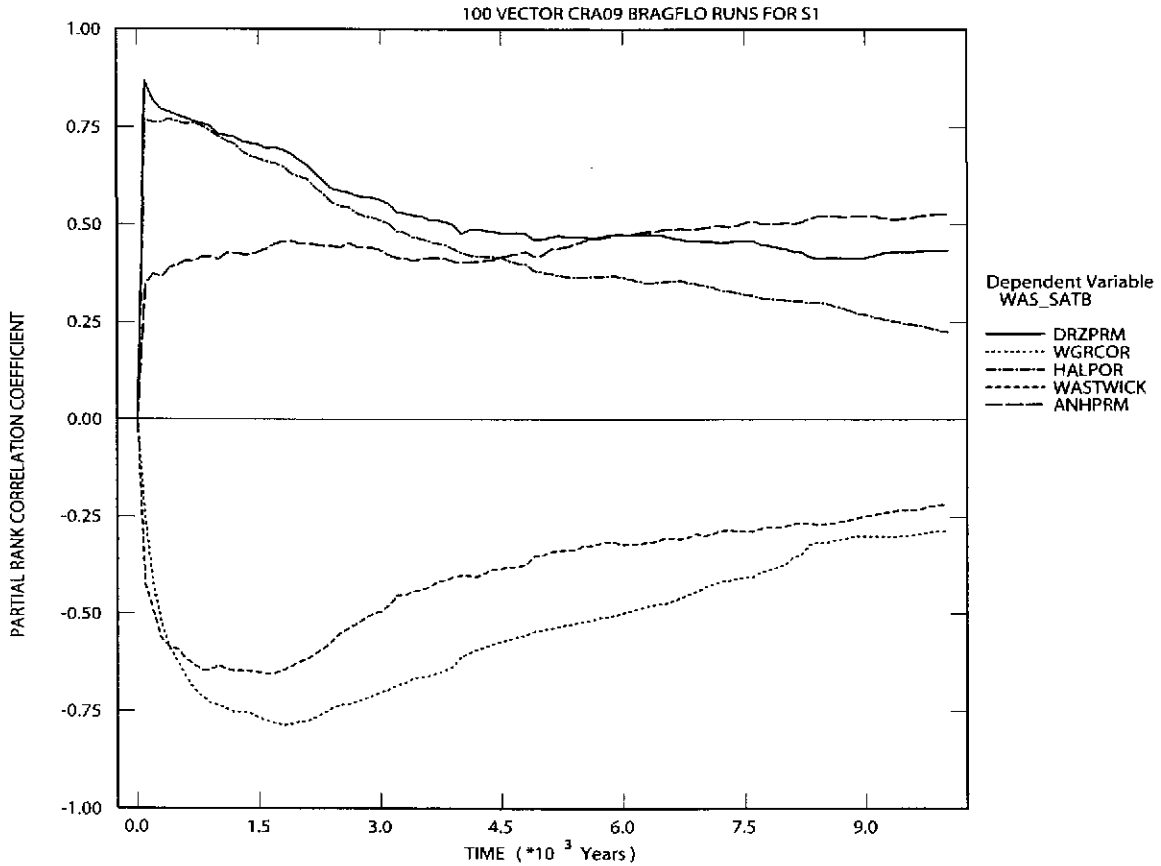


Figure 6-9. Primary correlations of brine saturation (dimensionless) in the waste panel with input parameters versus time (years), for Replicate R1, Scenario S1, CRA-2009 PA. Table 4-2 gives a description of the names in the legend.

Sensitivity Analysis for Brine Saturation in the Waste Panel CRA1BC BRAGFLO R1S1

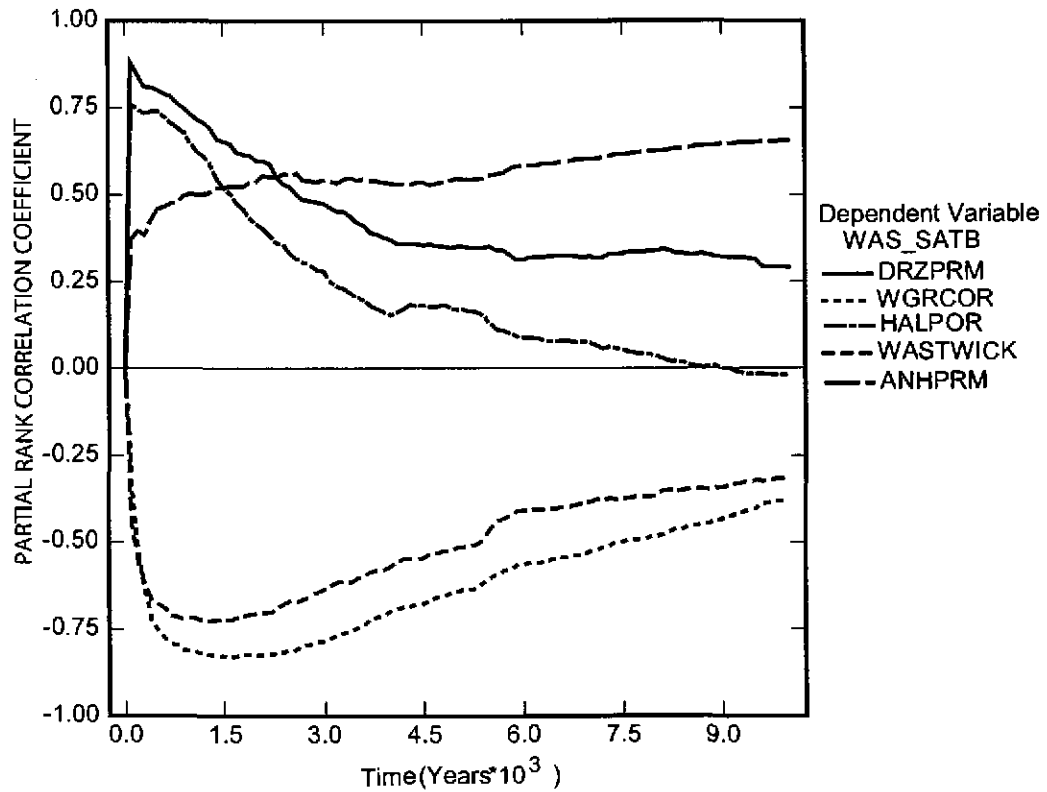
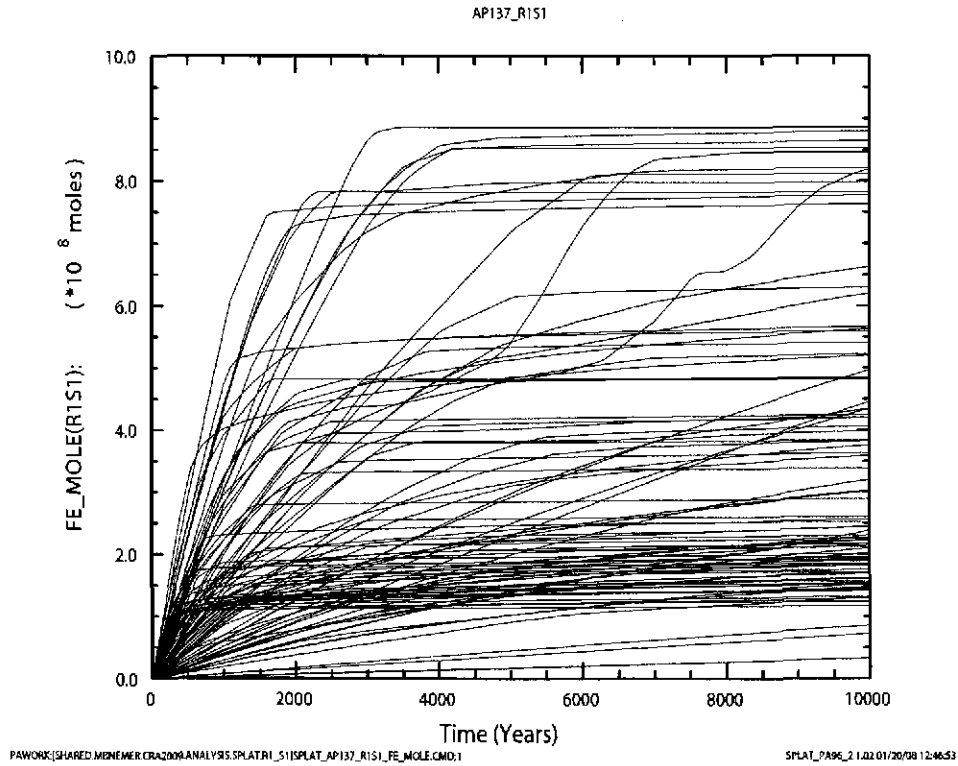
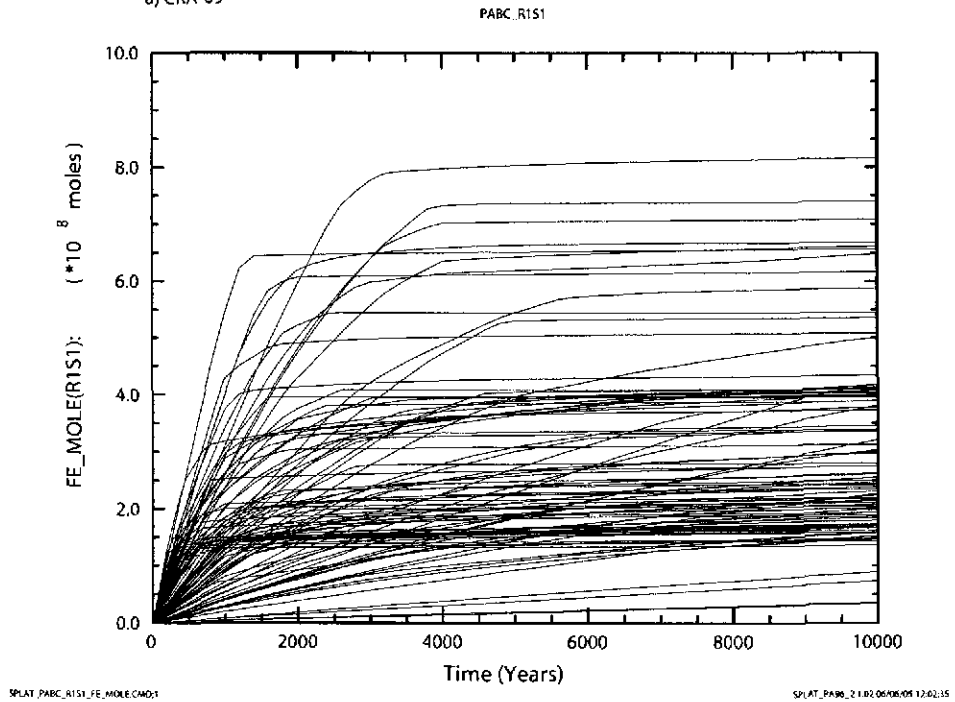


Figure 6-10. Primary correlations of brine saturation (dimensionless) in the waste panel with input parameters versus time (years), for Replicate R1, Scenario S1, CRA-2004 PABC. Table 4-2 gives a description of the names in the legend.

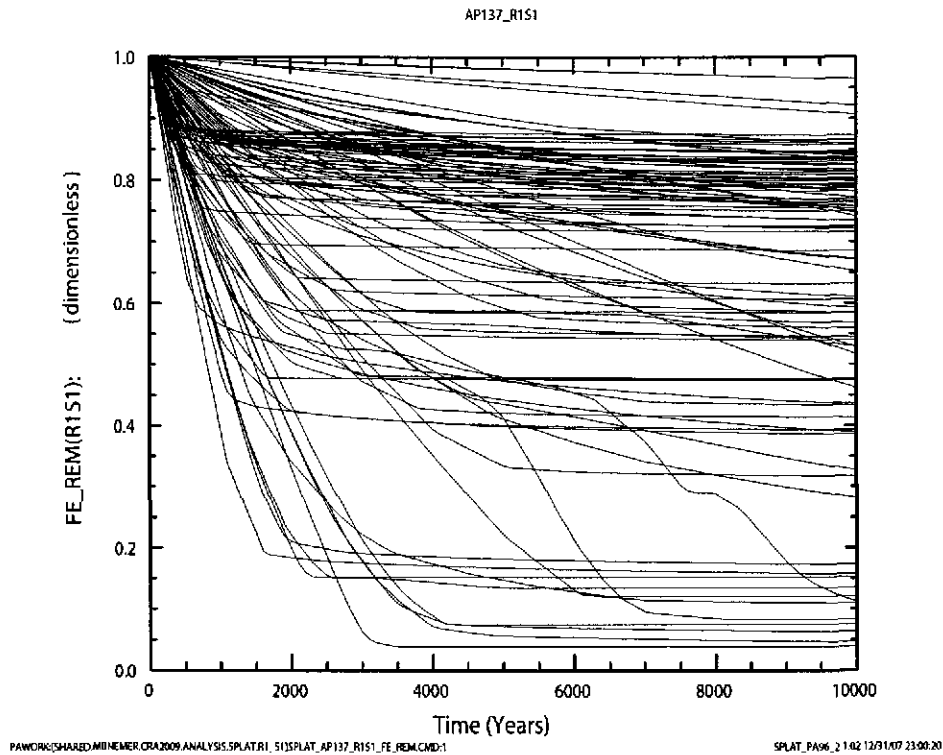


a) CRA-09

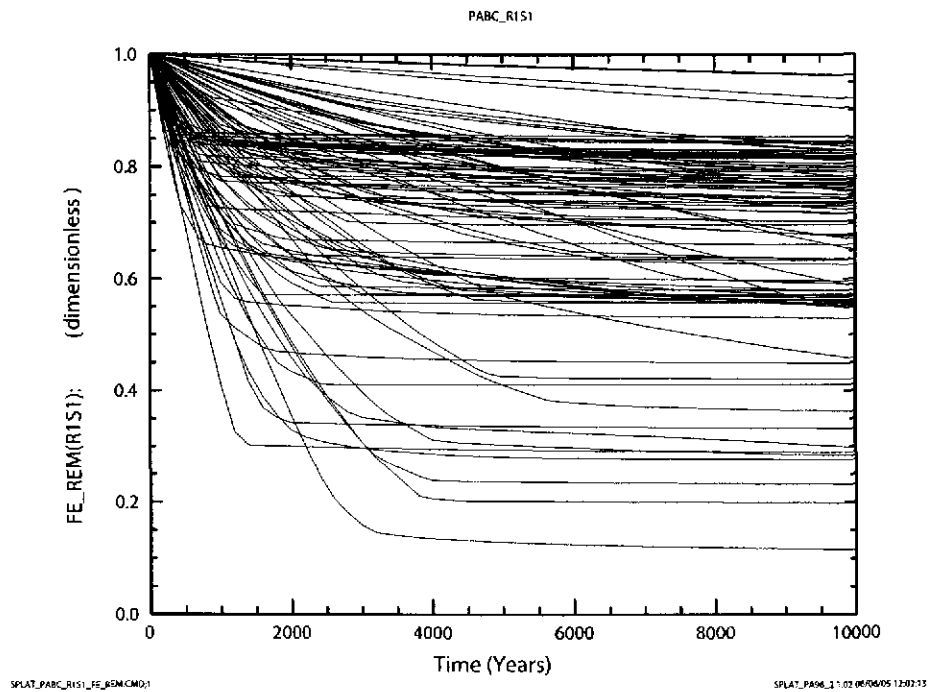


b) PABC

Figure 6-11. Cumulative gas generation (moles) by iron corrosion versus time (years) for all 100 vectors in Replicate R1, Scenario S1. Figure a) shows results from the CRA-2009 PA. Figure b) shows results from the CRA-2004 PABC.



a) CRA-09



b) PABC

Figure 6-12. Fraction of iron (dimensionless) remaining versus time (years) for all 100 vectors in Replicate R1, Scenario S1. Figure a) shows results from the CRA-2009 PA. Figure b) shows results from the CRA-2004 PABC.

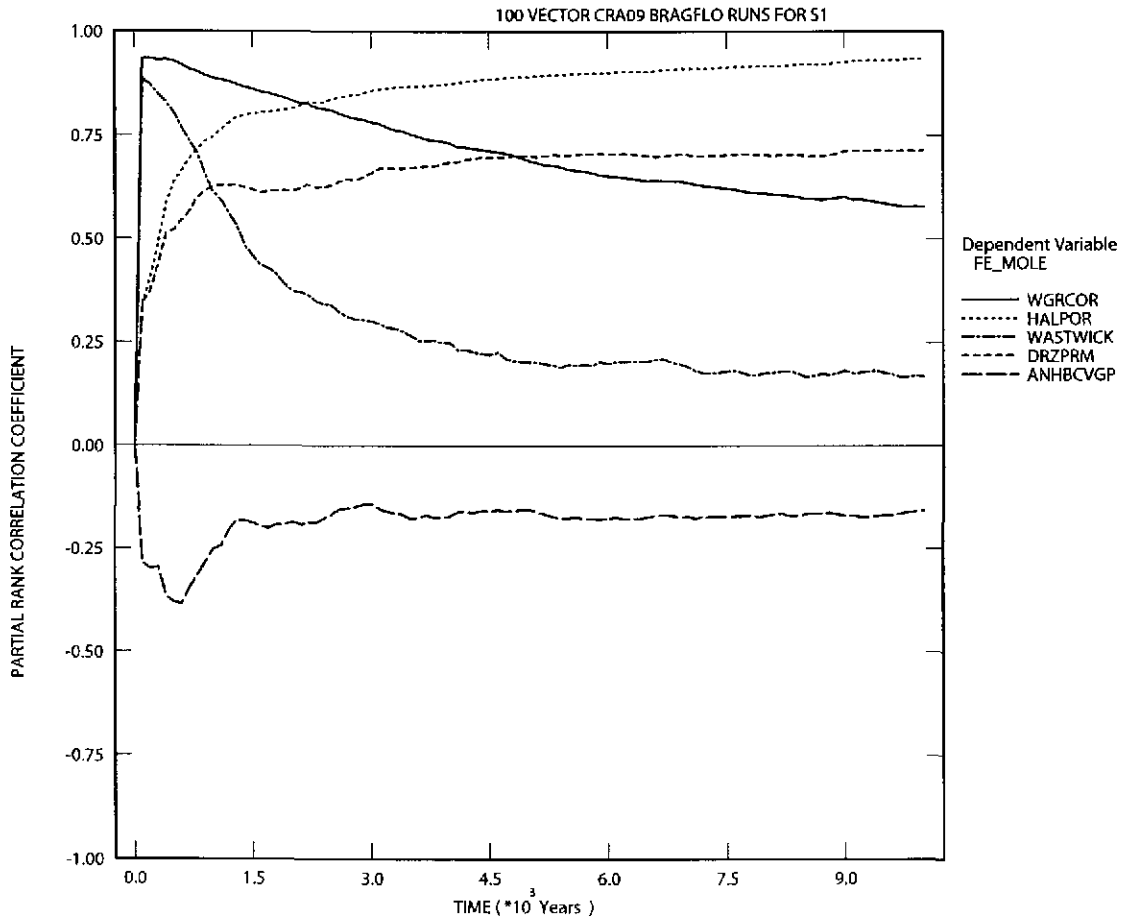


Figure 6-13. Primary correlations (dimensionless) of cumulative gas generation by corrosion with input parameters versus time (years) from the CRA-2009 PA, Replicate R1, Scenario S1. Table 4-2 gives a description of the names in the legend.

Sensitivity Analysis for Total Cumulative Gas Generation by Corrosion CRA1BC BRAGFLO R1S1

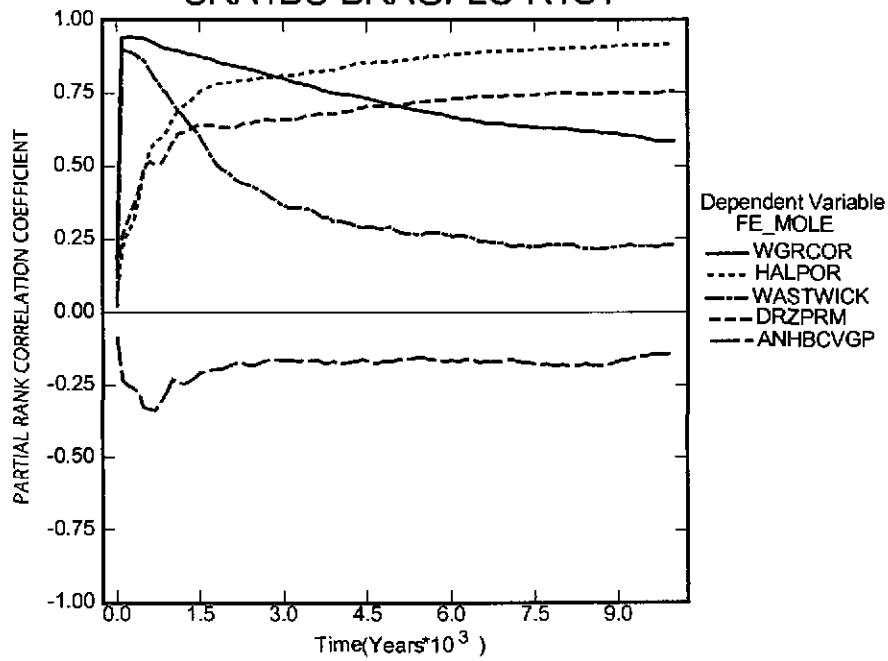
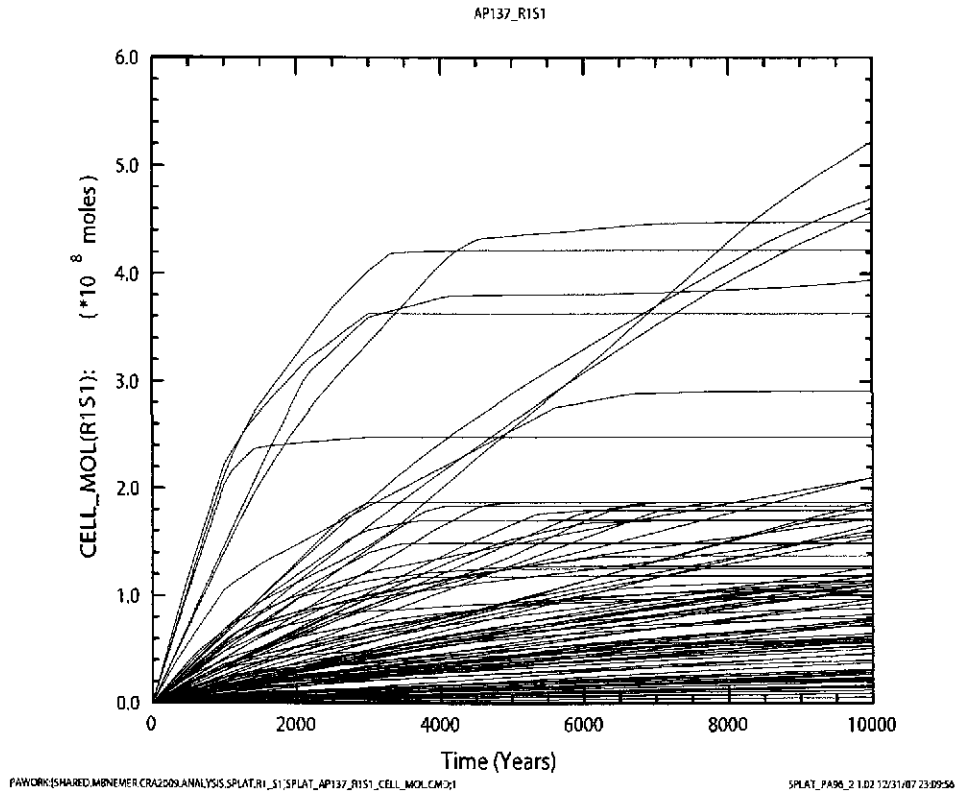
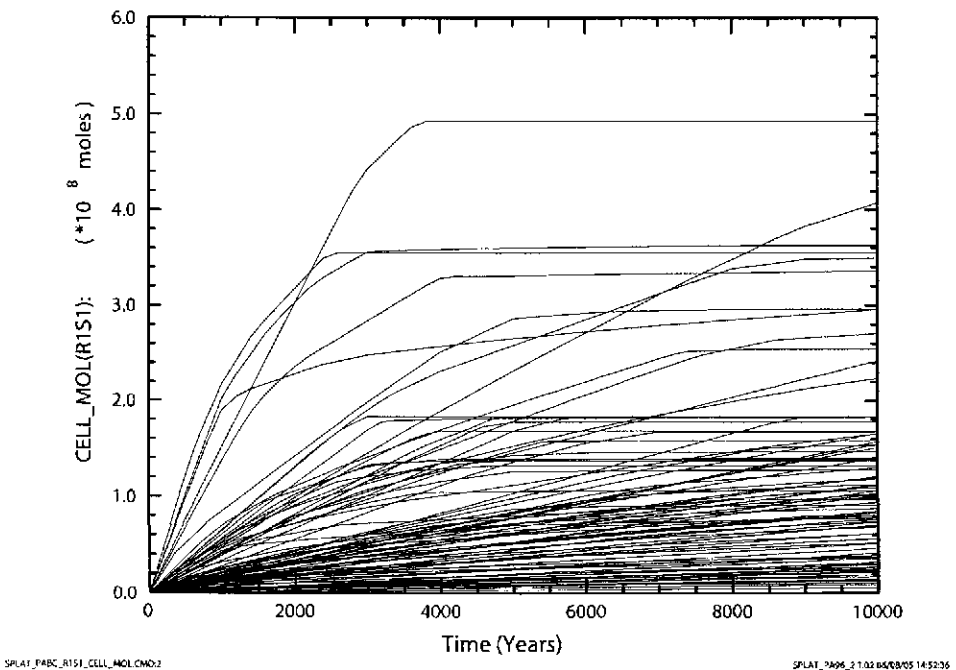


Figure 6-14. Primary correlations (dimensionless) of cumulative gas generation by corrosion with input parameters versus time (years) from the CRA-2004 PABC, Replicate R1, Scenario S1. Table 4-2 gives a description of the names in the legend.



a) CRA-09

PABC_R1S1



b) PABC

Figure 6-15. Cumulative gas generation (moles) due to microbial activity versus time (years) for all 100 vectors in Replicate R1, Scenario S1. Figure a) shows results from the CRA-2009 PA. Figure b) shows results from the CRA-2004 PABC.

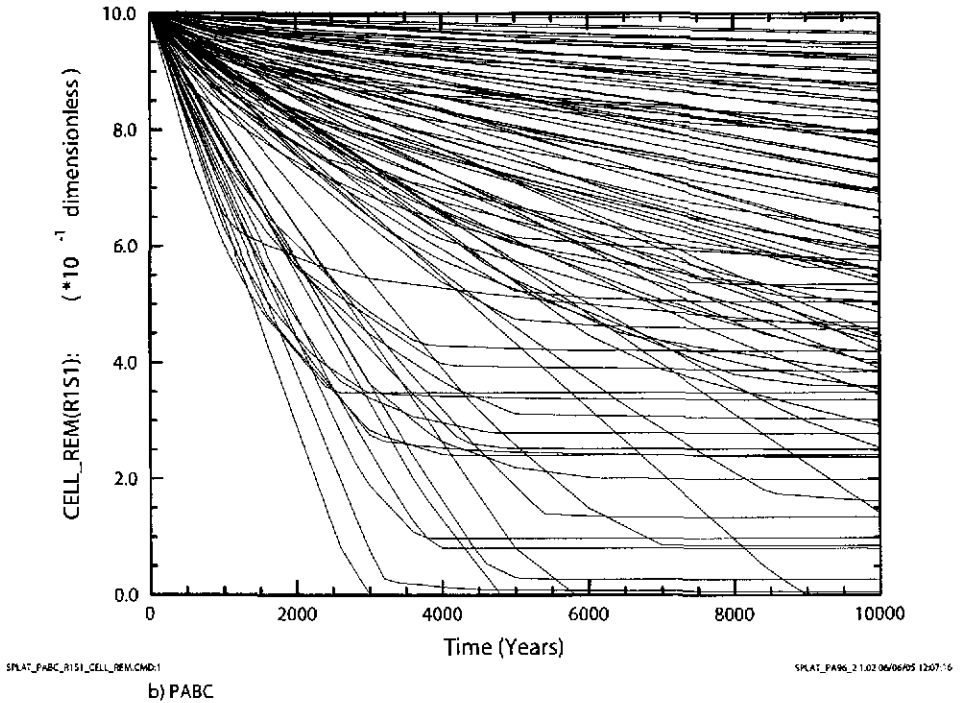
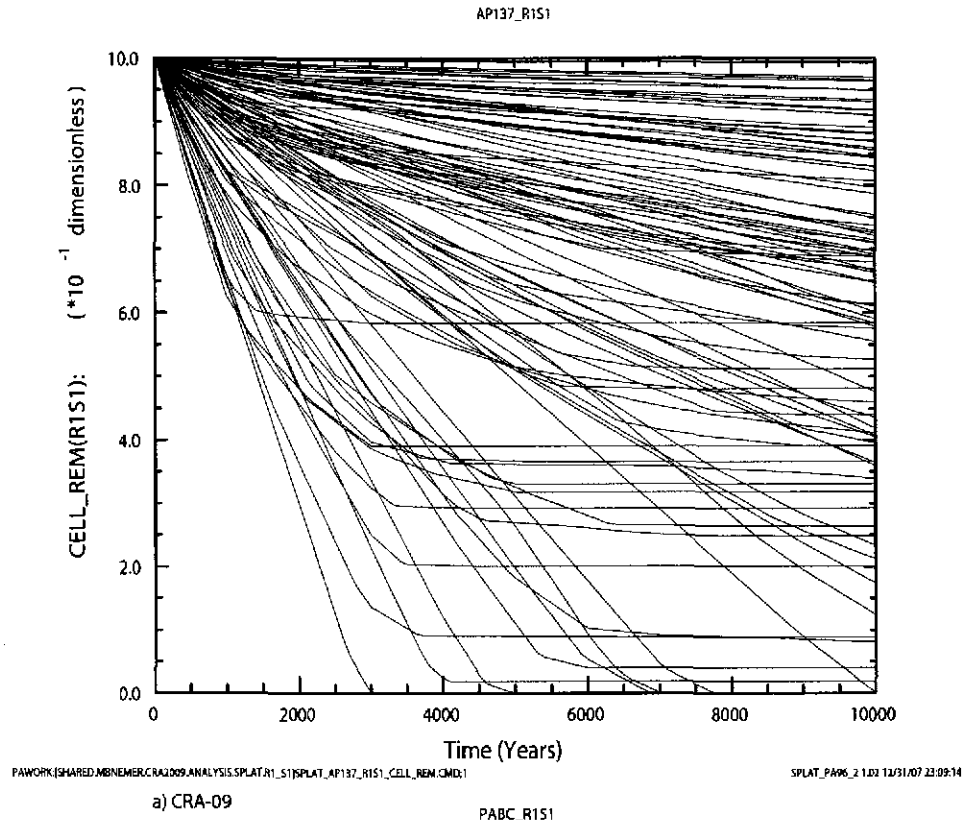


Figure 6-16. Remaining fraction of cellulose (dimensionless) versus time (years) for all 100 vectors in Replicate R1, Scenario S1. The remaining fraction of cellulose is either cellulose or CPR depending on the value of WAS_AREA:PROBDEG (see Subsection 5.1.1). Figure a) shows results from the CRA-2009 PA. Figure b) shows results from the CRA-2004 PABC.

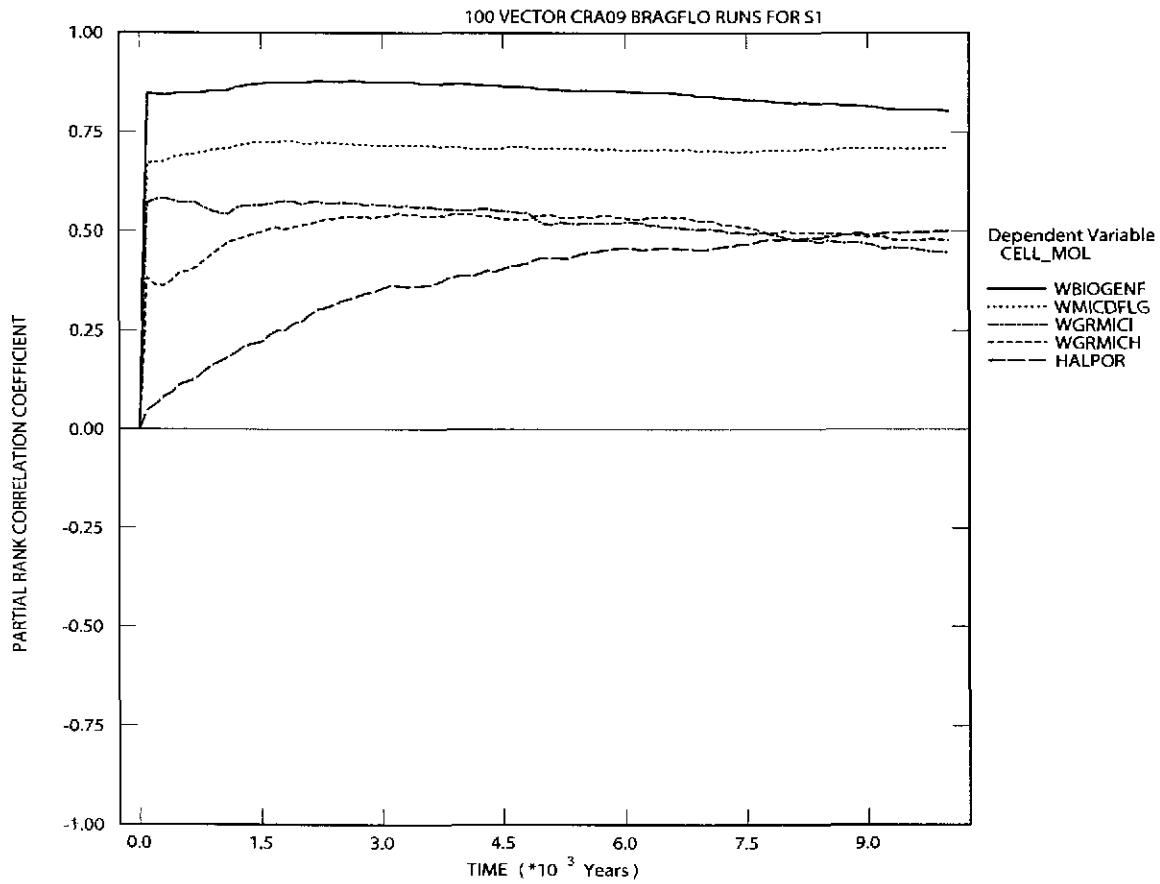


Figure 6-17. Primary correlations (dimensionless) of cumulative microbial gas generation with input parameters versus time (years), from the CRA-2009 PA, Replicate R1, Scenario S1. Table 4-2 gives a description of the names in the legend.

Sensitivity Analysis for Total Cumulative Microbial Gas Generation CRA1BC BRAGFLO R1S1

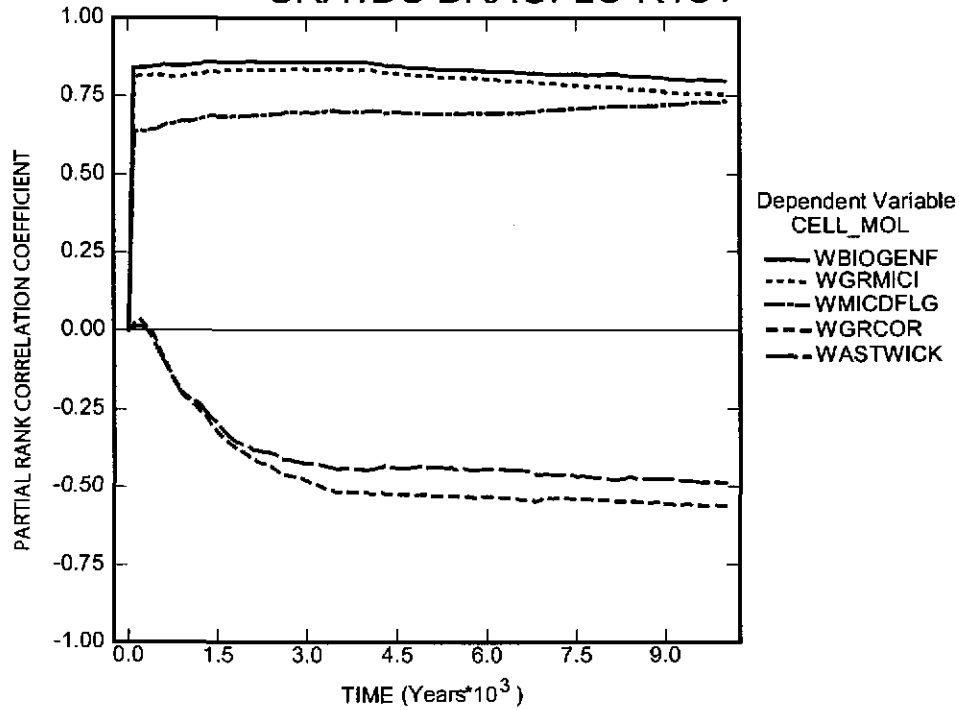


Figure 6-18. Primary correlations (dimensionless) of cumulative microbial gas generation with input parameters versus time (years), from the CRA-2004 PABC, Replicate R1, Scenario S1, CRA-2004 PABC. Table 4-2 gives a description of the names in the legend.

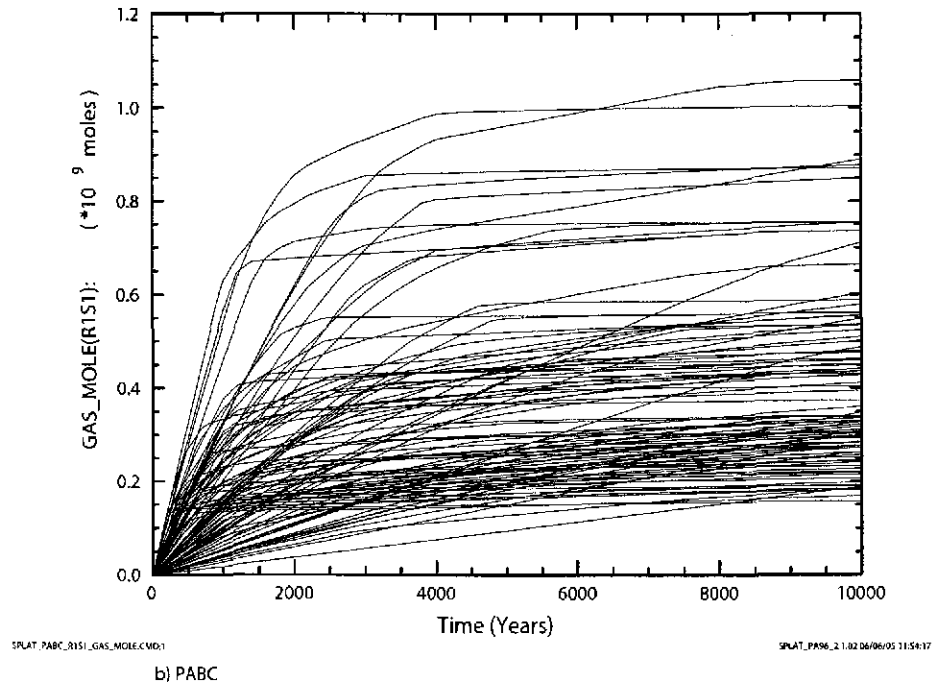
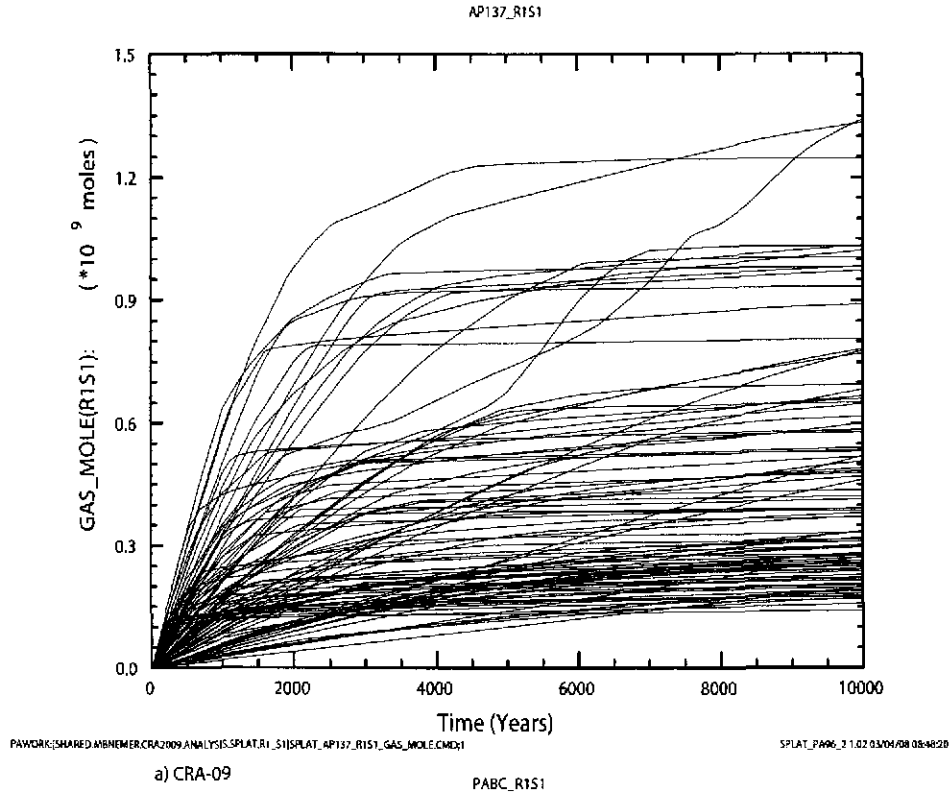


Figure 6-19. Total cumulative gas generation (moles) by all processes versus time (years) for all 100 vectors in Replicate R1, Scenario S1. Figure a) shows results from the CRA-2009 PA. Figure b) shows results from the CRA-2004 PABC.

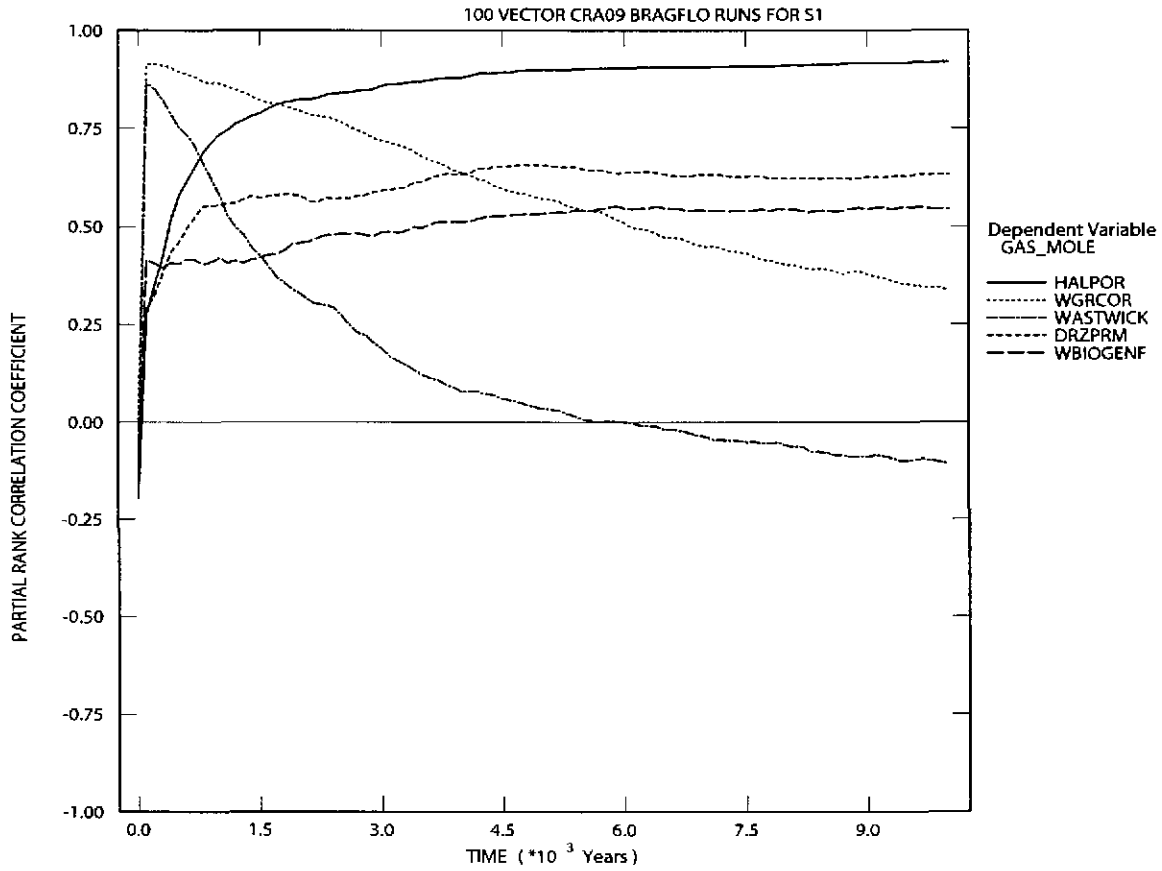


Figure 6-20. Primary correlations (dimensionless) of total cumulative gas generation with input parameters versus time (years) from the CRA-2009 PA, Replicate R1, Scenario S1. Table 4-2 gives a description of the names in the legend.

Sensitivity Analysis for Total Cumulative Gas Generation CRA1BC BRAGFLO R1S1

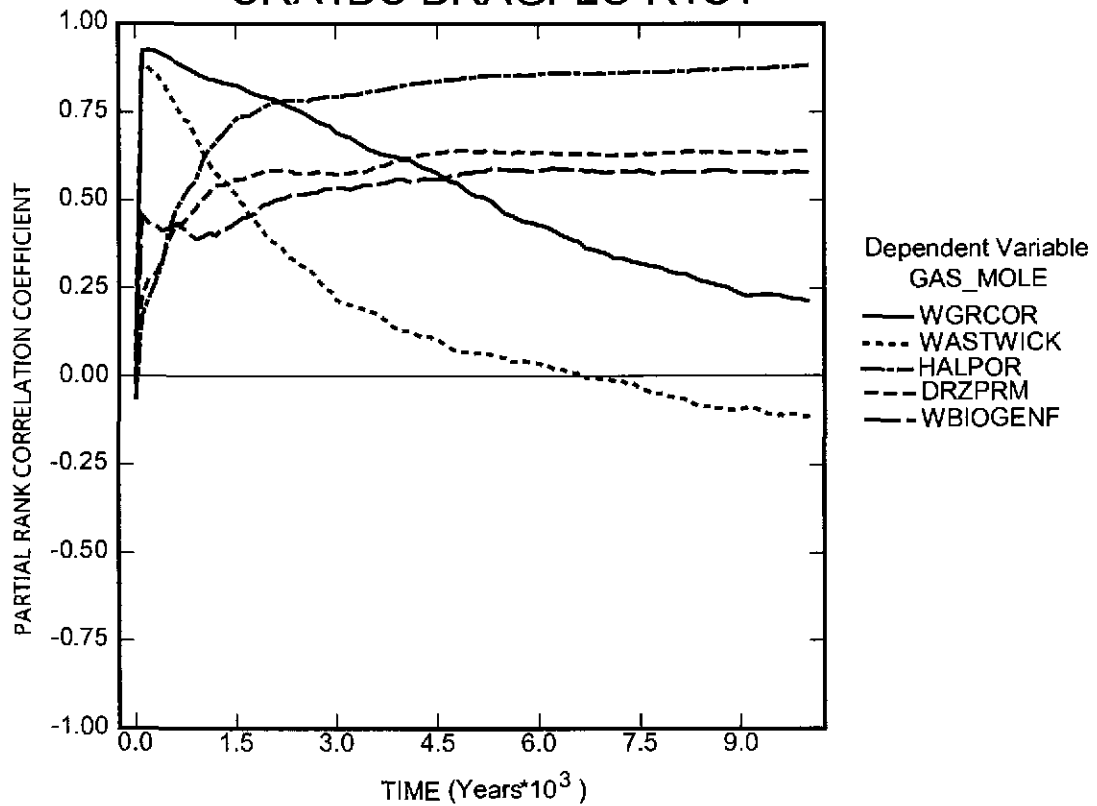


Figure 6-21. Primary correlations (dimensionless) of total cumulative gas generation with input parameters versus time (years) from the CRA-2004 PABC, Replicate R1, Scenario S1. Table 4-2 gives a description of the names in the legend.

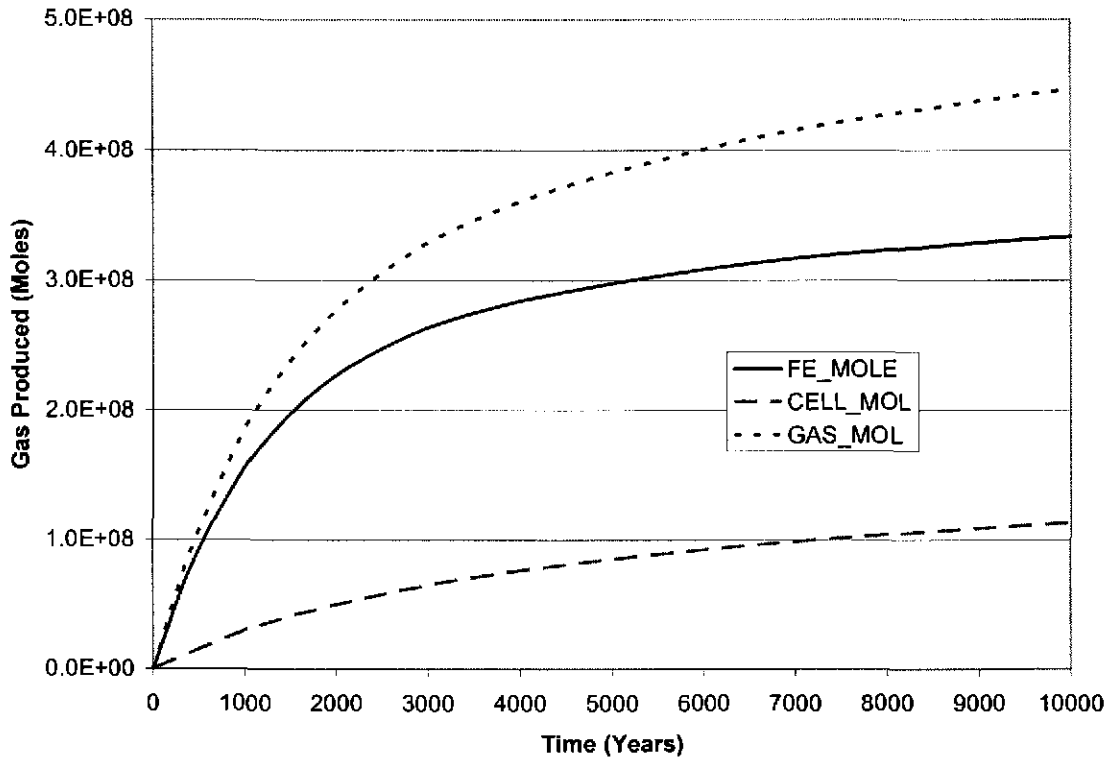


Figure 6-22. Cumulative gas generation (moles) by corrosion, by microbial activity and total versus time (years), averaged over 100 vectors from Replicate R1, Scenario S1 of the CRA-2009 PA.

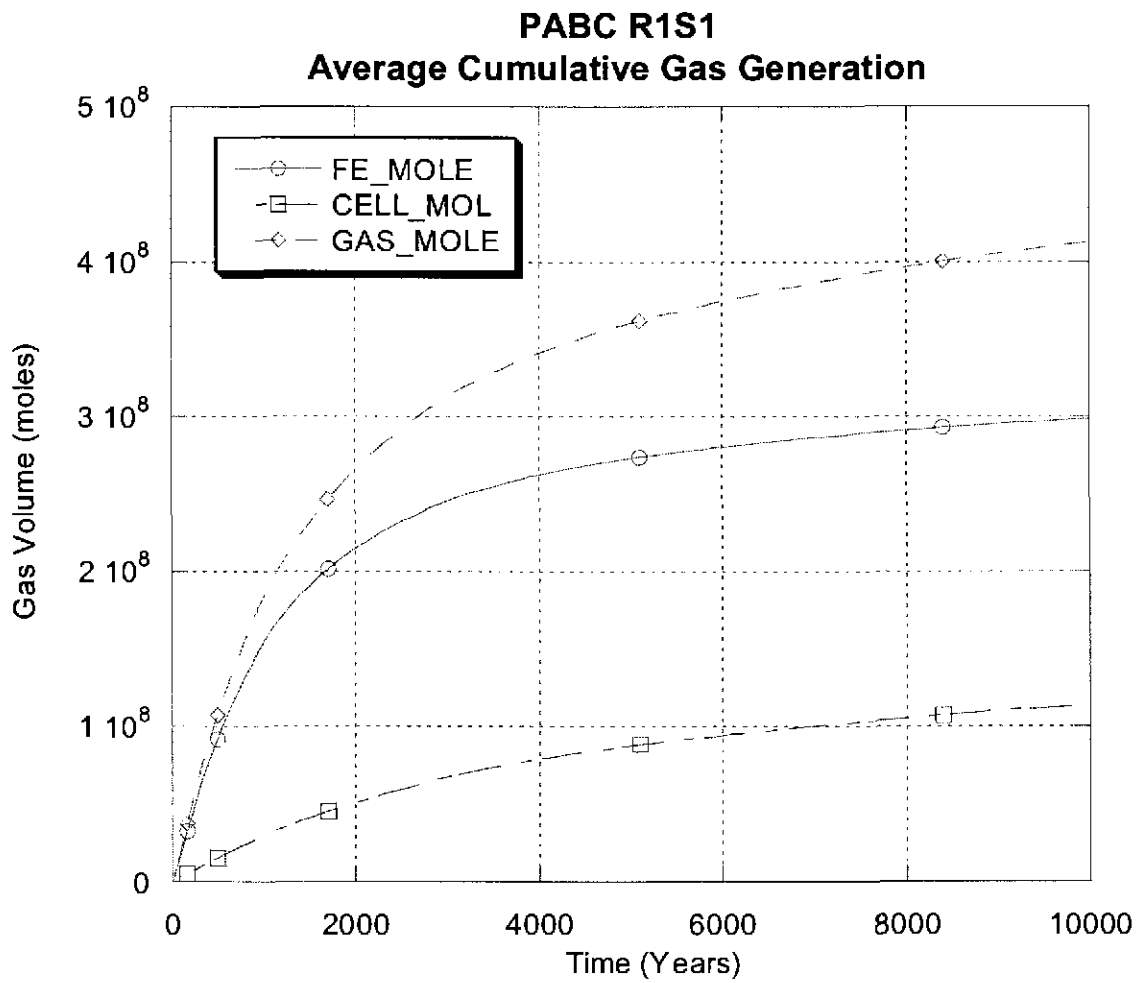
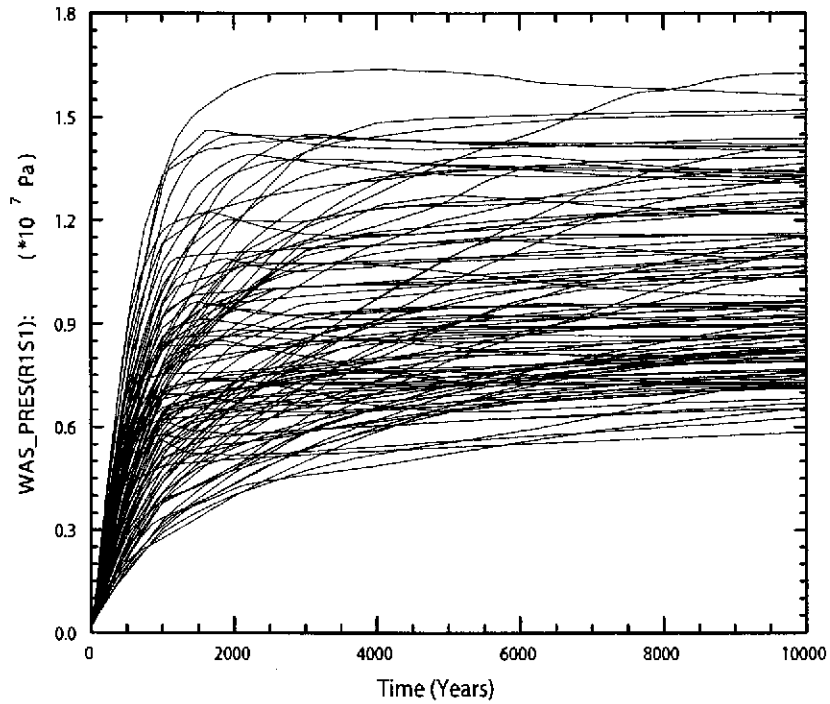


Figure 6-23. Cumulative gas generation (moles) by corrosion, by microbial activity and total versus time (years), averaged over 100 vectors from Replicate R1, Scenario S1 of the CRA-2004 PABC.

AP137_R151

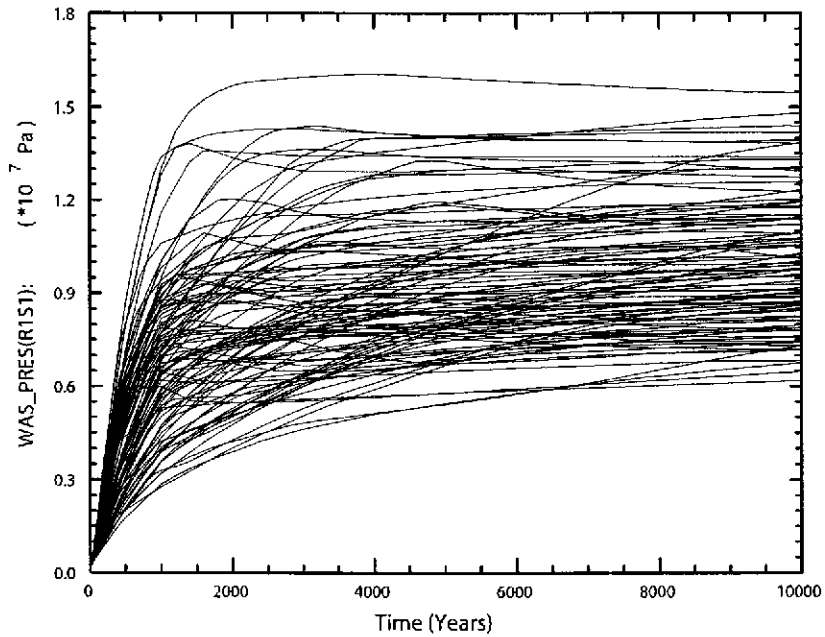


PAWORK\SHARED\MENEMER\CRA2009\ANALYSIS\SPLAT\R1_S1\SPLAT_AP137_R151_WAS_PRES.CMD:1

SPLAT_PARK_2.1.02.12/31/07 22:07:27

a) CRA-09

PABC_R151



SPLAT_PABC_R151_WAS_PRES.CMD:1

SPLAT_PARK_2.1.02.06/06/05 10:12:25

b) PABC

Figure 6-24. Volume averaged pressure (Pa) in the waste area versus time (years) for all 100 vectors in Replicate R1, Scenario S1. Figure a) shows results from the CRA-2009 PA. Figure b) shows results from the CRA-2004.

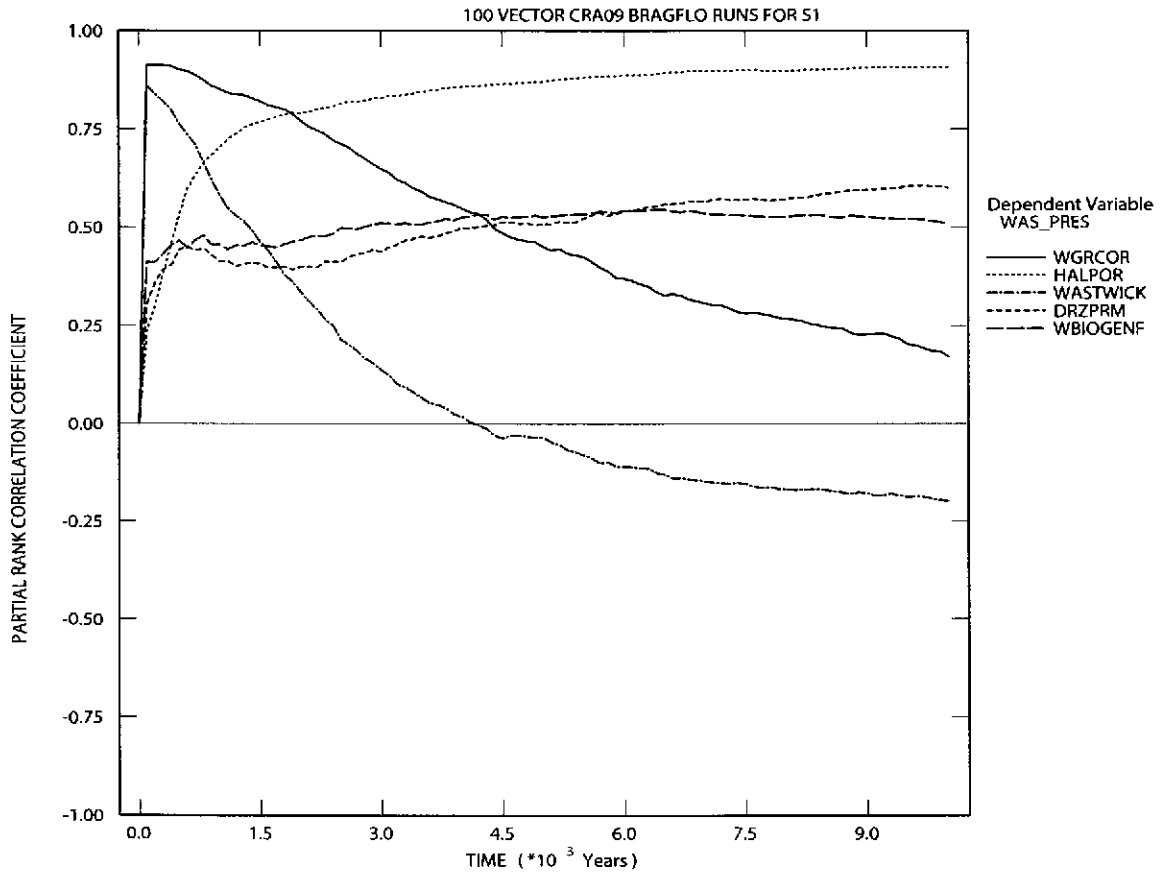


Figure 6-25. Primary correlations (dimensionless) of volume averaged pressure in the waste area with input parameters versus time (years) from the CRA-2009 PA, Replicate R1, Scenario S1. Table 4-2 gives a description of the names in the legend.

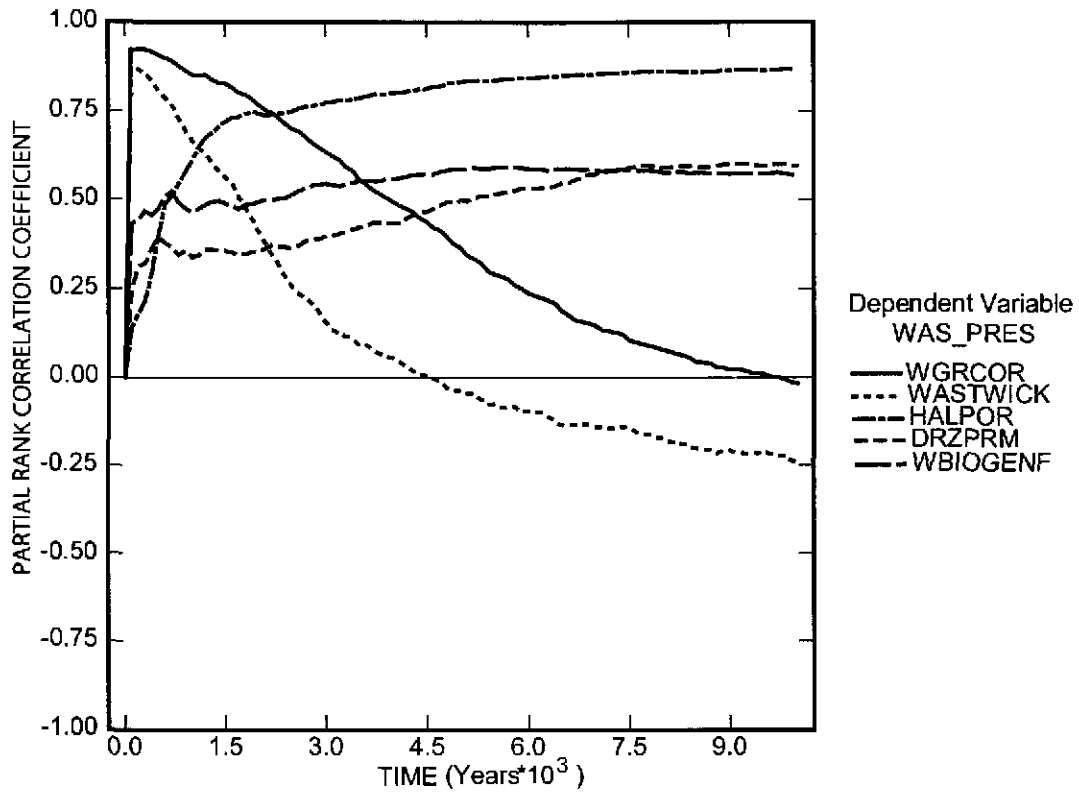
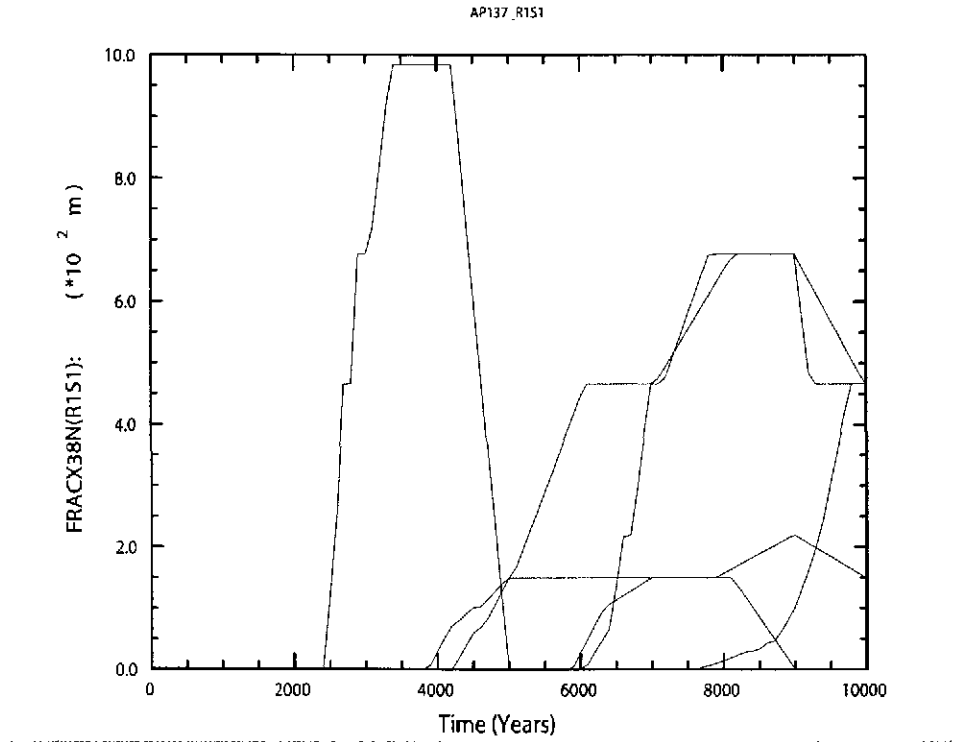
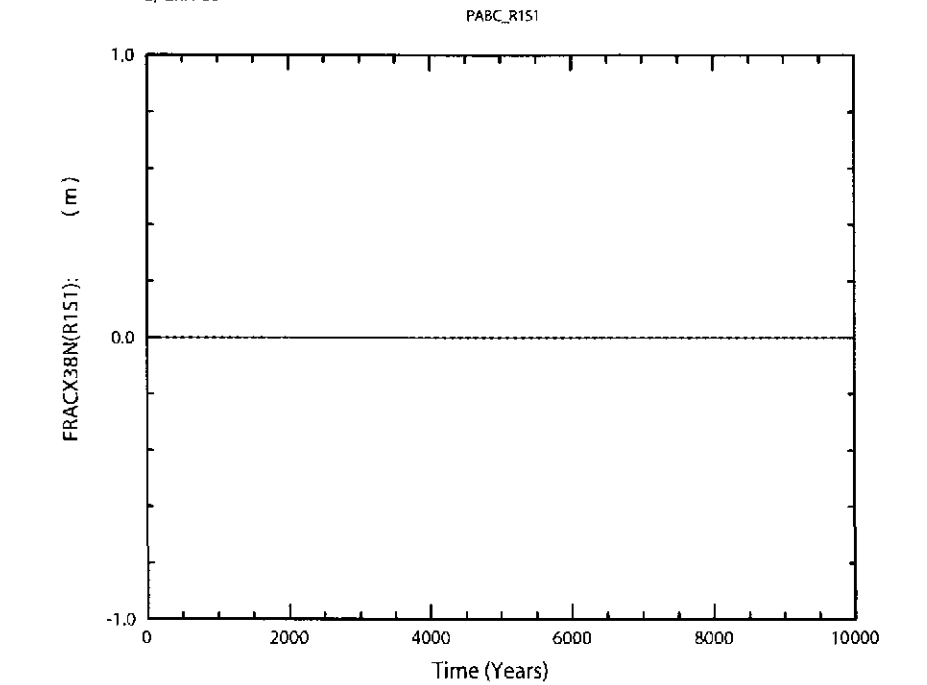


Figure 6-26. Primary correlations (dimensionless) of volume averaged pressure in the waste area with input parameters versus time (years) from the CRA-2004 PABC, Replicate R1, Scenario S1. Table 4-2 gives a description of the names in the legend.



a) CRA-09



b) PABC

Figure 6-27. Fracture length (m) in MB138 north of the repository versus time (years) for all 100 vectors in Replicate R1, Scenario S1. Figure a) shows results from the CRA-2009 PA. Figure b) shows results from the CRA-2004 PABC.

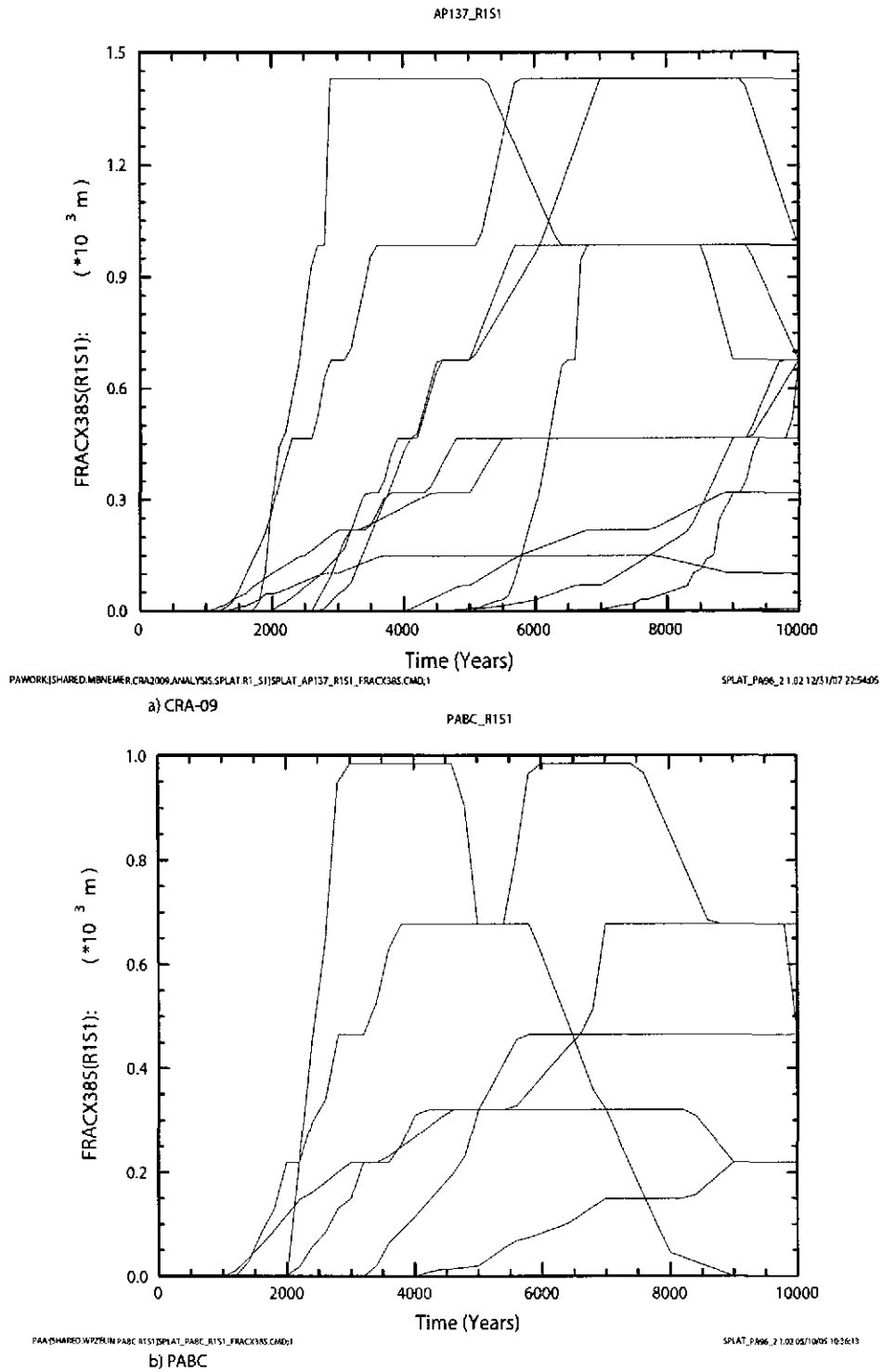
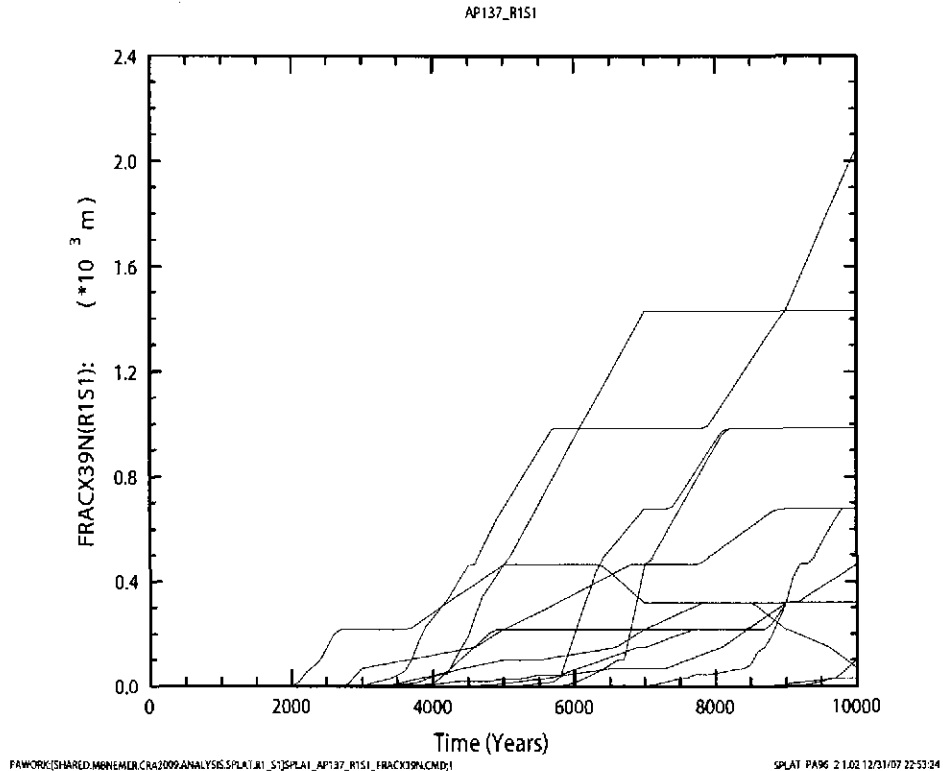
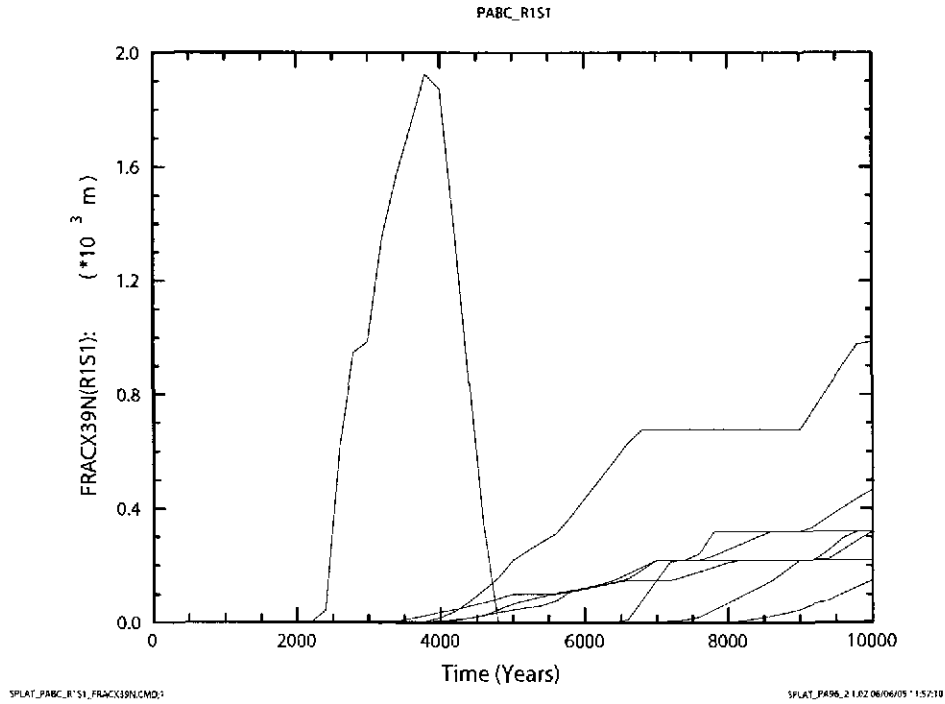


Figure 6-28. Fracture length (m) in MB138 south of the repository versus time (years) for all 100 vectors in Replicate R1, Scenario S1. Figure a) shows results from the CRA-2009 PA. Figure b) shows results from the CRA-2004 PABC.

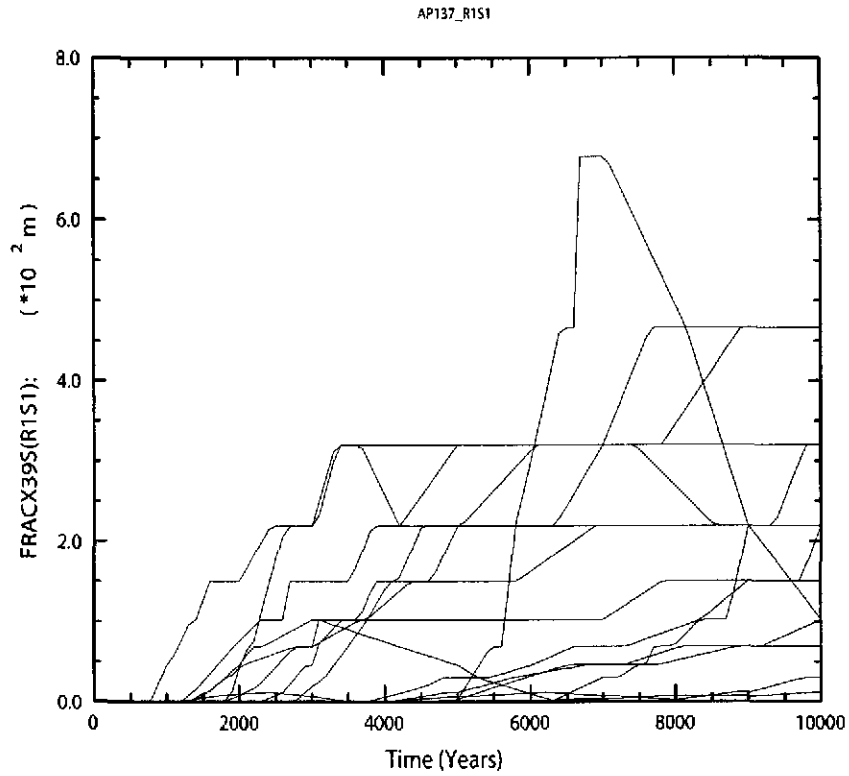


a) CRA-09



b) PABC

Figure 6-29. Fracture length (m) in MB139 north of the repository versus time (years) for all 100 vectors in Replicate R1, Scenario S1. Figure a) shows results from the CRA-2009 PA. Figure b) shows results from the CRA-2004 PABC.

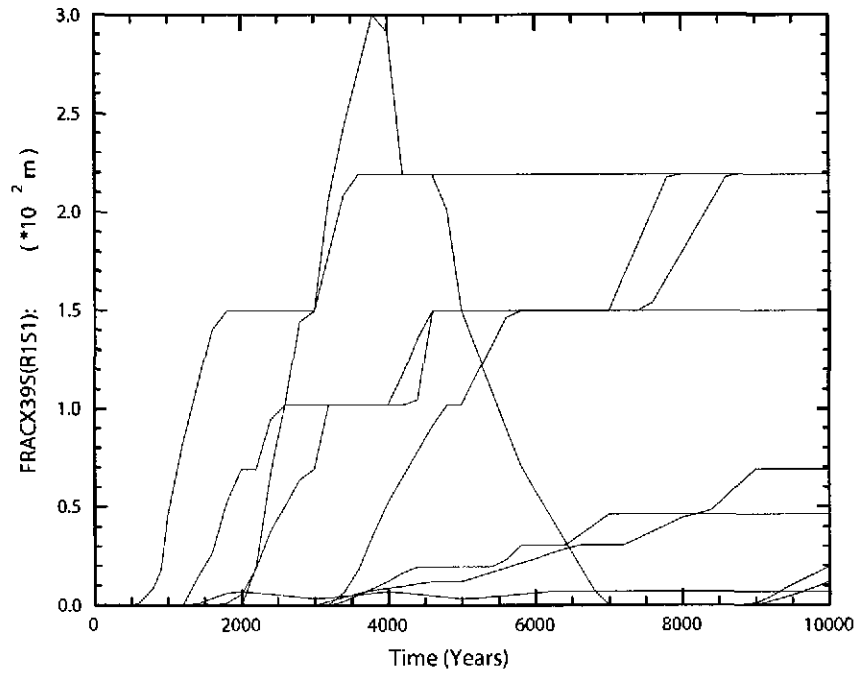


PAWDRK:\SHARED\MONITOR\CRA2009\ANALYSIS\SPLAT\R1_S1\SPLAT_AP137_R1S1_FRACX395.CMD;1

SPLAT_PAG6_21.02.12\31\07.22:52:43

a) CRA-09

PABC_R1S1

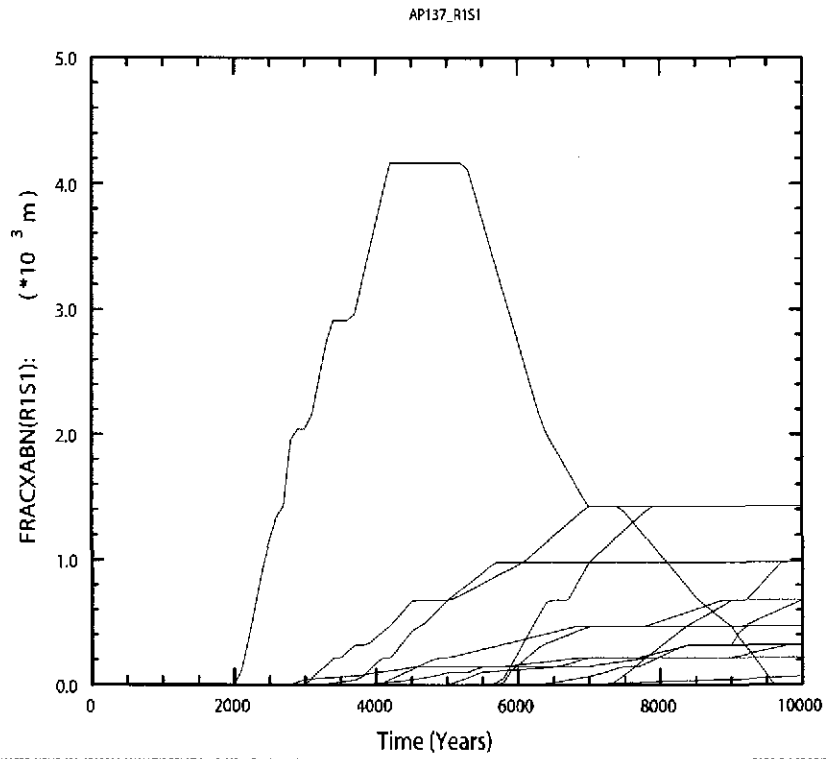


PAWDRK:\SHARED\MONITOR\PABC\R1S1\SPLAT_PABC_R1S1_FRACX395.CMD;1

SPLAT_PAG6_21.02.05\10\05.10:35:19

b) PABC

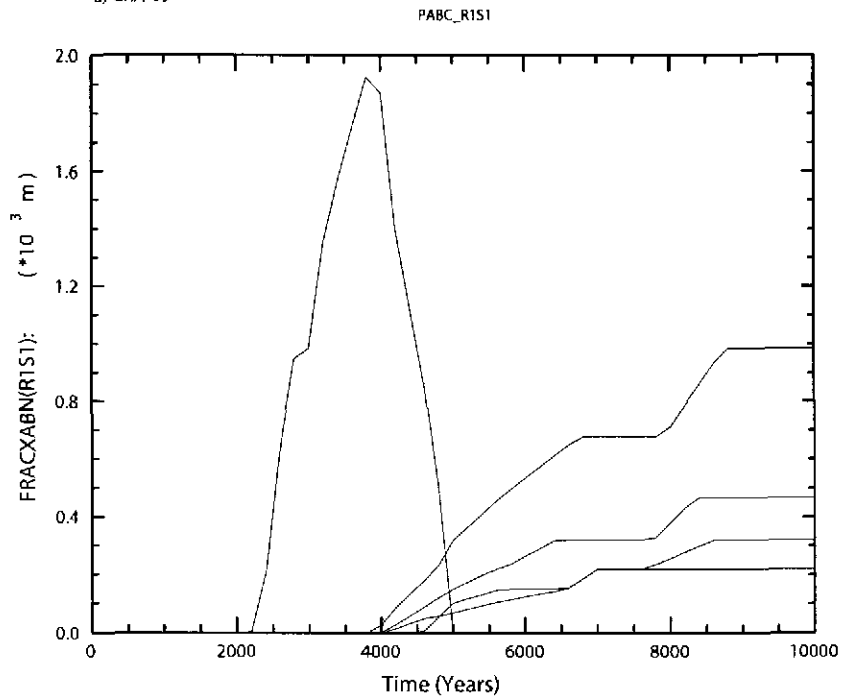
Figure 6-30. Fracture length (m) in MB139 south of the repository versus time (years) for all 100 vectors in Replicate R1, Scenario S1. Figure a) shows results from the CRA-2009 PA. Figure b) shows results from the CRA-2004 PABC.



FAWORK\SHARED\MEMEMER\CRA2009\ANALYSIS\SPLAT_R1_S1\PLAT_AP137_R1S1_FRACXABN.CMD1

SPLAT_PAB6_21.02 12/31/07 22:52:02

a) CRA-09



SPLAT_PABC_R1S1_FRACXABN.CMD1

SPLAT_PAB6_21.02 06/06/05 11:56:26

b) PABC

Figure 6-31. Fracture length in Anhydrite A&B (m) north of the repository versus time (years) for all 100 vectors in Replicate R1, Scenario S1. Figure a) shows results from the CRA-2009 PA. Figure b) shows results from the CRA-2004 PABC.

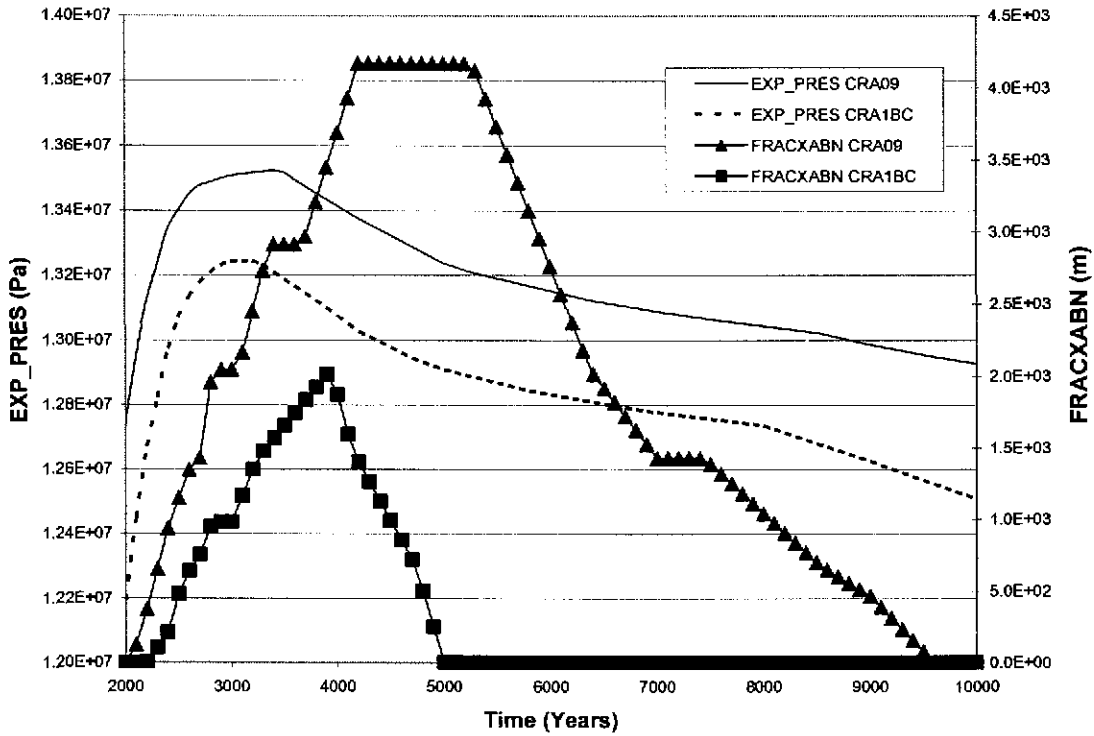
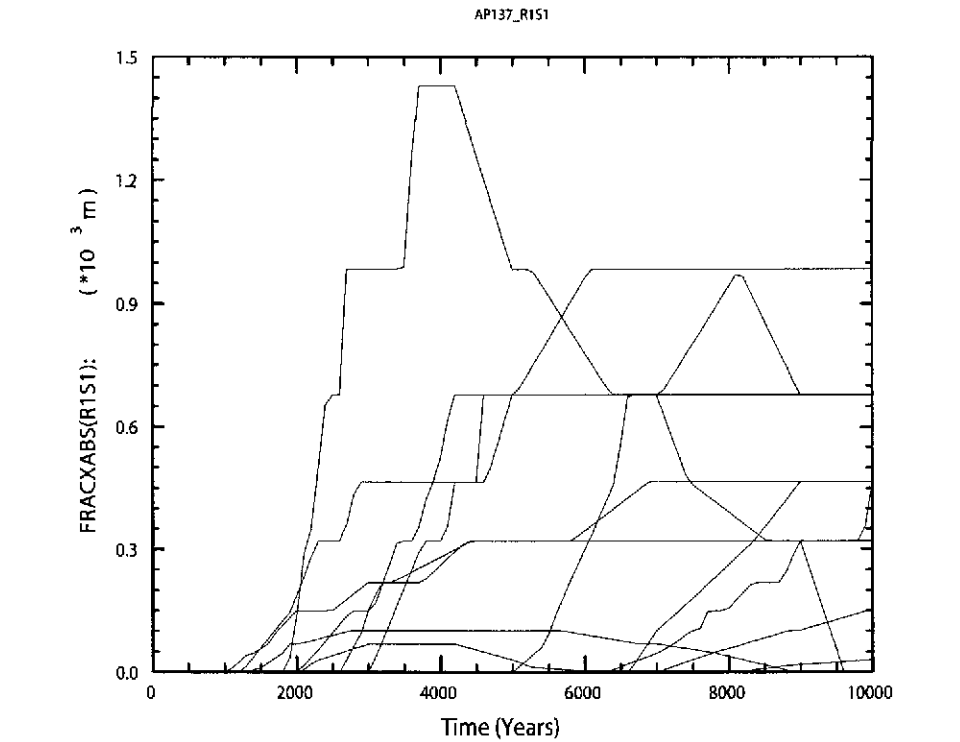
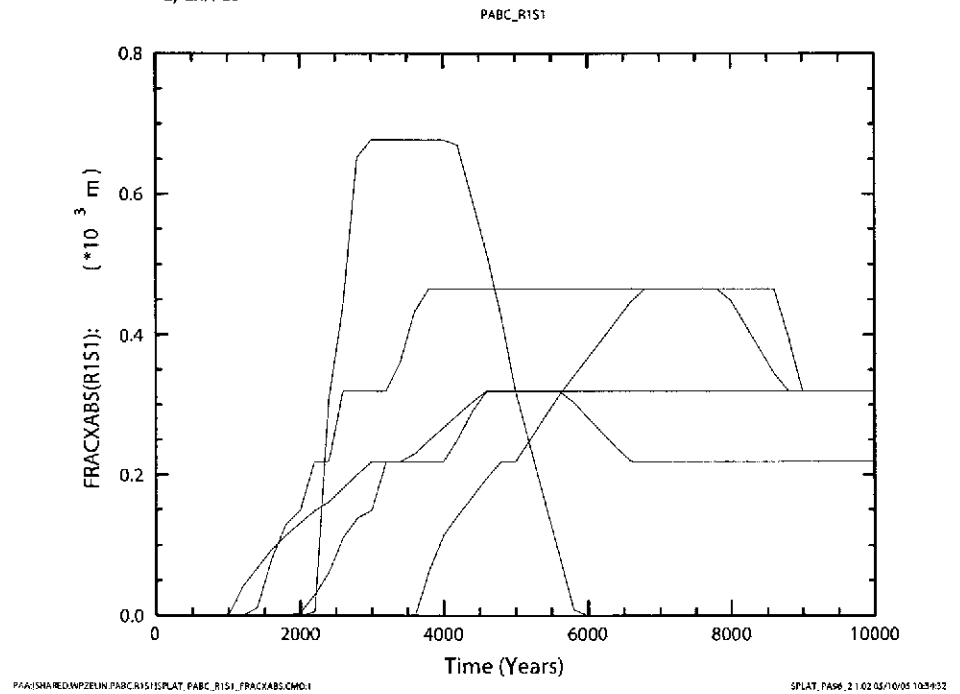


Figure 6-32. Pressure in Pa in the Experimental area EXP_PRES (left hand axis), and Fracture length in marker bed AB north of the repository FRACXABN (right hand axis), from Vector 53 of the CRA-2009 PA and the CRA-2004 PABC versus time.

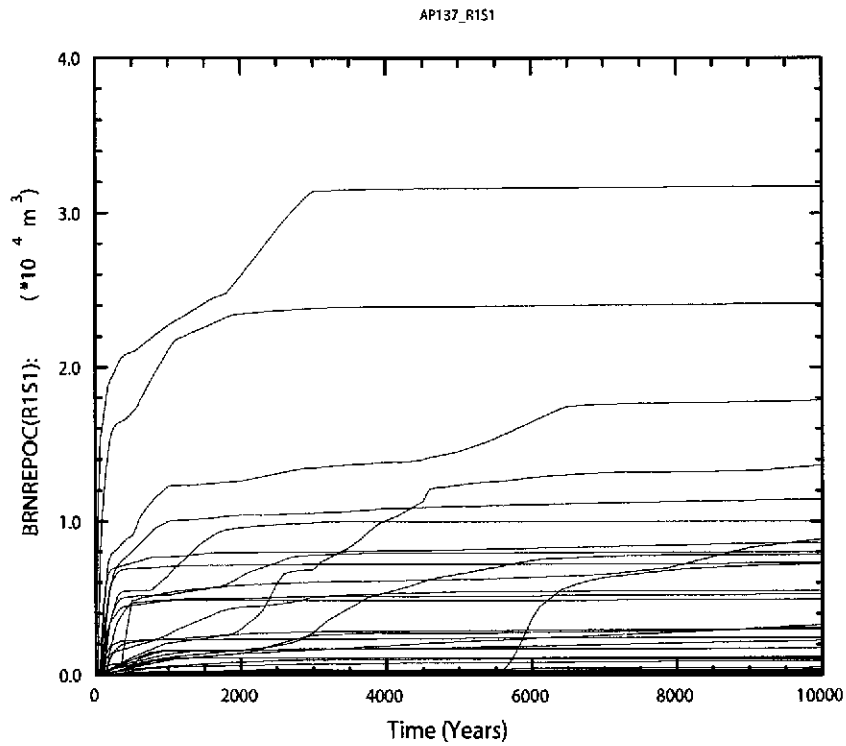


a) CRA-09



b) PABC

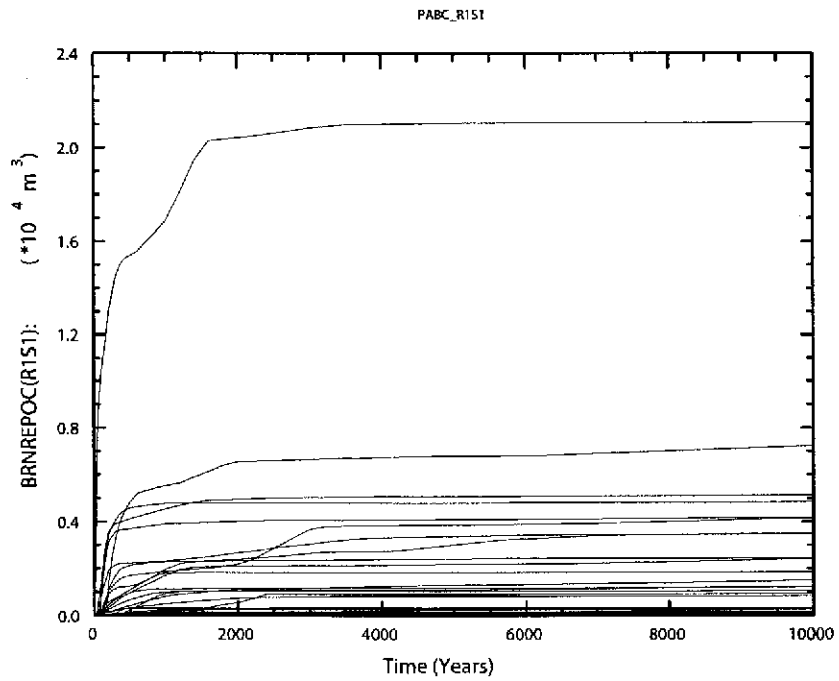
Figure 6-33. Fracture length in Anhydrite A and Anhydrite B (m) south of the repository versus time (years) for all 100 vectors in Replicate R1, Scenario S1. Figure a) shows results from the CRA-2009 PA. Figure b) shows results from the CRA-2004 PABC.



PAIWORK\SHARED\MHHEMER\CRA2009\ANALYSIS\SPLAT\R1_S1\SPLAT_AP137_R1S1_BRNREPOC.CMD:1

SPLAT_PA96_2.1.02.12/31/07 23:32:32

a) CRA-09



SPLAT_PABC_R1S1_BRNREPOC.CMD:1

SPLAT_PA96_2.1.02.06/06/05 10:444

b) PABC

Figure 6-34. Total cumulative brine flow (m^3) away from the repository versus time (years) for all 100 vectors in Replicate R1, Scenario S1. Figure a) shows results from the CRA-2009 PA. Figure b) shows results from the CRA-2004 PABC.

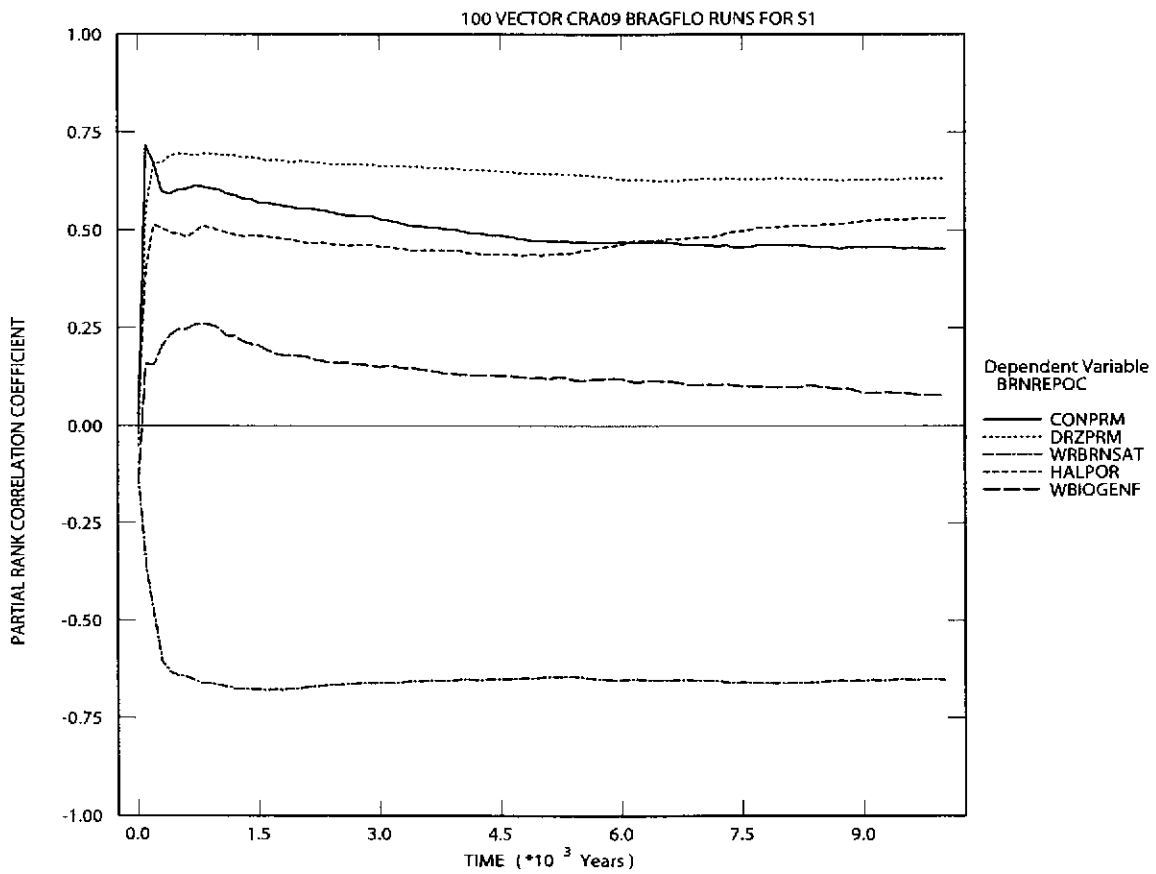


Figure 6-35. Primary correlations (dimensionless) of cumulative brine outflow from the repository with input parameters versus time (years) from the CRA-2009 PA, Replicate R1, Scenario S1. Table 4-2 gives a description of the names in the legend.

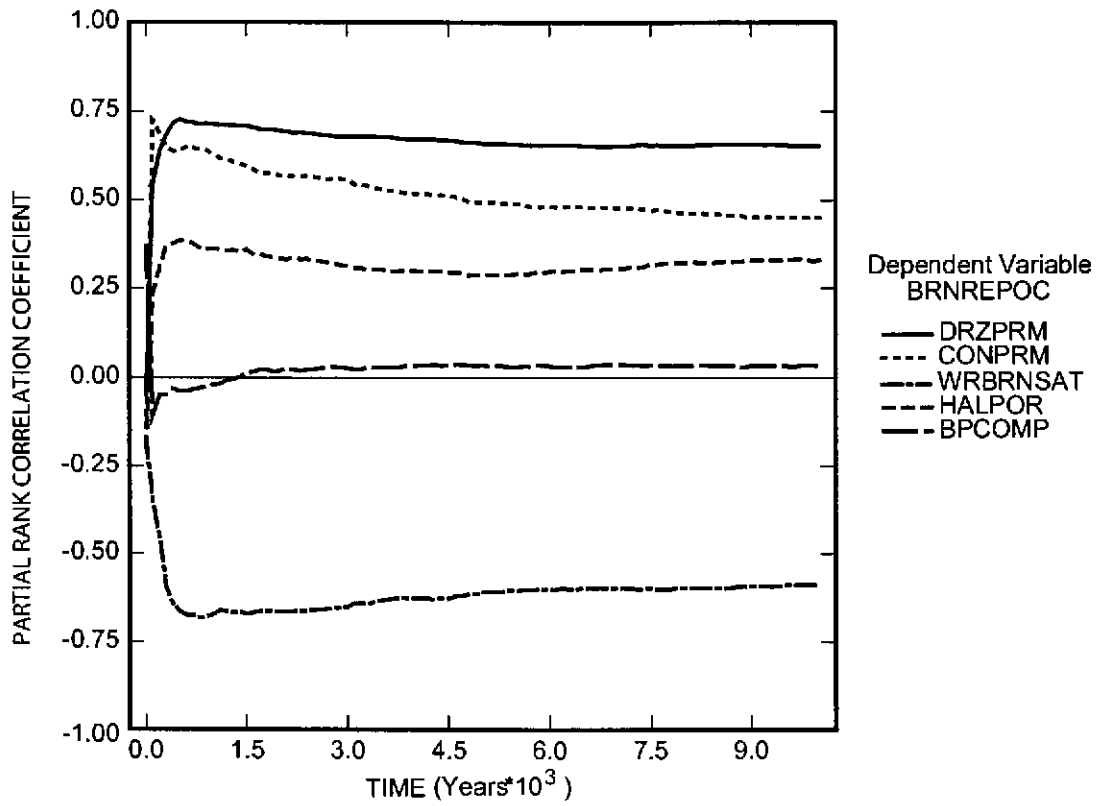


Figure 6-36. Primary correlations (dimensionless) of cumulative brine outflow from the repository with input parameters versus time (years) from the CRA-2004 PABC, Replicate R1, Scenario S1. Table 4-2 gives a description of the names in the legend.

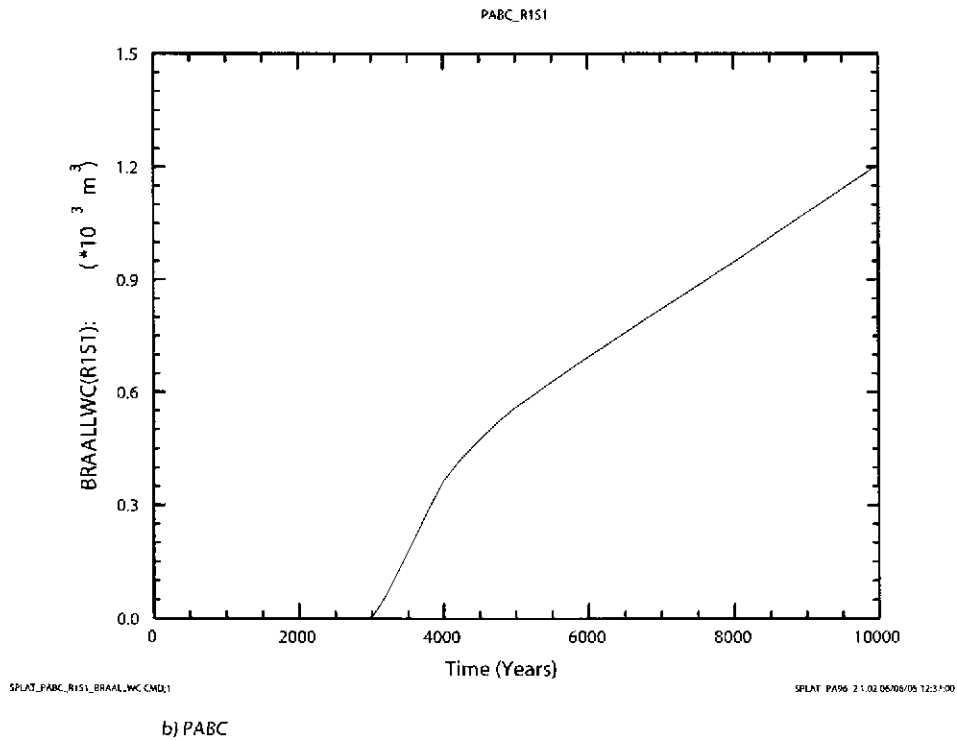
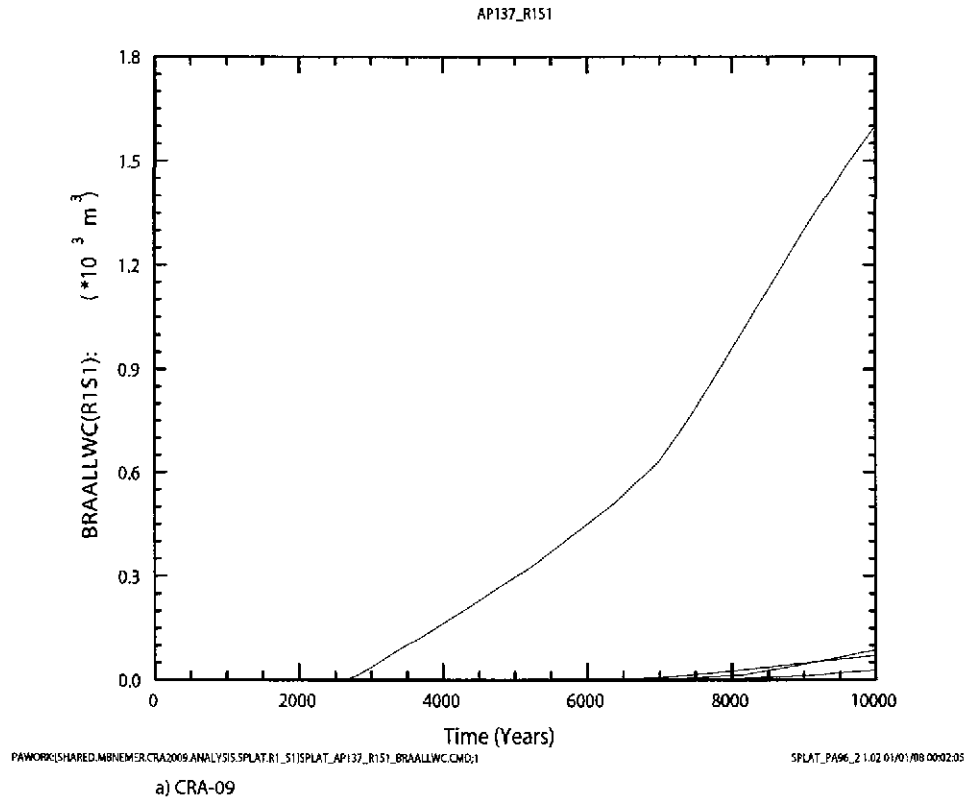


Figure 6-37. Cumulative brine flow (m^3) to the LWB versus time (years) for all 100 vectors in Replicate R1, Scenario S1. Figure a) shows results from the CRA-2009 PA. Figure b) shows results from the CRA-2004 PABC.

6.4 DRILLING DISTURBANCE SCENARIOS

Scenarios S2 through S6 evaluate the possible results of drilling intrusions into the repository. It is assumed that all boreholes in the Salado Flow Analysis are drilled through the repository in search of deeper resources. The potential consequences of encountering a pressurized brine pocket in the Castile (an E1 event) are considered in Scenarios S2 and S3. Boreholes that do not encounter pressurized brine (S4 and S5) are modeled in the Salado Flow grid as terminating at the base of the repository (an E2 event). Scenario S6 evaluates an E2 event followed by an E1 event. The specific sequences of material property changes in the model are listed in the following section. After Subsection 6.4.1, detailed results are presented for Scenario S2 and S4, which are representative of Scenarios S2-S6, except for the differences in the timing of the drilling intrusions. Brine releases to the Culebra are also presented for Scenario S6, as S6 is only used for determining the radionuclide source term to the Culebra in the PANEL application (Kanney and Leigh 2005).

6.4.1 Sequence of Events

Five drilling disturbance scenarios are considered in this part of the Salado Flow Analysis. The sequence of events for each is summarized below:

Scenario S2 (E1 event)

- 200 years: change in lower shaft material properties.
- 350 years: borehole intrusion (E1) through the Waste Panel into a hypothetical pressurized brine reservoir in the underlying Castile Formation. Concrete borehole plugs are immediately emplaced in the borehole at the Culebra and at the surface.
- 550 years: Borehole plugs fail and the borehole (top to bottom) is assumed to have properties equivalent to sand (material: BH_SAND).
- 1,550 years: the permeability of the borehole between the repository and the Castile Formation decreases due to creep closure of the salt (material: BH_CREEP).

Scenario S3 (E1 event)

- 200 years: change in lower shaft material properties.
- 1,000 years: borehole intrusion (E1) through the Waste Panel into a hypothetical pressurized brine reservoir in the underlying Castile Formation. Concrete borehole plugs are immediately emplaced in the borehole at the Culebra and at the surface.
- 1,200 years: Borehole plugs fail and the borehole (top to bottom) is assumed to have properties equivalent to sand (material: BH_SAND).
- 2,200 years: the permeability of the borehole between the repository and the Castile Formation decreases due to creep closure of the salt (material: BH_CREEP).

Scenario S4 (E2 event)

- 200 years: change in lower shaft material properties.

- 350 years: borehole intrusion (E2) through a Waste Panel terminating at the base of the DRZ in the modeling grid (no connection to the underlying Castile Formation). Two plugs are present in the upper part of the borehole.
- 550 years: Borehole plugs fail and the borehole (top to bottom) is assumed to have properties equivalent to sand (material: BH_SAND).

Scenario S5 (E2 event)

- 200 years: change in lower shaft material properties.
- 1,000 years: borehole intrusion (E2) through a Waste Panel terminating at the base of the DRZ in the modeling grid (no connection to the underlying Castile Formation). Two plugs are present in the upper part of the borehole.
- 1,200 years: Borehole plugs fail and the borehole (top to bottom) is assumed to have properties equivalent to sand (material: BH_SAND).

Scenario S6 (E2,E1 events)

- 200 years: change in lower shaft material properties.
- 1,000 years: borehole intrusion (E2) through a Waste Panel terminating at the base of the DRZ in the modeling grid (no connection to the underlying Castile Formation) Borehole filled with sand.
- 2,000 years: borehole intrusion (E1) through a Waste Panel into a hypothetical pressurized brine reservoir in the underlying Castile Formation
- 2,200 years: Borehole plugs fail and the borehole (top to bottom) is assumed to have properties equivalent to sand (material: BH_SAND).
- 3,200 years: the permeability of the borehole between the repository and the Castile Formation decreases due to creep closure of the salt (material: BH_CREEP).

6.4.2 Halite Creep

Drilling intrusions have relatively little effect on the range of porosities in the repository compared to the undisturbed scenario, because most creep closure occurs prior to the drilling event. However, changes in pressure due to the intrusion do have a small but recognizable impact on porosity, which is the primary measure of creep closure in the waste areas. Figure 6-38 and Figure 6-39 show the volume averaged porosity in all waste areas versus time for Scenarios S2 and S4, for the CRA-2009 PA and the CRA-2009 PABC. There is little difference in the two analyses, which is confirmed by statistics given in Table 6-13.

Table 6-13. Statistics of porosity volume-averaged over all waste-filled areas at 10,000 years for Replicate R1, Scenarios S2 and S4 for the CRA-2009 PA and CRA-2004 PABC.

W_R_POR (dimensionless)	CRA-2009 PA		CRA-2004 PABC	
	S2	S4	S2	S4
Minimum	9.08E-02	5.90E-02	9.76E-02	5.71E-02
Average	1.52E-01	1.28E-01	1.51E-01	1.26E-01
Maximum	2.17E-01	2.08E-01	2.11E-01	2.04E-01

6.4.3 Brine Inflow

Table 6-14 summarizes statistics for S2 and S4 for BRNREPTC, the cumulative brine flow into the repository. The average inflows for the CRA-2009 PA and the CRA-2004 PABC differ slightly. The average brine inflow in S2 is greater in the CRA-2009 PA than in the CRA-2004 PABC. Some of this increase is attributable to the increased DRZ porosity, which can be seen by looking at the amount of brine that enters the repository under undisturbed conditions (Table 6-5).

Table 6-14 Statistics for cumulative brine flow into the repository at 10,000 years Replicate R1, Scenarios S2 and S4 for the CRA-2009 PA and CRA-2004 PABC.

(BRNREPTC) (m ³)	CRA-2009 PA		CRA-2004 PABC	
	S2	S4	S2	S4
Minimum	9.53E+03	8.55E+02	9.32E+03	8.05E+02
Average	3.86E+04	1.92E+04	3.19E+04	1.31E+04
Maximum	2.01E+05	8.66E+04	1.99E+05	4.71E+04

Figure 6-40 and Figure 6-41 show plots of brine flow into the repository versus time for all 100 vectors in Scenarios S2 and S4 for the CRA-2009 PA and the CRA-2004 PABC. The graphs visually confirm the statistics listed above in Table 6-14.

Figure 6-42 and Figure 6-43 show the total volume of brine in the repository versus time for all 100 vectors in Scenarios S2 and S4 of Replicate R1. The results from Scenario S2 show a spike in brine volume at the intrusion time as one would expect. The volume then decreases with time due to increasing pressure, associated brine flow up the borehole, and brine consumption from steel corrosion. The results for Scenario S4 show a similar decrease after the borehole plugs fail. Scenario S4 has no intrusion into the Castile brine pocket.

6.4.4 Brine Saturation

Figure 6-44 and Figure 6-45 show brine saturation (WAS_SATB) in the Waste Panel versus time for all 100 vectors, for Scenarios S2 and S4, for the CRA-2009 PA and the CRA-2004 PABC. The direct consequence of greater brine inflow associated with a drilling intrusion is higher brine saturation in the waste areas. For Scenario S2, brine saturation in the Waste Panel increases immediately to a value close to 1 after a drilling intrusion into a pressurized brine pocket in the Castile (350 years).

Figure 6-46 - Figure 6-47 shows the PRCC's for brine saturation in the Waste Panel WAS_SATB for Scenario S2, from the CRA-2009 PA and the CRA-2004 PABC. Figure 6-48 - Figure 6-49 shows the PRCC's for Scenario S4 from the same analyses. The permeability of the DRZ (DRZPRM) and the borehole (BHPERM) exhibit the largest positive correlations. High permeability in these materials allows brine to flow into the waste areas. Negative correlations with the steel corrosion rate (WGRCOR) and the waste wicking factor (WASTWICK) are evident because high values of these parameters lead to faster brine consumption.

6.4.5 Gas Generation

Table 6-15 summarizes average cumulative gas generation information at 10,000 years for Scenarios S2 and S4. The CRA-2009 PA and the CRA-2004 PABC are similar. Drilling intrusions do not appreciably affect gas generation by microbial activity, but gas generation by corrosion is greater in the E1 scenario (S2) than in the E2 (S4) scenario. The increase is due to increased availability of brine, which is a limiting factor for corrosion. At 10,000 years, the average brine saturation in the Waste Panel (WAS_SATB) in the E1 scenario is greater than in the E2 scenario.

Table 6-15. Brine saturation and cumulative gas generation at 10,000 years averaged over 100 vectors for Replicate R1 for the CRA-2009 and CRA-2004 PABC.

Property	CRA-2009 PA		CRA-2004 PABC	
	S2	S4	S2	S4
WAS_SATB (dimensionless)	8.15E-01	4.03E-01	8.00E-01	3.76E-01
GAS_MOLE (moles)	5.28E+08	5.02E+08	4.83E+08	4.48E+08
FE_MOLE (moles)	3.92E+08	3.62E+08	3.57E+08	3.24E+08
CELL_MOL (moles)	1.36E+08	1.40E+08	1.26E+08	1.24E+08

Figure 6-50 and Figure 6-51 show the cumulative amount of gas produced by iron corrosion versus time, and Figure 6-56 and Figure 6-57 show the fraction of iron remaining versus time. The results for gas produced by iron corrosion in the CRA-2009 PA are very similar to that of the CRA-2004 PABC. Figure 6-52- Figure 6-53 and Figure 6-54 - Figure 6-55 show the PRCC's for gas generation by iron corrosion versus time for the CRA-2009 PA and the CRA-2004 PABC. Variables such as the steel corrosion rate (WGRCOR), halite porosity (HALPOR), DRZ permeability (DRZPRM), and the waste wicking factor (WASTWICK) show the highest positive correlations with gas generation by iron corrosion. These correlations are reasonable because these variables all influence the net gas generation rate from corrosion. The borehole permeability (BHPERM) shows a strong positive correlation in S4, presumably because it serves as a conduit for brine to enter the repository from the upper DRZ, Culebra Formation, and Dewey Lake Formation (bore hole does not penetrate the castile brine pocket in S4).

Figure 6-58 and Figure 6-59 show the cumulative amount of gas produced by microbial gas generation, Figure 6-65 and Figure 6-66 show the fraction of cellulose (cellulose or CPR depending on the value of WAS_AREA:PROBDEG, see Subsection 5.4 of Nemer and Stein 2005). No large differences between CRA-2009 PA and CRA-2004 PABC results are evident. Figure 6-60 - Figure 6-61 and Figure 6-62 - Figure 6-63 show the PRCC's for the cumulative amount of gas generation by microbial activity versus time for the CRA-2009 PA and the CRA-2004 PABC. Besides variables that are directly related to the rate of microbial gas-generation (BIOGENFC, GRATMICI), the only variables with an important correlation are the corrosion rate and the wicking factor. It's interesting to note that in the CRA-2004 PABC, the wicking factor and the iron corrosion rate both have negative correlations with microbial gas generation, however these do not show up in the CRA-2009 PA. Although brine saturation in Figure 6-46 is negatively correlated with the wicking factor and the iron corrosion rate, these variables do not appear to be important enough to limit microbial gas generation shown in Figure 6-60.

In Figure 6-64 we have plotted for S2 ($\text{CELL_MOL}_{\text{CRA09}} - \text{CELL_MOL}_{\text{CRA1BC}} / \text{CELL_MOL}_{\text{CRA1BC}}$, versus $\text{GRATMICH}_{\text{CRA09}} / \text{GRATMICH}_{\text{CRA1BC}} - \text{GRATMICH}_{\text{CRA1BC}} / \text{GRATMICH}_{\text{CRA1BC}}$, where the subscripts CRA09 and CRA1BC indicate the CRA-2009 PA and the CRA-2004 PABC analysis, GRATMICH is the humid microbial gas generation rate, and GRATMICH is the inundated microbial gas generated rate. In other words Figure 6-64 is a scatter plot showing the difference in the amount of microbial gas generated versus the difference in the humid rate, for each vector. The difference in the humid rate is due to the new method by which it is sampled, as discussed in Subsection 5.1.3. According to the R^2 value, about 30 % of the difference in CELL_MOL is attributable to the new humid rate sampling methodology.

Figure 6-67 and Figure 6-68 show the total cumulative amount of gas produced versus time from all gas-generation processes. The differences between the CRA-2009 and the CRA-2004 PABC are small. Figure 6-69 - Figure 6-70 and Figure 6-71 - Figure 6-72 show the PRCC's for total cumulative gas generation by all processes versus time for the CRA-2009 PA and the CRA-2004 PABC. Halite porosity has the largest positive correlation, owing to the fact that corrosion accounts for more gas generation than microbial activity.

6.4.6 Pressure

Pressures in the disturbed scenarios are identical to pressures in the undisturbed scenarios until the drilling intrusion occurs. Following the intrusion pressures in the Waste Panel tend to change rapidly, especially once the borehole plugs fail 200 years after the intrusion. Table 6-16 shows statistics of the volume average pressure in the Waste Panel at 10,000 years. The differences between the CRA-2009 PA and the CRA-2004 PABC are small.

Table 6-16. Statistics on the volume averaged pressure in the waste panel at 10,000 years for Replicate R1 for the CRA-2009 PA and CRA-2004 PABC.

WAS_PRES (Pa)	CRA-2009 PA		CRA-2004 PABC	
	S2	S4	S2	S4
Minimum	4.52E+06	1.10E+06	4.70E+06	1.21E+06
Average	8.58E+06	6.49E+06	8.53E+06	6.39E+06
Maximum	1.48E+07	1.39E+07	1.42E+07	1.35E+07

Figure 6-73 and Figure 6-74 show the volume averaged pressure in the Waste Panel (WAS_PRES) versus time for all 100 vectors in Replicate R1, for the CRA-2009 PA and the CRA-2004 PABC. As the figures indicate there aren't significant differences between the two analyses. Figure 6-75 - Figure 6-76 and Figure 6-77 - Figure 6-78 show PRCC's for WAS_PRES versus time for Scenarios S2 and S4 from the CRA-2009 PA and the CRA-2004 PABC. The figures indicate that borehole permeability has the strongest negative correlation, as this is the primary means by which pressure may escape the repository. Castile brine pocket pressure has a strong positive correlation with pressure at the time of an intrusion, which subsequently decreases with time.

6.4.7 Rock Fracturing

The consequence of rock fracturing is modeled in the DRZ and marker beds with a model that alters the permeability of these units as pressures increase above a fracture initiation pressure. Figure 6-79 through

Figure 6-90 show the fracturing length in marker beds 138, 139 and Anhydrite A&B, north and south of the repository. Vector 53 shows a large but transient fracture length which begins at 2000 years, similar to S1 but not as large. Fracturing has little impact on brine flow out of the repository for the disturbed scenarios. In the disturbed scenarios brine migrates out of the borehole.

6.4.8 Brine Flow Out of the Repository

Figure 6-91 and Figure 6-92 show cumulative brine flow out of the Waste Panel. Figure 6-93 and Figure 6-94 show cumulative brine flow away from the repository (BRNREPOC) versus time for Scenarios S2 and S4, for the CRA-2009 PA and the CRA-2004 PABC. The results from the two analyses are similar. This is confirmed by statistics at 10,000 years given below in Table 6-17.

Table 6-17. Statistics on cumulative brine flow out of the repository at 10,000 years for Replicate R1 for CRA-2009 PA and CRA-2004 PABC.

BRNREPOC (m ³)	CRA-2009 PA		CRA-2004 PABC	
	S2	S4	S2	S4
Minimum	9.70E+02	1.31E+00	8.20E+02	1.41E+00
Average	1.66E+04	2.71E+03	1.48E+04	1.36E+03
Maximum	1.79E+05	3.35E+04	1.78E+05	2.13E+04

Figure 6-95 - Figure 6-96 and Figure 6-97 - Figure 6-98 show PRCC's for BRNREPOC versus time for Scenario S2 and S4, from the CRA-2009 PA and the CRA-2004 PABC. In both scenarios, DRZ and borehole permeabilities have the strongest positive correlations.

Figure 6-99 and Figure 6-100 show the cumulative brine flow to the Culebra formation in Scenarios S2 and S4. Figure 6-101 and Figure 6-102 show cumulative brine flow to the LWB. Table 6-18 gives statistics on these flows at 10,000 years for S2, S4 and S6. Scenario S6 was included here because flow to the Culebra formation were slightly higher in S6 compared to S2, and because the results of S6 are only used to determine the radionuclide source term to the Culebra formation in the PANEL application (Kanney and Leigh 2005). The results indicate slightly higher brine flow to the Culebra formation and lower brine flow to the LWB in the CRA-2009 PA compared to the CRA-2004 PABC.

Table 6-19 shows statistics on cumulative brine flow to the Magenta and the Dewey Lake formations for scenarios S2 and S6. The results shown in Table 6-19 show that the maximum cumulative brine flow to the Magenta and Dewey Lake formations over the 10,000-year regulatory period are three to four orders of magnitude lower than flow to the Culebra formation. In looking at the results of Table 6-18 and Table 6-19, it's important to note that the Los Medanos, Tamarisk, and Forty Niner formations are set in the WIPP PAPDB to be essentially impermeable to liquid and gas flow in order to maximize the amount of brine flow into the

Culebra formation. This modeling approach was designed to add conservatism (Dotson 1996) to radionuclide release calculations since the Culebra formation is known to be the most transmissive unit above the repository. However, treating the Tamarisk and Forty-niner formations as impermeable should also over-estimate brine flow to the Magenta formation.

Table 6-18. Statistics on cumulative brine flow to the Culebra formation, and the LWB at 10,000 years for Replicate R1, for the CRA-2009 PA and CRA-2004 PABC. BRNBHRCC and BRAALLWC are variables calculated in the ALG2 post-processing step (see Table 4-1 and Appendix B).

Cumulative brine releases to the Culebra BRNBHRCC (m ³)	CRA-2009 PA			CRA-2004 PABC		
	S2	S4	S6	S2	S4	S6
Minimum	6.28E-01	1.81E-01	4.10E+00	6.35E-01	2.27E-01	4.04E+00
Average	9.52E+03	1.04E+02	9.62E+03	9.51E+03	1.09E+02	9.58E+03
Maximum	1.72E+05	1.56E+03	1.75E+05	1.72E+05	1.46E+03	1.75E+05

Cumulative brine releases to the LWB BRAALLWC (m ³)	CRA-2009 PA		CRA-2004 PABC	
	S2	S4	S2	S4
Minimum	4.79E-05	4.79E-05	4.96E-05	4.96E-05
Average	1.40E+01	1.25E+01	8.31E+00	7.43E+00
Maximum	1.28E+03	1.17E+03	8.28E+02	7.42E+02

Table 6-19. Statistics on cumulative brine flow to the Magenta and the Dewey Lake formations at 10,000 years for Replicate R1 of the CRA-2009 PA and the CRA-2009 PABC. BRNBHUP4 and BRNBHUP6 are variables that were calculated in a ALG2 post-processing step that is described above in Subsection 6.4.8.

Cumulative brine releases to the Magenta BRNBHUP4 (m ³)	CRA-2009 PA		CRA-2004 PABC	
	S2	S6	S2	S6
Minimum	2.20E-19	6.28E-19	2.20E-19	6.28E-19
Average	1.65E-01	8.51E-05	1.34E-01	1.10E-05
Maximum	4.03E+00	7.44E-03	4.19E+00	8.53E-05

Cumulative brine releases to the Dewey Lake BRNBHUP6 (m ³)	CRA-2009 PA		CRA-2004 PABC	
	S2	S6	S2	S6
Minimum	0.00E+00	0.00E+00	0.00E+00	0.00E+00
Average	2.91E-02	0.00E+00	3.12E-02	0.00E+00
Maximum	5.03E-01	0.00+00	5.75E-01	0.00E+00

6.4.9 Figures for Subsection 6.4

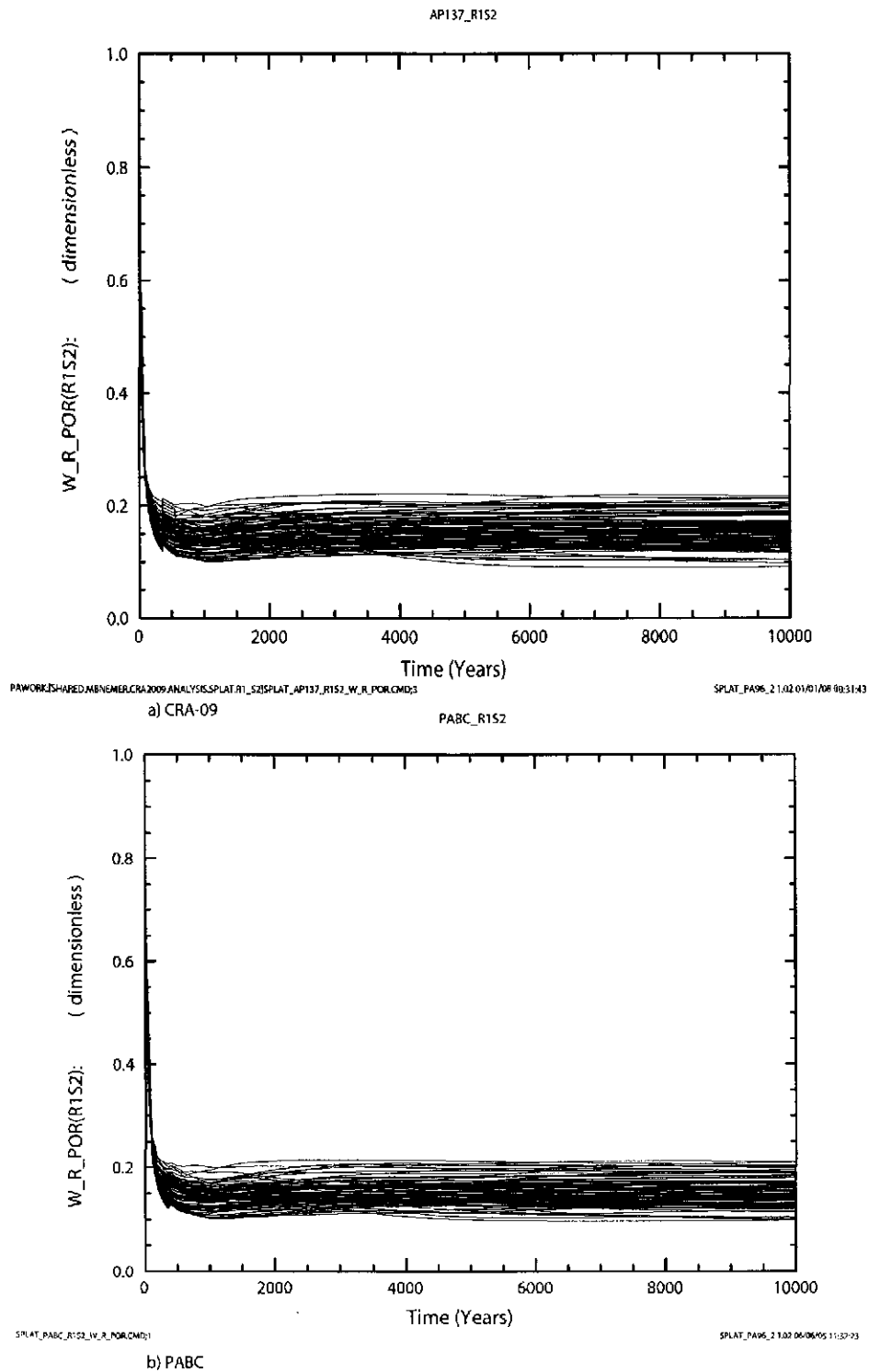
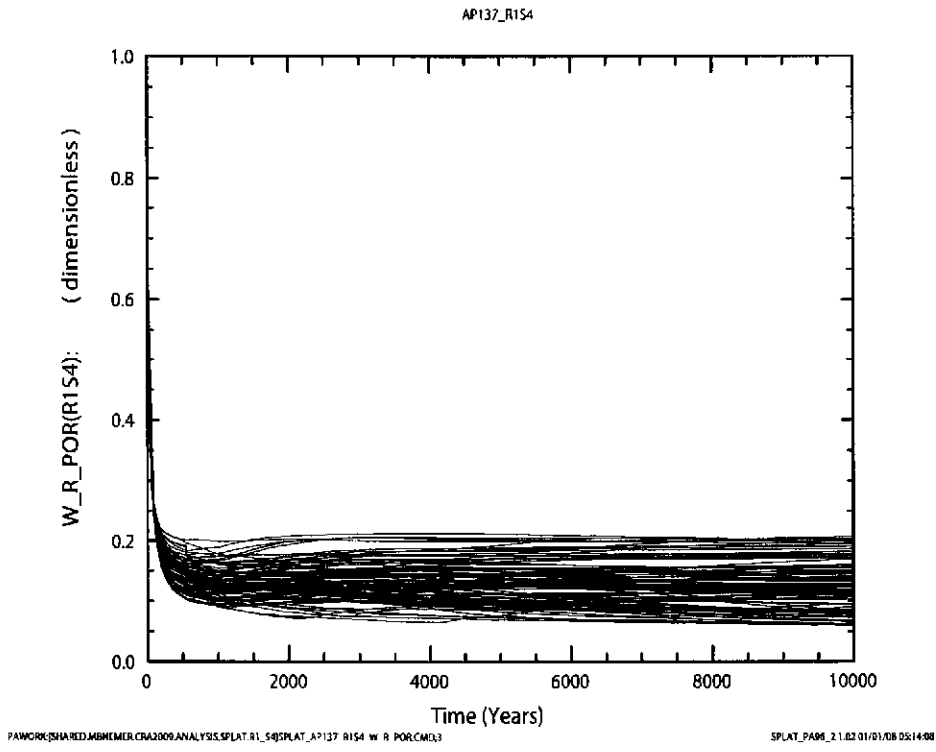
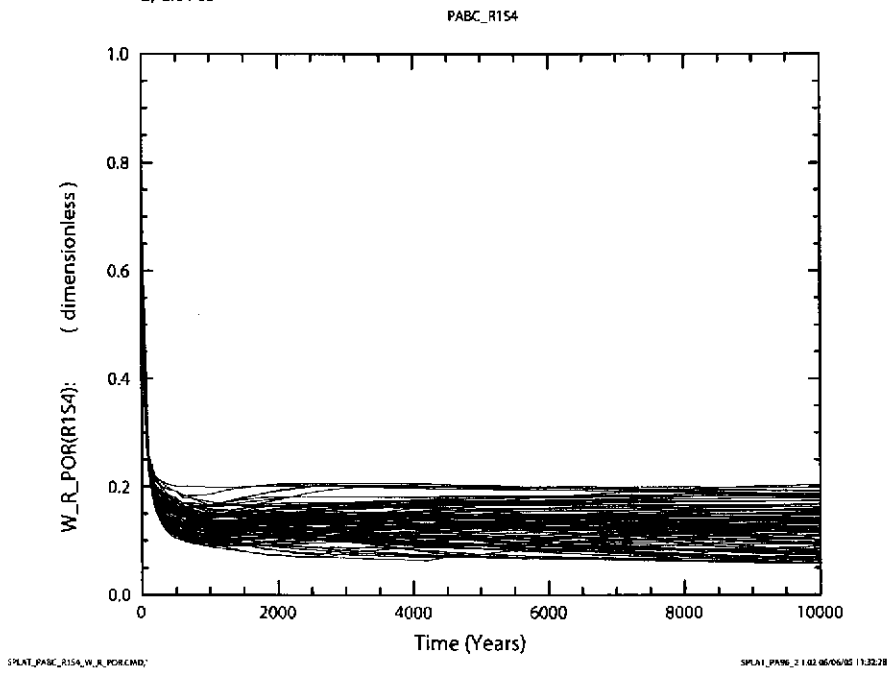


Figure 6-38. Volume averaged porosity (dimensionless) in all waste regions versus time (years) for all 100 vectors in Replicate R1, Scenario S2. Figure a) shows results from the CRA-2009 PA. Figure b) shows results from the CRA-2004 PABC.

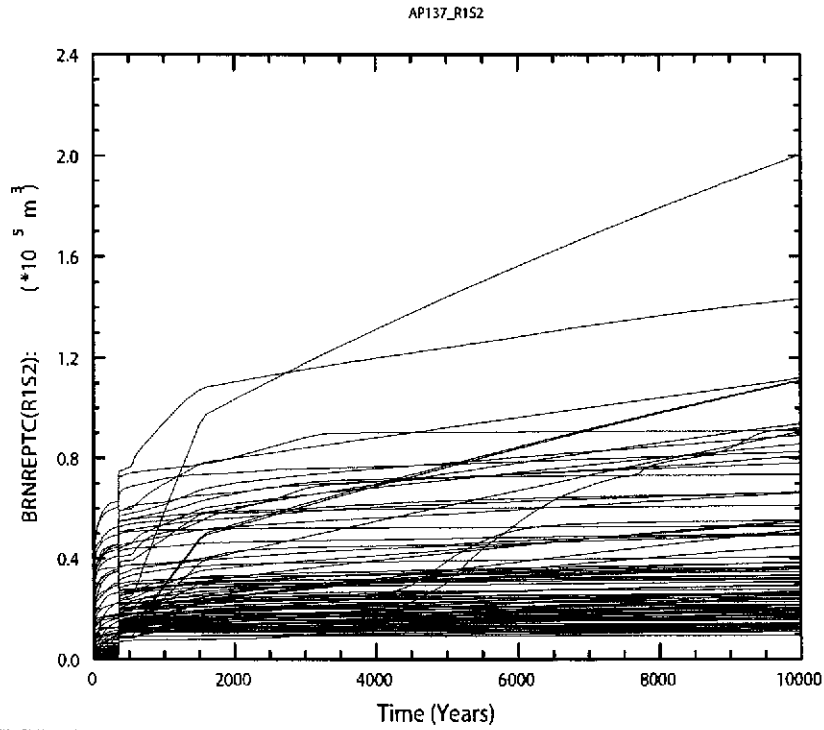


a) CRA-09



b) PABC

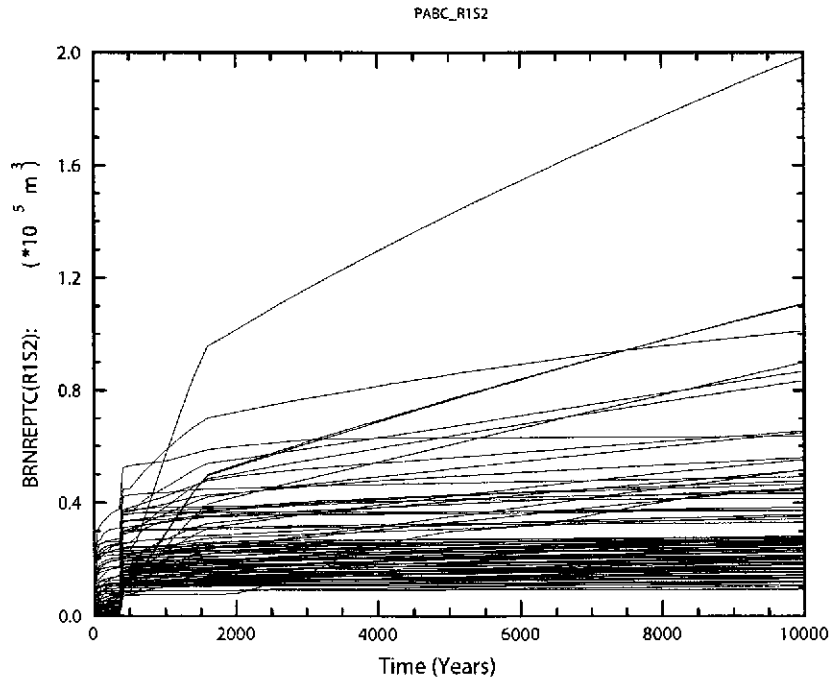
Figure 6-39. Volume averaged porosity (dimensionless) in all waste regions versus time (years) for all 100 vectors in Replicate R1, Scenario S4. Figure a) shows results from the CRA-2009 PA. Figure b) shows results from the CRA-2004 PABC.



PAW00K\SHARED\MBNEMER\CRA2009\ANALYSIS\SPLAT_R1_S2\SPLAT_AP137_R152_BRNREPTC.MD:3

SPLAT_PAGE_2 11/02/01/01/08 01:53:22

a) CRA-09

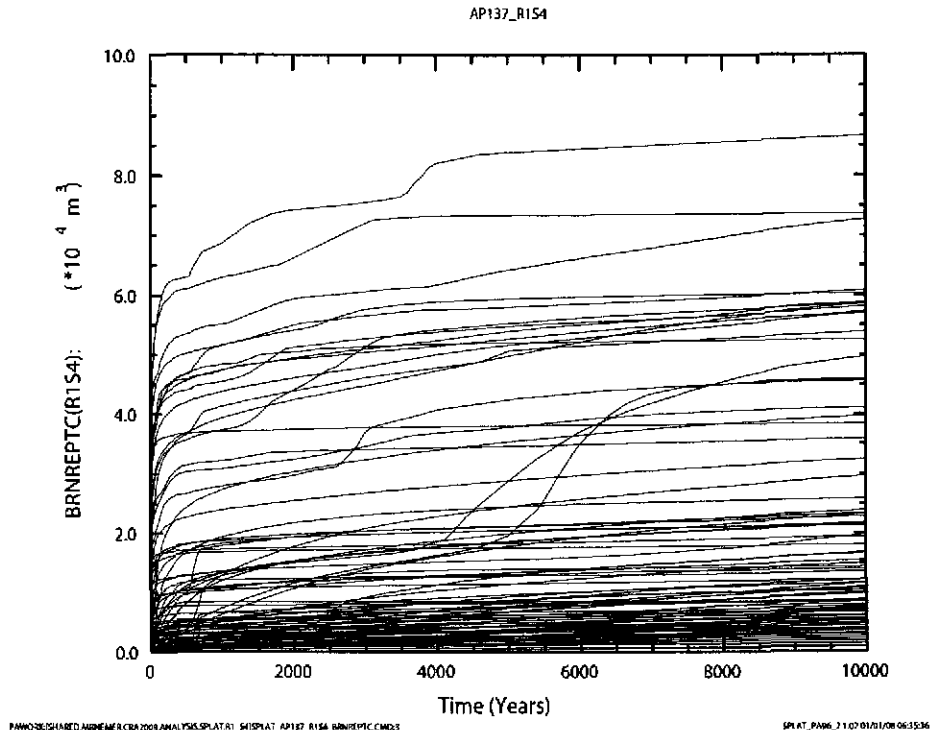


SPLAT_PABC_R152_BRNREPTC.MD:1

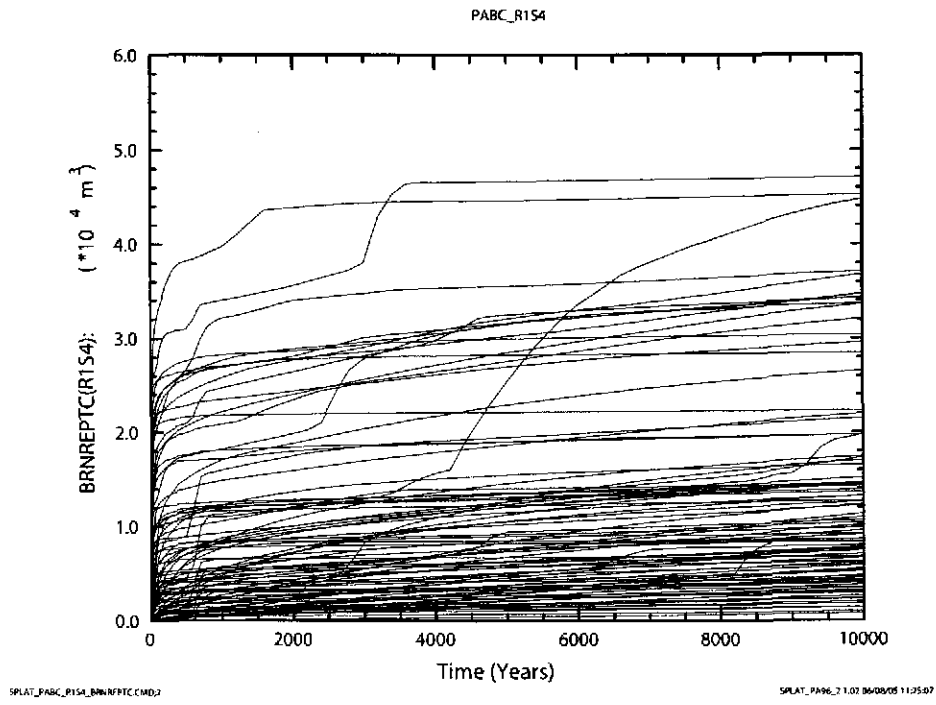
SPLAT_PAGE_7 11/02/06/00/15 12:18:48

b) PABC

Figure 6-40. Total cumulative inflow (m^3) of brine into the repository versus time (years) for all 100 vectors in Replicate R1, Scenario S2. Figure a) shows results from the CRA-2009 PA. Figure b) shows results from the CRA-2004 PABC.

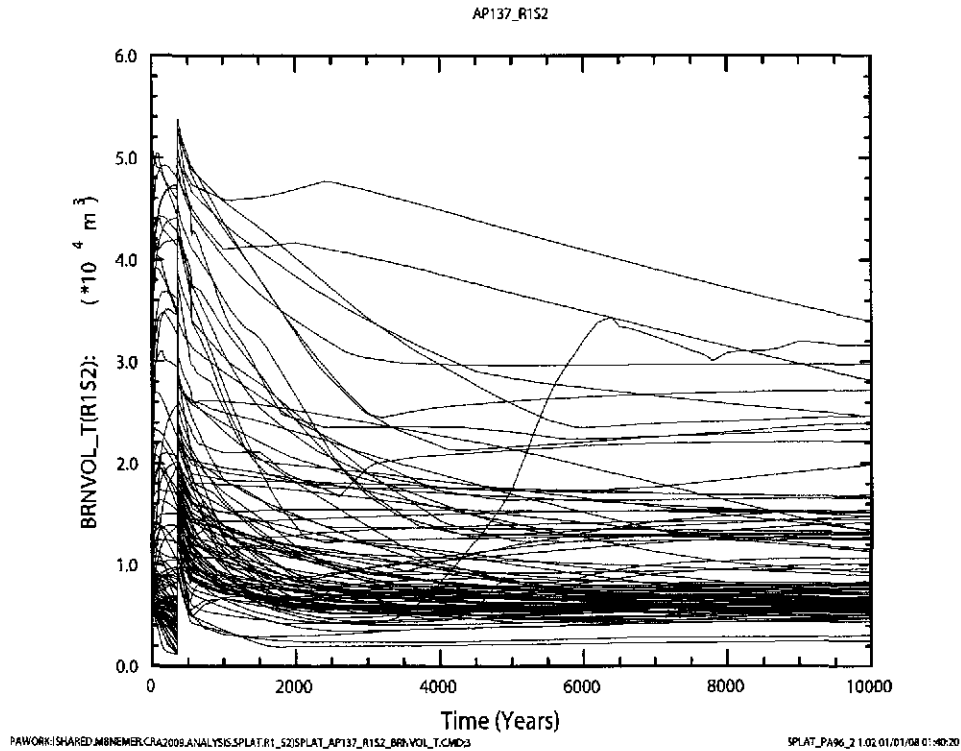


a) CRA-09

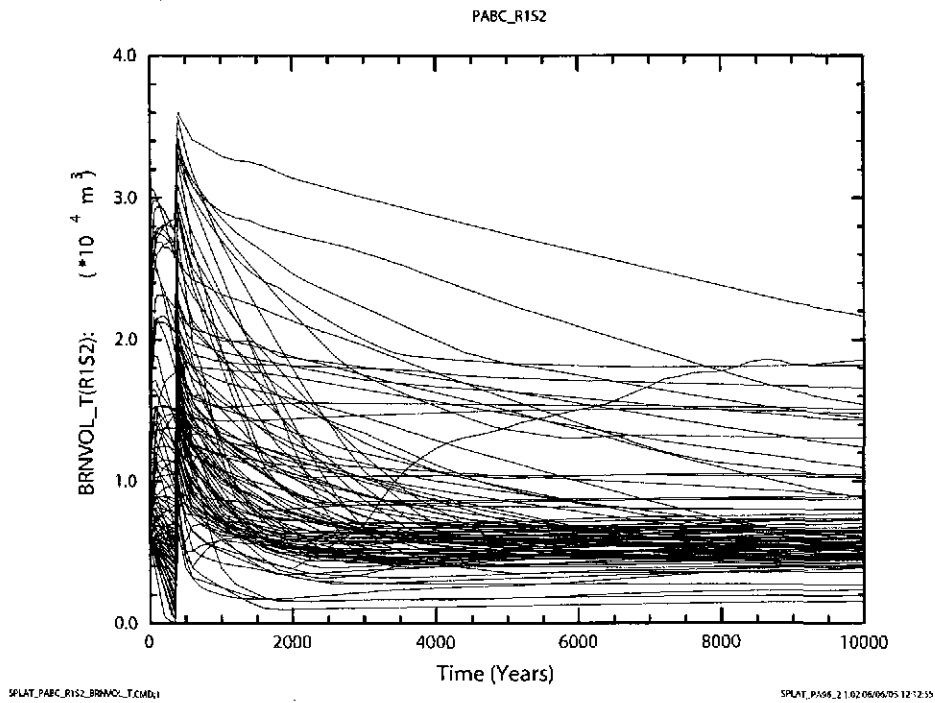


b) PABC

Figure 6-41. Total cumulative inflow of brine (m^3) into the repository versus time (years) for all 100 vectors in Replicate R1, Scenario S4. Figure a) shows results from the CRA-2009 PA. Figure b) shows results from the CRA-2004 PABC.



a) CRA-09



b) PABC

Figure 6-42. Total volume (m^3) of brine in the repository versus time (years) for all 100 vectors in Replicate R1, Scenario S2. Figure a) shows results from the CRA-2009 PA. Figure b) shows results from the CRA-2004 PABC.

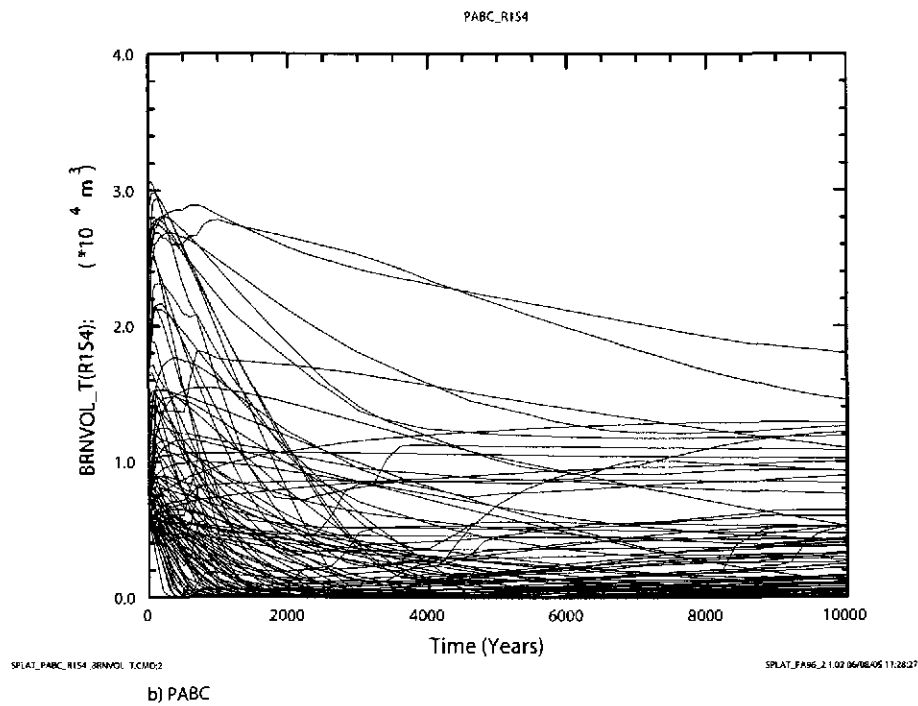
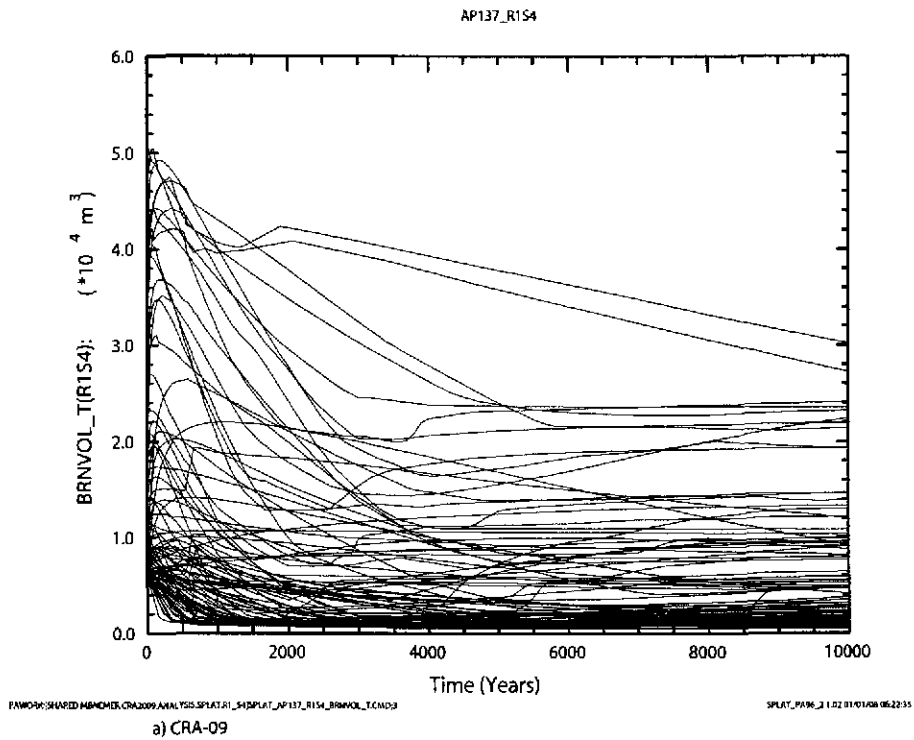
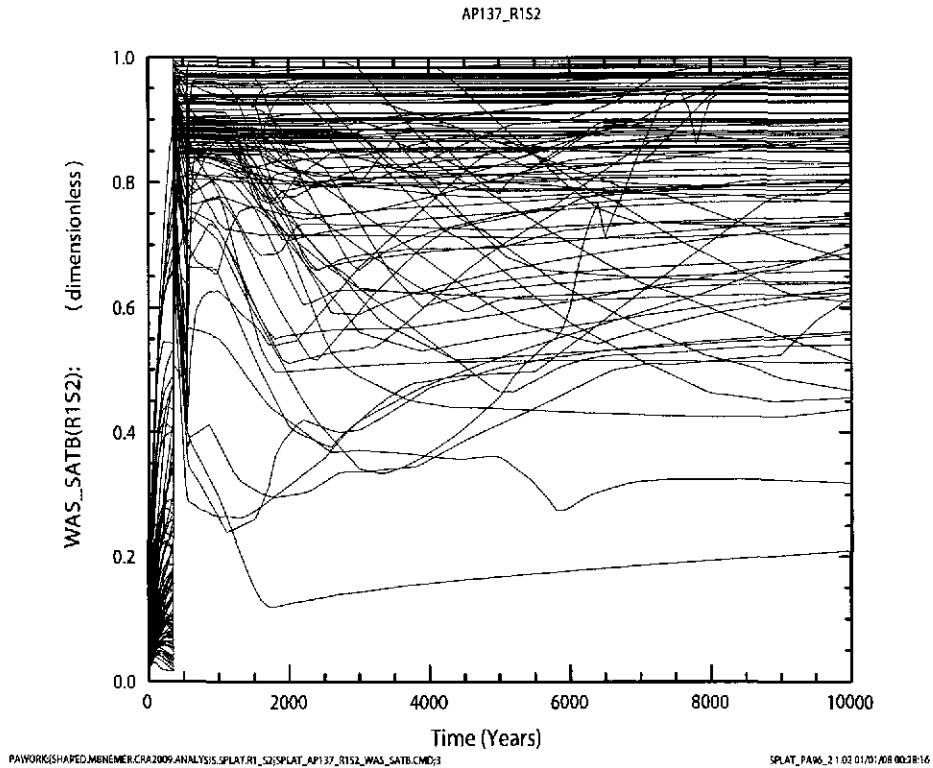
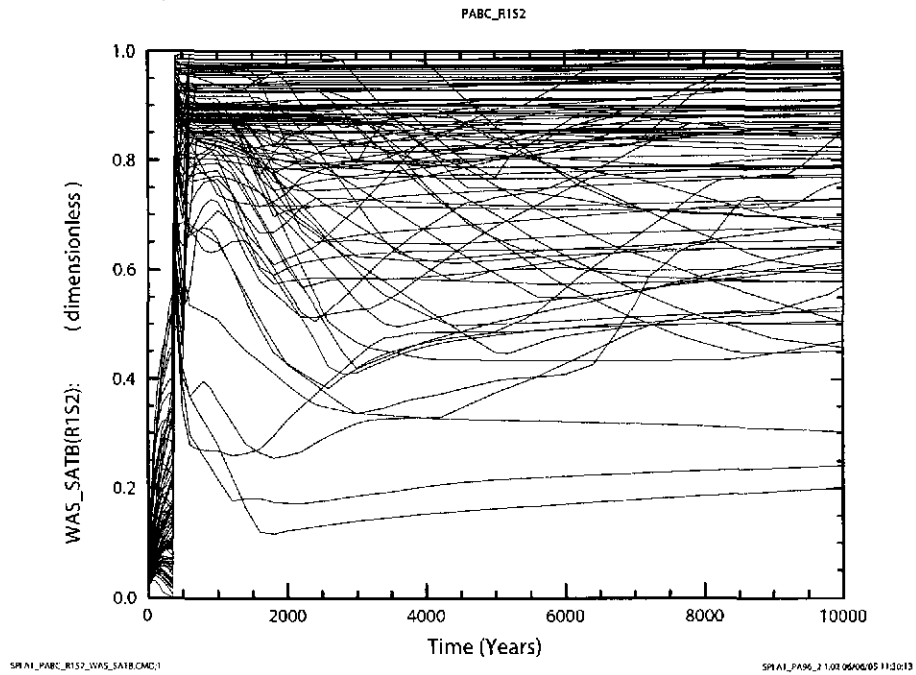


Figure 6-43. Total volume (m^3) of brine in the repository versus time (years) for all 100 vectors in Replicate R1, Scenario S4. Figure a) shows results from the CRA-2009 PA. Figure b) shows results from the CRA-2004 PABC.

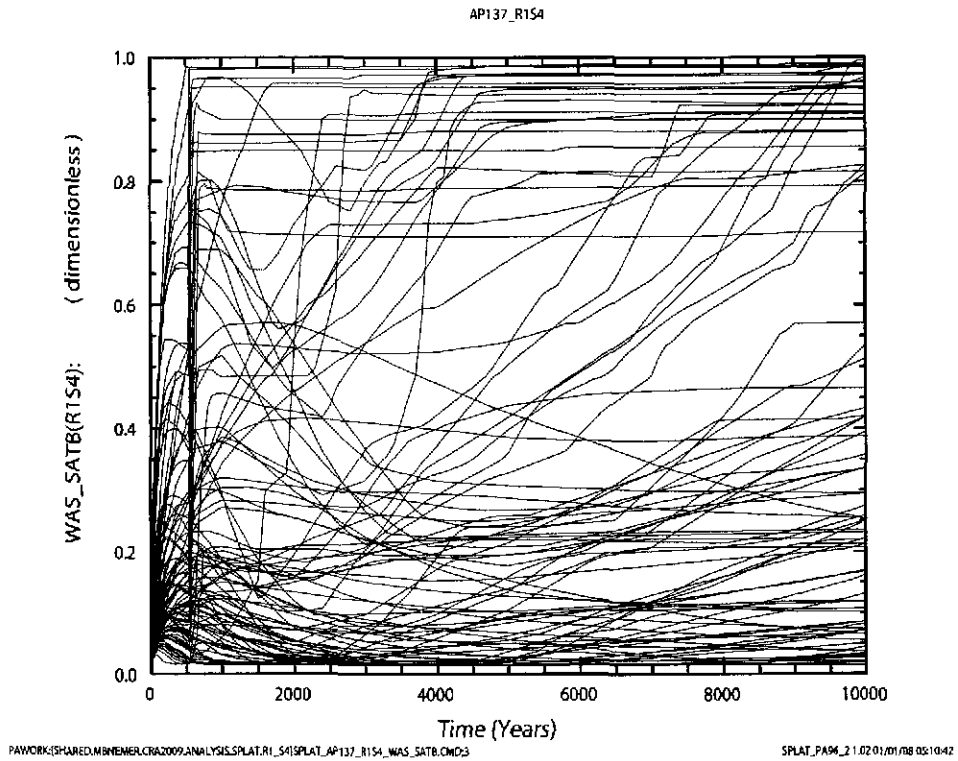


a) CRA-09

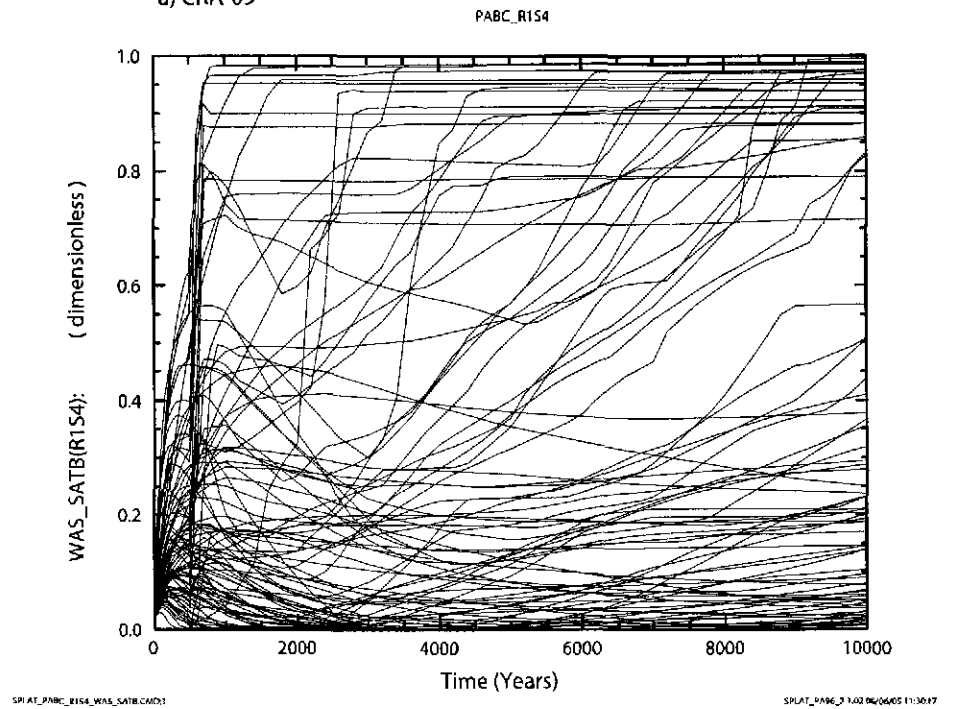


b) PABC

Figure 6-44. Brine saturation (dimensionless) in the Waste Panel versus time (years) for all 100 vectors in Replicate R1, Scenario S2. Figure a) shows results from the CRA-2009 PA. Figure b) shows results from the CRA-2004 PABC.



a) CRA-09



b) PABC

Figure 6-45. Brine saturation (dimensionless) in the waste panel versus time (years) for all 100 vectors in Replicate R1, Scenario S4. Figure a) shows results from the CRA-2009 PA. Figure b) shows results from the CRA-2004 PABC.

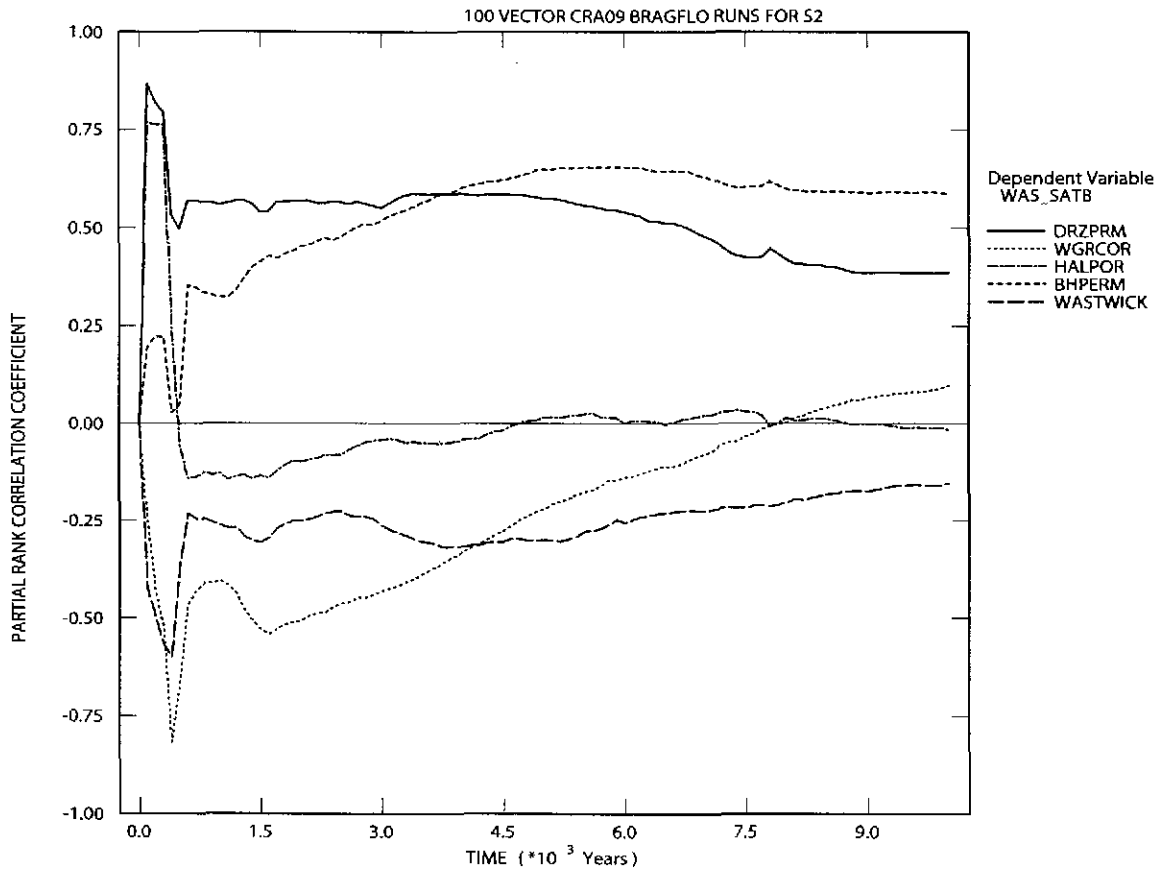


Figure 6-46. Primary correlations of brine saturation (dimensionless) in the Waste Panel with input parameters versus time (years) from the CRA-2009 PA, Replicate R1, Scenario S2. Table 4-2 gives a description of the names in the legend.

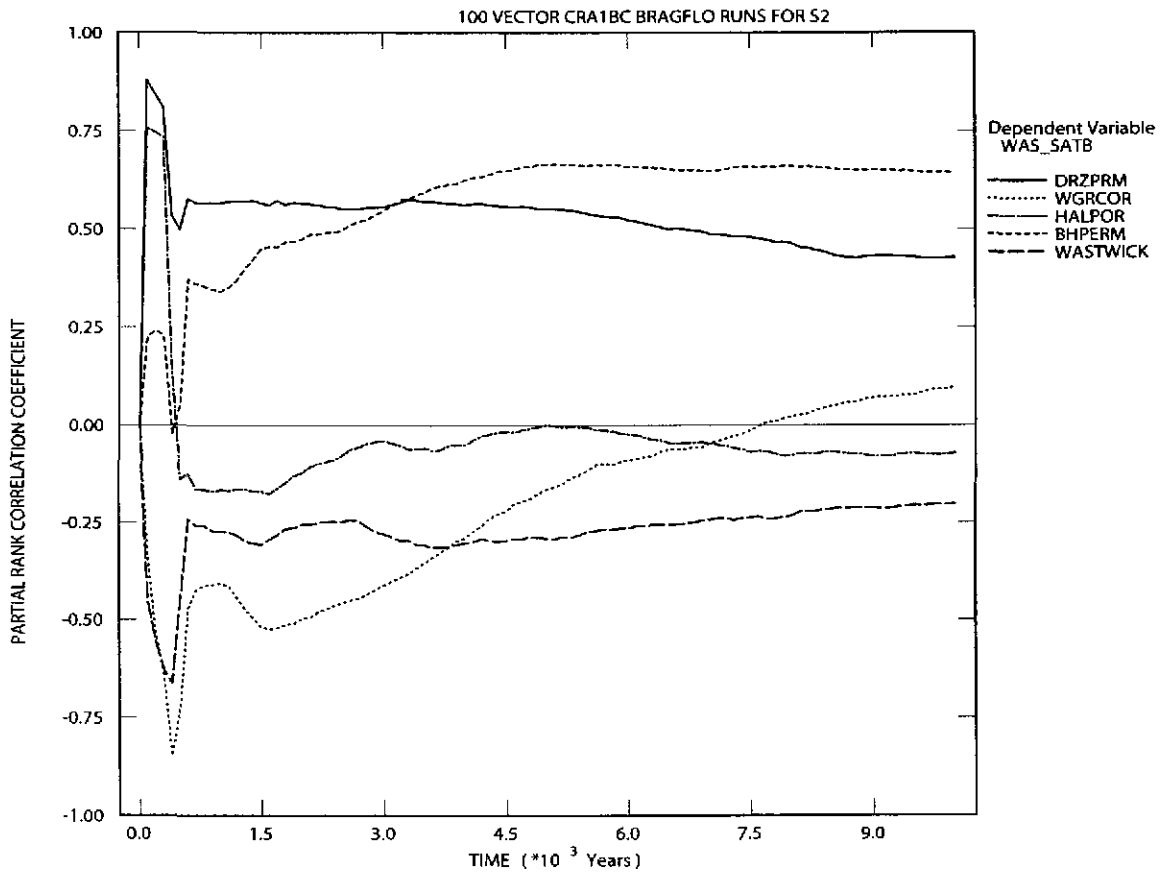


Figure 6-47. Primary correlations of brine saturation (dimensionless) in the Waste Panel with input parameters versus time (years) from the CRA-2004 PABC, Replicate R1, Scenario S2. Table 4-2 gives a description of the names in the legend.

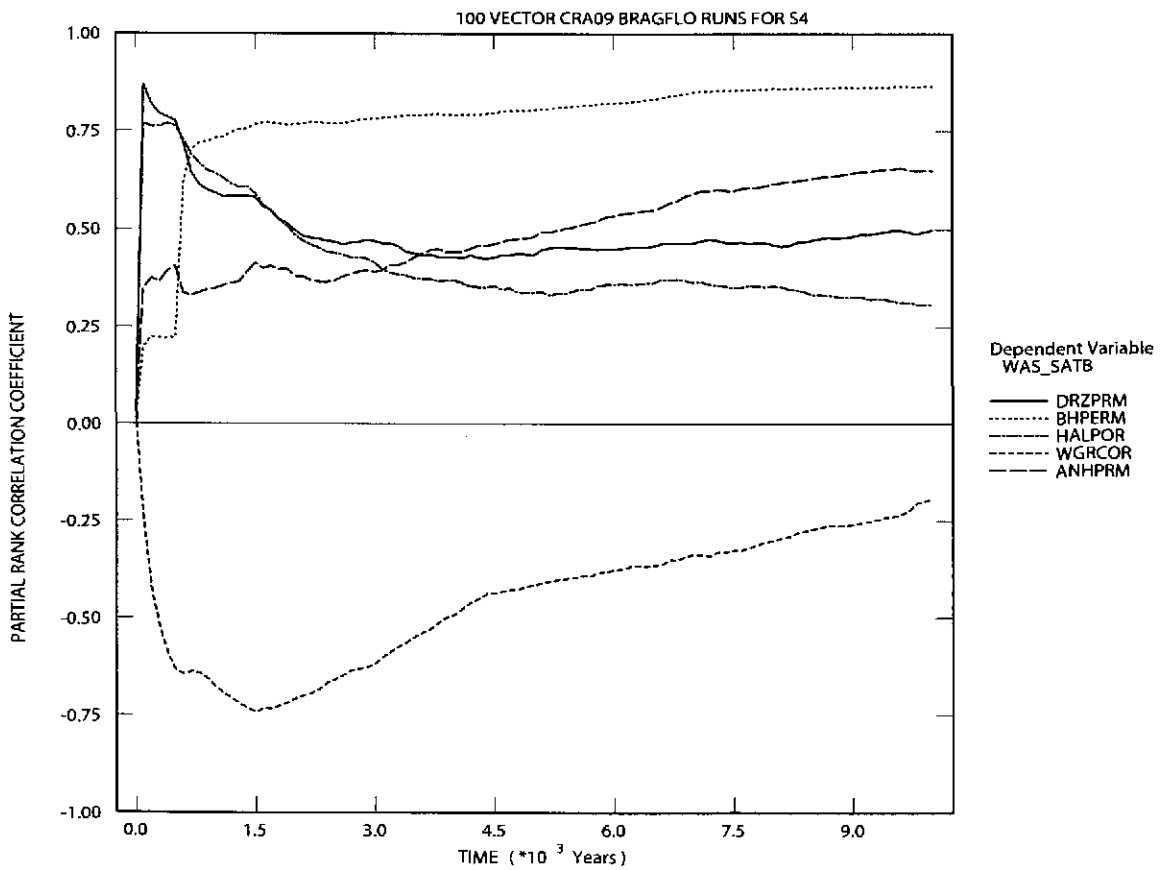


Figure 6-48. Primary correlations of brine saturation (dimensionless) in the waste panel with input parameters versus time (years) from the CRA-2009 PA, Replicate R1, Scenario S4. Table 4-2 gives a description of the names in the legend.

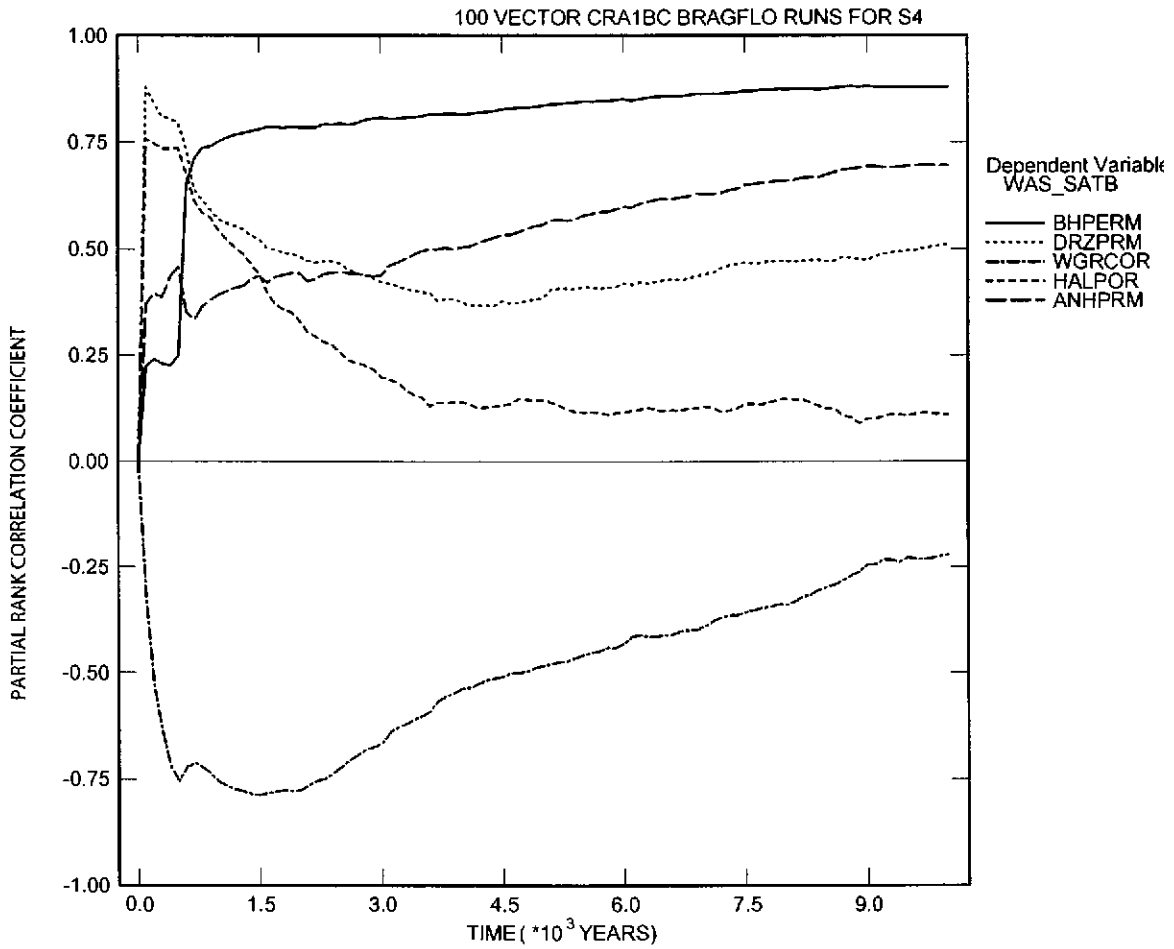
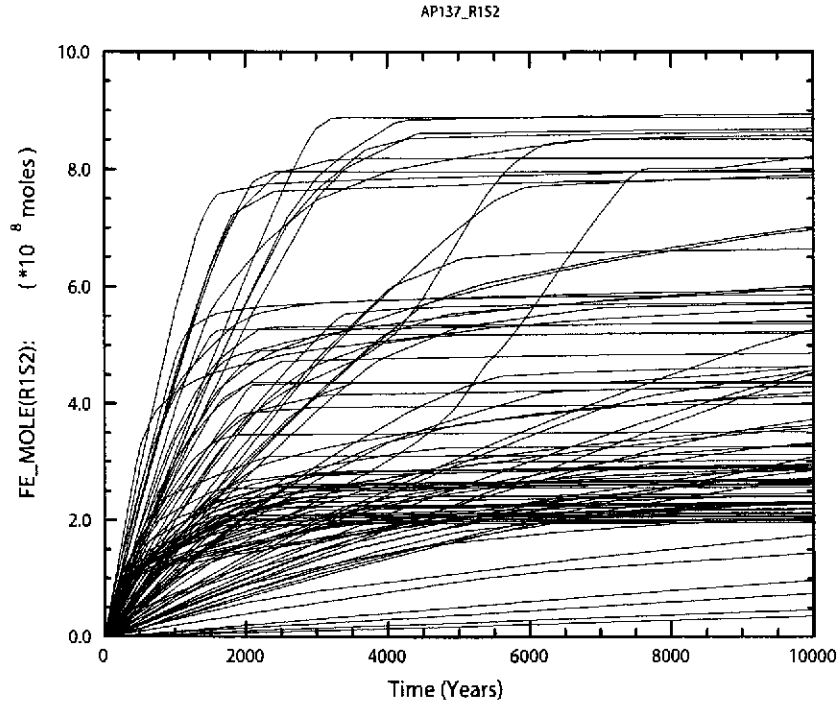
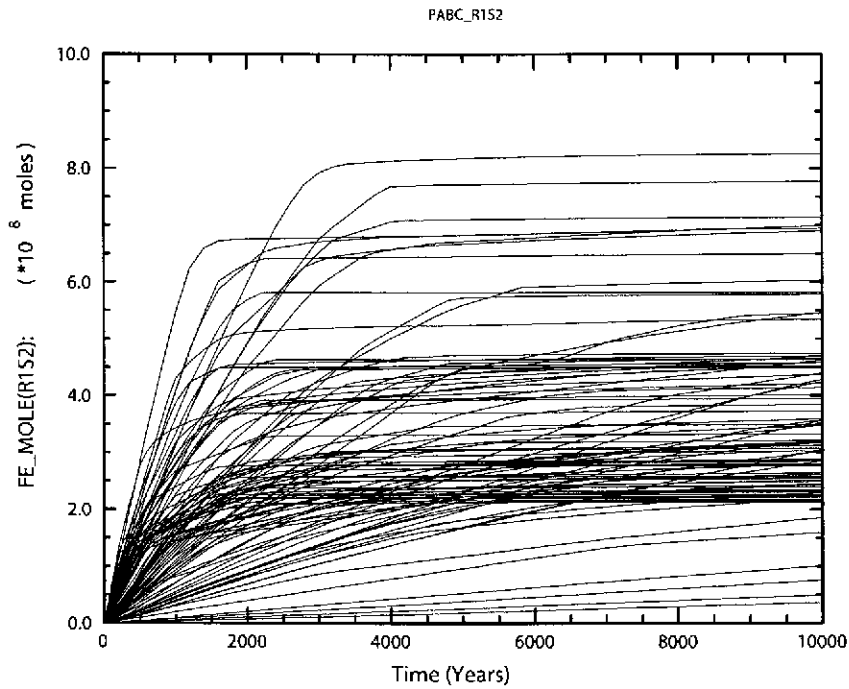


Figure 6-49. Primary correlations of brine saturation (dimensionless) in the waste panel with input parameters versus time (years) from the CRA-2004 PABC, Replicate R1, Scenario S4. Table 4-2 gives a description of the names in the legend.

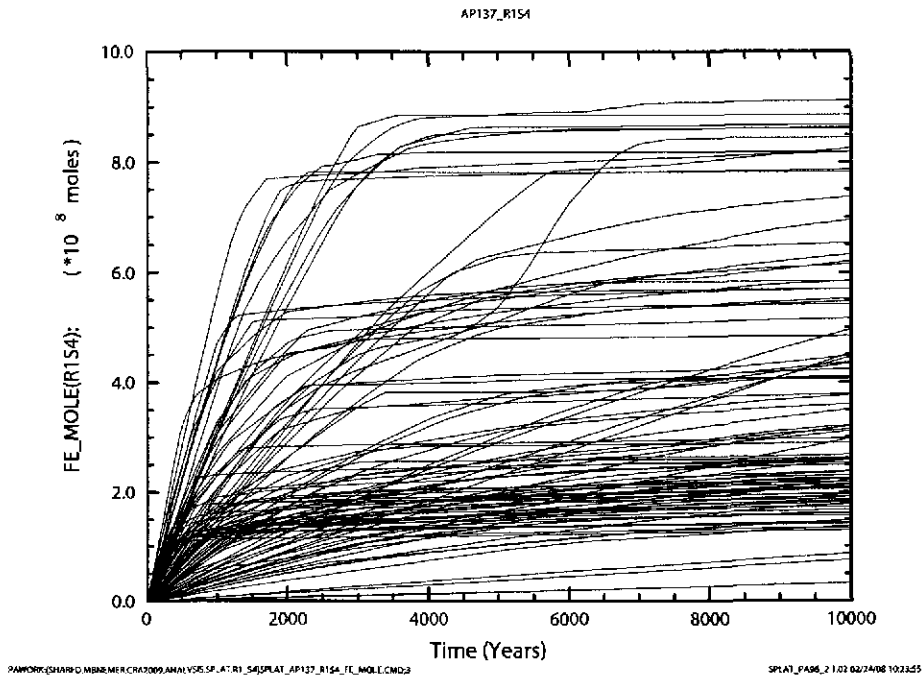


a) CRA-09

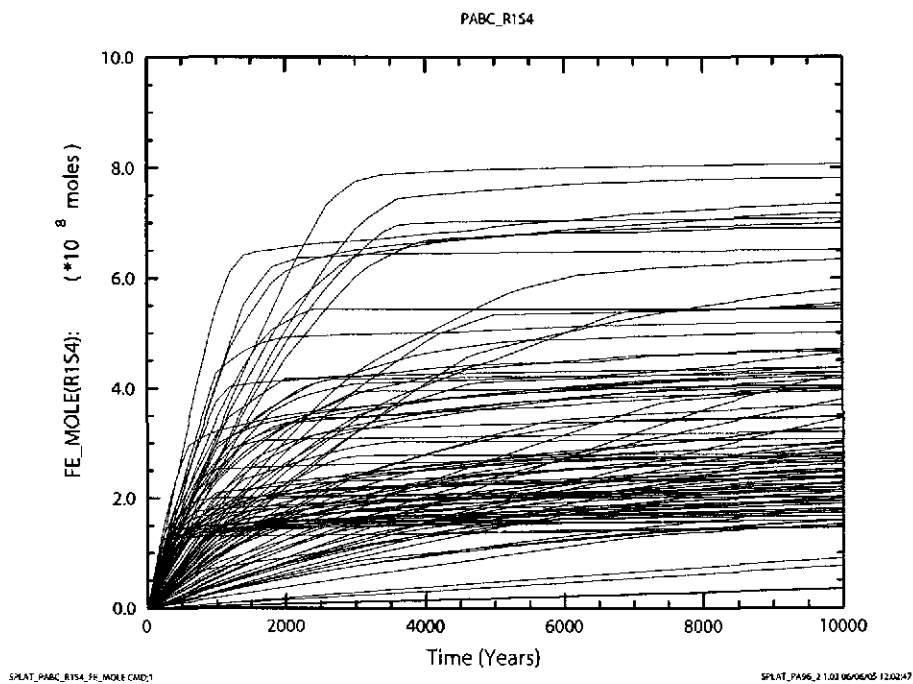


b) PABC

Figure 6-50. Cumulative moles of gas (moles) produced by iron corrosion versus time (years) for all 100 vectors in Replicate R1, Scenario S2. Figure a) shows results from the CRA-2009 PA. Figure b) shows results from the CRA-2004 PABC.



a) CRA-09



b) PABC

Figure 6-51. Cumulative moles of gas (moles) produced by iron corrosion versus time (years) for all 100 vectors in Replicate R1, Scenario S4. Figure a) shows results from the CRA-2009 PA. Figure b) shows results from the CRA-2004 PABC.

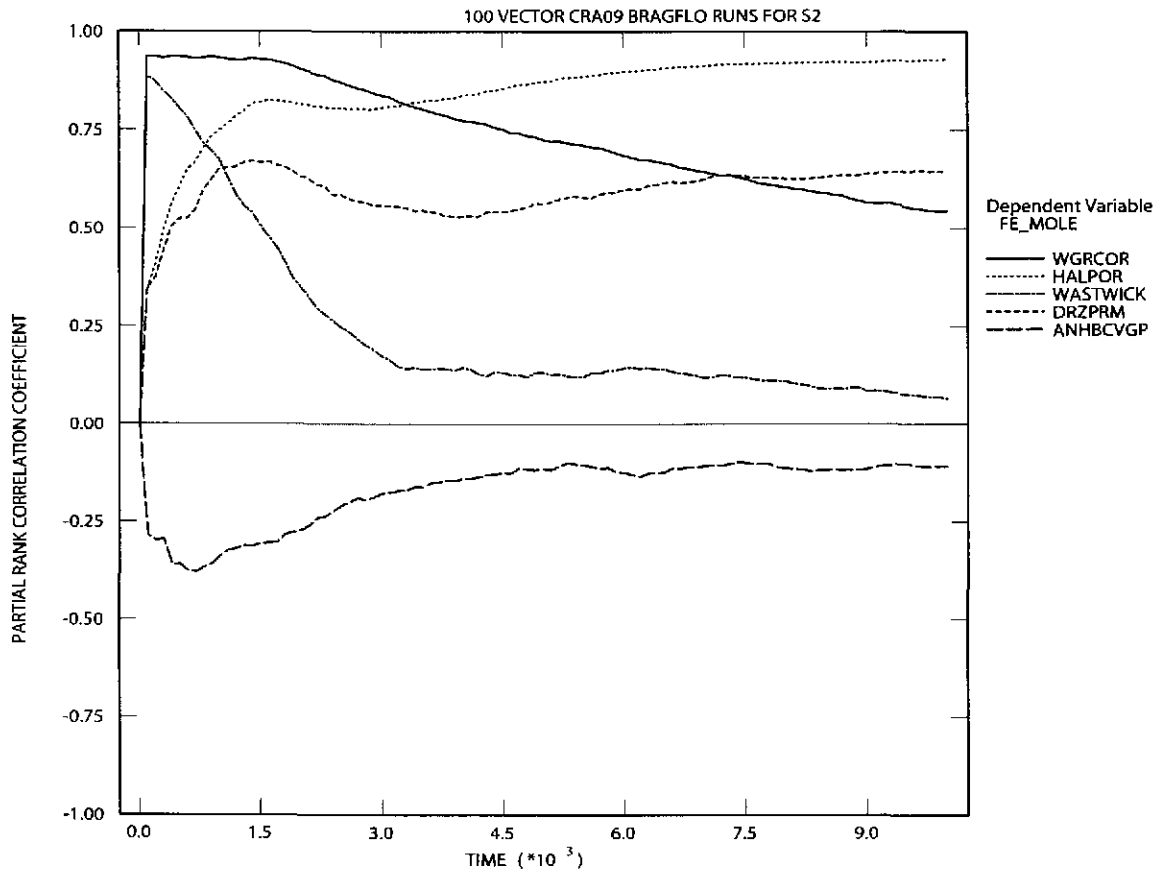


Figure 6-52. Primary correlations of cumulative amount (moles) of gas produced by iron corrosion in the waste panel with input parameters versus time (years) from the CRA-2009 PA, Replicate R1, Scenario S2. Table 4-2 gives a description of the names in the legend.

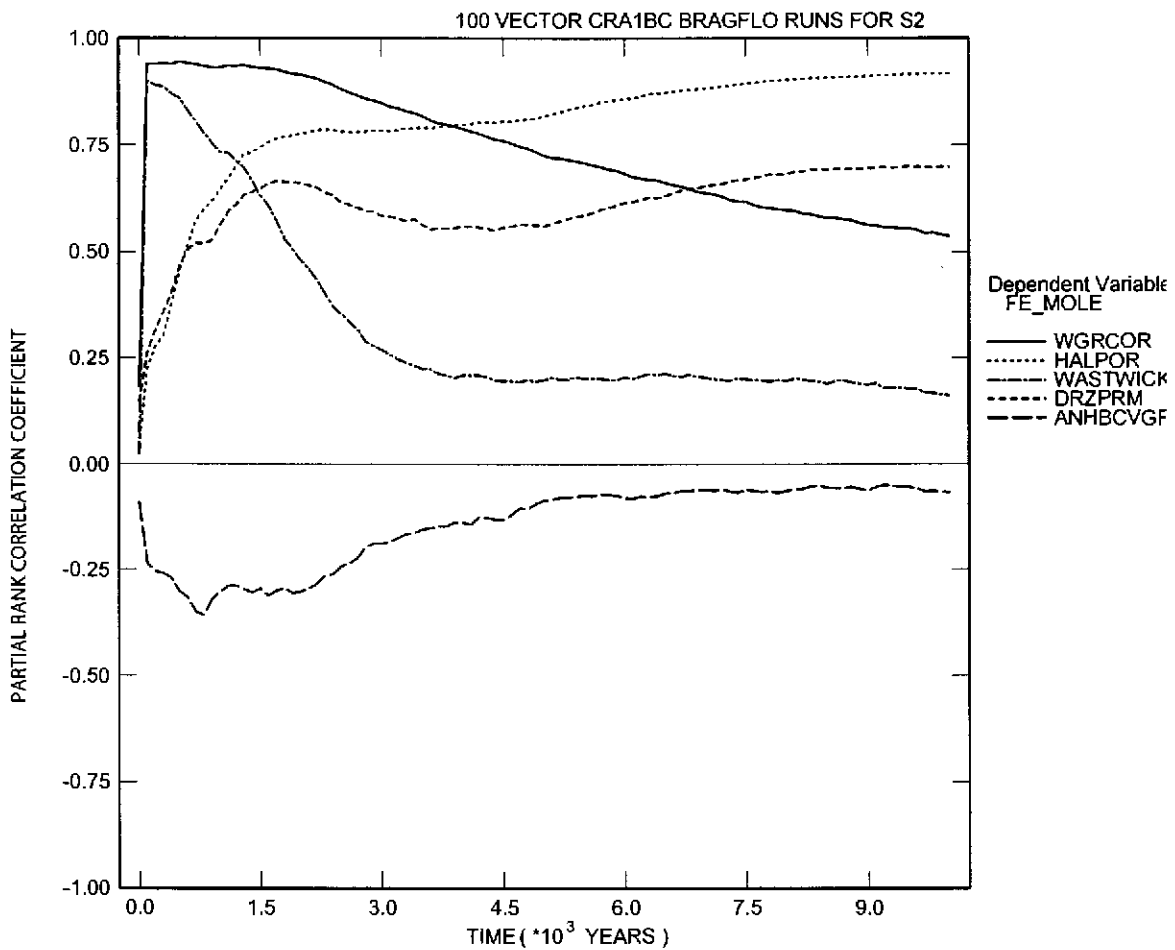


Figure 6-53. Primary correlations of cumulative amount (moles) of gas produced by iron corrosion in the waste panel with input parameters versus time (years) from the CRA-2004 PABC, Replicate R1, Scenario S2. Table 4-2 gives a description of the names in the legend.

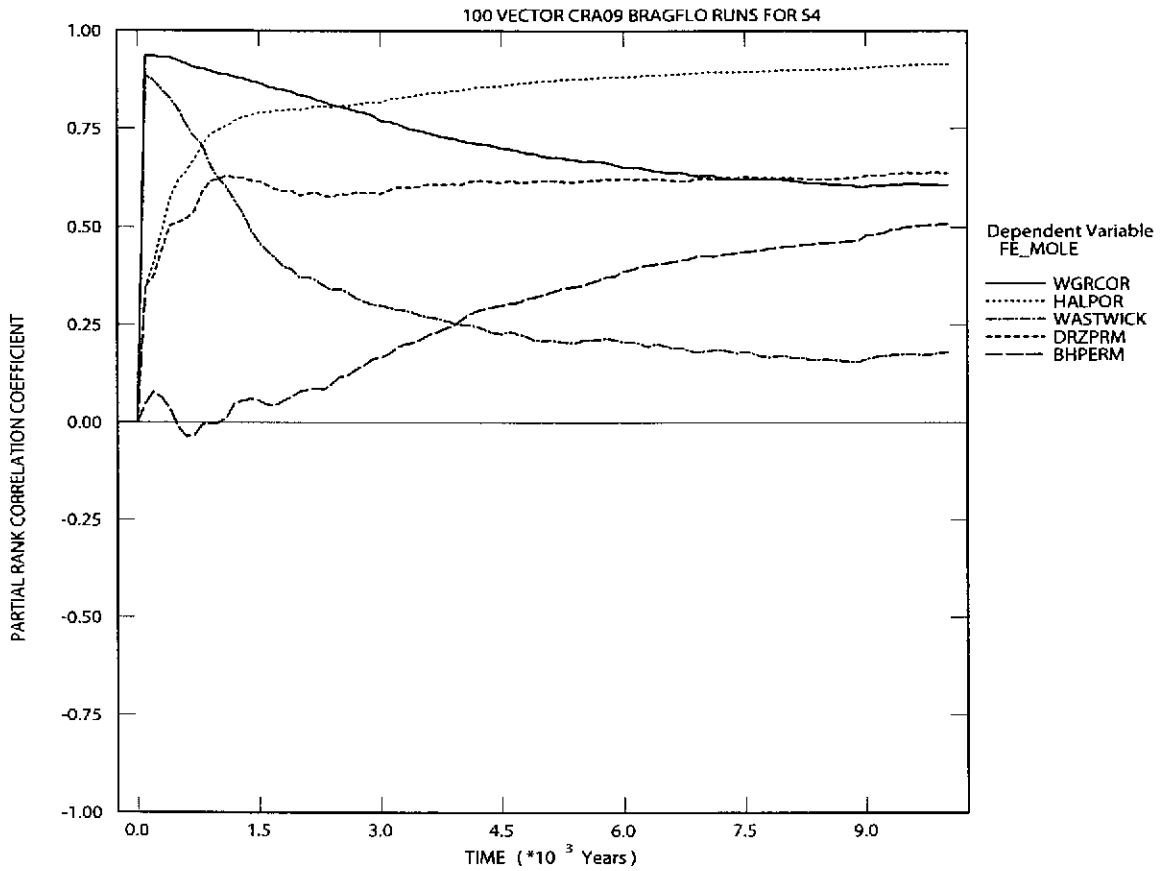


Figure 6-54. Primary correlations of cumulative amount (moles) of gas produced by iron corrosion in the waste panel with input parameters versus time (years) from the CRA-2009 PA, Replicate R1, Scenario S4. Table 4-2 gives a description of the names in the legend.

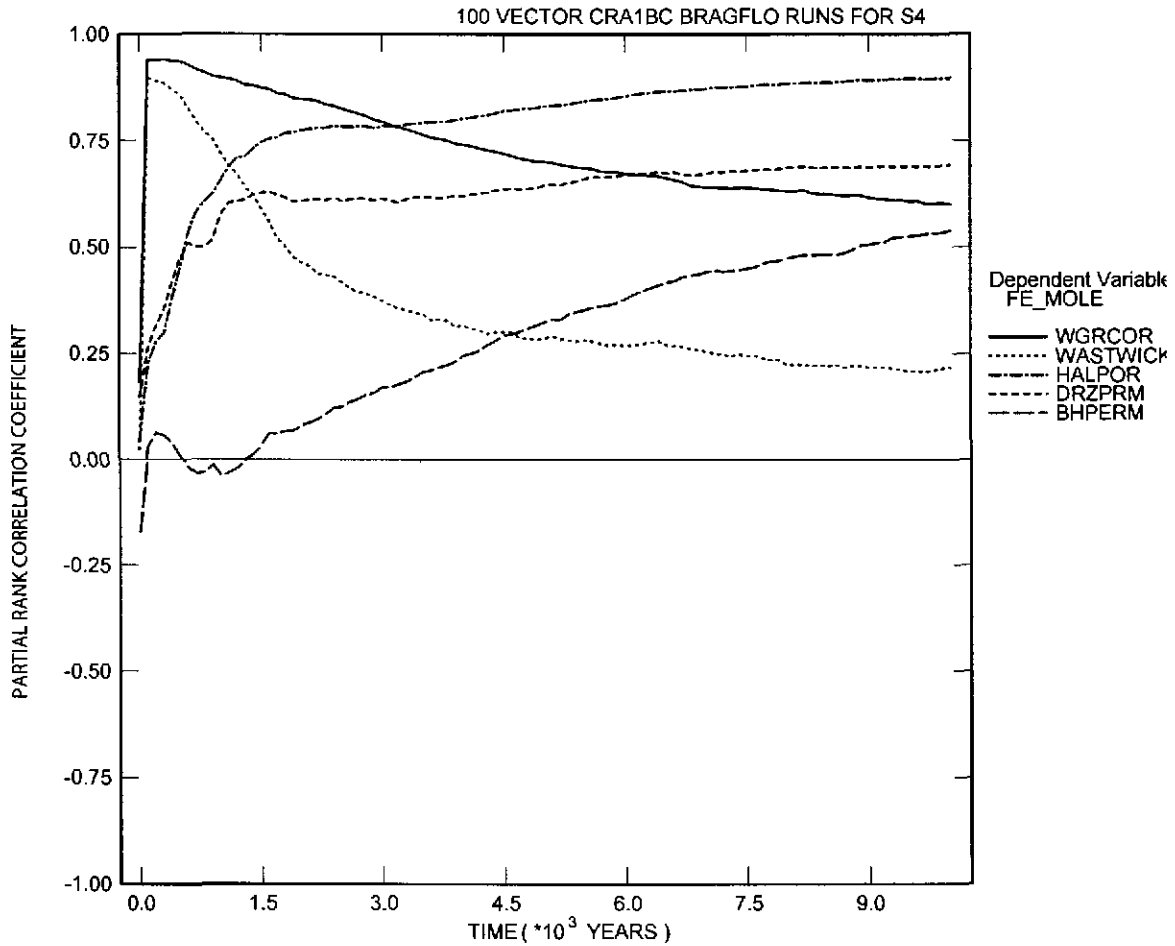
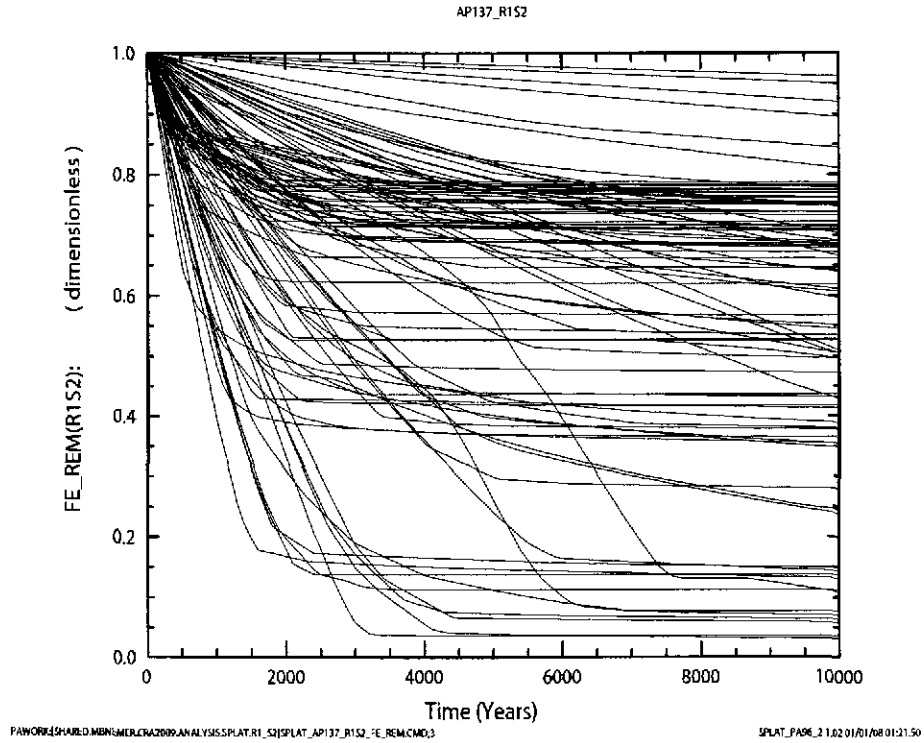
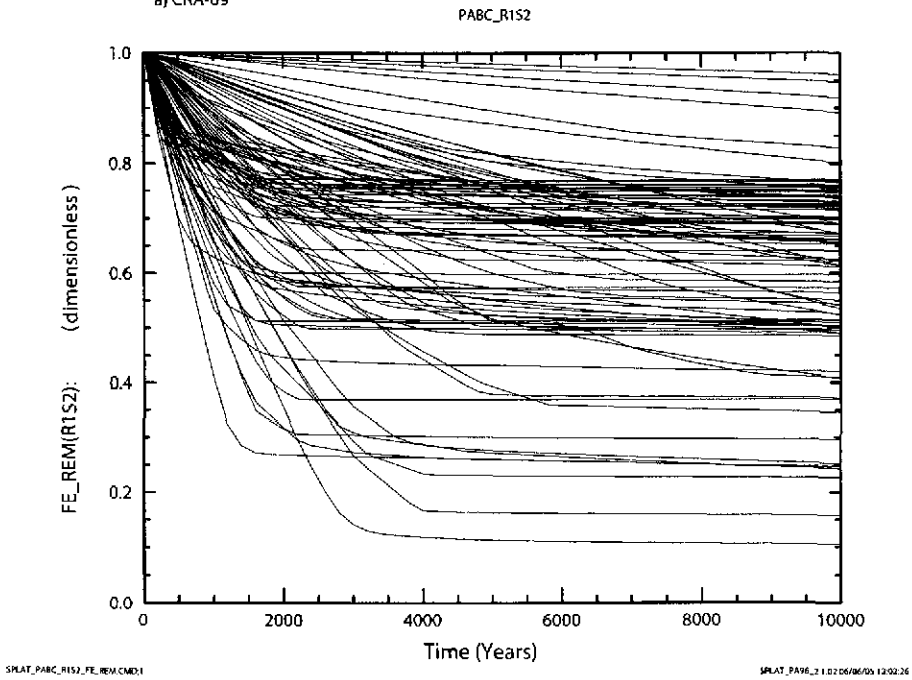


Figure 6-55. Primary correlations of cumulative amount (moles) of gas produced by iron corrosion in the waste panel with input parameters versus time (years) from the CRA-2004 PABC, Replicate R1, Scenario S4. Table 4-2 gives a description of the names in the legend.

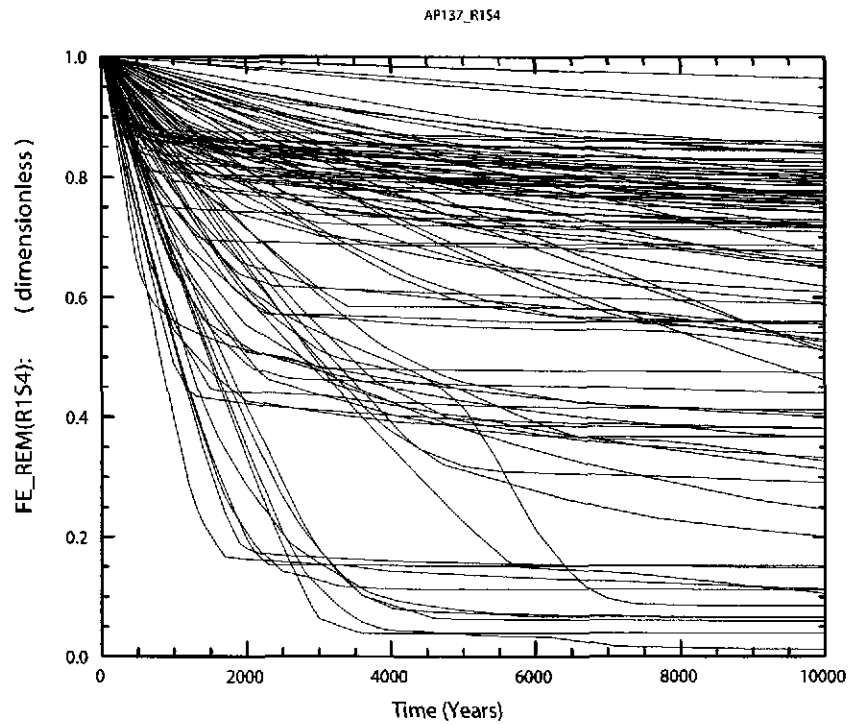


a) CRA-09



b) PABC

Figure 6-56. Fraction of iron (dimensionless) remaining versus time (years) for all 100 vectors in Replicate R1, Scenario S2. Figure a) shows results from the CRA-2009 PA. Figure b) shows results from the CRA-2004 PABC.

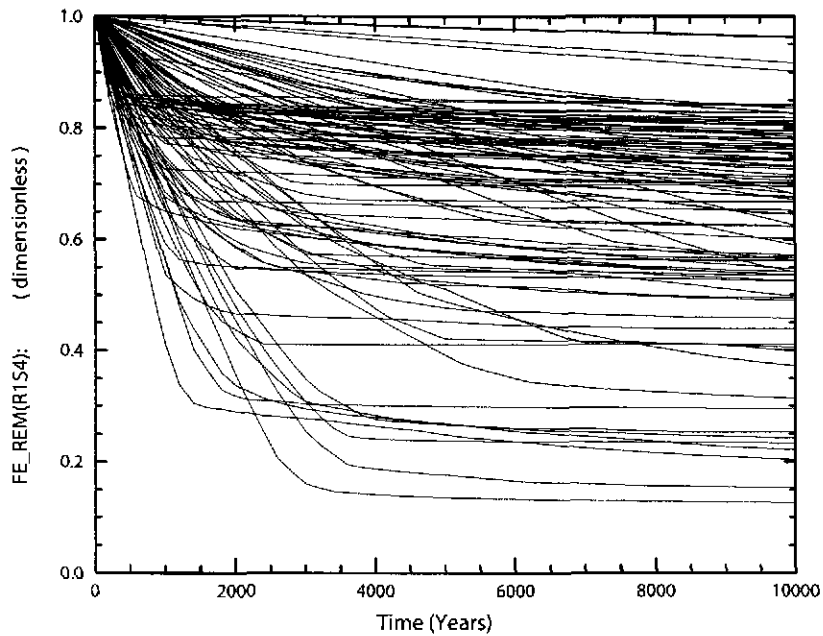


PAWORK\SHARED\MENEMER\CRA2009\ANALYSIS\SPLAT\R1_S4\SPLAT_AP137_R1S4_FE_REM.CMD.3

SPLAT_PA96_2110201401A80604.10

a) CRA-09

PABC_R1S4



SPLAT_PARC_R1S4_FE_REM.CMD.1

SPLAT_PA96_211020600AS120025

a) PABC

Figure 6-57. Fraction of iron (dimensionless) remaining versus time (years) for all 100 vectors in Replicate R1, Scenario S4. Figure a) shows results from the CRA-2009 PA. Figure b) shows results from the CRA-2004 PABC.

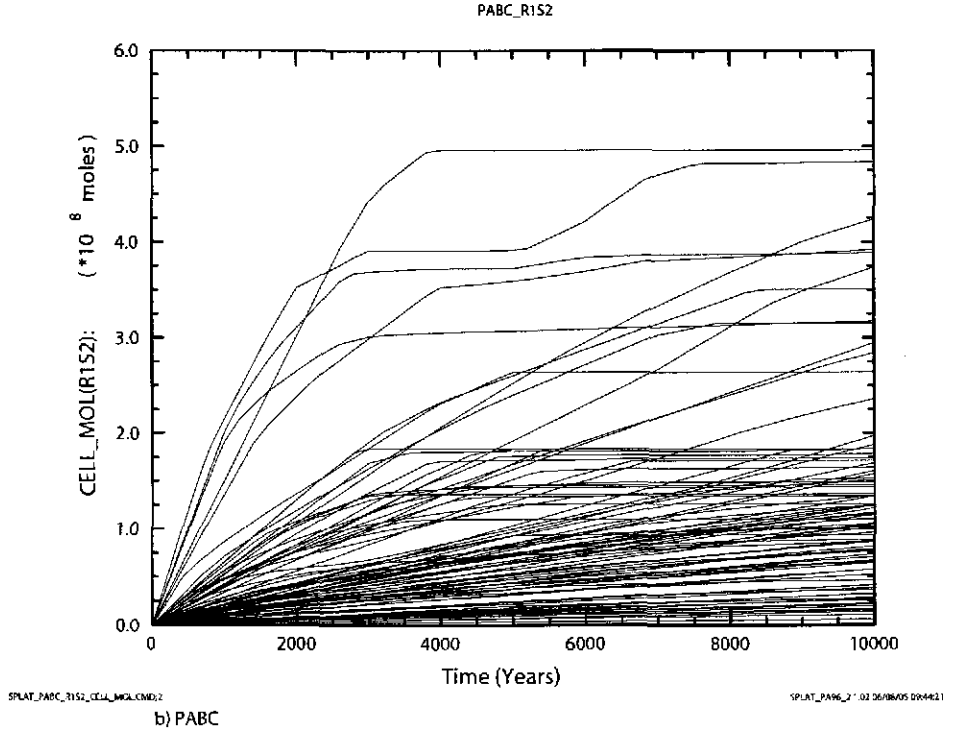
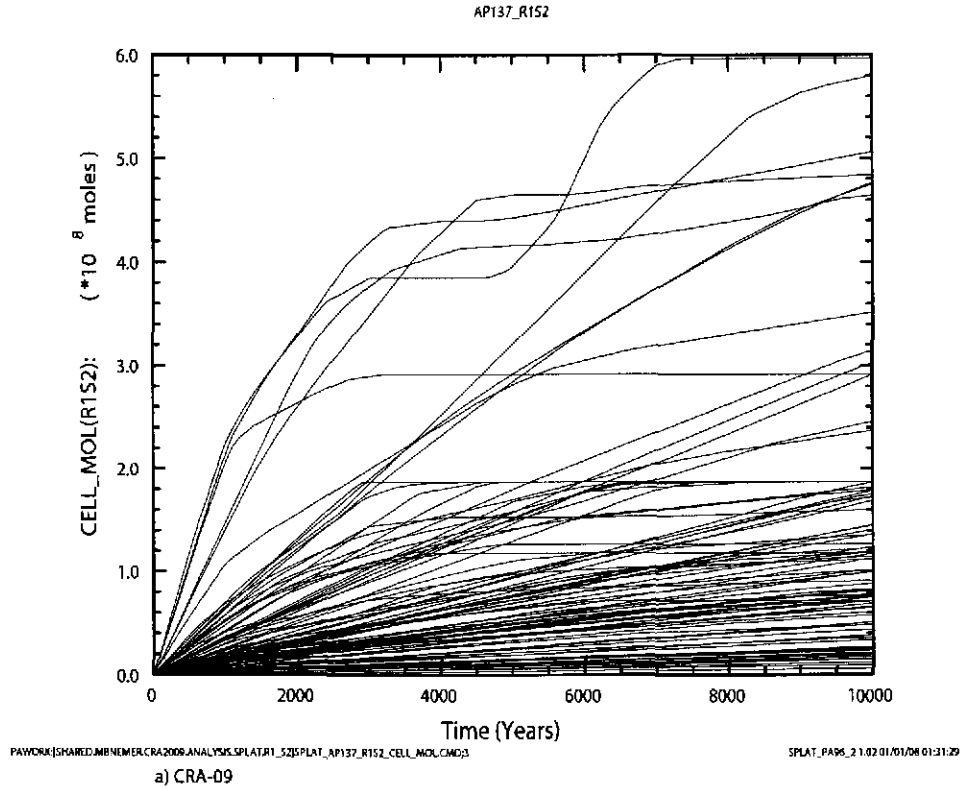


Figure 6-58. Cumulative amount of gas (moles) produced by microbial gas generation versus time (years) for all 100 vectors in Replicate R1, Scenario S2. Figure a) shows results from the CRA-2009 PA. Figure b) shows results from the CRA-2004 PABC.

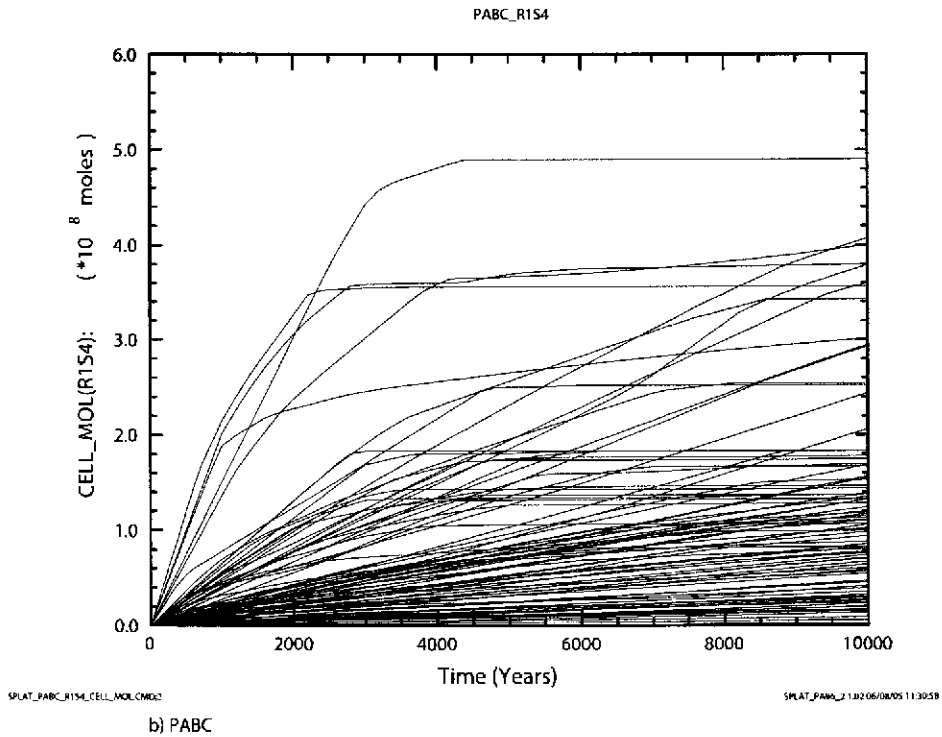
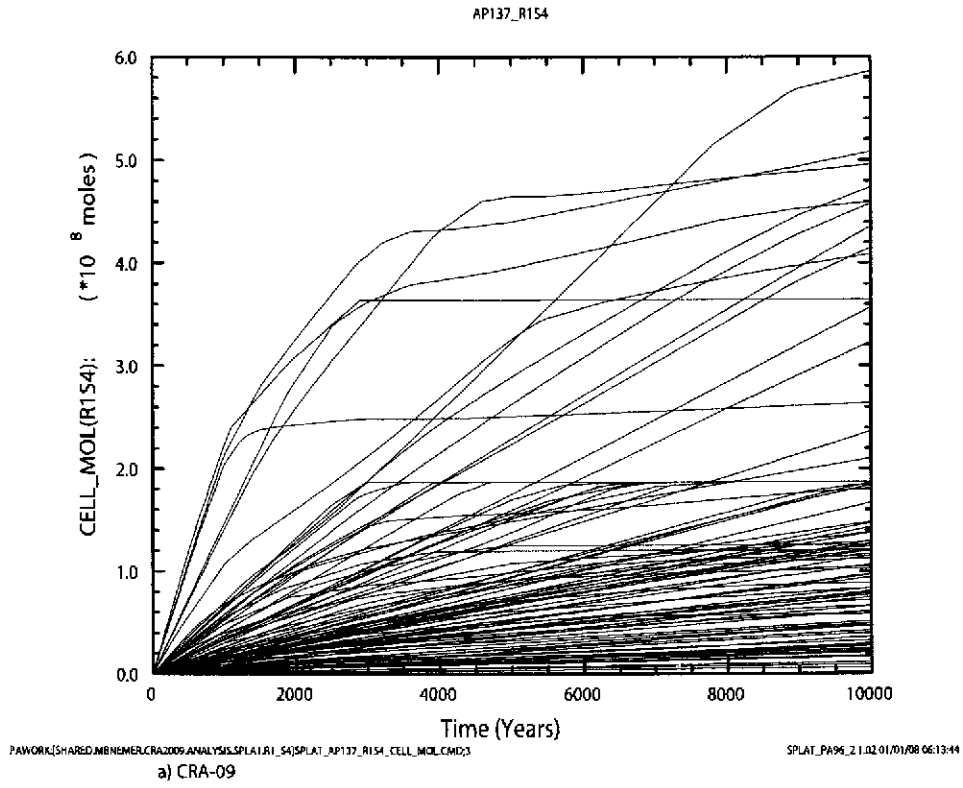


Figure 6-59. Cumulative amount of gas (moles) produced by microbial gas generation versus time (years) for all 100 vectors in Replicate R1, Scenario S4. Figure a) shows results from the CRA-2009 PA. Figure b) shows results from the CRA-2004 PABC.

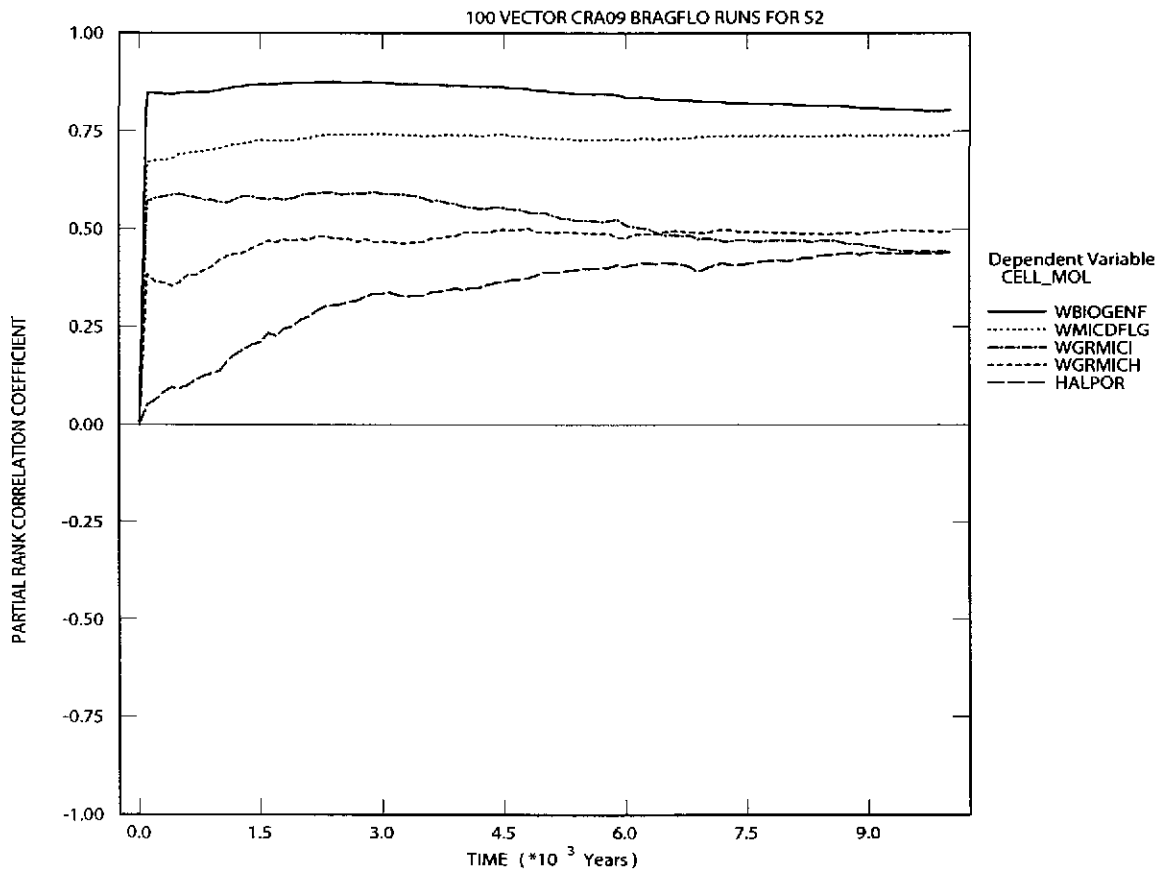
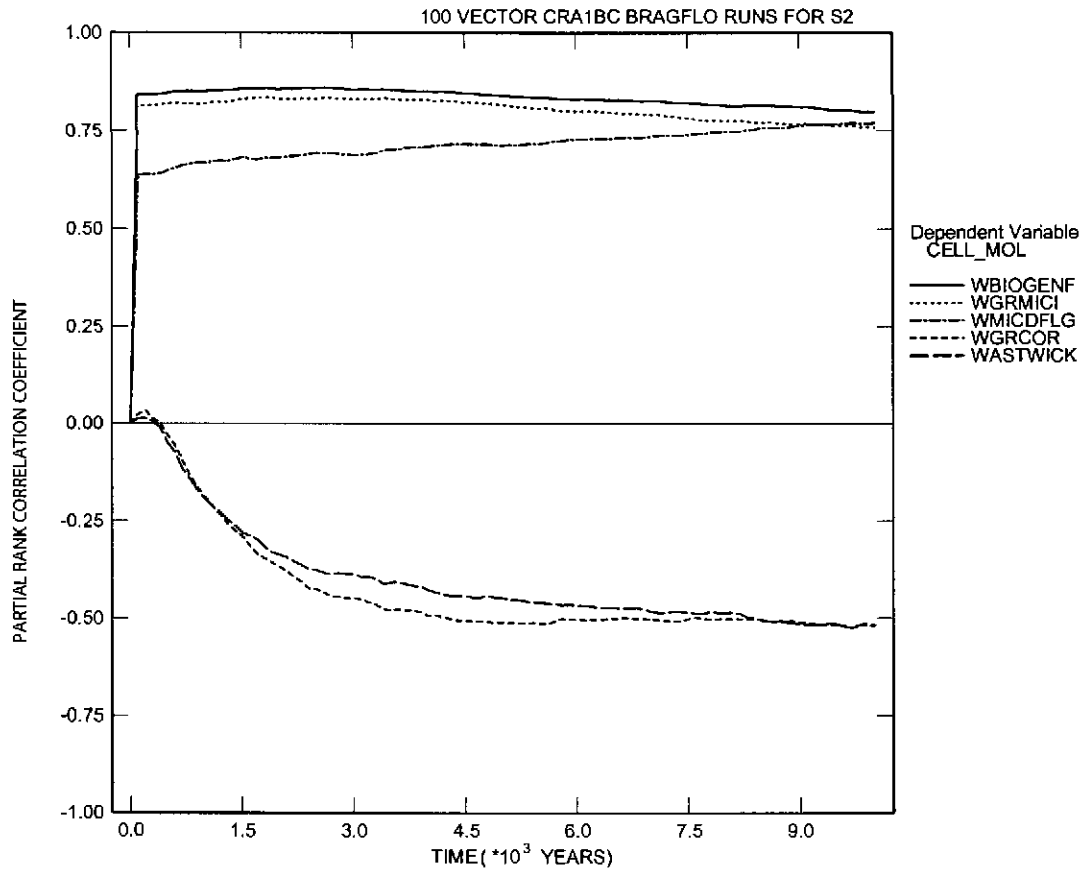


Figure 6-60. Primary correlations of cumulative amount (moles) of gas produced by microbial gas generation in the waste panel with input parameters versus time (years) from the CRA-2009 PA, Replicate R1, Scenario S2. Table 4-2 gives a description of the names in the legend.



PCCSRC_S2.INP;3

PCCSRC_PA96 2.21 06/08/05 10:19

Figure 6-61. Primary correlations of cumulative amount (moles) of gas produced by microbial gas generation in the waste panel with input parameters versus time (years) from the CRA-2004 PABC, Replicate R1, Scenario S2. Table 4-2 gives a description of the names in the legend.

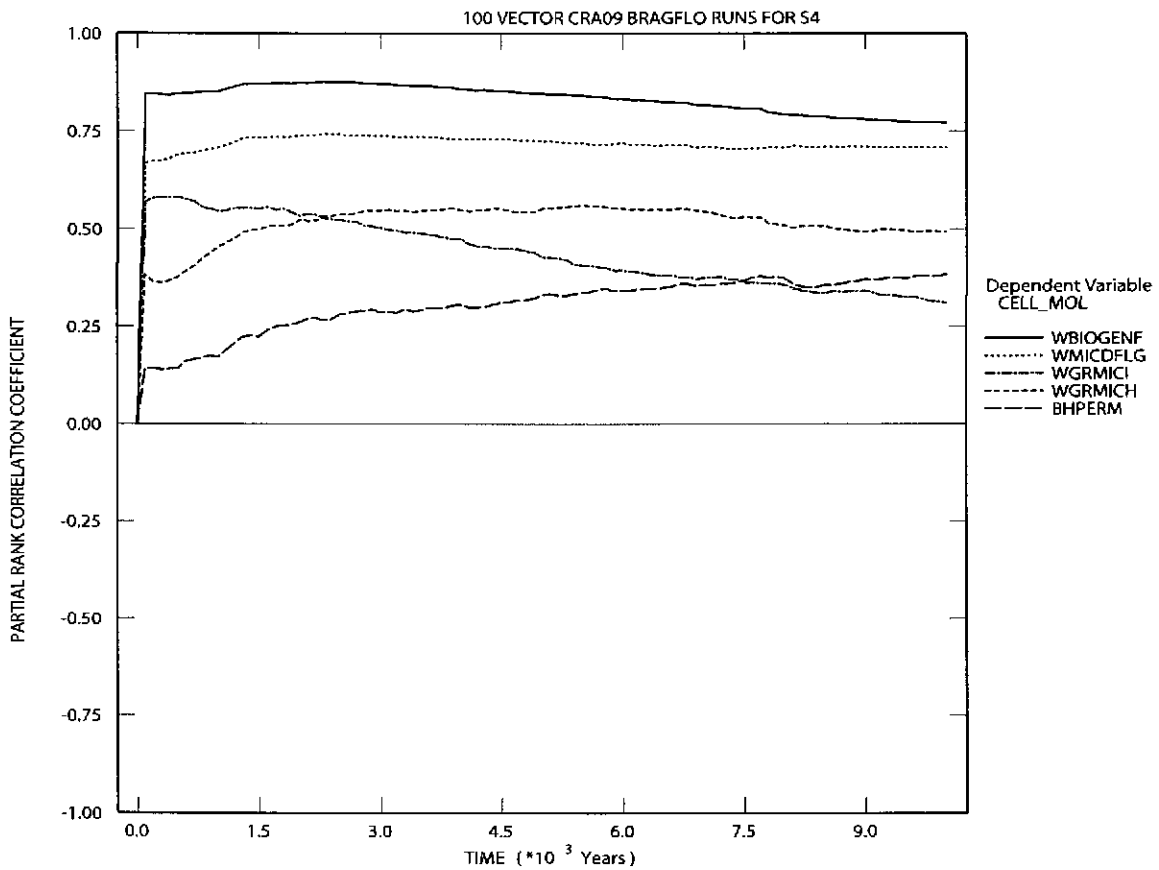


Figure 6-62. Primary correlations of cumulative amount (moles) of gas produced by microbial gas generation in the Waste Panel with input parameters versus time (years) from the CRA-2009 PA, Replicate R1, Scenario S4. Table 4-2 gives a description of the names in the legend.

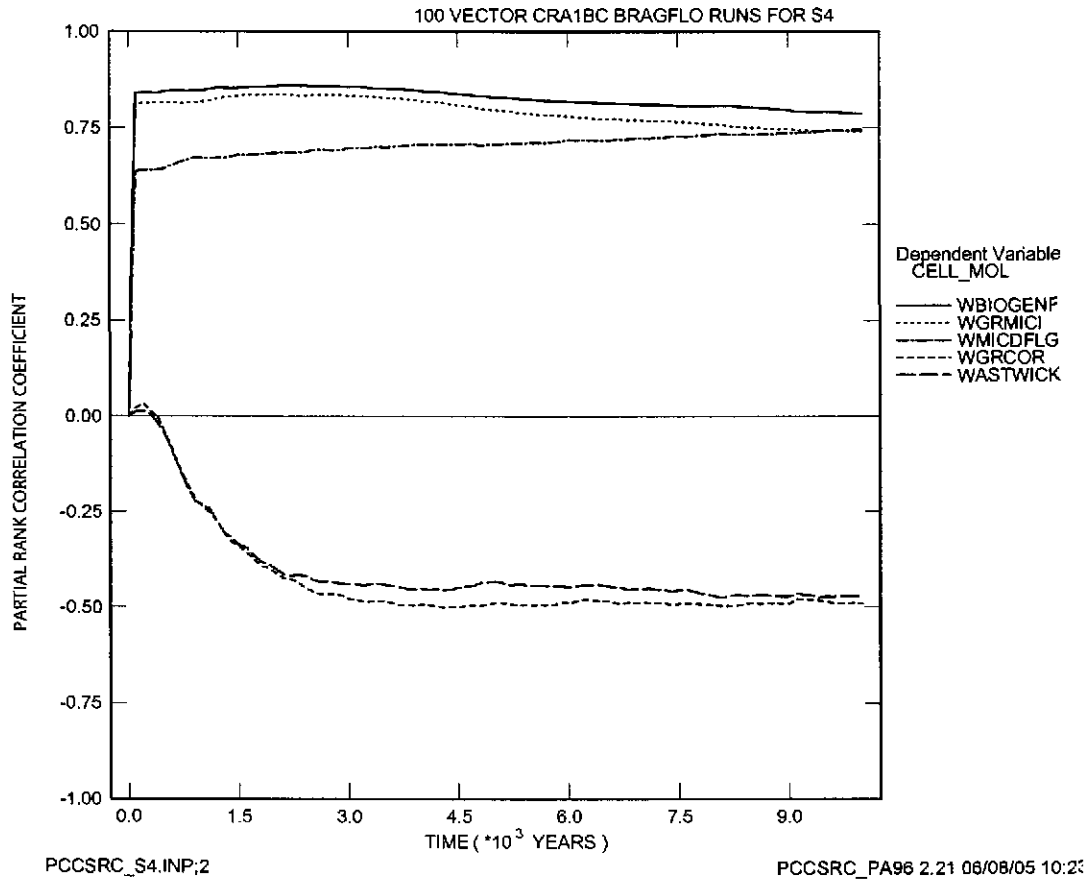


Figure 6-63. Primary correlations of cumulative amount (moles) of gas produced by microbial gas generation in the Waste Panel with input parameters versus time (years) from the CRA-2004 PABC, Replicate R1, Scenario S4. Table 4-2 gives a description of the names in the legend.

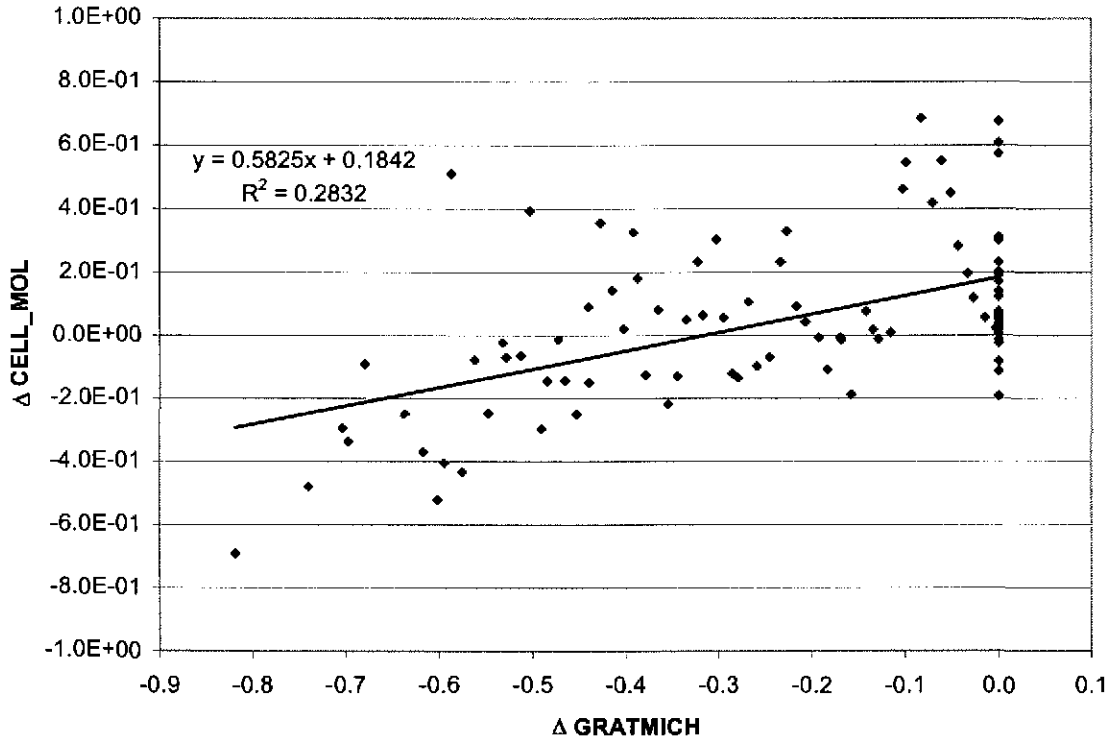
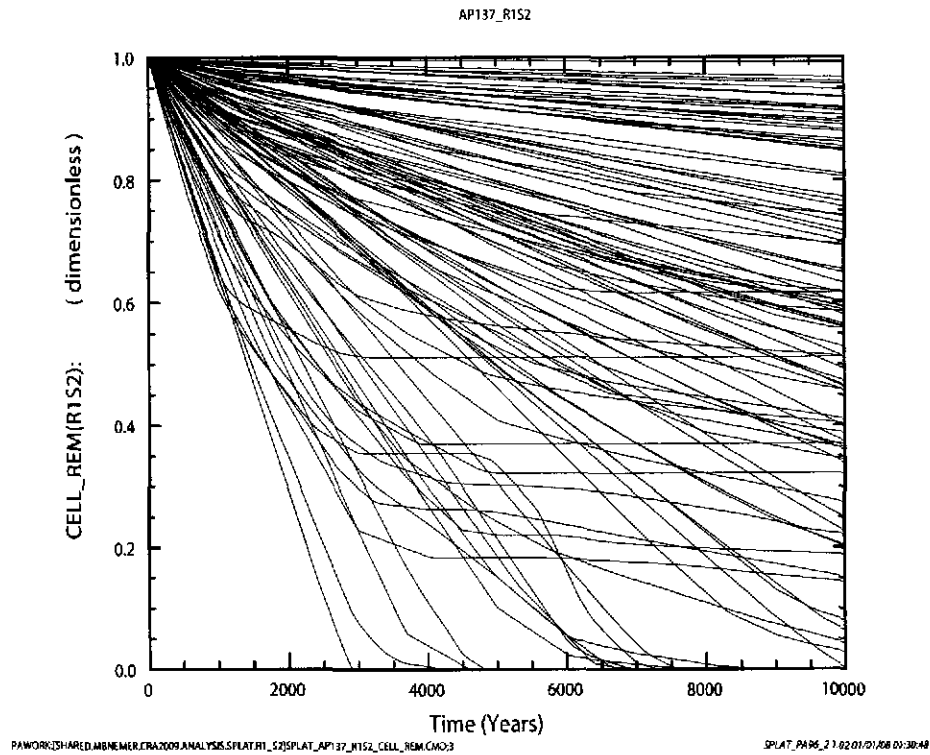
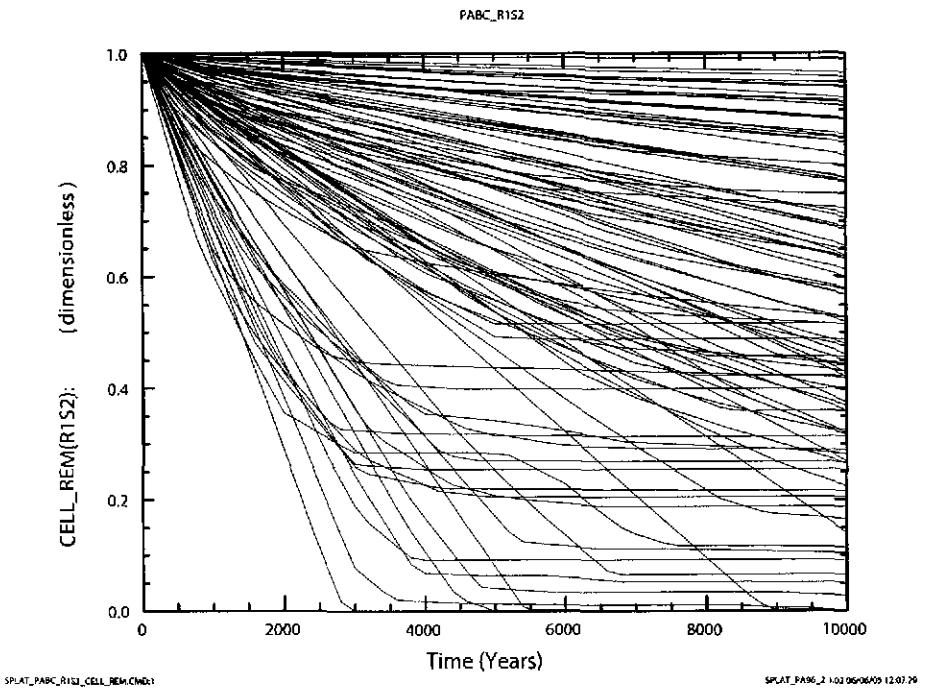


Figure 6-64. Difference in amount of microbial gas produced at 10,000 years from the CRA-2009 PA and the CRA-2004 PABC (normalized by CELL_MOL from the CRA-2004 PABC) versus the difference in the humid gas generation rates from the two analyses (the humid gas generation rates from each analysis are normalized by their respective inundated microbial gas-generation rates).

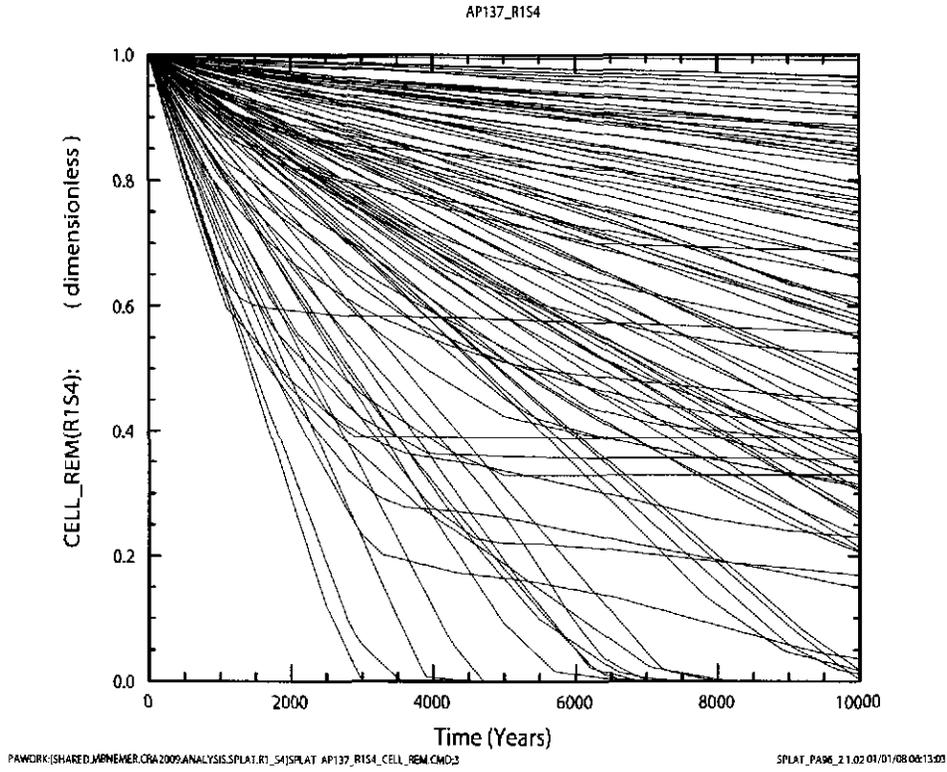


a) CRA-09

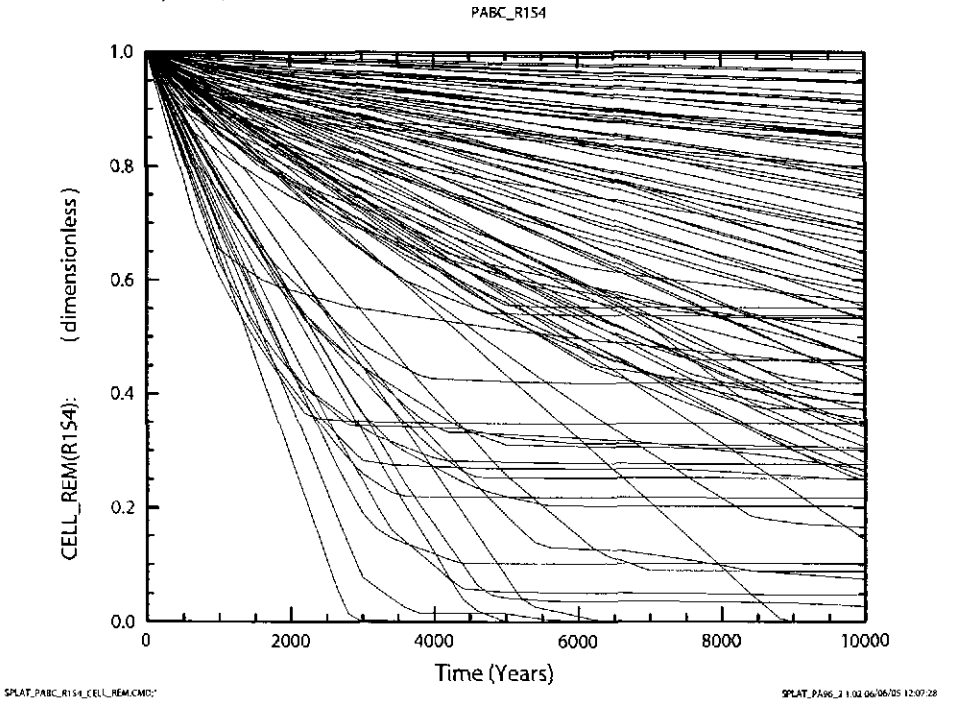


b) PABC

Figure 6-65. Fraction of cellulose (dimensionless) remaining versus time (years) for all 100 vectors in Replicate R1, Scenario S2. Fraction of cellulose is either cellulose or CPR depending on the value of WAS_AREA:PROBDEG (see Subsection 5.1.1). Figure a) shows results from the CRA-2009 PA. Figure b) shows results from the CRA-2004 PABC.

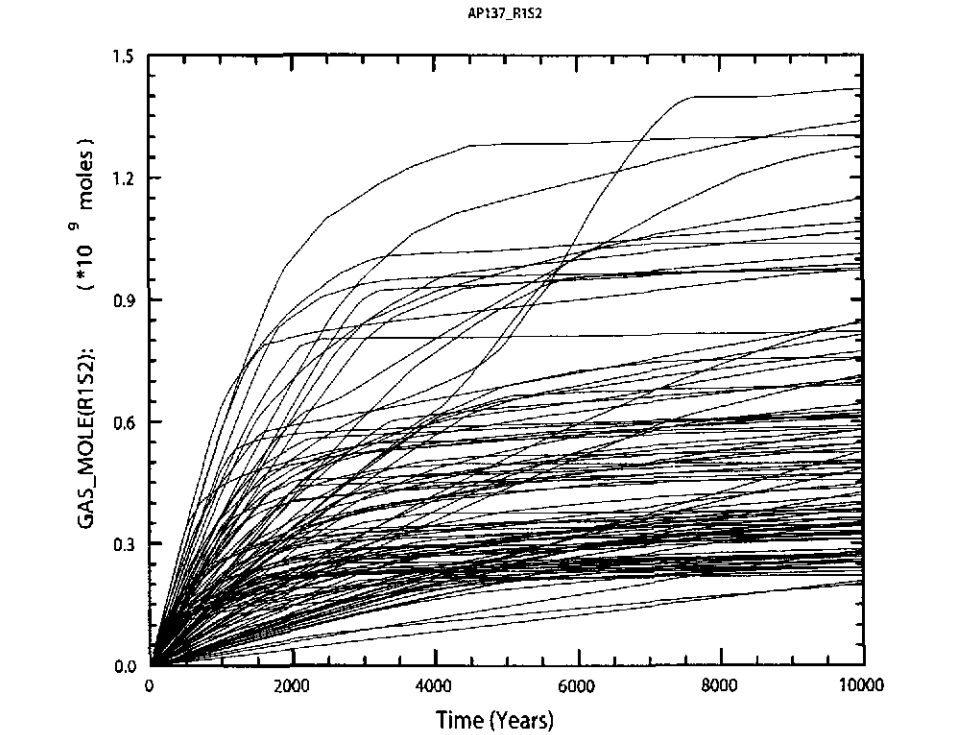


a) CRA-09

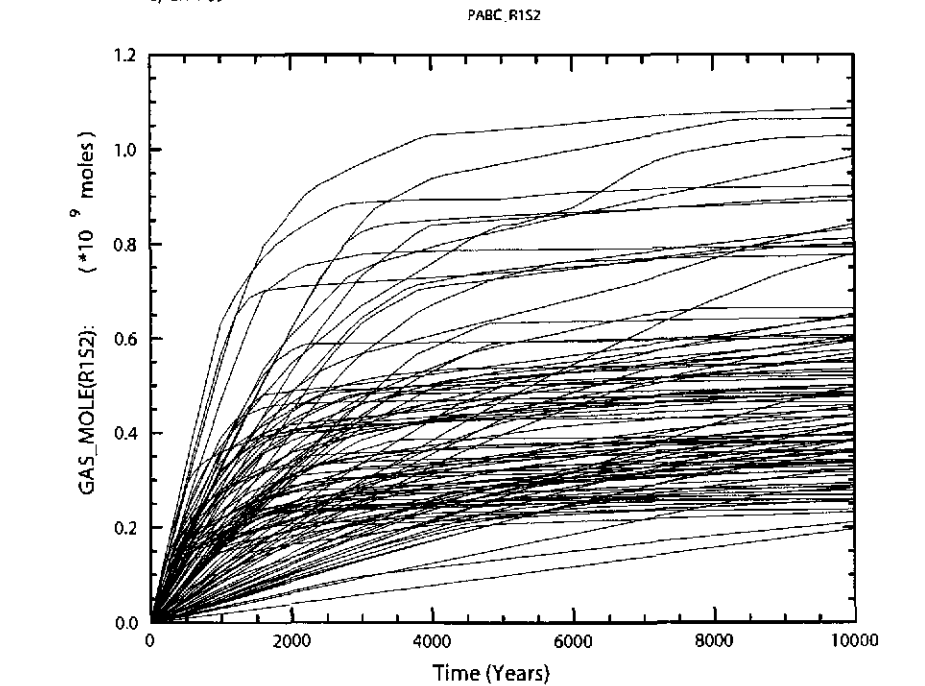


b) PABC

Figure 6-66. Fraction of cellulose (dimensionless) remaining versus time (years) for all 100 vectors in Replicate R1, Scenario S4. Fraction of cellulose is either cellulose or CPR depending on the value of WAS_AREA:PROBDEG (see Subsection 5.1.1). Figure a) shows results from the CRA-2009 PA. Figure b) shows results from the CRA-2004 PABC.



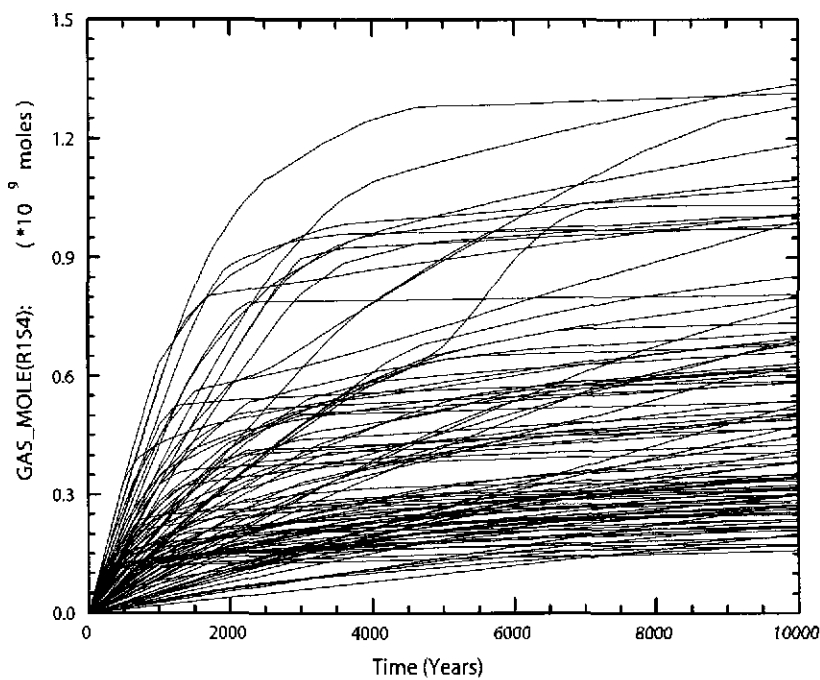
a) CRA-09



b) PABC

Figure 6-67. Total cumulative amount of gas (moles) generated versus time (years) for all 100 vectors in Replicate R1, Scenario S2. Figure a) shows results from the CRA-2009 PA. Figure b) shows results from the CRA-2004 PABC.

AP137_R1S4

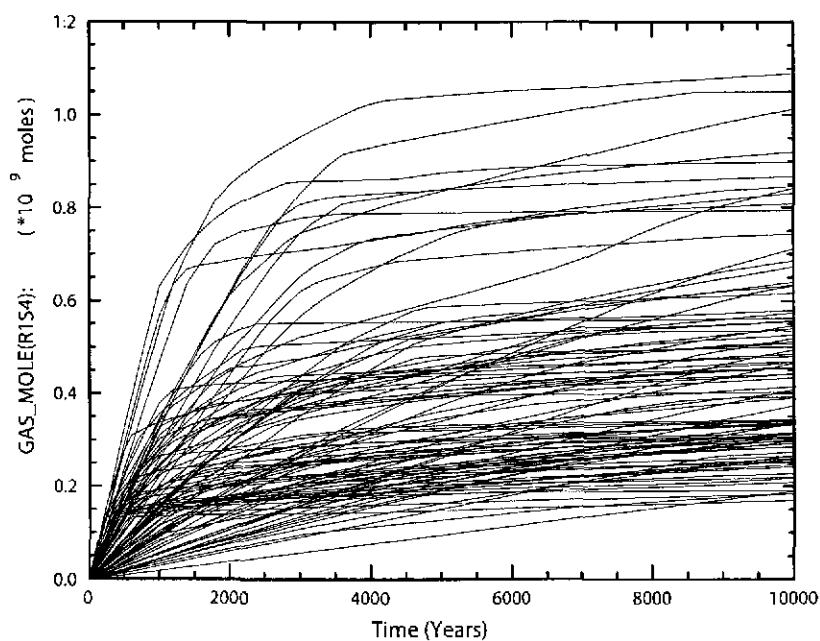


PAWOR\SHARE\AR\B\M\ES\CRA2009\ANALYSIS\SPLAT\R1_S4\SPLAT_AP137_R1S4_GAS_MOLE.CMD3

SPLAT_PAG6_2 1.07 05/04/09 11:07:06

a) CRA-09

PABC_R1S4



SPLAT_PABC_R1S4_GAS_MOLE.CMD3

SPLAT_PAG6_2 1.02 06/06/05 11:54:39

b) PABC

Figure 6-68. Total cumulative amount of gas (moles) generated versus time (years) for all 100 vectors in Replicate R1, Scenario S4. Figure a) shows results from the CRA-2009 PA. Figure b) shows results from the CRA-2004 PABC.

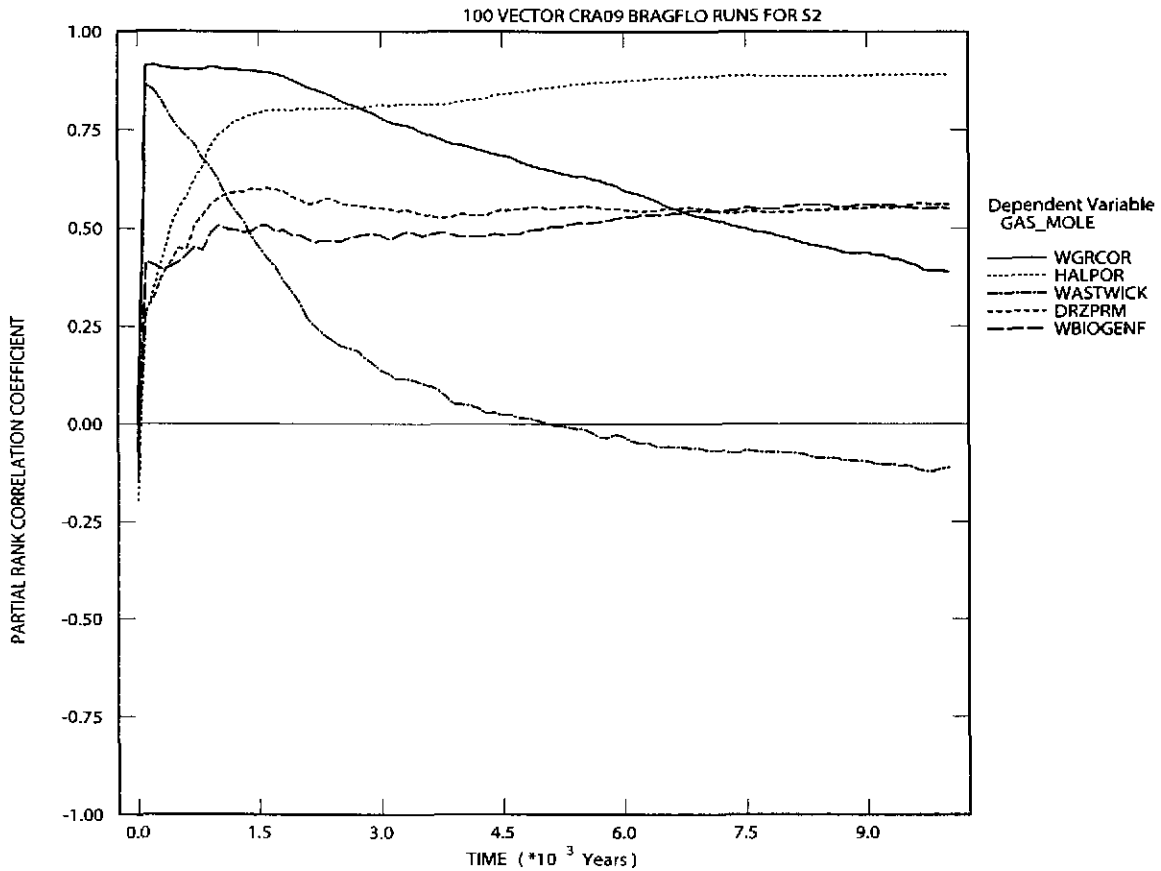


Figure 6-69. Primary correlations for total cumulative amount (moles) of gas produced in the waste panel with input parameters, versus time (years) from the CRA-2009 PA Replicate R1, Scenario S2. Table 4-2 gives a description of the names in the legend.

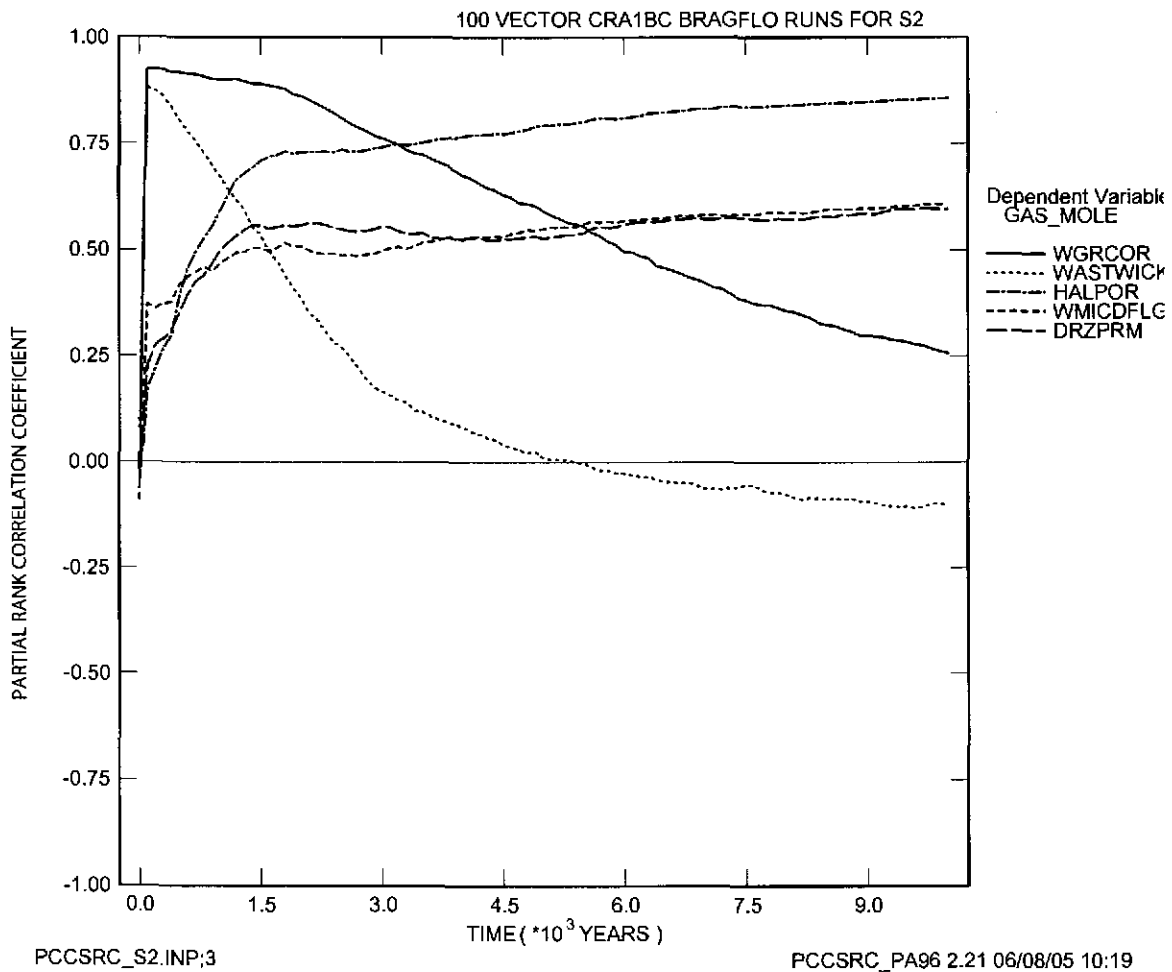


Figure 6-70. Primary correlations of total cumulative amount (moles) of gas produced in the waste panel with input parameters, versus time (years) from the CRA-2004 PABC Replicate R1, Scenario S2. Table 4-2 gives a description of the names in the legend.

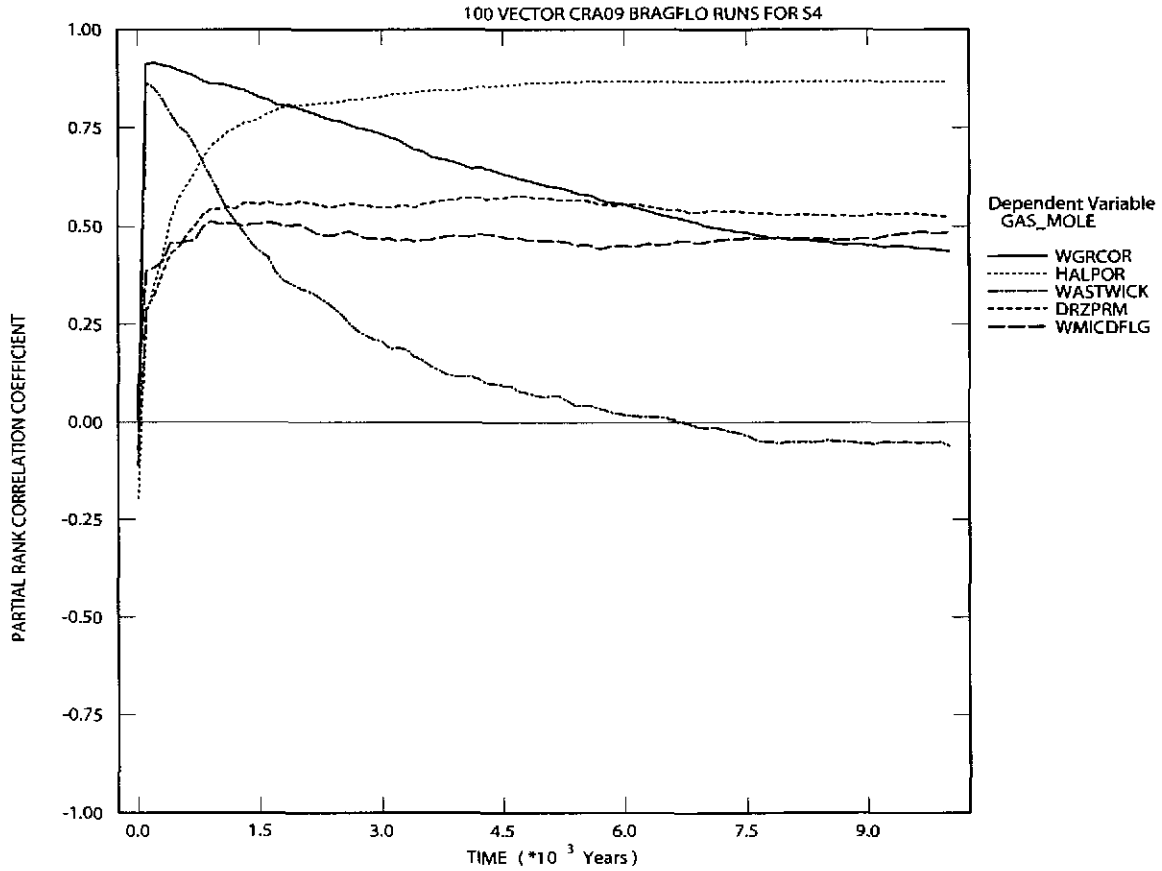


Figure 6-71. Primary correlations of total cumulative amount (moles) of gas produced in the Waste Panel with input parameters, versus time (years) from the CRA-2009 PA Replicate R1, Scenario S4. Table 4-2 gives a description of the names in the legend.

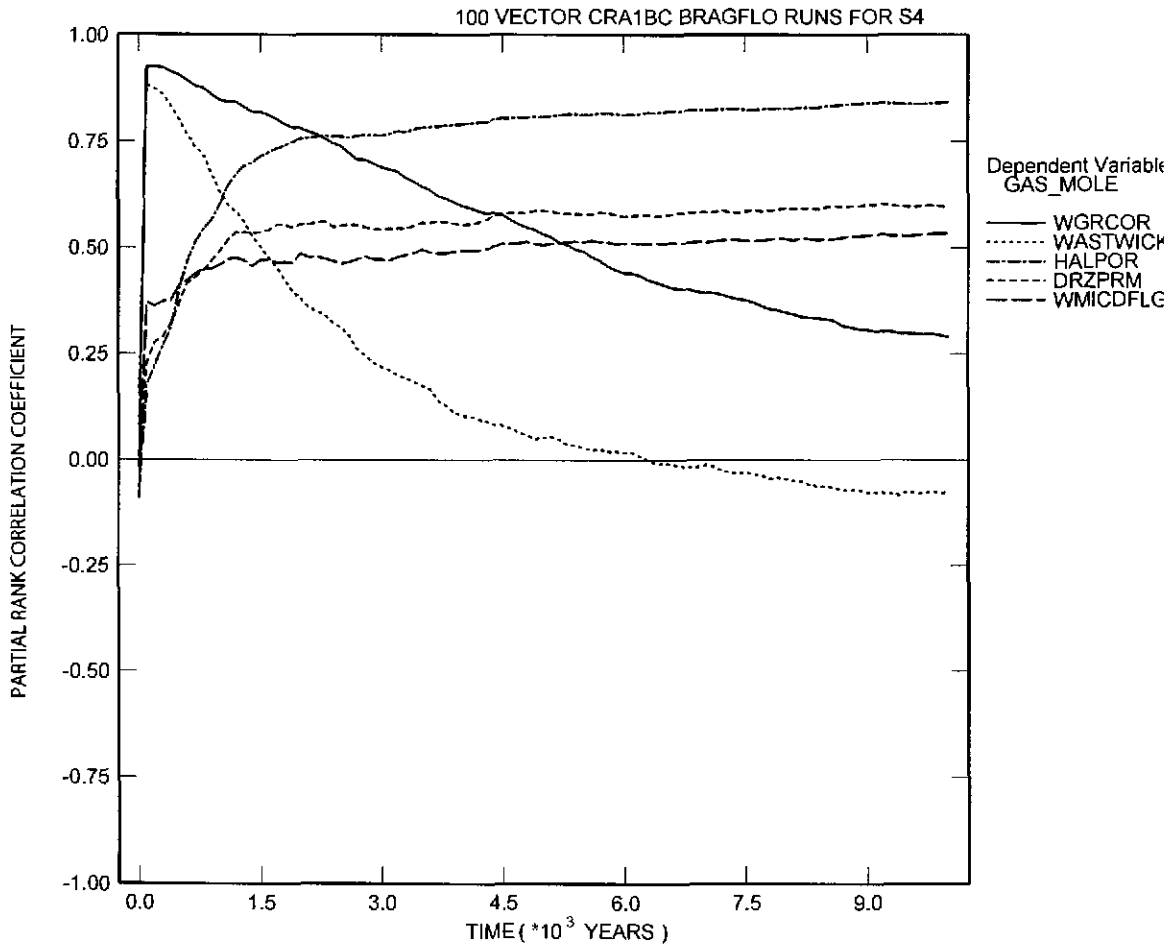
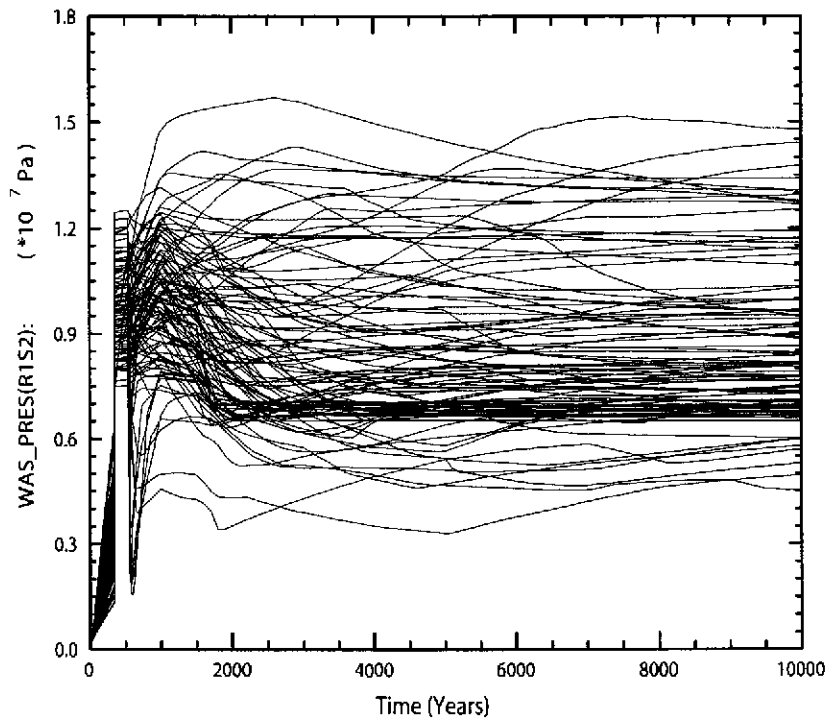


Figure 6-72. Primary correlations of total cumulative amount (moles) of gas produced in the Waste Panel with input parameters, versus time (years) from the CRA-2004 PABC Replicate R1, Scenario S4. Table 4-2 gives a description of the names in the legend.

AP137_R1S2

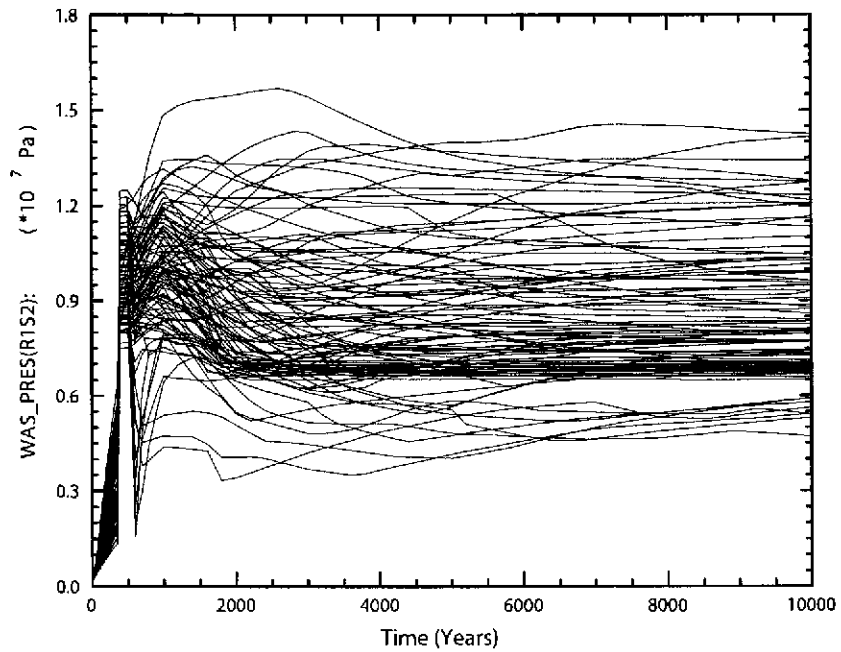


PAWORK\SHAREDMB\NEMER\CRA2009\ANALYSIS\SPLAT_RT_SIS\SPLAT_AP137_R1S2_WAS_PRES.CMD;1

SPLAT_PAS6_21.02.01\01\08\002857

a) CRA-09

PABC_R1S2



SPLAT_PABC_R1S2_WAS_PRES.CMD;1

SPLAT_PAS6_21.02.06\0A\05113034

b) PABC

Figure 6-73. Volume averaged pressure (Pa) in the waste area versus time (years) for all 100 vectors in Replicate R1, Scenario S2. Figure a) shows results from the CRA-2009 PA. Figure b) shows results from the CRA-2004 PABC.

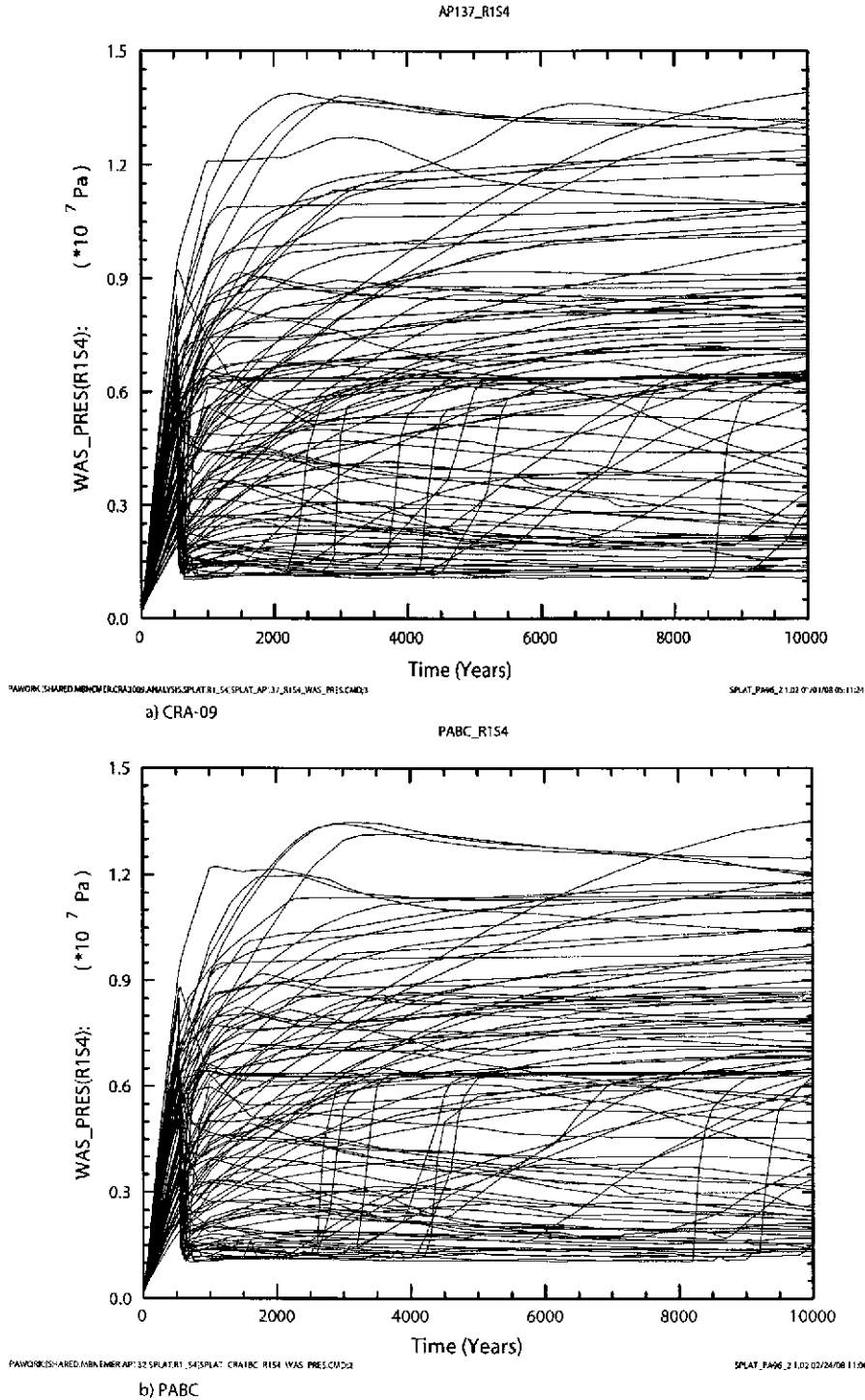


Figure 6-74. Volume averaged pressure (Pa) in the waste area versus time (years) for all 100 vectors in Replicate R1, Scenario S4. Figure a) shows results from the CRA-2009 PA. Figure b) shows results from the CRA-2004 PABC.

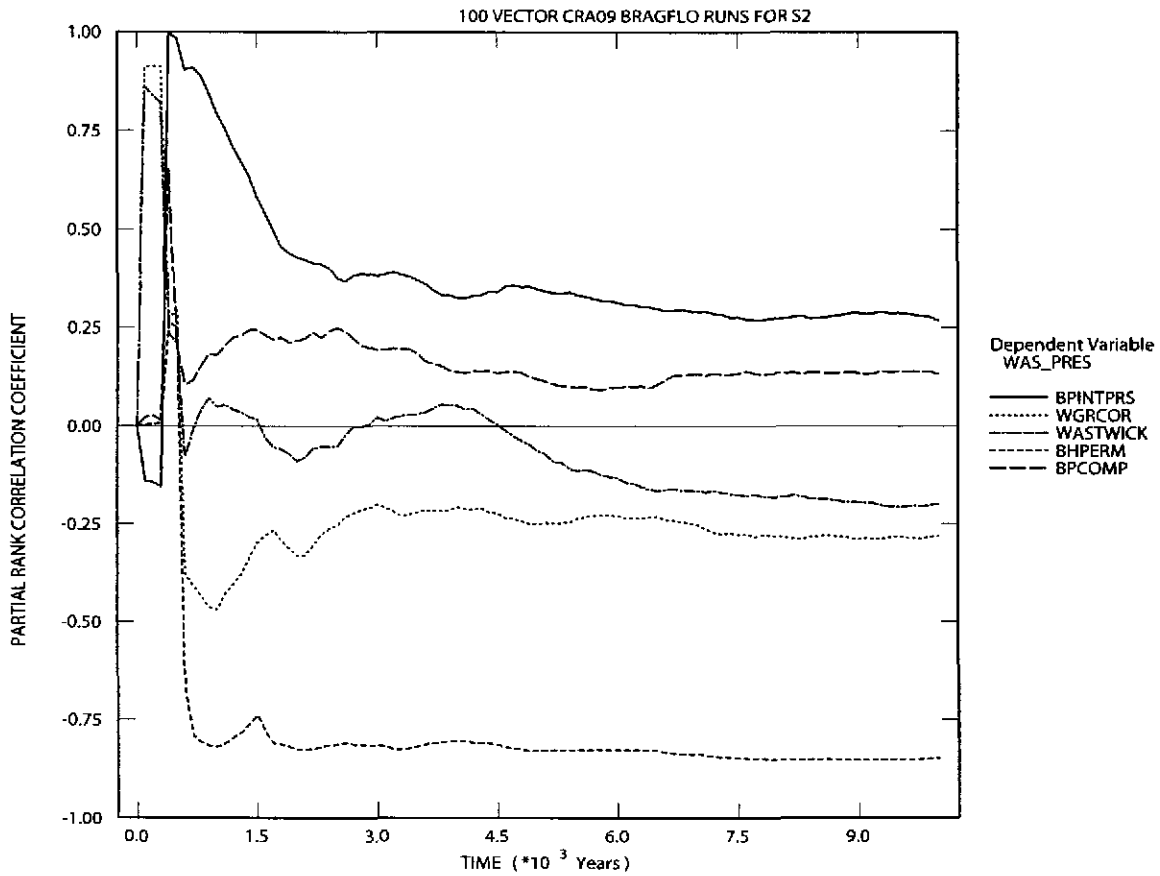


Figure 6-75. Primary correlations (dimensionless) of volume averaged pressure in the waste panel with input parameters versus time (years) from the CRA-2009 PA Replicate R1, Scenario S2. Table 4-2 gives a description of the names in the legend.

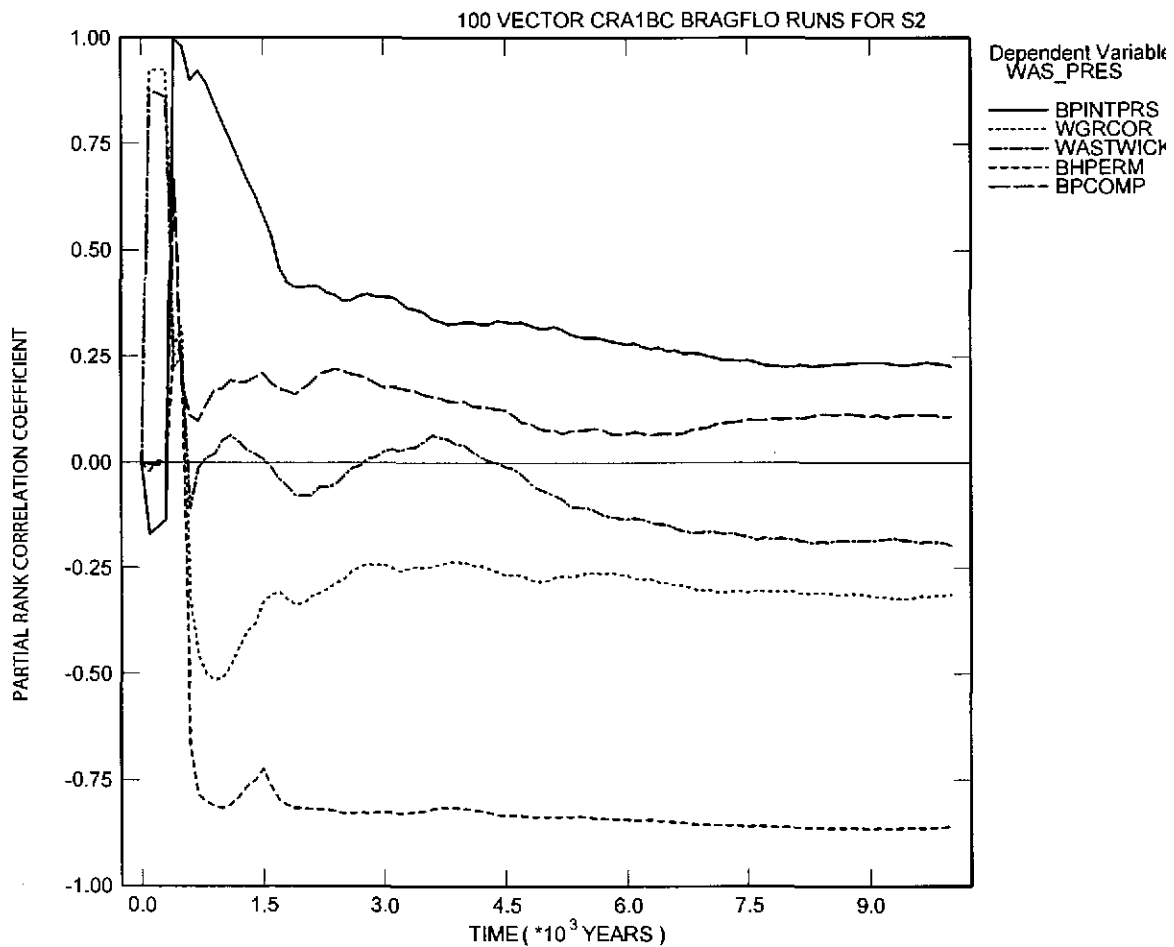


Figure 6-76. Primary correlations (dimensionless) of volume averaged pressure in the waste panel with input parameters versus time (years) from the CRA-2004 PABC Replicate R1, Scenario S2. Table 4-2 gives a description of the names in the legend.

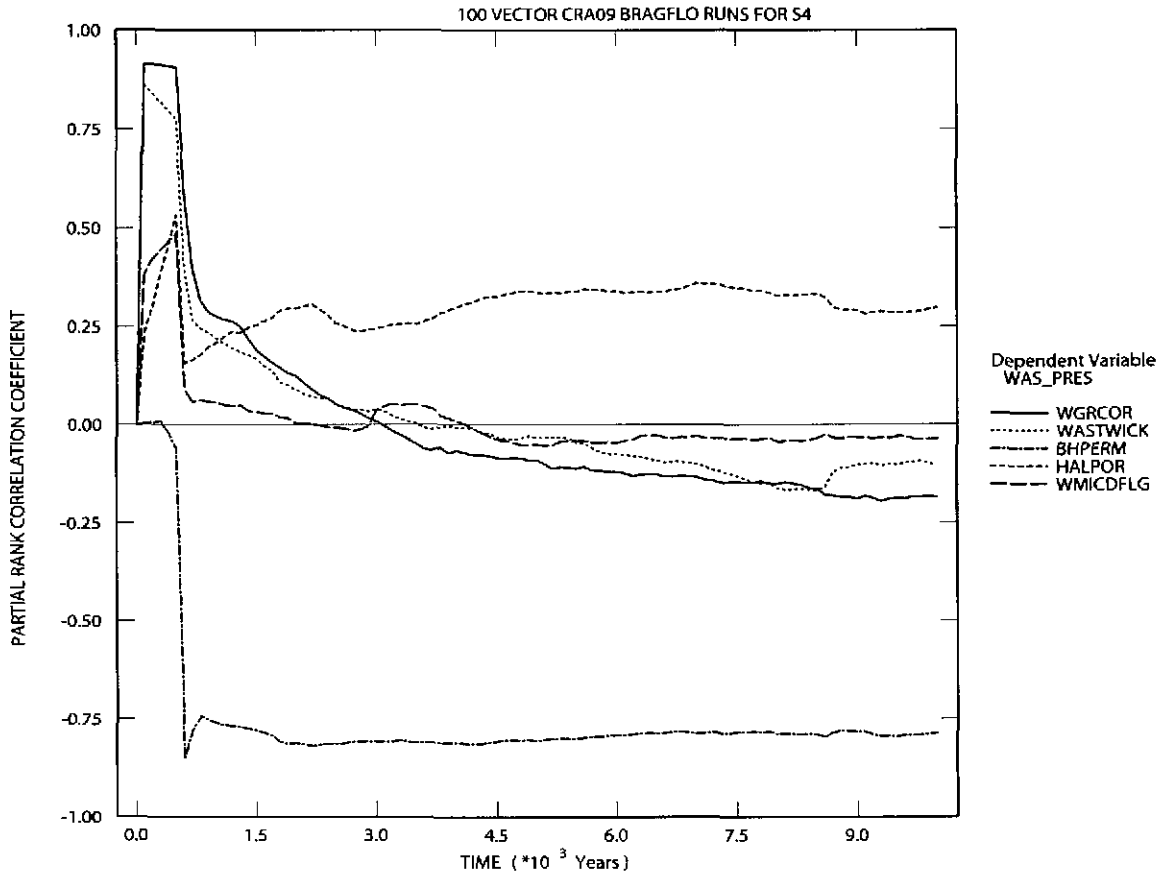


Figure 6-77. Primary correlations (dimensionless) of volume averaged pressure in the waste panel with input parameters versus time (years) from the CRA-2009 PA Replicate R1, Scenario S4. Table 4-2 gives a description of the names in the legend.

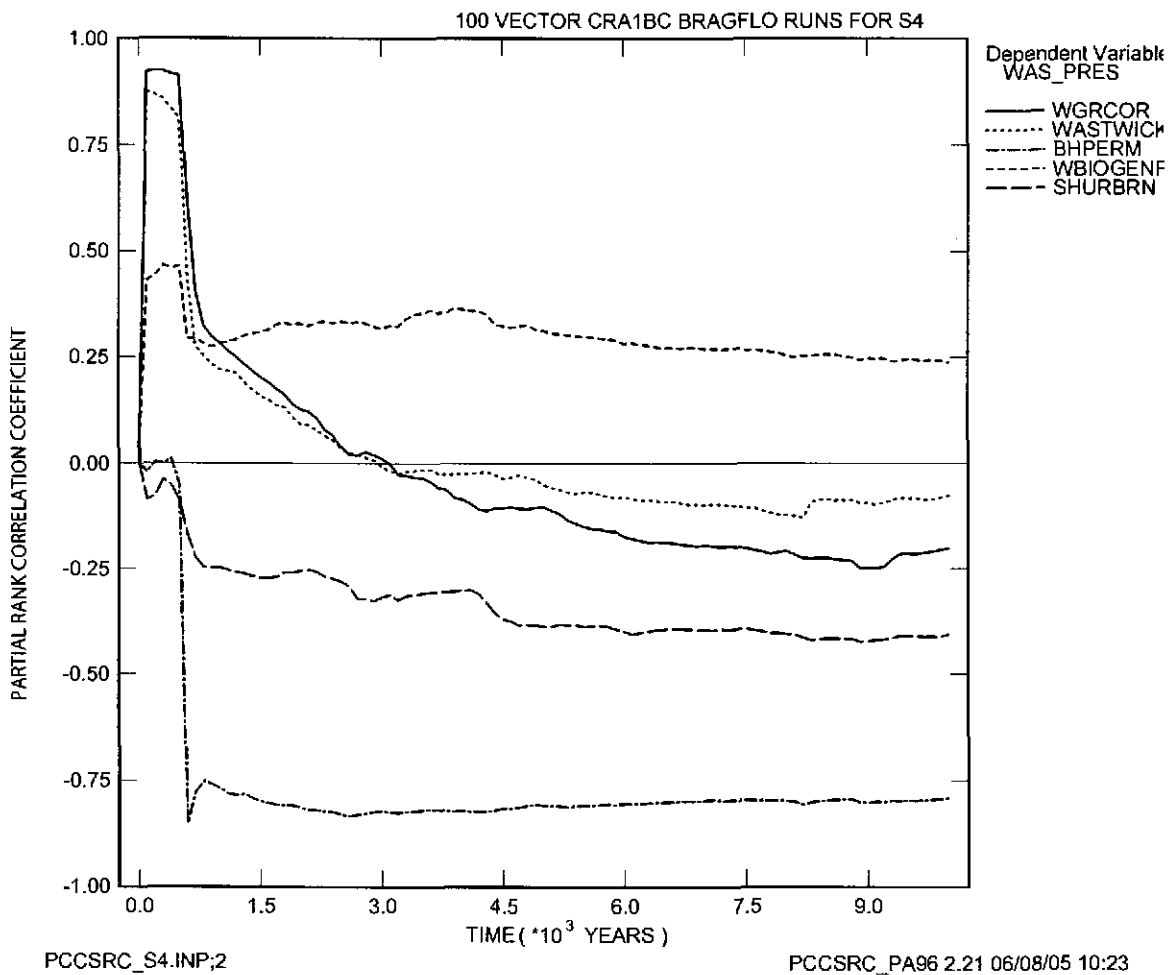
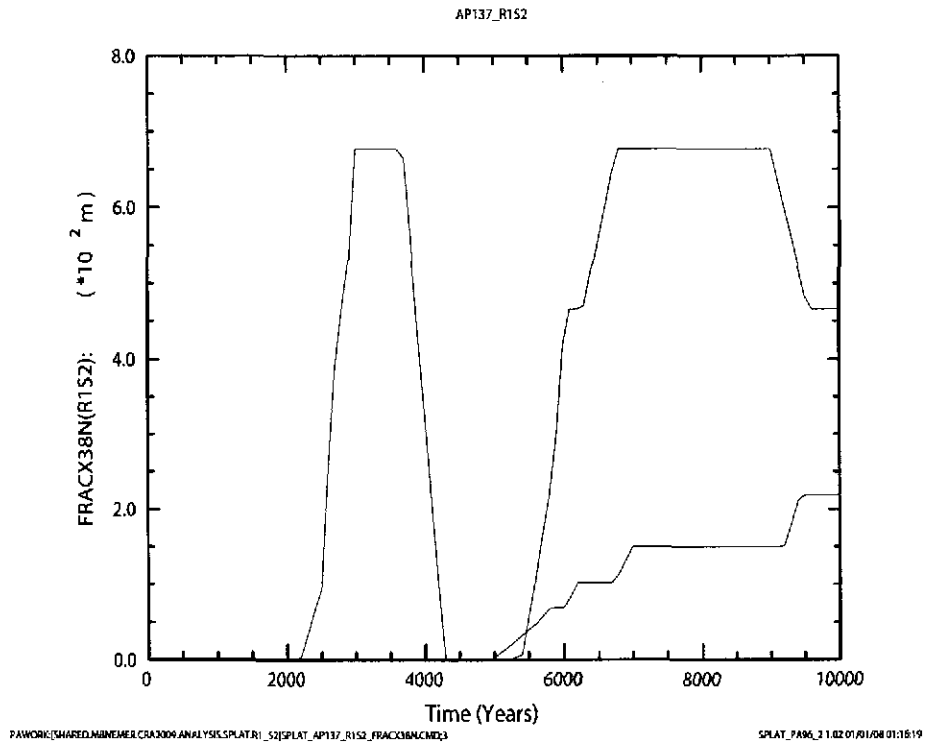
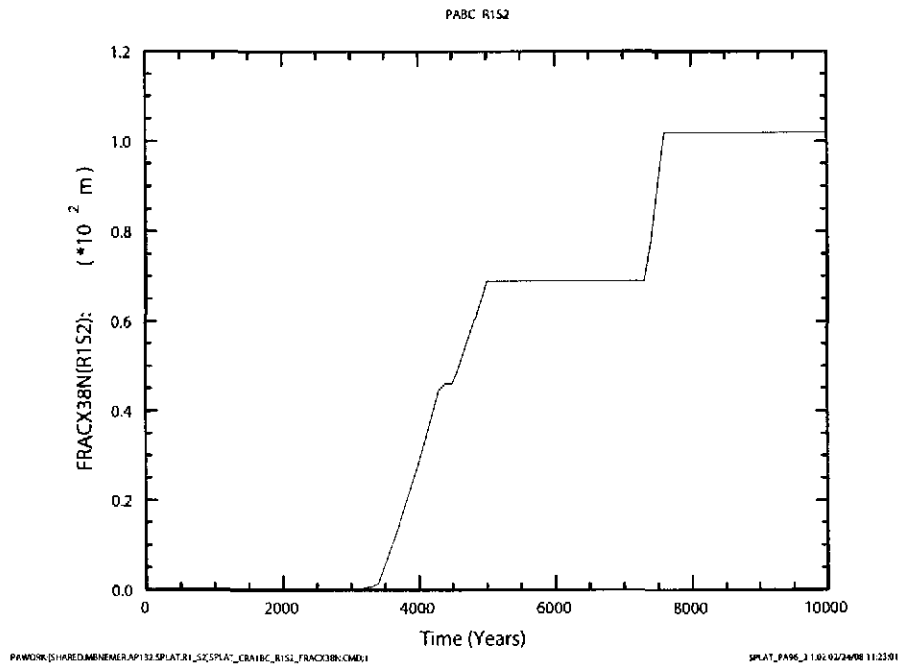


Figure 6-78. Primary correlations (dimensionless) of volume averaged pressure in the waste panel with input parameters versus time (years) from the CRA-2004 PABC Replicate R1, Scenario S4. Table 4-2 gives a description of the names in the legend.

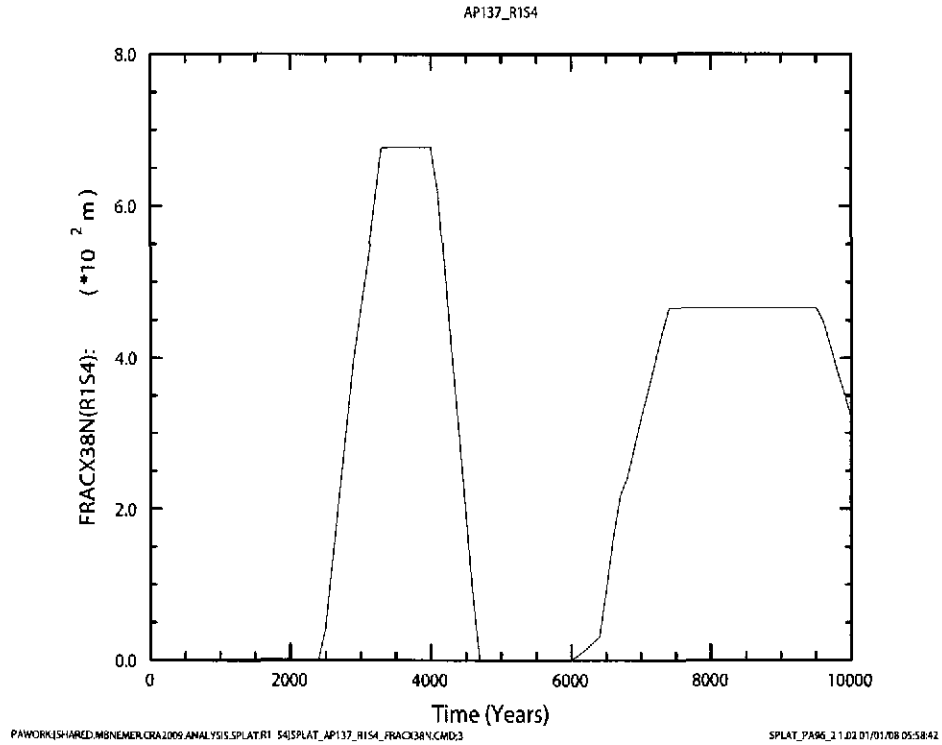


a) CRA-09

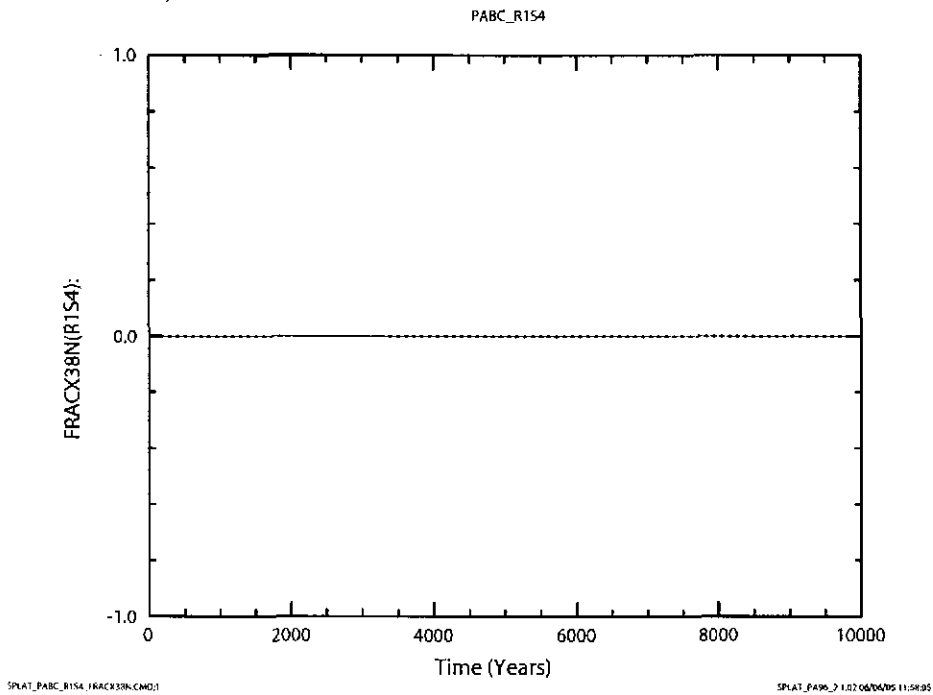


b) PABC

Figure 6-79. Fracture length (m) in MB138, north of the repository versus time (years) for all 100 vectors in Replicate R1, Scenario S2. Figure a) shows results from the CRA-2009 PA. Figure b) shows results from the CRA-2004 PABC.

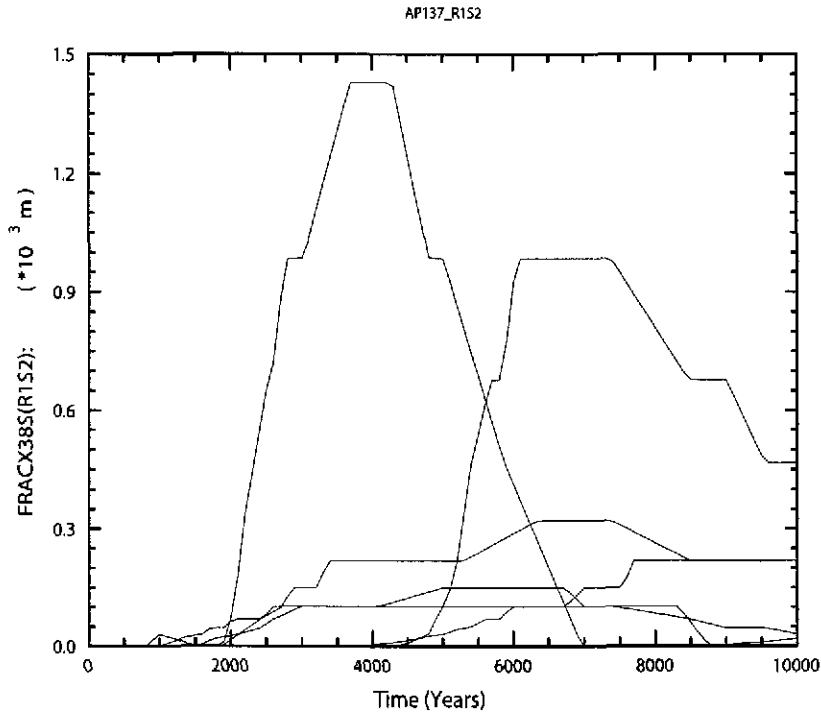


a) CRA-09

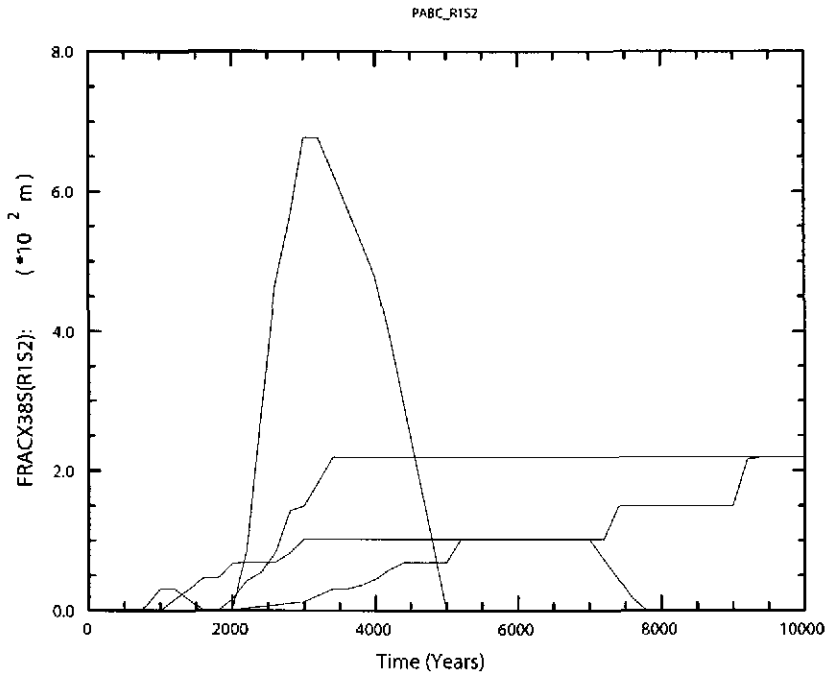


b) PABC

Figure 6-80. Fracture length (m) in MB138, north of the repository versus time (years) for all 100 vectors in Replicate R1, Scenario S4. Figure a) shows results from the CRA-2009 PA. Figure b) shows results from the CRA-2004 PABC.



a) CRA-09



b) PABC

Figure 6-81. Fracture length (m) in MB138, south of the repository versus time (years) for all 100 vectors in Replicate R1, Scenario S2. Figure a) shows results from the CRA-2009 PA. Figure b) shows results from the CRA-2004 PABC.

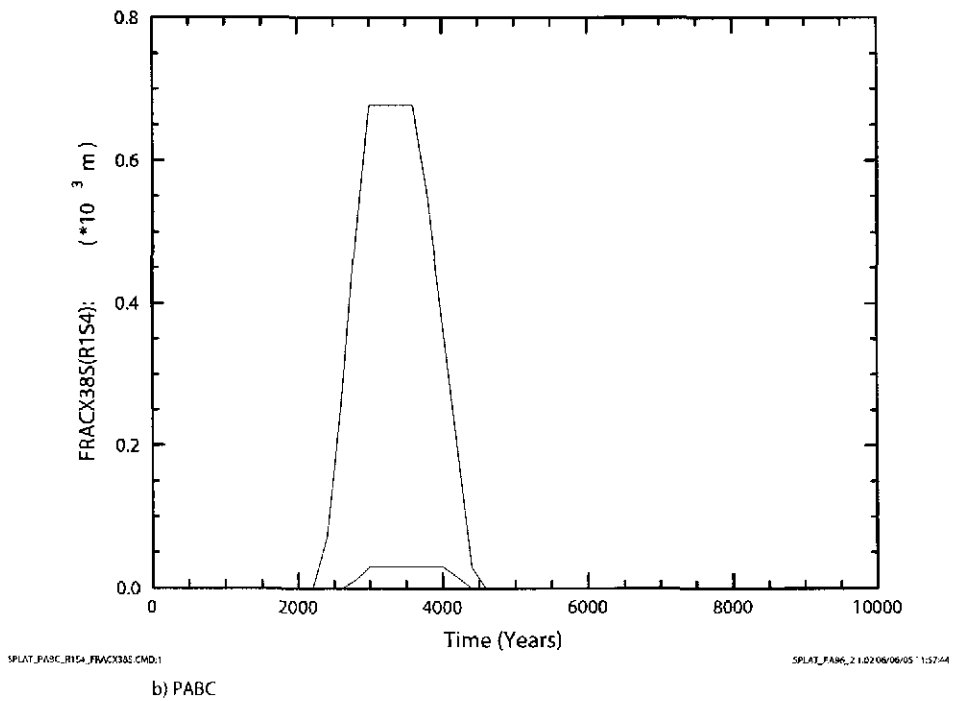
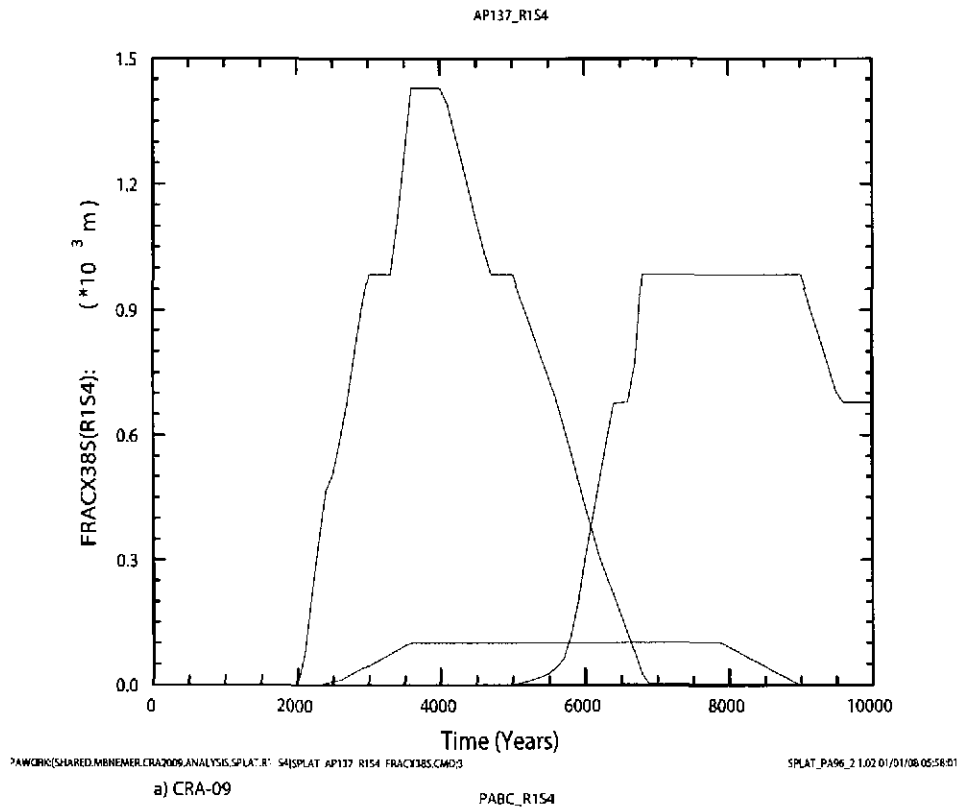


Figure 6-82. Fracture length (m) in MB138, south of the repository versus time (years) for all 100 vectors in Replicate R1, Scenario S4. Figure a) shows results from the CRA-2009 PA. Figure b) shows results from the CRA-2004 PABC.

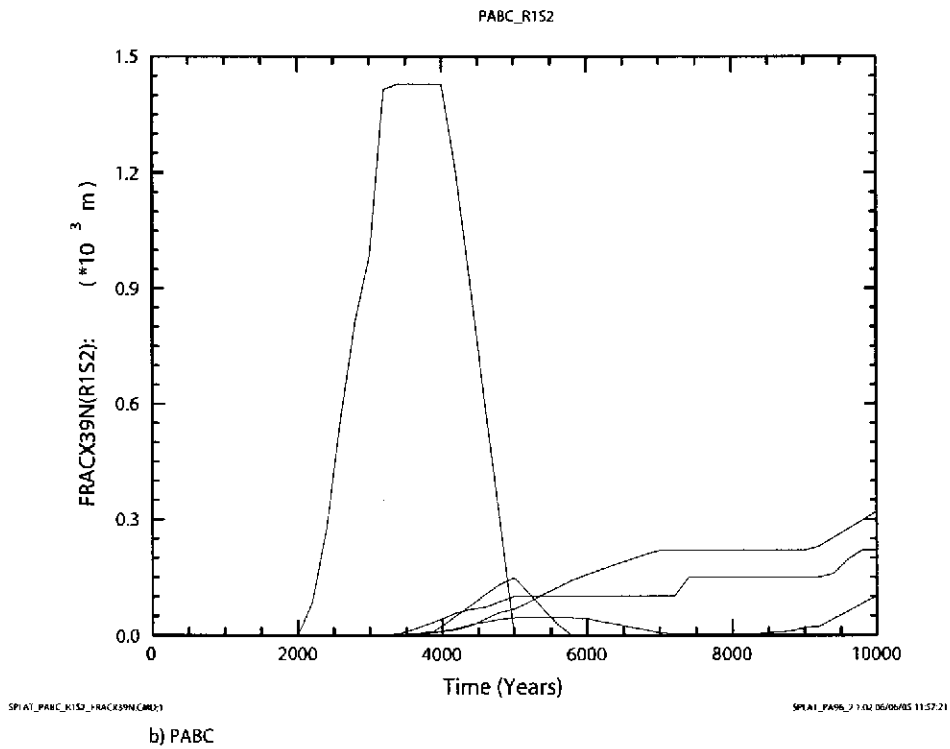
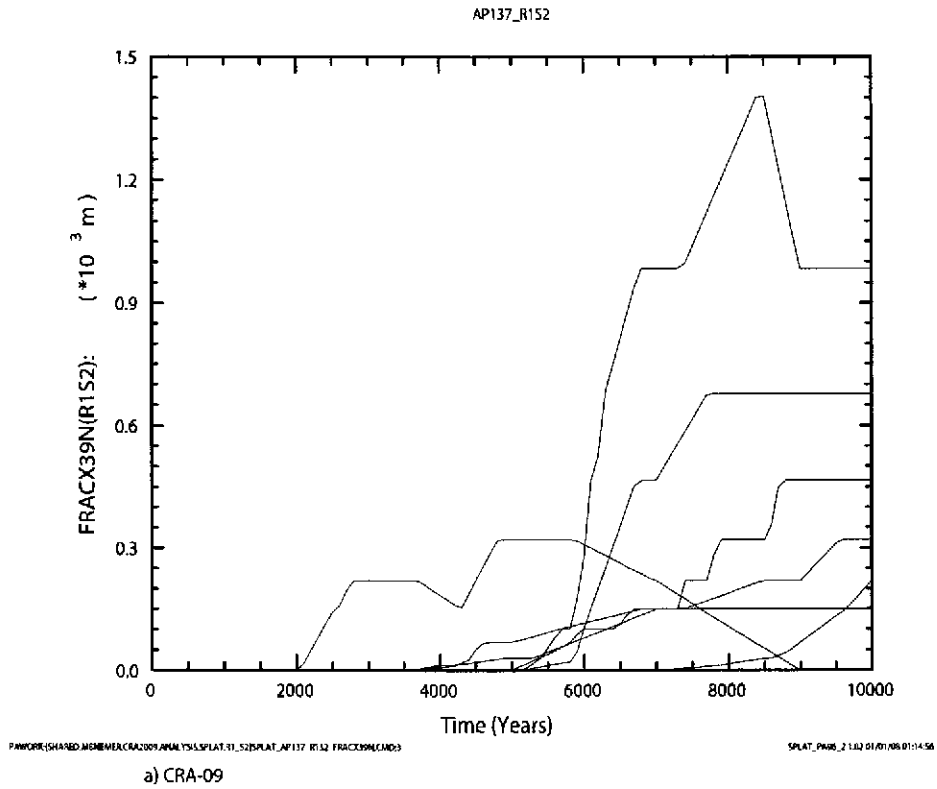
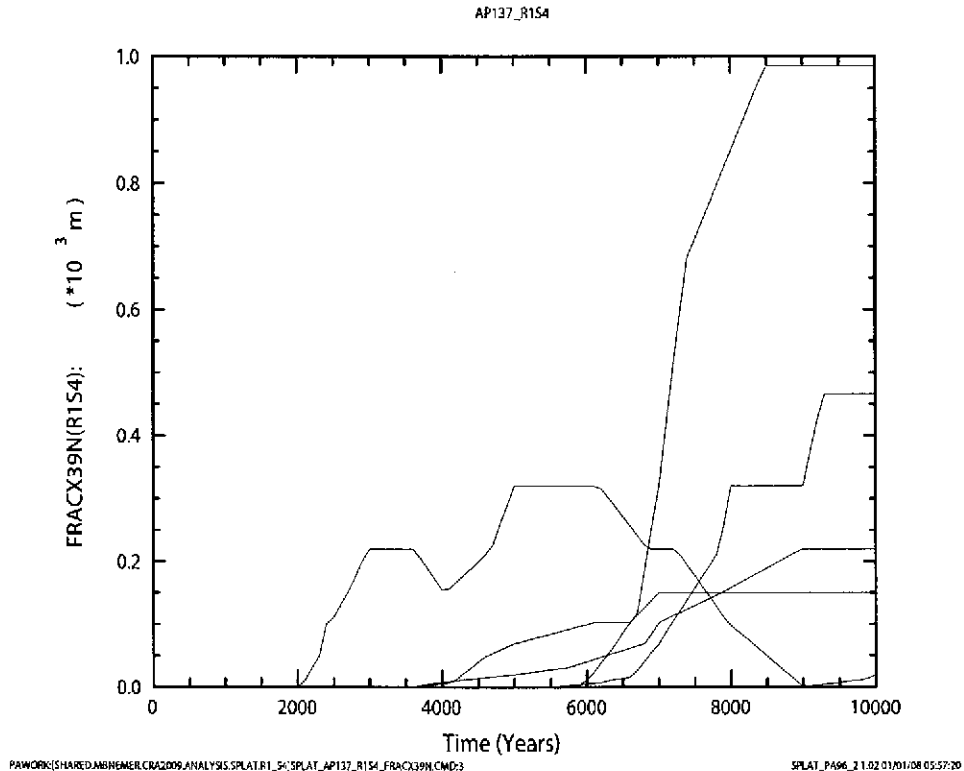
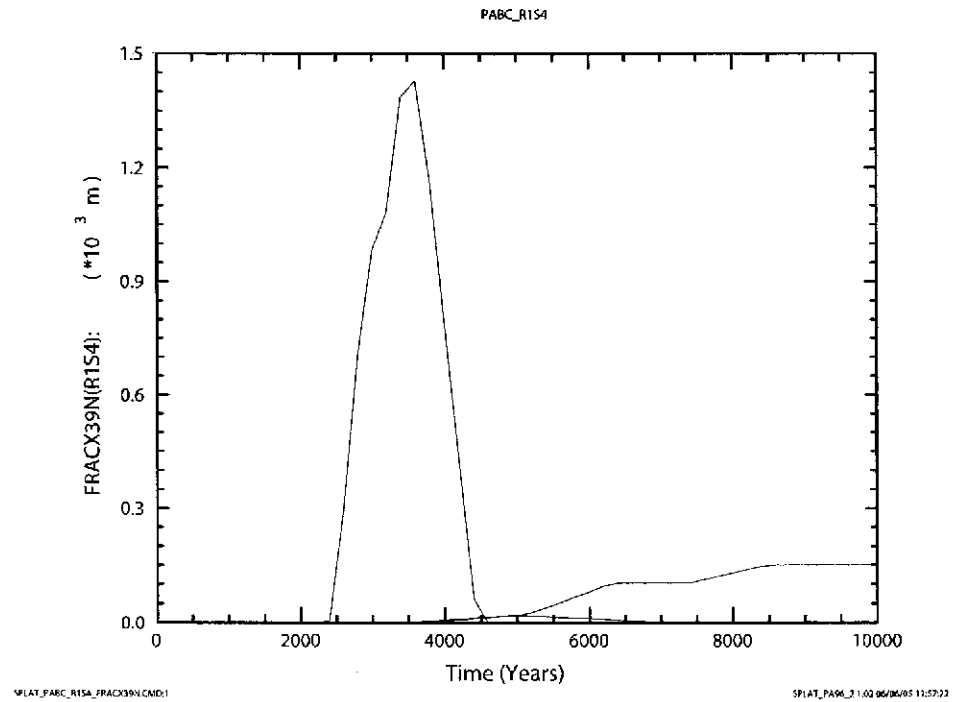


Figure 6-83. Fracture length (m) in MB139, north of the repository versus time (years) for all 100 vectors in Replicate R1, Scenario S2. Figure a) shows results from the CRA-2009 PA. Figure b) shows results from the CRA-2004 PABC.



a) CRA-09



b) PABC

Figure 6-84. Fracture length (m) in MB139, north of the repository versus time (years) for all 100 vectors in Replicate R1, Scenario S4. Figure a) shows results from the CRA-2009 PA. Figure b) shows results from the CRA-2004 PABC.

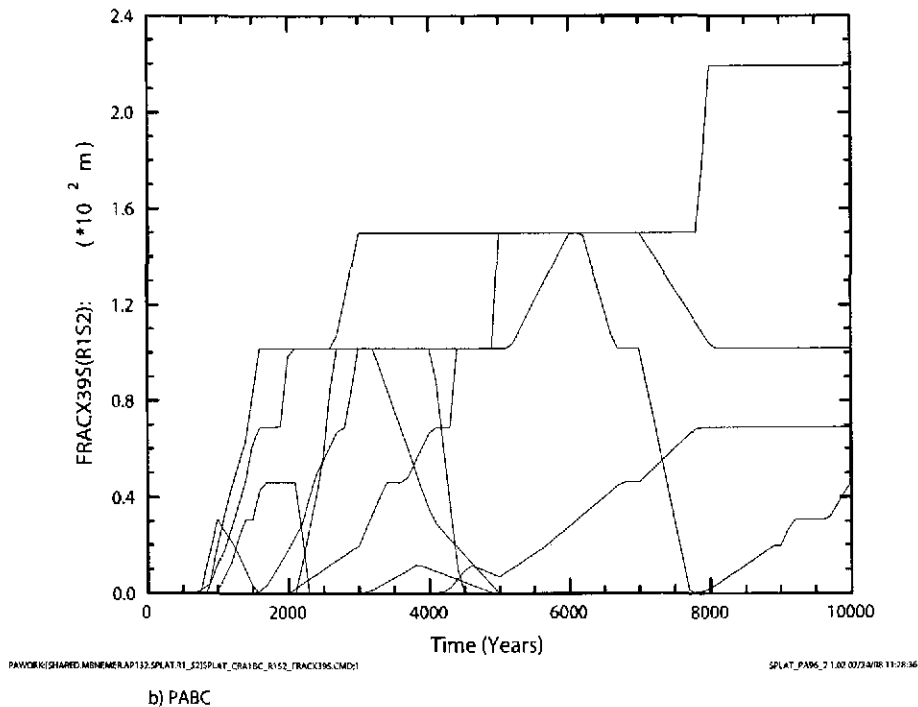
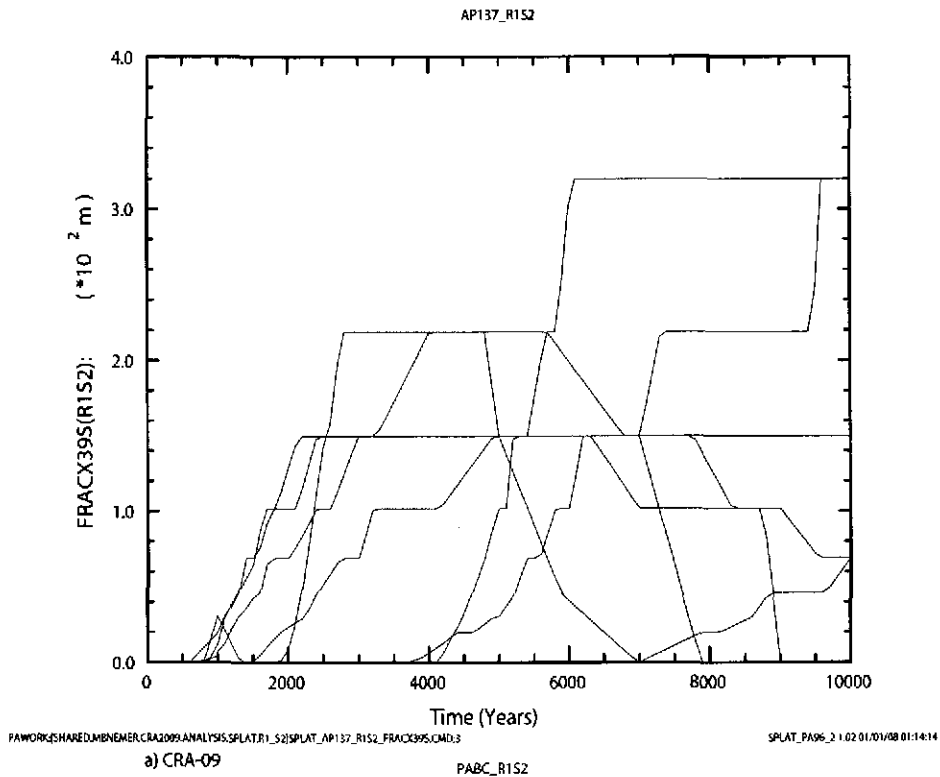
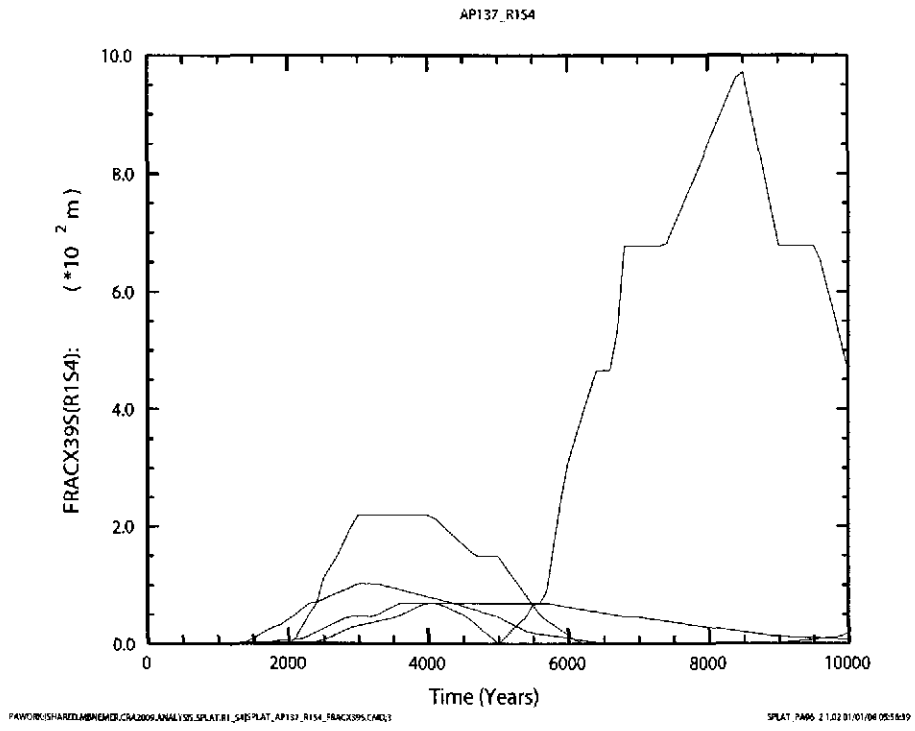
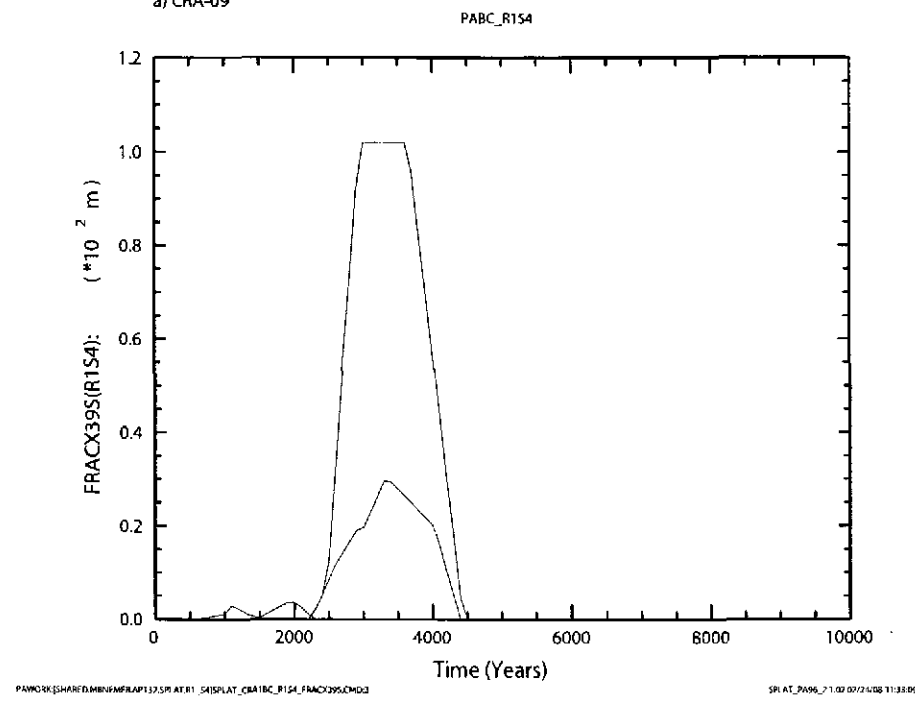


Figure 6-85. Fracture length (m) in MB139, south of the repository versus time (years) for all 100 vectors in Replicate R1, Scenario S2. Figure a) shows results from the CRA-2009 PA. Figure b) shows results from the CRA-2004 PABC.

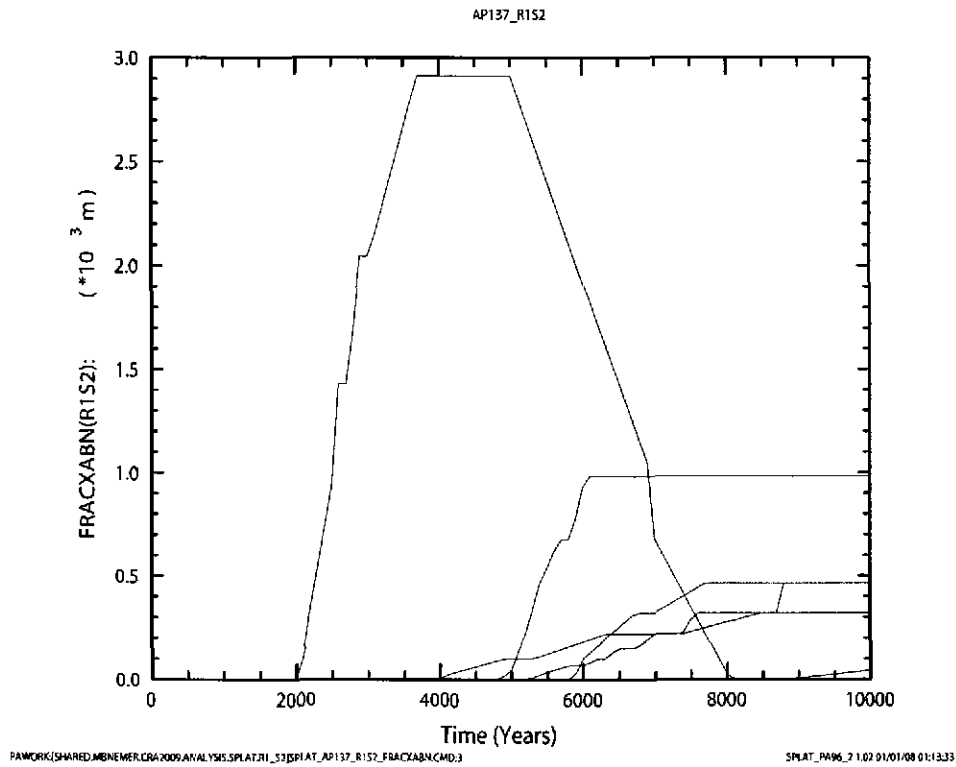


a) CRA-09



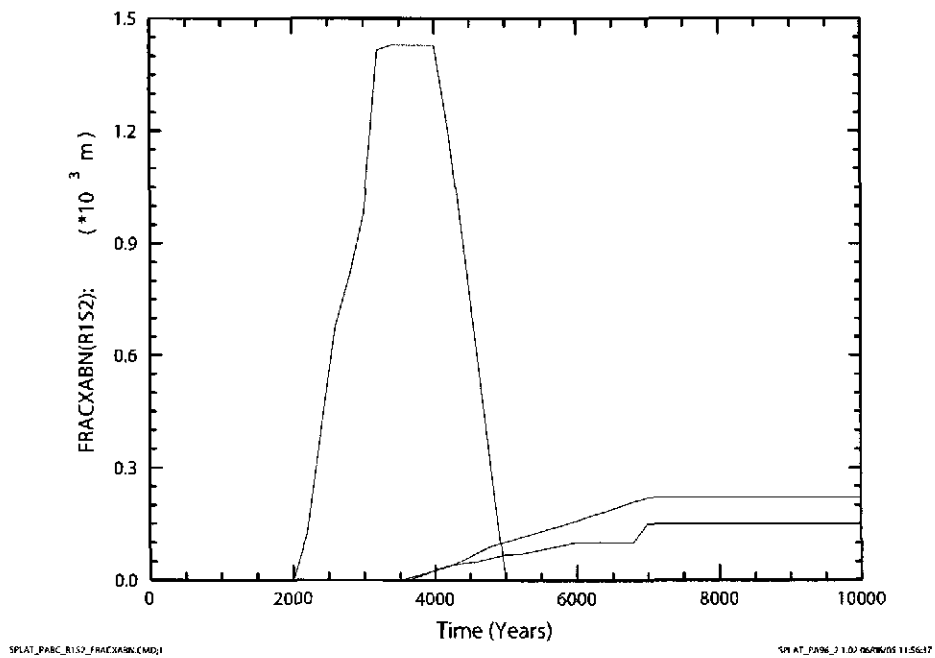
b) PABC

Figure 6-86. Fracture length (m) in MB139, south of the repository versus time (years) for all 100 vectors in Replicate R1, Scenario S4. Figure a) shows results from the CRA-2009 PA. Figure b) shows results from the CRA-2004 PABC.



a) CRA-09

PABC R1S2



b) PABC

Figure 6-87. Fracture length (m) in Anhydrite A&B, north of the repository versus time (years) for all 100 vectors in Replicate R1, Scenario S2. Figure a) shows results from the CRA-2009 PA. Figure b) shows results from the CRA-2004 PABC.

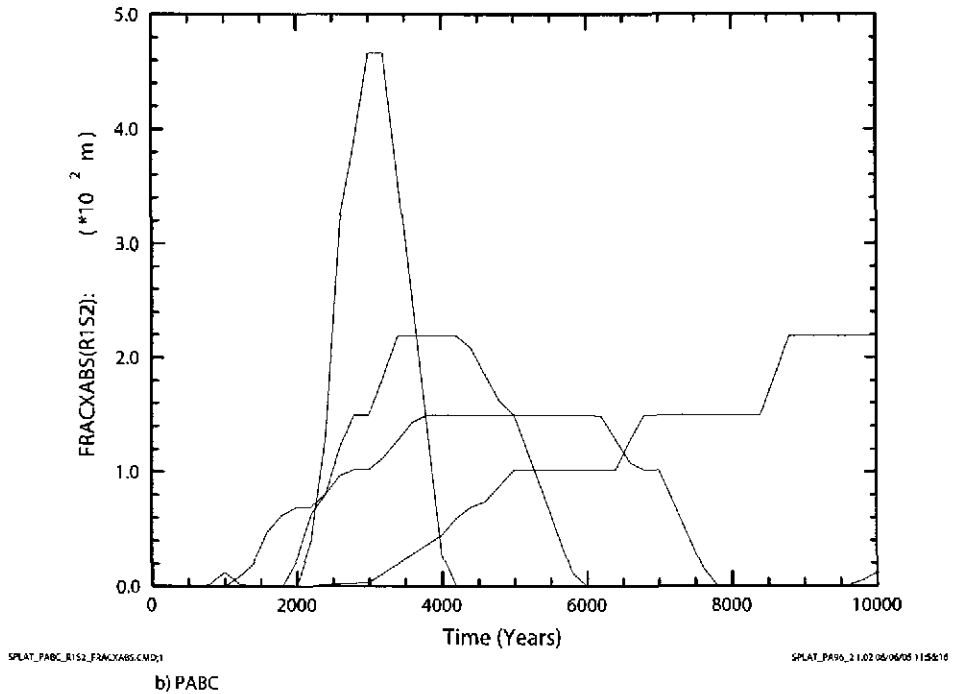
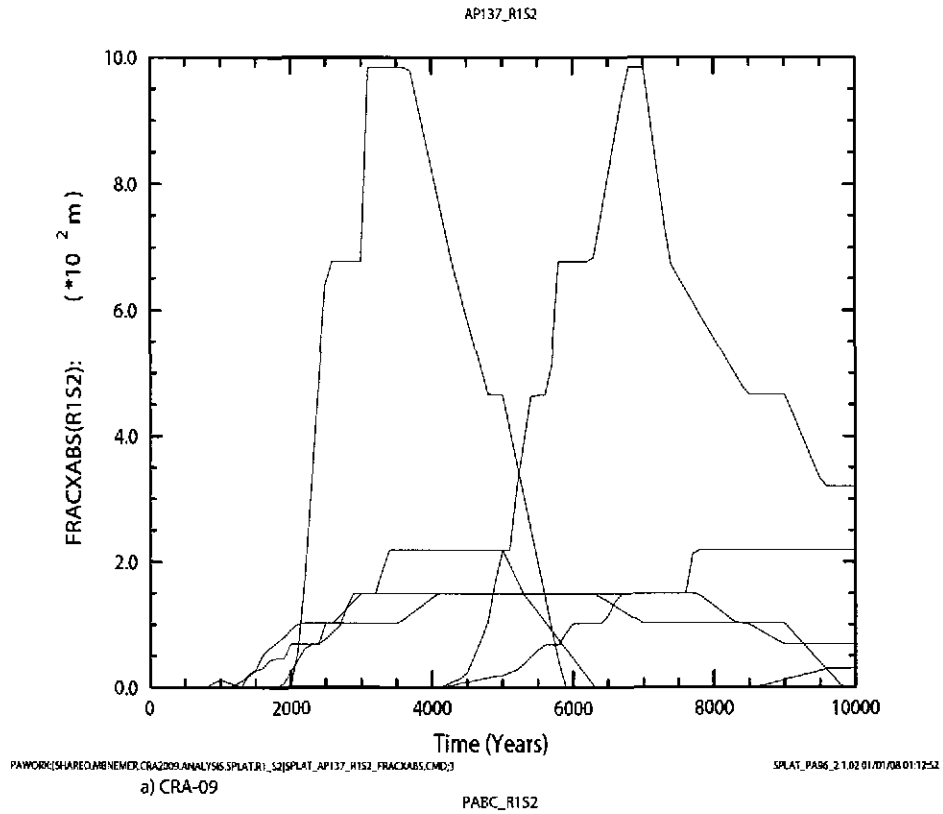


Figure 6-89. Fracture length (m) in Anhydrite A&B, south of the repository versus time (years) for all 100 vectors in Replicate R1, Scenario S2. Figure a) shows results from the CRA-2009 PA. Figure b) shows results from the CRA-2004 PABC.

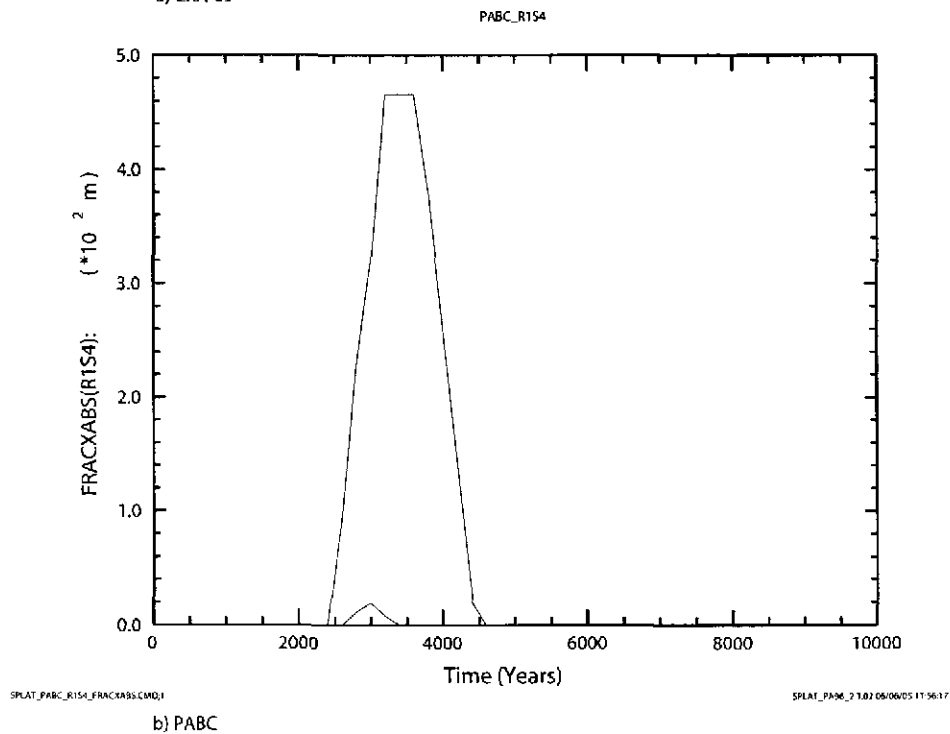
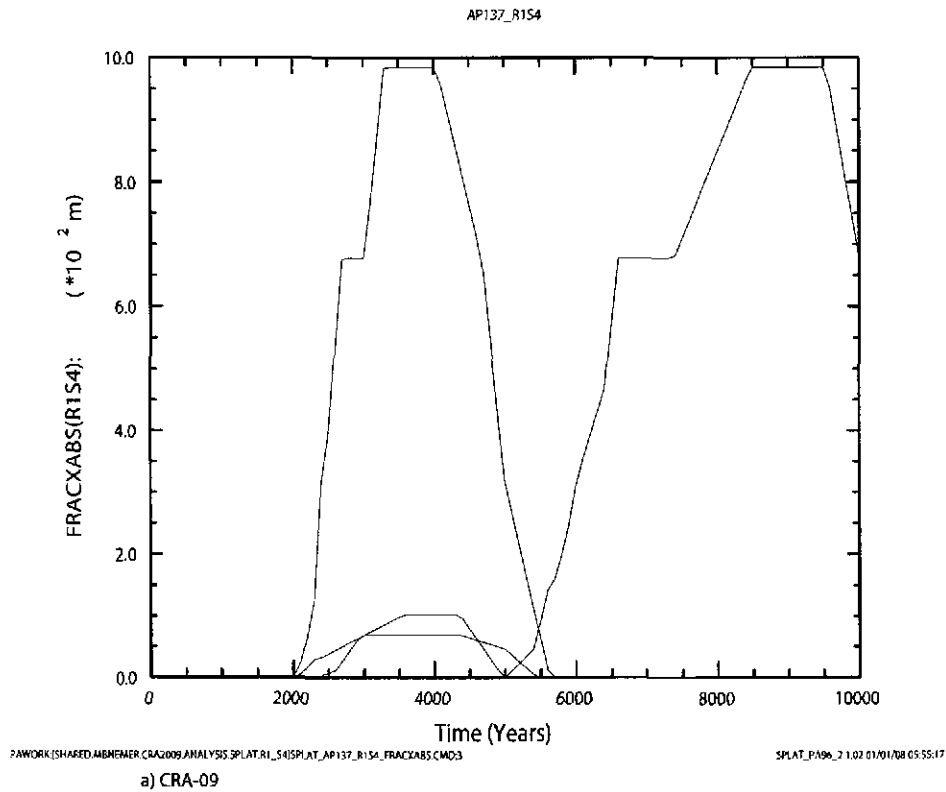
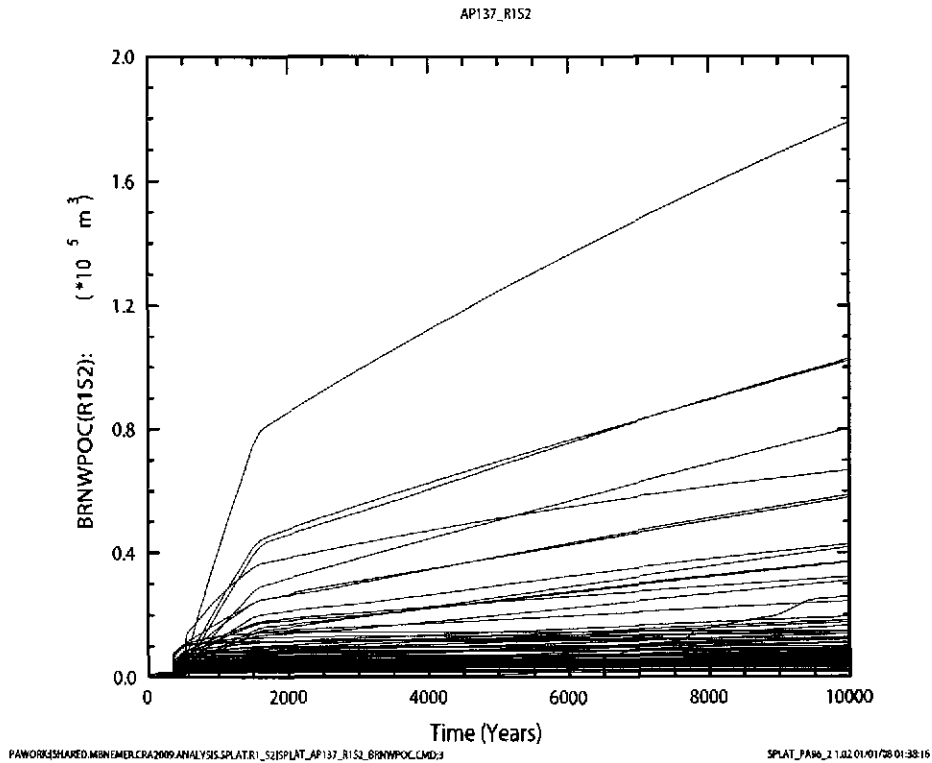
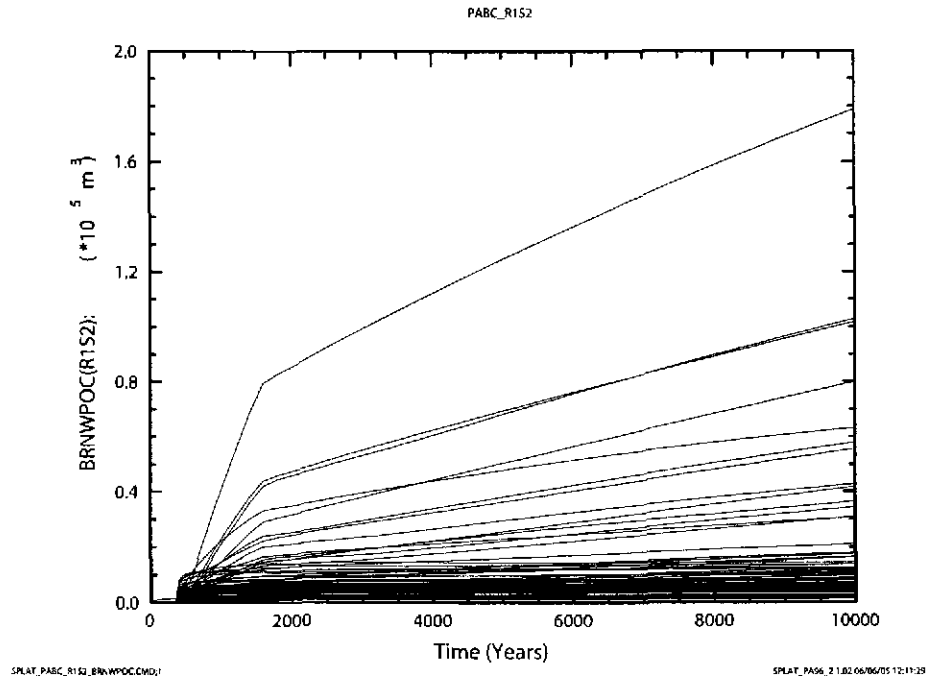


Figure 6-90. Fracture length (m) in Anhydrite A&B, south of the repository versus time (years) for all 100 vectors in Replicate R1, Scenario S4. Figure a) shows results from the CRA-2009 PA. Figure b) shows results from the CRA-2004 PABC.



a) CRA-09



b) PABC

Figure 6-91. Total cumulative brine flow (m^3) out of the waste panel versus time (years) for all 100 vectors in Replicate R1, Scenario S2. Figure a) shows results from the CRA-2009 PA. Figure b) shows results from the CRA-2004 PABC.

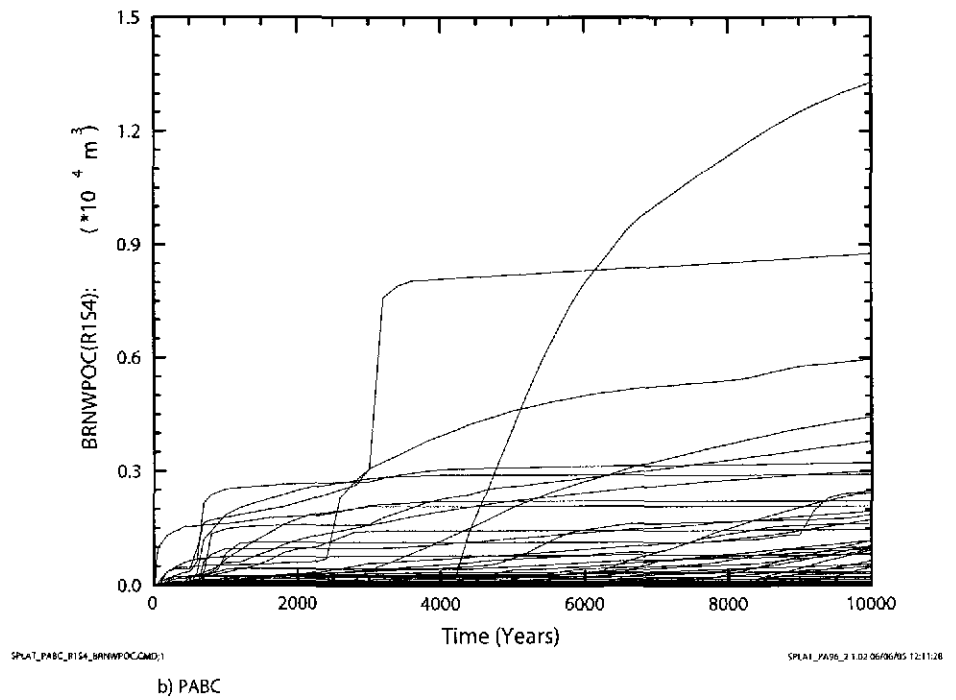
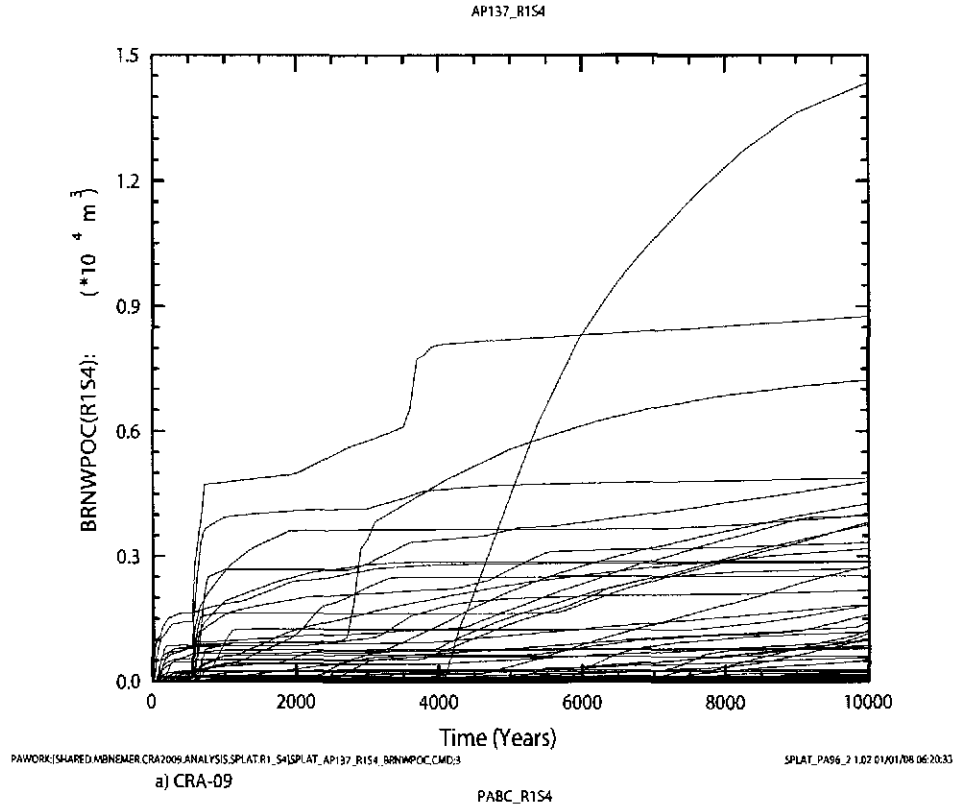


Figure 6-92. Total cumulative brine flow (m^3) out of the Waste Panel, versus time (years) for all 100 vectors in Replicate R1, Scenario S4. Figure a) shows results from the CRA-2009 PA. Figure b) shows results from the CRA-2004 PABC.

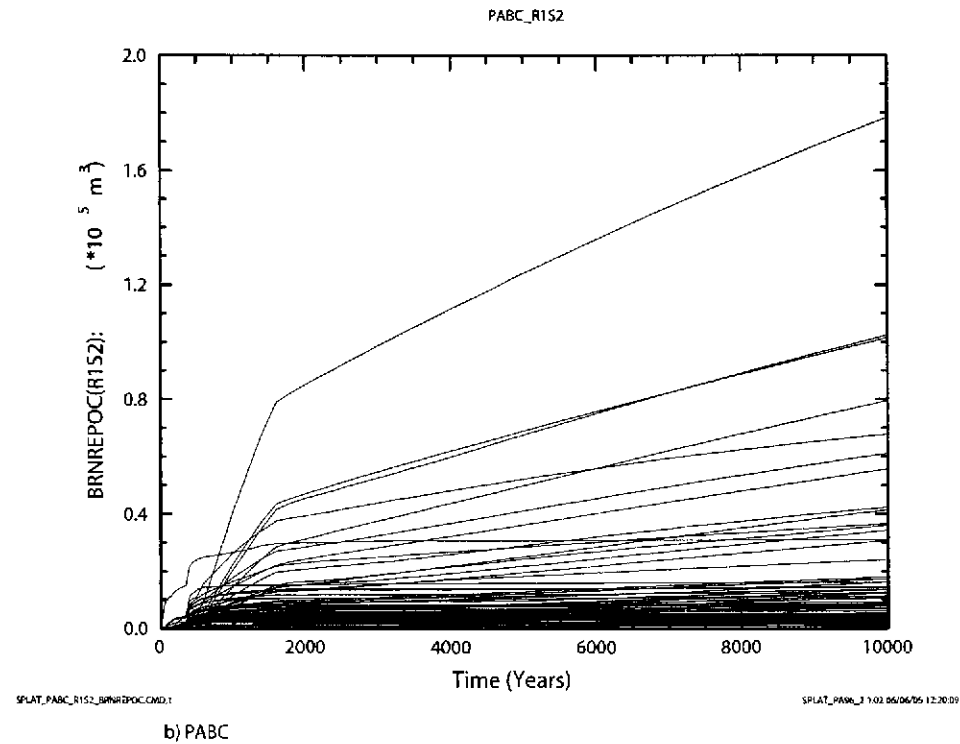
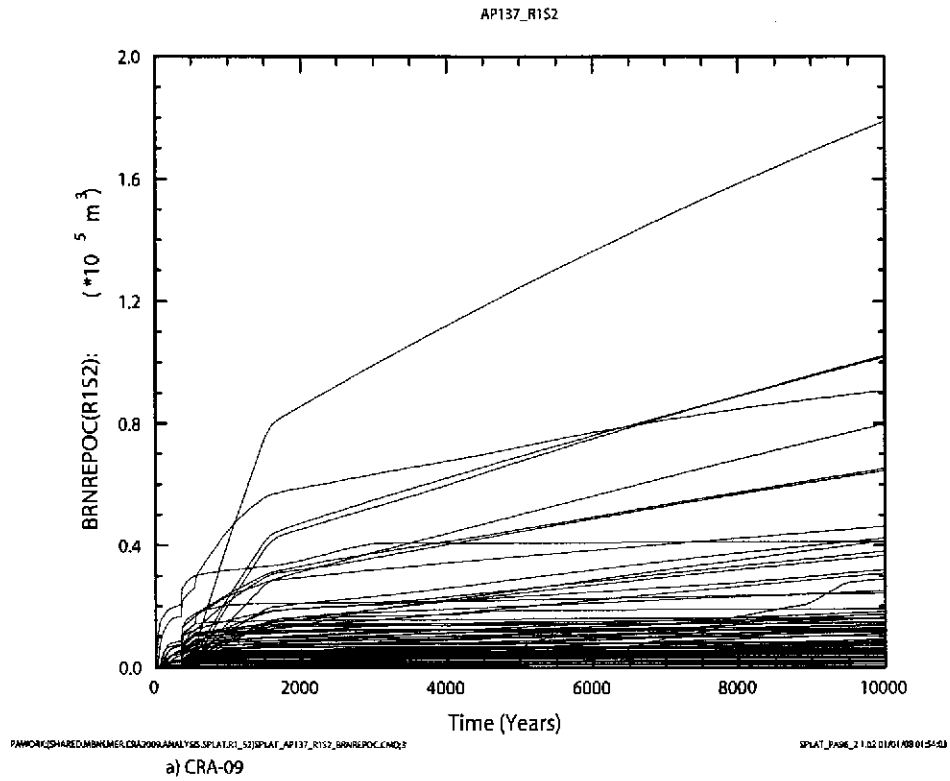
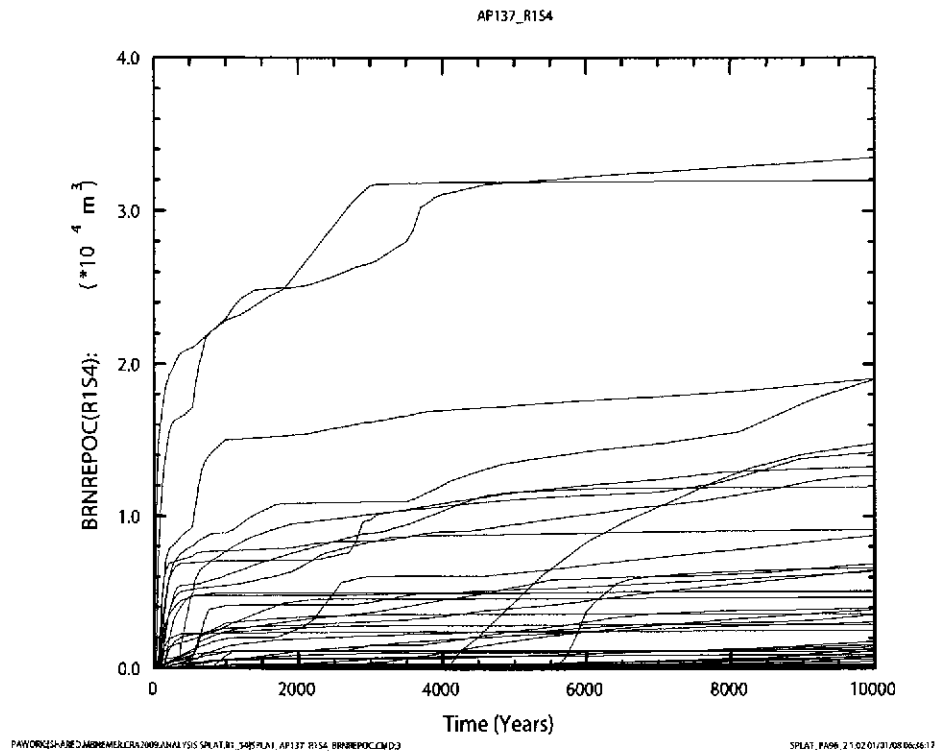
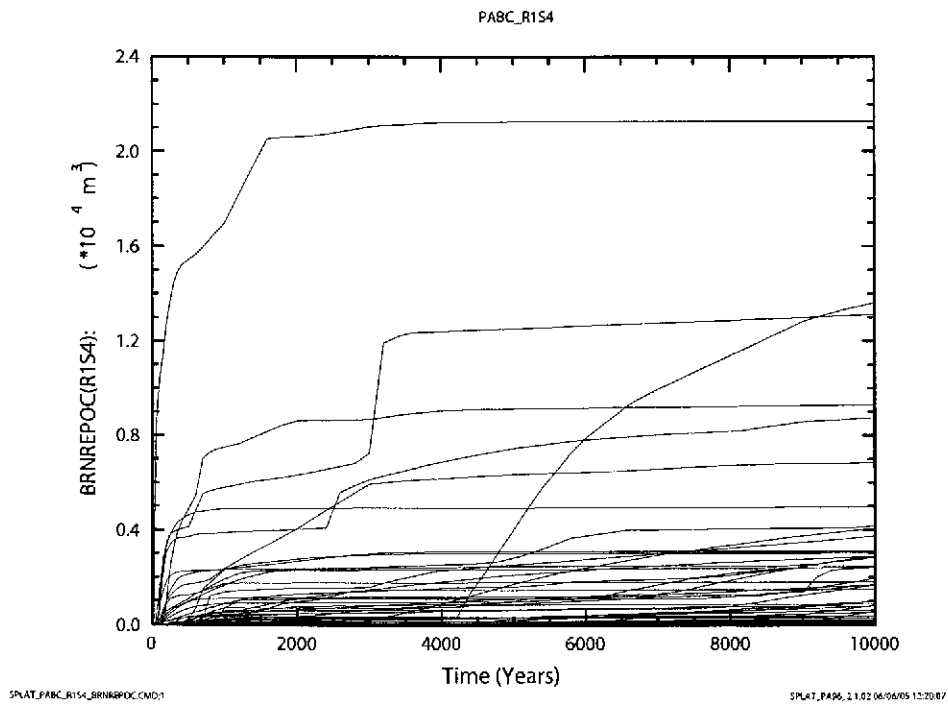


Figure 6-93. Cumulative brine flow (m^3) out of the repository versus time (years) for all 100 vectors in Replicate R1, Scenario S2. Figure a) shows results from the CRA-2009 PA. Figure b) shows results from the CRA-2004 PABC.



a) CRA-09



b) PABC

Figure 6-94. Cumulative brine flow (m³) out of the repository versus time (years) for all 100 vectors in Replicate R1, Scenario S4. Figure a) shows results from the CRA-2009 PA. Figure b) shows results from the CRA-2004 PABC.

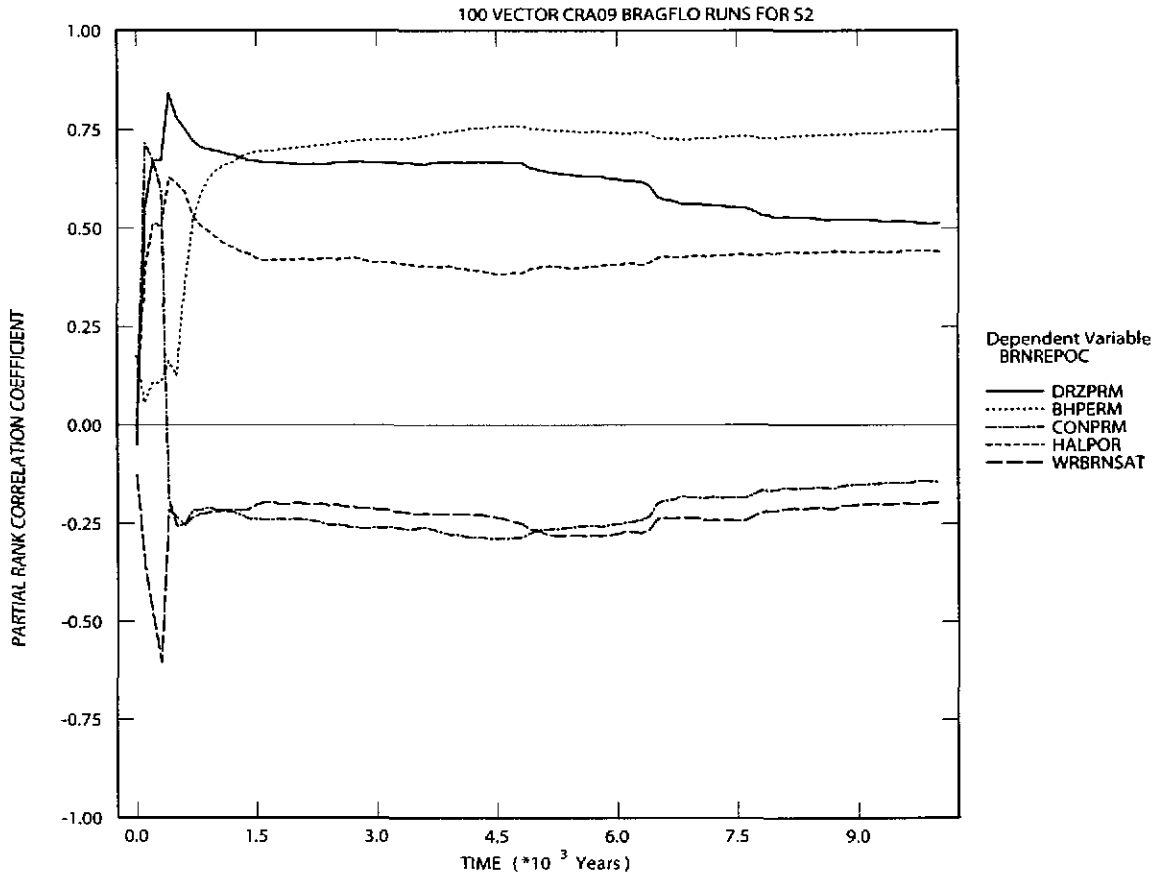


Figure 6-95. Primary correlations (dimensionless) of brine flow out of the repository with input parameters versus time (years) from the CRA-2009 PA Replicate R1, Scenario S2. Table 4-2 gives a description of the names in the legend.

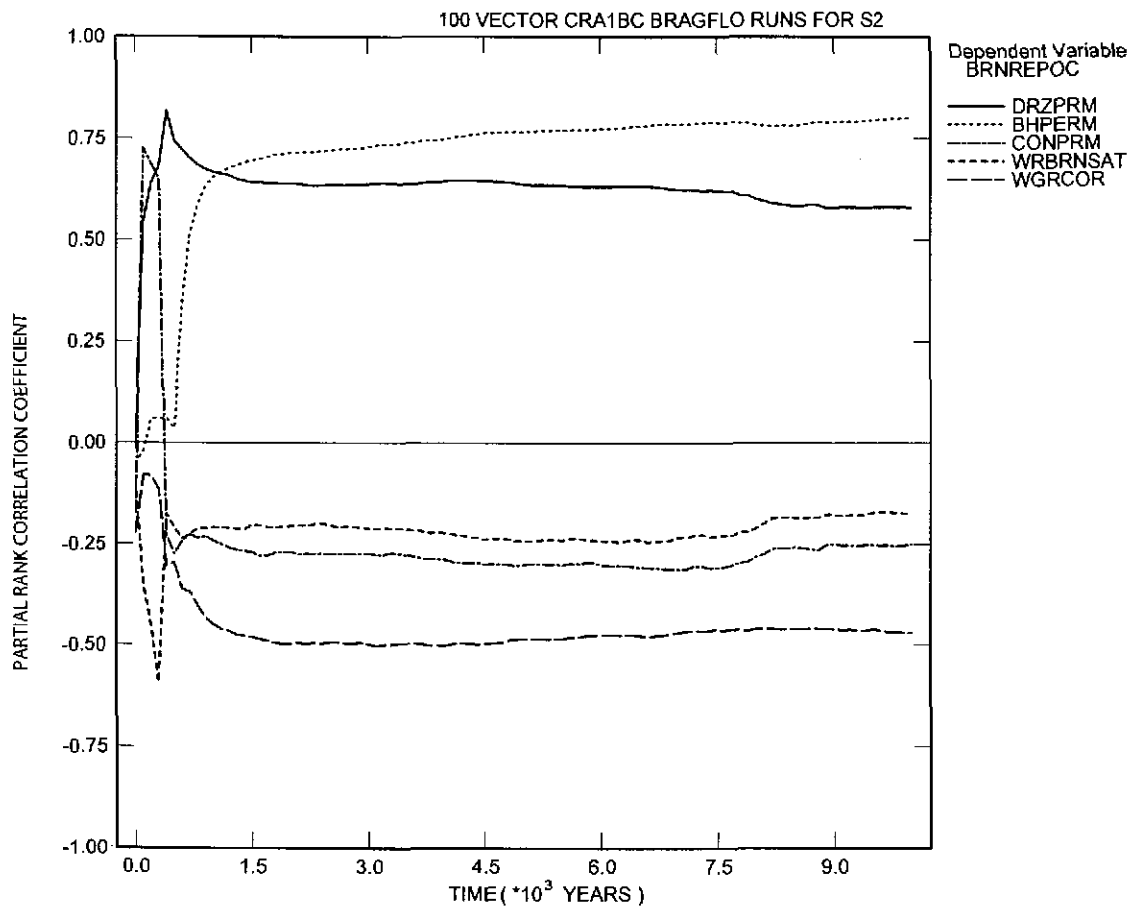


Figure 6-96. Primary correlations (dimensionless) of brine flow out of the repository with input parameters versus time (years) from the CRA-2004 PABC Replicate R1, Scenario S2. Table 4-2 gives a description of the names in the legend.

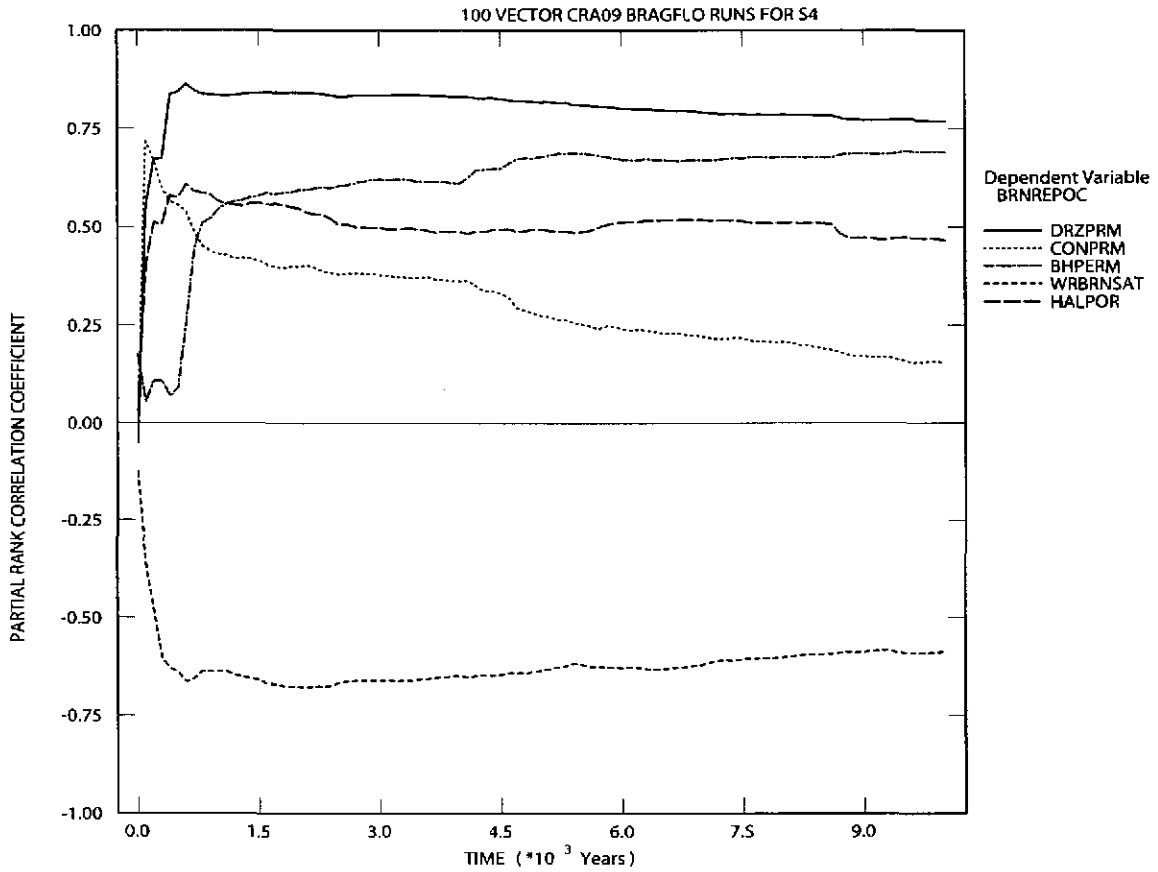
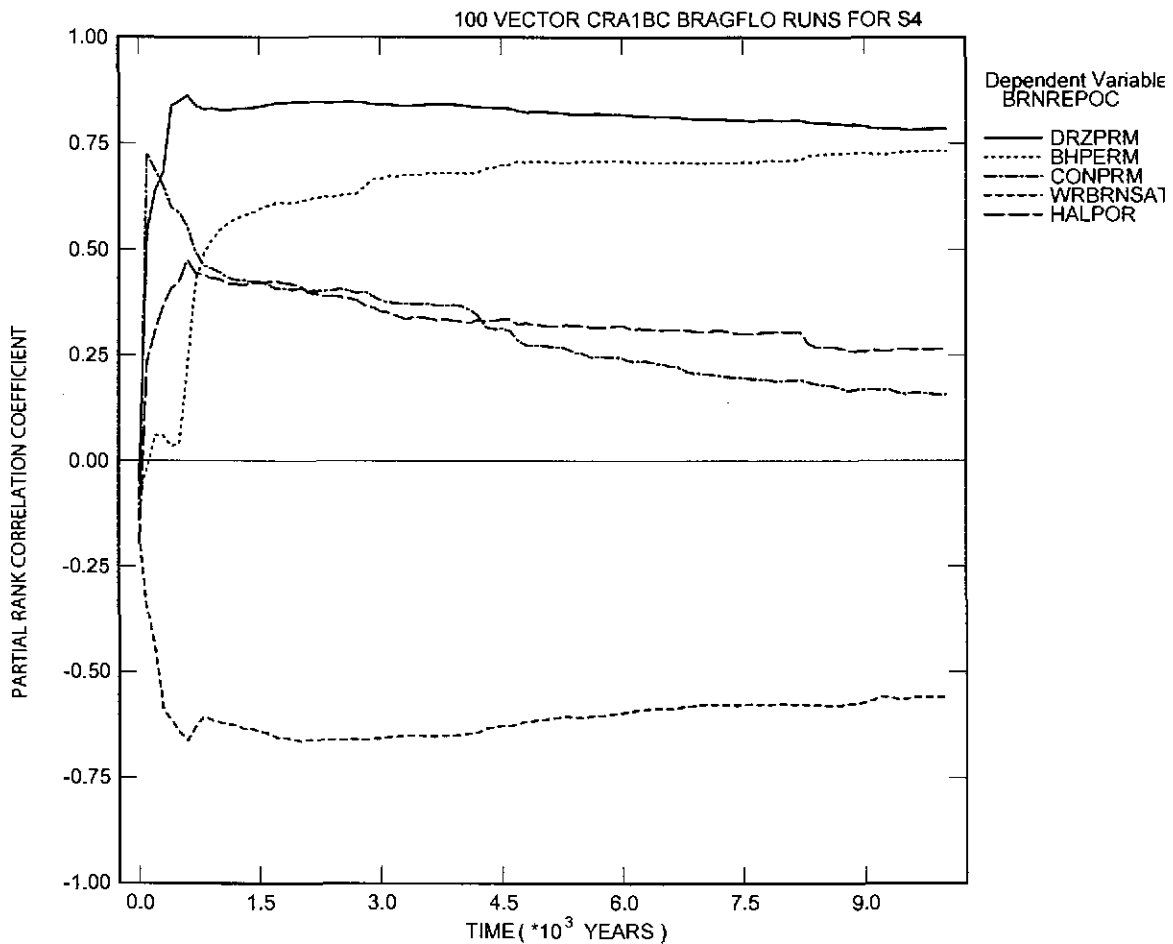


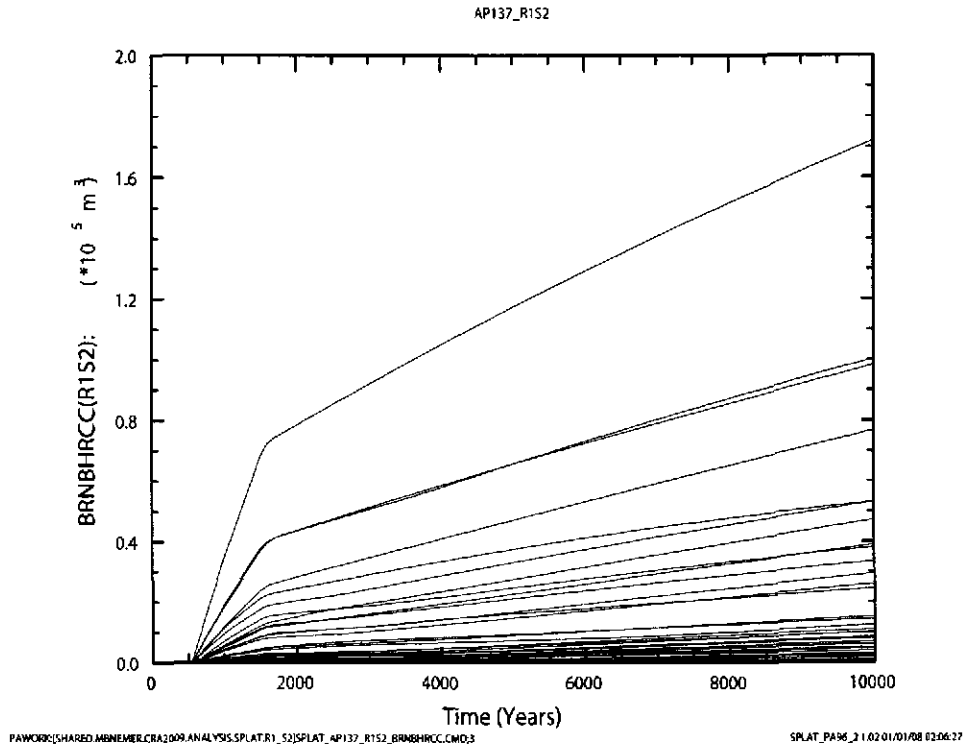
Figure 6-97. Primary correlations (dimensionless) of brine flow out of the repository with input parameters versus time (years) from the CRA-2009 PA Replicate R1, Scenario S4. Table 4-2 gives a description of the names in the legend.



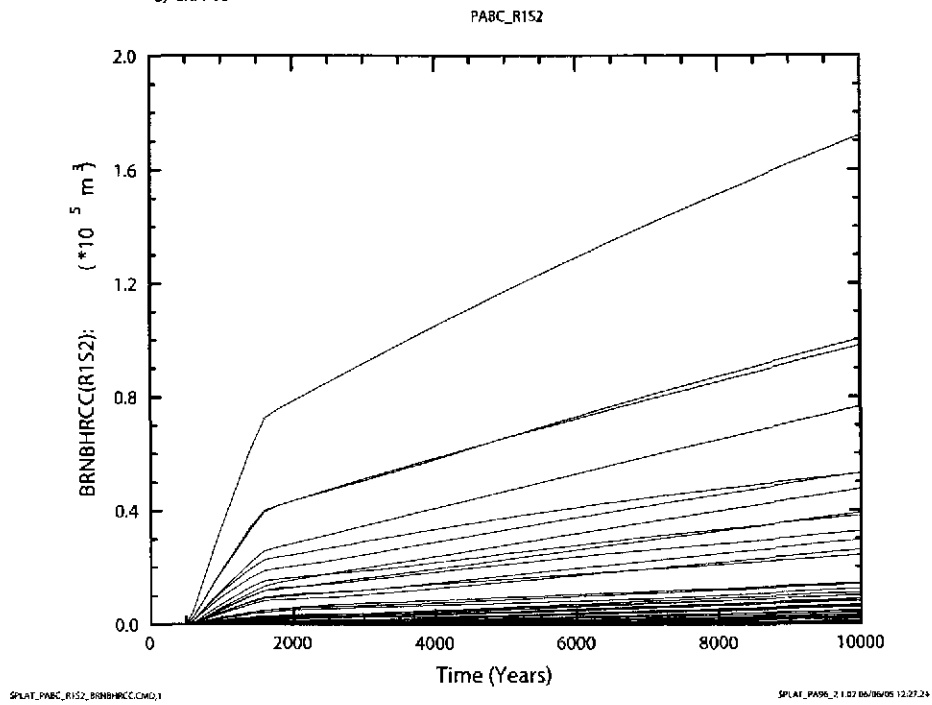
PCCSRC_S4.INP;2

PCCSRC_PA96 2.21 06/08/05 10:23

Figure 6-98. Primary correlations (dimensionless) of brine flow out of the repository with input parameters versus time (years) from the CRA-2004 PABC Replicate R1, Scenario S4. Table 4-2 gives a description of the names in the legend.



a) CRA-09



b) PABC

Figure 6-99. Cumulative brine flow (m³) to the Culebra formation versus time (years) for all 100 vectors in Replicate R1, Scenario S2. Figure a) shows results from the CRA-2009 PA. Figure b) shows results from the CRA-2004 PABC.

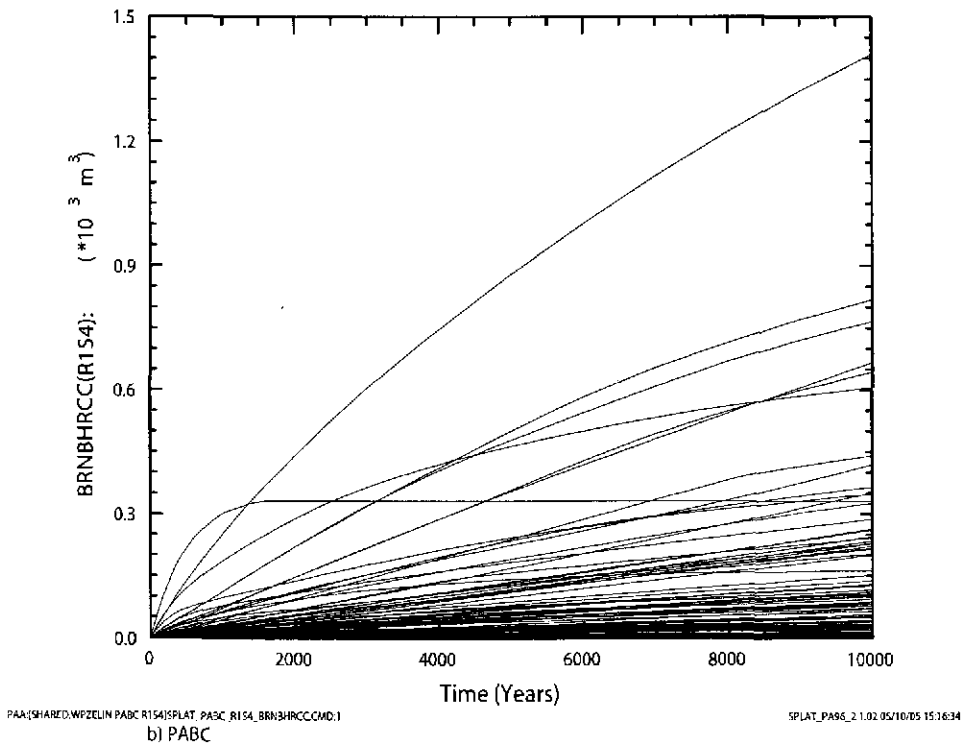
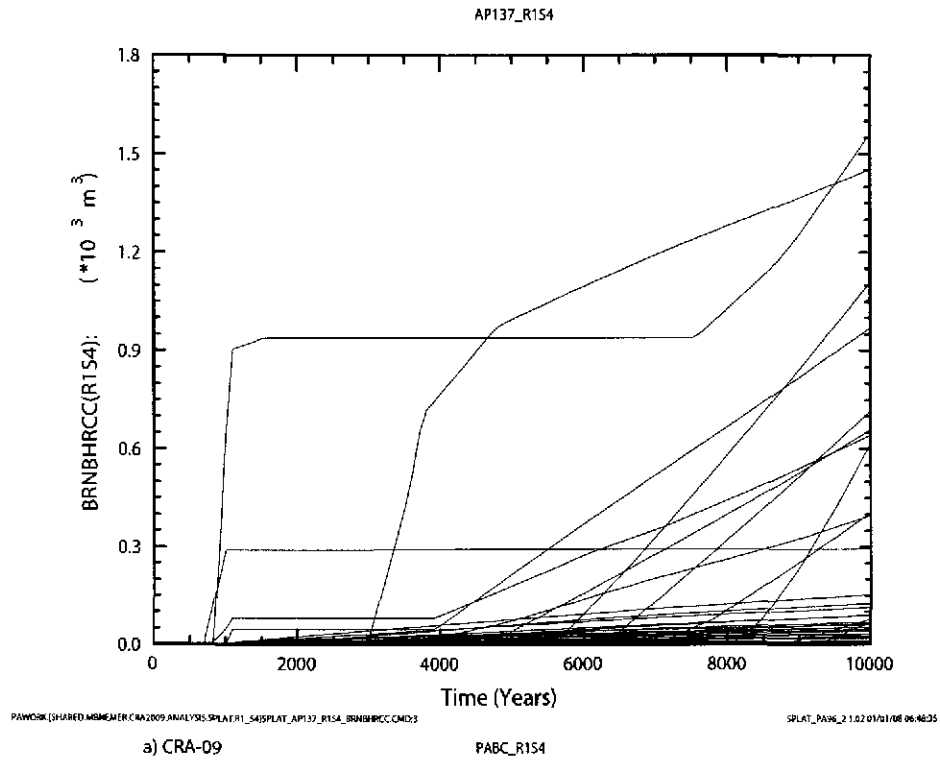
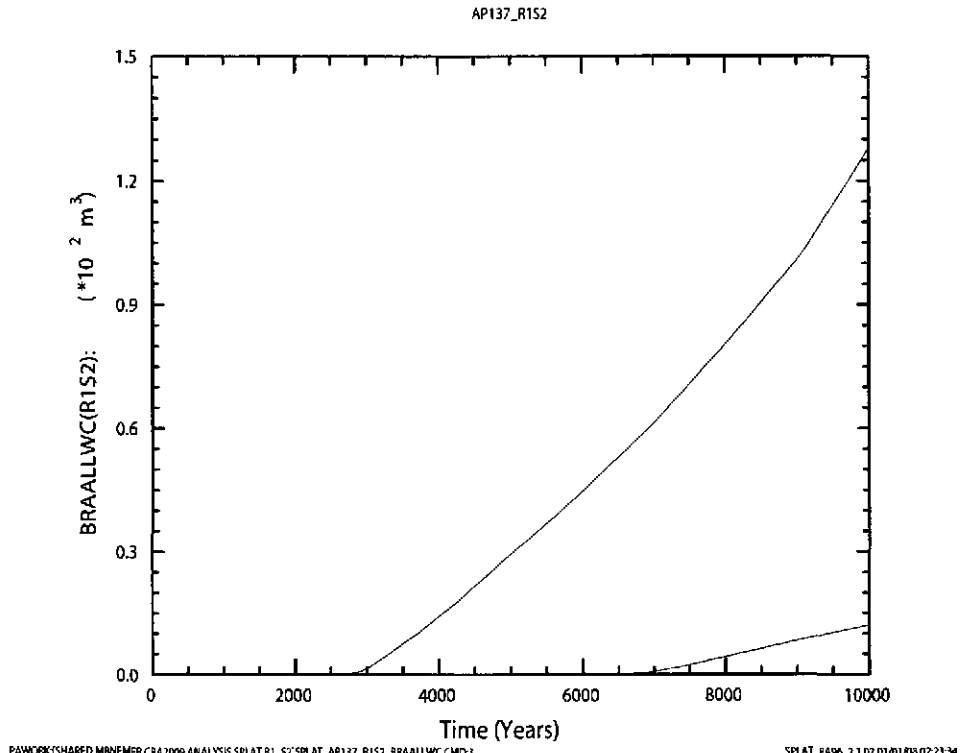
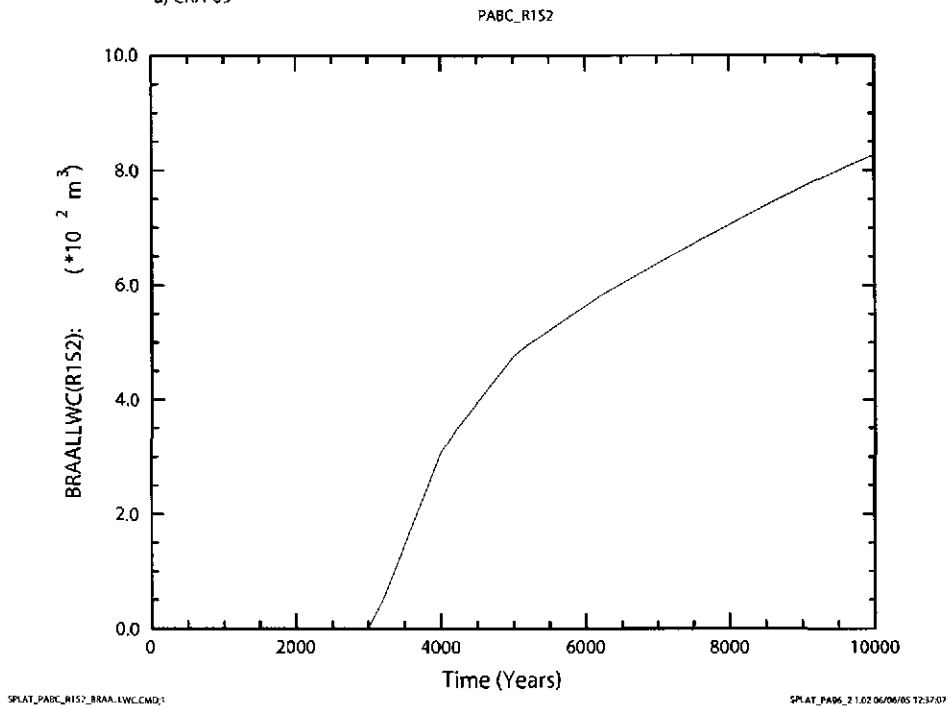


Figure 6-100. Cumulative brine flow (m^3) to the Culebra formation versus time (years) for all 100 vectors in Replicate R1, Scenario S4. Figure a) shows results from the CRA-2009 PA. Figure b) shows results from the CRA-2004 PABC.

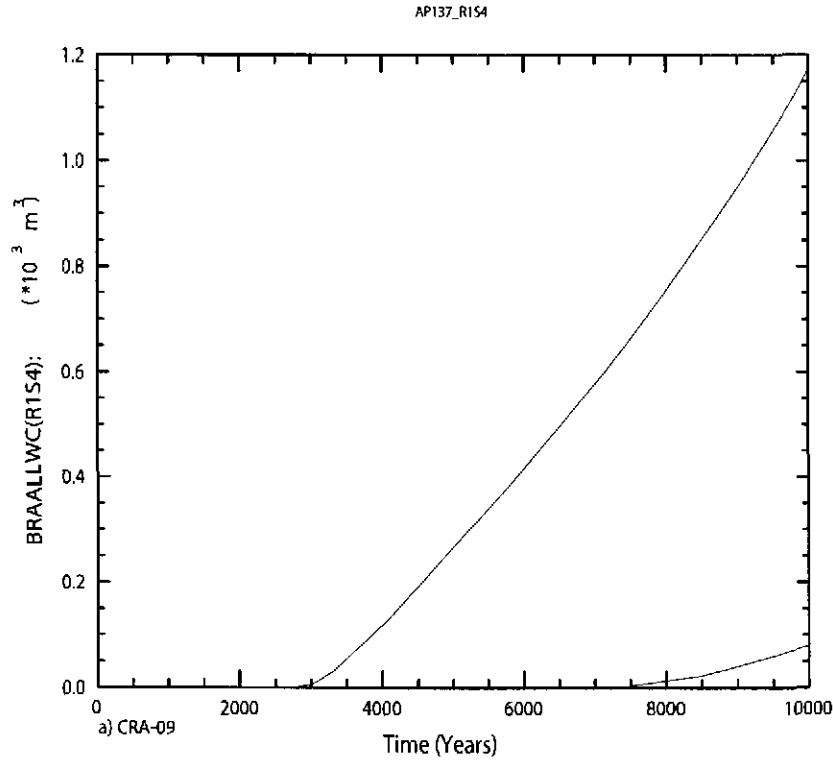


a) CRA-09



b) PABC

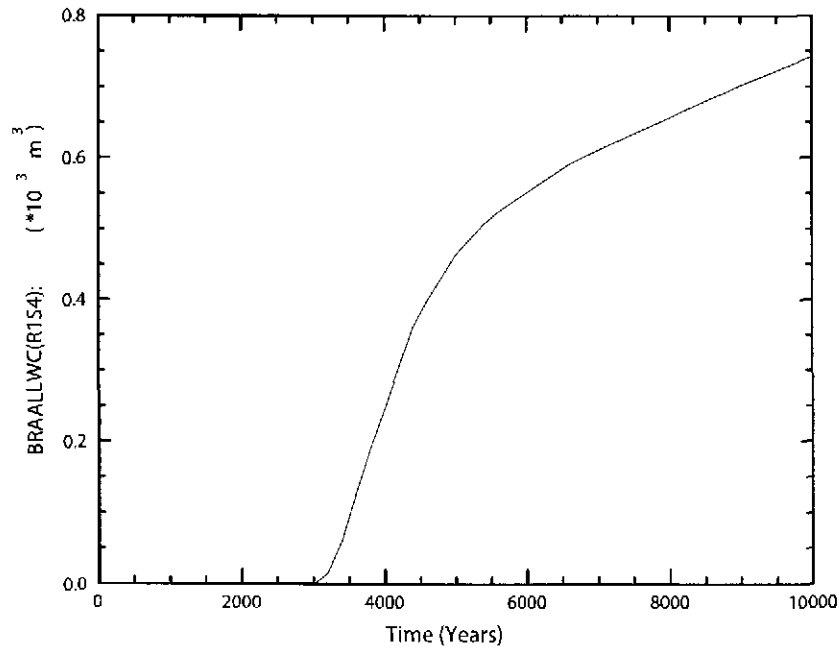
Figure 6-101. Cumulative brine flow (m^3) to the LWB versus time (years) for all 100 vectors in Replicate R1, Scenario S2. Figure a) shows results from the CRA-2009 PA. Figure b) shows results from the CRA-2004 PABC.



PAWWORK\SHARID\MB\EMER\CRA2009\ANALYSIS\SPLAT\R1_S4\SPLAT_AP137_R1S4_BRAALLWC.CH03

SPLAT_PAGE_21.02.01\01\08 07:05:40

PABC_R1S4



SPLAT_PABC_R1S4_BRAALLWC.CH01

SPLAT_PAGE_21.02.06\06\05 12:37:04

Figure 6-102. Cumulative brine flow (m^3) to the LWB versus time (years) for all 100 vectors in Replicate R1, Scenario S4. Figure a) shows results from the CRA-2009 PA. Figure b) shows results from the CRA-2004 PABC.

6.5 COMPARISON OF REPLICATES

The Salado Flow Analysis employs three replicates to confirm the statistical reliability of the primary analysis of Replicate R1. Each is composed of the same six scenarios, but each replicate uses a different Latin Hypercube set of sampled input parameters.

Comparison of results from the three replicates is based upon three key output variables. These variables are chosen because of their importance to other models, which calculate releases that are tallied in the final CCDFs. All of these variables are discussed in detail for Replicate R1 in Subsection 6:

- WAS_PRES - pressure in the waste panel
- WAS_SATB - brine saturation in the waste panel
- BRNREPOC - cumulative brine flow away from the repository

Figure 6-103 and Figure 6-104 show volume averaged pressure in the Waste Panel (WAS_PRES) versus time, averaged over 100 vectors, from Scenario S1, Replicates R1-R3, from the CRA-2009 PA and the CRA-2004 PABC. The differences in the replicates are about the same relative magnitude in the two analyses. Figure 6-105 and Figure 6-106 show the brine saturation in the Waste Panel (WAS_SATB) versus time for the same set of analyses. Figure 6-107 and Figure 6-108 show the cumulative brine flow away from the repository (BRNREPOC) for the same set of analyses. The differences between replicates are greater for WAS_SATB and BRNREPOC than for WAS_PRES but no greater in the CRA-2009 PA than was seen in the CRA-2004 PABC.

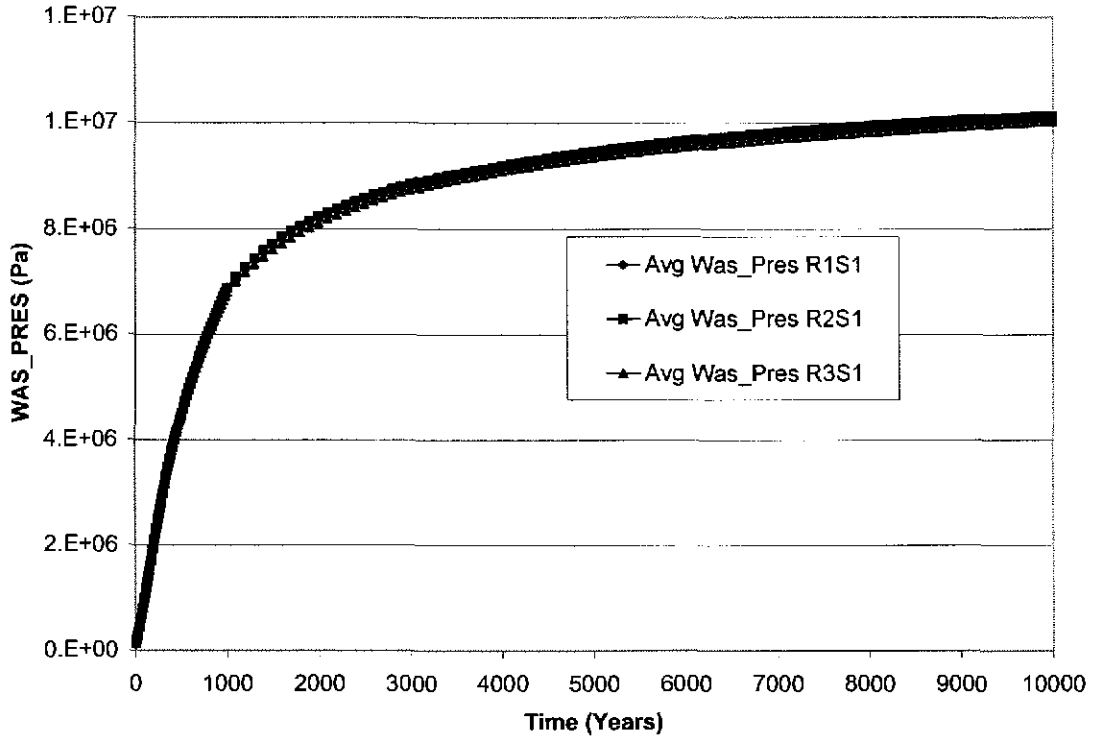


Figure 6-103. Vector-averaged pressure (Pa) in the waste area versus time (years) from the CRA-2009 PA, Scenario S1, Replicates R1-R3.

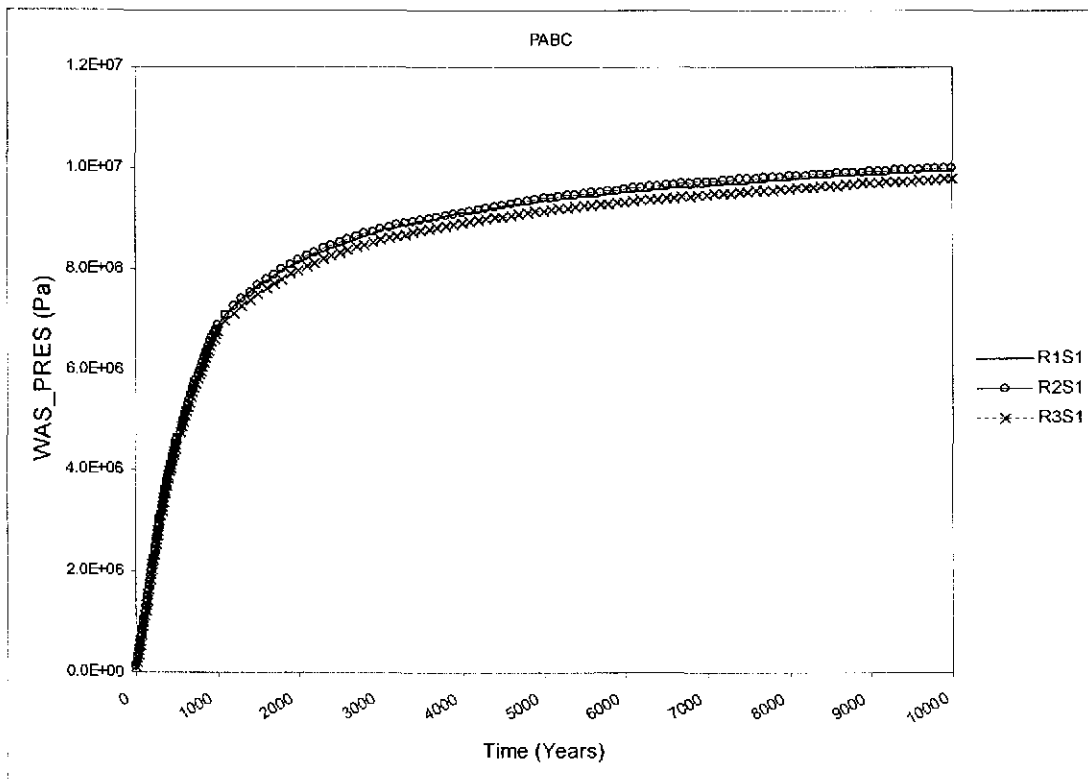


Figure 6-104. Vector-averaged pressure (Pa) in the waste area versus time (years) from the CRA-2004 PABC, Scenario S1, Replicates R1-R3.

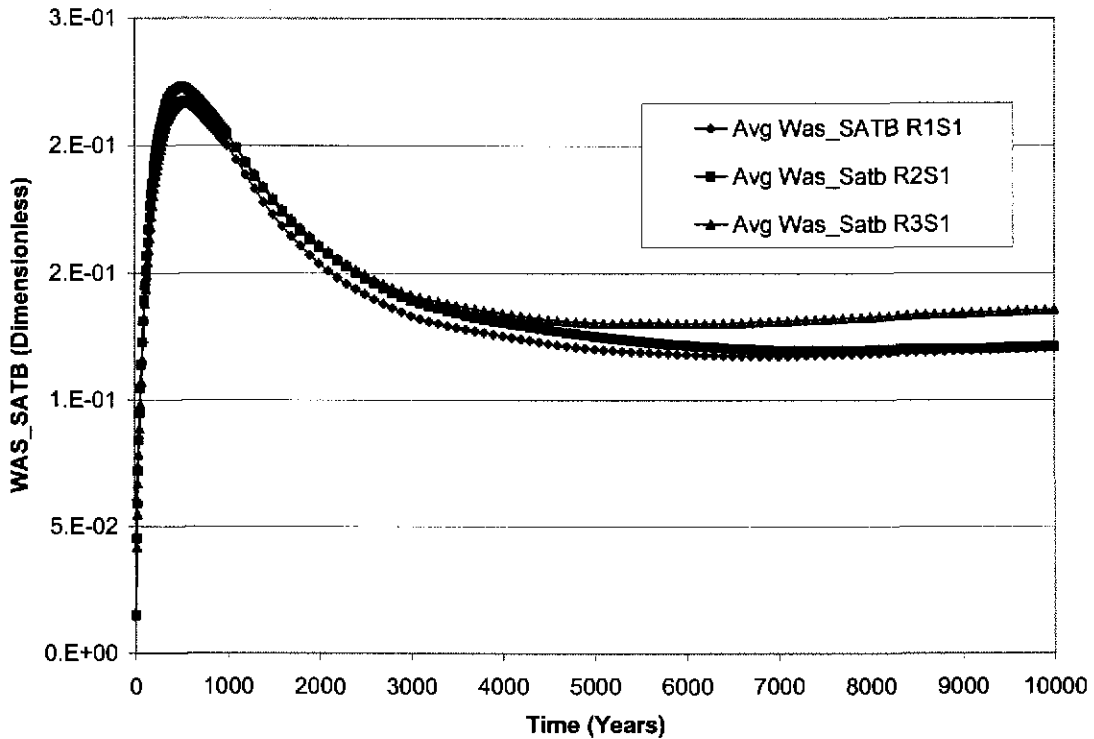


Figure 6-105. Vector-averaged brine saturation (dimensionless) in the waste panel versus time (years)) from the CRA-2009 PA, Scenario S1, Replicates R1-R3.

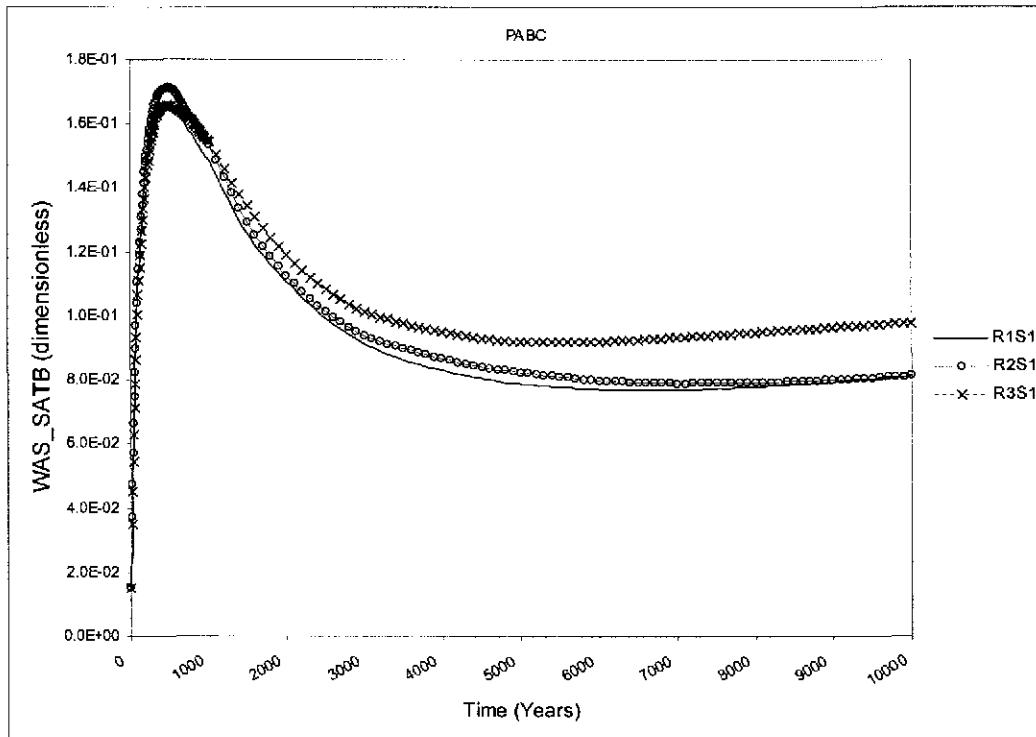


Figure 6-106. Vector-averaged brine saturation (dimensionless) in the waste panel versus time (years)) from the CRA-2004 PABC, Scenario S1, Replicates R1-R3. Note that brine saturation axis maximum is set at 0.18 to emphasize the differences.

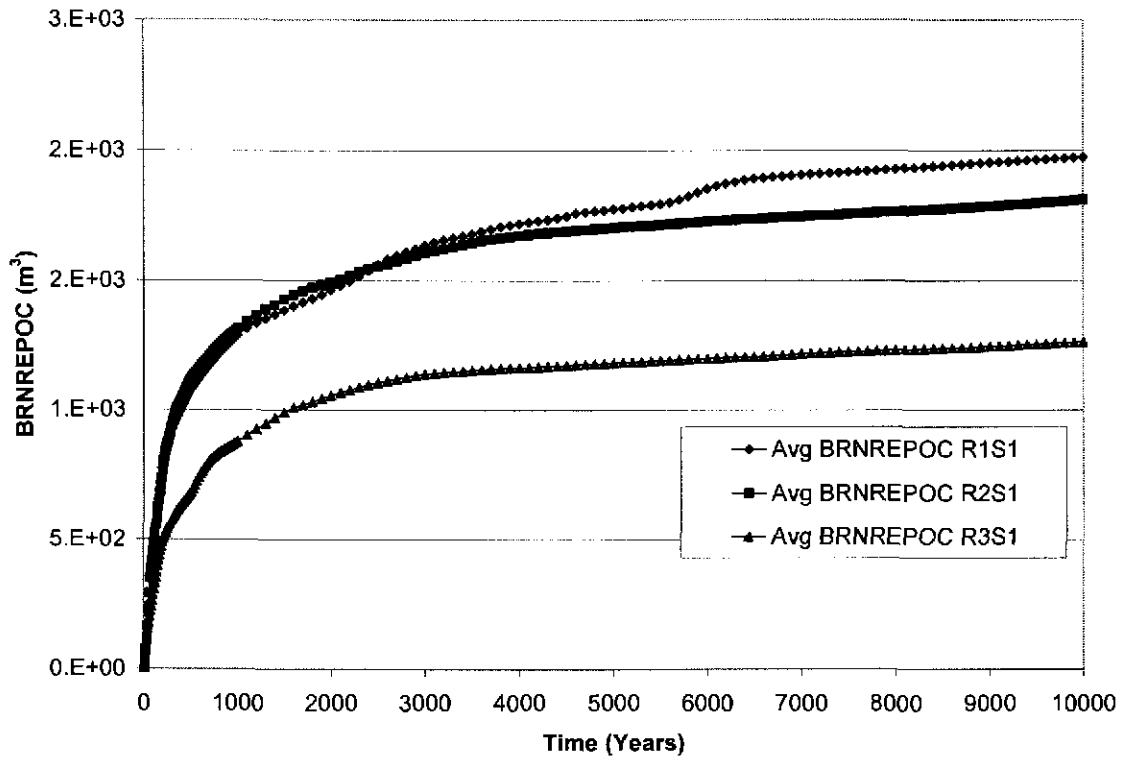


Figure 6-107. Vector-averaged cumulative brine flow (m^3) away from the repository versus time (years) from the CRA-2009 PA, Scenario S1, Replicates R1-R3.

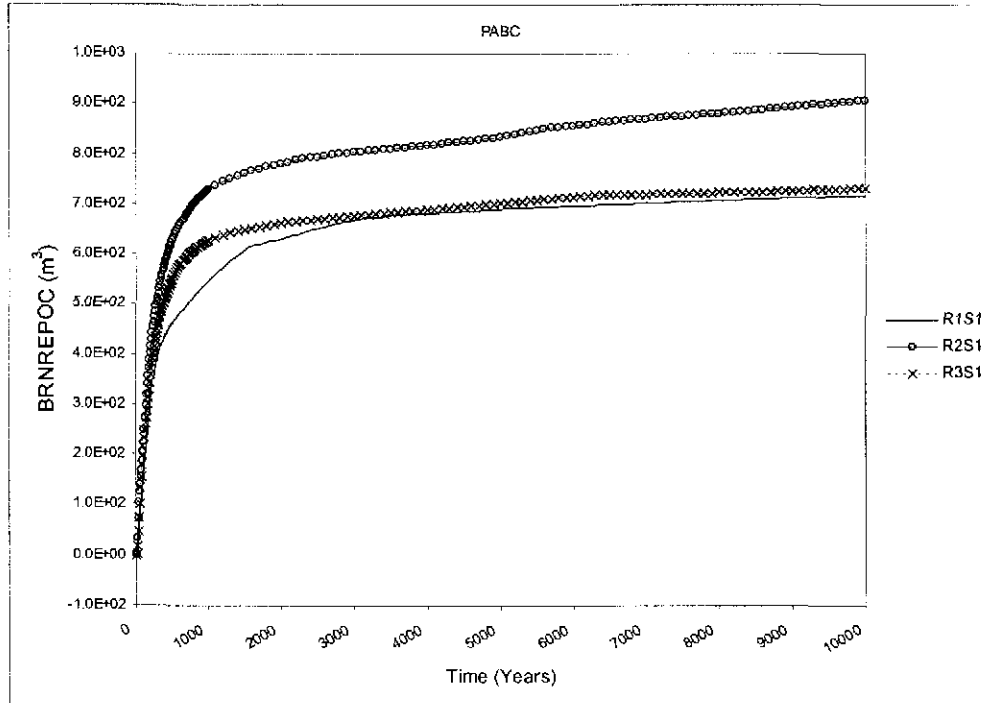


Figure 6-108. Vector-averaged cumulative brine flow (m^3) away from the repository versus time (years) from the CRA-2004 PABC, Scenario S1, Replicates 1-3.

7 SUMMARY AND CONCLUSIONS

The BRAGFLO analysis contained herein provides essential outputs that are needed by other PA process models in order to calculate total releases from the repository. Results of the CRA-2009 PA and CRA-2004 PABC were compared. For the S1 scenario, pressures and saturations in the CRA-2009 PA and the CRA-2004 PABC were similar at 10,000 years. Brine flows into the repository were generally greater in the CRA-2009 PA than the CRA-2004 PABC due to the higher DRZ porosities (see Subsection 5.1.2).

Microbial gas generation was slightly higher in the CRA-2009 PA than the CRA-2004 PABC owing to the addition of the emplacement materials (see Subsection 5.1.1) and the increased DRZ porosity (Subsection 5.1.2). The new methodology for sampling the humid rate had a modest effect on microbial gas generation, which is as it was intended.

The changes to the BRAGFLO code had little effect on the results other than to cause fewer exception vectors when the repository becomes dry. Because these vectors are generally at lower pressures and saturations, their effect is minimal on repository performance.

In the CRA-2009 PA fracture lengths were generally higher than in the CRA-2004 PABC, however this result should be understood with the caveat that the pressures generating these larger fracture lengths were only slightly different than that of the CRA-2004 PABC. It should also be noted that the larger fracture length did not lead to a significantly larger brine release to the Land Withdrawal Boundary.

8 REFERENCES

APPENDIX A: ALGEBRACDB (ALG2) OUTPUT VARIABLES IN STEP 5

Name	Type/Units	Description
FE_KG	Steel (kg)	Remaining Mass Of Steel
CELL_KG	Cellulose (kg)	Remaining Mass Of Cellulose
MGO_KG	Magnesium Oxide (kg)	Remaining Mass of Magnesium Oxide
FE_REM	Fraction of Initial Steel	Remaining Fraction Of Steel
CELL_REM	Fraction of Initial Cellulose	Remaining Fraction Of Cellulose
MGO_REM	Fraction of Initial Magnesium Oxide	Remaining Fraction of Magnesium Oxide
FE_MOLE	Gas (moles)	Cumulative Gas Generation By Corrosion
CELL_MOL	Gas (moles)	Cumulative Gas Generation By Total Microbial Activity
GAS_MOLE	Gas (moles)	Cumulative Total Gas Generation
FE_MOL_D	Gas (moles/drum)	Cumulative Gas Generation By Corrosion
CELMOL_D	Gas (moles/drum)	Cumulative Gas Generation By Total Microbial Activity (CELL_MOL/DRUMTOT)
GASMOL_D	Gas (moles/drum)	Cumulative Total Gas Generation
GAS_FE_V	Gas Volume (m ³)	Cumulative Gas Generation By Corrosion
GAS_CMH	Gas Volume (m ³)	Cumulative Gas Generation By Humid Microbial Activity
GAS_CMI	Gas Volume (m ³)	Cumulative Gas Generation By Inundated Microbial Activity
GAS_C_V	Gas Volume (m ³)	Cumulative Gas Generation By Total Microbial Activity (CELL_MOL)
GAS_VOL	Gas Volume (m ³)	Cumulative Total Gas Generation
WAS_PRES	Pressure (Pa)	Volume-Averaged Pressure: Waste Panel
SRR_PRES	Pressure (Pa)	Volume-Averaged Pressure: RoR South
NRR_PRES	Pressure (Pa)	Volume-Averaged Pressure: RoR North
REP_PRES	Pressure (Pa)	Volume-Averaged Pressure: RoR (North + South)
OPS_PRES	Pressure (Pa)	Volume-Averaged Pressure: Ops Region
EXP_PRES	Pressure (Pa)	Volume-Averaged Pressure: Exp Region
W_R_PRES	Pressure (Pa)	Volume-Averaged Pressure: All Waste Regions
B_P_PRES	Pressure (Pa)	Volume-Averaged Pressure: Castille Brine Pocket
PORVOL_T	Pore Volume (m ³)	Total Pore Volume In The Repository
DZU_PRES	Pressure (Pa)	Volume-Averaged Pressure: DRZ above the repository
DZL_PRES	Pressure (Pa)	Volume-Averaged Pressure: DRZ below the repository
BRNVOL_W	Brine Volume (m ³)	Brine Volume: Waste Panel
BRNVOL_S	Brine Volume (m ³)	Brine Volume: RoR South
BRNVOL_N	Brine Volume (m ³)	Brine Volume: RoR North

Name	Type/Units	Description
BRNVOL_R	Brine Volume (m ³)	Brine Volume: RoR (North + South)
BRNVOL_T	Brine Volume (m ³)	Brine Volume: All Waste Regions
BRNVOL_O	Brine Volume (m ³)	Brine Volume: Ops Region
BRNVOL_E	Brine Volume (m ³)	Brine Volume: Exp Region
BRNVOL_A	Brine Volume (m ³)	Brine Volume: All Excavated Areas
WAS_SATG	Gas Saturation (dimensionless)	Volume-Averaged Gas Saturation: Waste Panel
SRR_SATG	Gas Saturation (dimensionless)	Volume-Averaged Gas Saturation: RoR South
NRR_SATG	Gas Saturation (dimensionless)	Volume-Averaged Gas Saturation: RoR North
REP_SATG	Gas Saturation (dimensionless)	Volume-Averaged Gas Saturation: RoR (North + South)
OPS_SATG	Gas Saturation (dimensionless)	Volume-Averaged Gas Saturation: Ops Region
EXP_SATG	Gas Saturation (dimensionless)	Volume-Averaged Gas Saturation: Exp Region
NWA_SATG	Gas Saturation (dimensionless)	Volume-Averaged Gas Saturation: Ops + Exp Regions
W_R_SATG	Gas Saturation (dimensionless)	Volume-Averaged Gas Saturation: All Waste Regions
B_P_SATG	Gas Saturation (dimensionless)	Volume-Averaged Gas Saturation: Castille Brine Pocket
WAS_SATB	Brine Saturation (dimensionless)	Volume-Averaged Brine Saturation: Waste Panel
SRR_SATB	Brine Saturation (dimensionless)	Volume-Averaged Brine Saturation: RoR South
NRR_SATB	Brine Saturation (dimensionless)	Volume-Averaged Brine Saturation: RoR North
REP_SATB	Brine Saturation (dimensionless)	Volume-Averaged Brine Saturation: RoR (North + South)
OPS_SATB	Brine Saturation (dimensionless)	Volume-Averaged Brine Saturation: Ops Region
EXP_SATB	Brine Saturation (dimensionless)	Volume-Averaged Brine Saturation: Exp Region
W_R_SATB	Brine Saturation (dimensionless)	Volume-Averaged Brine Saturation: All Waste Regions
NWA_SATB	Brine Saturation (dimensionless)	Volume-Averaged Brine Saturation: Ops + Exp Regions
B_P_SATB	Brine Saturation (dimensionless)	Volume-Averaged Brine Saturation: Castille Brine Pocket
WAS_POR	Porosity (dimensionless)	Volume-Averaged Porosity: Waste Panel
SRR_POR	Porosity (dimensionless)	Volume-Averaged Porosity: RoR South
NRR_POR	Porosity (dimensionless)	Volume-Averaged Porosity: RoR North
REP_POR	Porosity (dimensionless)	Volume-Averaged Porosity: RoR (North + South)
OPS_POR	Porosity (dimensionless)	Volume-Averaged Porosity: Ops Region
EXP_POR	Porosity (dimensionless)	Volume-Averaged Porosity: Exp Region
W_R_POR	Porosity (dimensionless)	Volume-Averaged Porosity: All Waste Regions
NWA_POR	Porosity (dimensionless)	Volume-Averaged Porosity: Ops + Exp Regions
BRN_RMV	Brine Volume (m ³)	Brine Consumed
BRNREPTC	Brine Volume (m ³)	Total Brineflow Into Repository
BRNEXIC	Brine Volume (m ³)	Total Brineflow Into Excavated Areas

Name	Type/Units	Description
BRNWPIC	Brine Volume (m ³)	Total Brineflow Into Waste Panel
BNWPSFLW	Brine Volume (m ³)	Total Brineflow Into Waste Panel Through the Plane of the Panel Closure
BRNSRRIC	Brine Volume (m ³)	Total Brineflow Into RoR South
BRNNRRIC	Brine Volume (m ³)	Total Brineflow Into RoR North
BNRRSFLW	Brine Volume (m ³)	Total Brineflow Into RoR Through the Plane of the Panel Closure
BRNRRIC	Brine Volume (m ³)	Total Brineflow Into RoR (North + South)
BRNORIC	Brine Volume (m ³)	Total Brineflow Into Ops Region
BRNEAIC	Brine Volume (m ³)	Total Brineflow Into Exp Region
BRNREPOC	Brine Volume (m ³)	Total Brineflow Out Of Repository
BRNEXOC	Brine Volume (m ³)	Total Brineflow Out of All Excavated Areas
BRNREPNC	Brine Volume (m ³)	Net Brineflow Into Repository
BRNWPOC	Brine Volume (m ³)	Total Brinflow Out Of Waste Panel
BNWPNFLW	Brine Volume (m ³)	Total Brineflow Out Of Waste Panel Across the Panel Closure Plane
BRNWFNC	Brine Volume (m ³)	Net Brineflow Into Waste Panel
BRNSRROC	Brine Volume (m ³)	Total Brinflow Out Of RoR South
BRNSRRNC	Brine Volume (m ³)	Net Brineflow Into RoR South
BRNNRROC	Brine Volume (m ³)	Total Brinflow Out Of RoR North
BRNNRRNC	Brine Volume (m ³)	Net Brineflow Into RoR North
BRNRROC	Brine Volume (m ³)	Total Brinflow Out Of RoR (North + South)
BRNEXNC	Brine Volume (m ³)	Net Brineflow Into All Experimental Areas
BRNRRNC	Brine Volume (m ³)	Net Brineflow Into RoR (North + South)
BRNOROC	Brine Volume (m ³)	Total Brinflow Out Of Ops Region
BRNORNC	Brine Volume (m ³)	Net Brineflow Into Ops Region
BRNEAOC	Brine Volume (m ³)	Total Brinflow Out Of Exp Region
BRNEANC	Brine Volume (m ³)	Net Brineflow Into Exp Region
BRNBHUPP	Brine Volume (m ³)	Brineflow Up Borehole: Bottom Of Waste Panel (@Element 1410)
BRNBHUPC	Brine Volume (m ³)	Brineflow Up Borehole: Bottom Of Upper DRZ (@Element 1168)
BRNBHRCC	Brine Volume (m ³)	Brineflow Up Borehole: Culebra/Unnamed Contact (@Element 1845)
BRNBHRUC	Brine Volume (m ³)	Brineflow Up Borehole: Dewey Lake/49er Contact (@Element 1979)
BRNBHRSC	Brine Volume (m ³)	Brineflow Up Borehole: Santa Rosa (@Element 2155)
BNBHLDZ	Brine Volume (m ³)	Brineflow Up Borehole: Bottom Of Lower DRZ (@Element 1111)
BNBHURZ	Brine Volume (m ³)	Brineflow Up Borehole: Top Of Upper DRZ (@Element 1493)
BRNBHDPP	Brine Volume (m ³)	Brineflow Down Borehole: Bottom Of Waste Panel (@Element 1410)

Name	Type/Units	Description
BRNBHDPC	Brine Volume (m ³)	Brineflow Down Borehole: Bottom Of Upper DRZ (@Element 1168)
BNBHDDRZ	Brine Volume (m ³)	Brineflow Down Borehole: Santa Rosa (@Element 1364)
BNBHDRCC	Brine Volume (m ³)	Brineflow Down Borehole: Culebra/Unnamed Contact (@Element 1845)
BRNSHRSC	Brine Volume (m ³)	Brineflow up shaft: Santa Rosa (@element 1364)
BNSHDSCZ	Brine Volume (m ³)	Brineflow down shaft: Santa Rosa (@element 1496)
BRNSHRUC	Brine Volume (m ³)	Brineflow up shaft: Dewey Lake/49er Contact (@element 1493)
BNSHDRUZ	Brine Volume (m ³)	Brineflow Down Shaft: Dewey Lake/49er Contact (@Element 1493)
BRNSHRCC	Brine Volume (m ³)	Brineflow up Shaft: Culebra/unamed Contact (@element 1489)
BNSHDRCC	Brine Volume (m ³)	Brineflow down Shaft: Culebra/unamed Contact (@element 1489)
BNSHUDRZ	Brine Volume (m ³)	Brineflow up Shaft: MB138/U_DRZ Contact (@element 1381)
BNSHDDRZ	Brine Volume (m ³)	Brineflow down Shaft: MB138/U_DRZ Contact (@element 1381)
BRNSHABC	Brine Volume (m ³)	Brineflow Up Shaft: Anhy AB/CONC MON Contact (@element 1315)
BRNBHUP1	Brine Volume (m ³)	Total Brineflow up the Borehole: (@element 1644)
BRNBHUP2	Brine Volume (m ³)	Total Brineflow up the Borehole: (@element 1845)
BRNBHUP3	Brine Volume (m ³)	Total Brineflow up the Borehole: (@element 1711)
BRNBHUP4	Brine Volume (m ³)	Total Brineflow up the Borehole: (@element 1912)
BRNBHUP5	Brine Volume (m ³)	Total Brineflow up the Borehole: (@element 1778)
BRNBHUP6	Brine Volume (m ³)	Total Brineflow up the Borehole: (@element 1979)
BRNBHUP7	Brine Volume (m ³)	Total Brineflow up the Borehole: (@element 2021)
BRNBHUP8	Brine Volume (m ³)	Total Brineflow up the Borehole: (@element 2113)
BRNBHUP9	Brine Volume (m ³)	Total Brineflow up the Borehole: (@element 2155)
BRNBHUP0	Brine Volume (m ³)	Total Brineflow up the Borehole: (@element 1410)
BNSHDABC	Brine Volume (m ³)	Brineflow down Shaft: Anhy AB/CONC MON Contact (@element 1315)
BRM38NIC	Brine Volume (m ³)	Total Lateral Brineflow Out Of MB Toward Repository: MB 138, North
BRAABNIC	Brine Volume (m ³)	Total Lateral Brineflow Out Of MB Toward Repository: Anhydrite A & B, North
BRM39NIC	Brine Volume (m ³)	Total Lateral Brineflow Out Of MB Toward Repository: MB 139, North
BRM38SIC	Brine Volume (m ³)	Total Lateral Brineflow Out Of MB Toward Repository: MB 138, South
BRAABSIC	Brine Volume (m ³)	Total Lateral Brineflow Out Of MB Toward Repository: Anhydrite A & B, South
BRM39SIC	Brine Volume (m ³)	Total Lateral Brineflow Out Of MB Toward Repository: MB 139, South
BRAALIC	Brine Volume (m ³)	Total Lateral Brineflow Out Of MB Toward Repository: All Marker Beds
BRM38NOC	Brine Volume (m ³)	Total Lateral Brineflow Into MB Away From Repository: MB 138, North

Name	Type/Units	Description
BRAABNOC	Brine Volume (m ³)	Total Lateral Brineflow Into MB Away From Repository: Anhydrite A & B, North
BRM39NOC	Brine Volume (m ³)	Total Lateral Brineflow Into MB Away From Repository: MB 139, North
BRM38SOC	Brine Volume (m ³)	Total Lateral Brineflow Into MB Away From Repository: MB 138, South
Name	Type/Units	Description
BRAABSOC	Brine Volume (m ³)	Total Lateral Brineflow Into MB Away From Repository: Anhydrite A & B, South
BRM39SOC	Brine Volume (m ³)	Total Lateral Brineflow Into MB Away From Repository: MB 139, South
BRAALOC	Brine Volume (m ³)	Total Lateral Brineflow Into MB Away From Repository: All Marker Beds
BRM38NNC	Brine Volume (m ³)	Net Lateral Brineflow Through MB: MB 138, North
BRAABNNC	Brine Volume (m ³)	Net Lateral Brineflow Through MB: Anhydrite A & B, North
BRM39NNC	Brine Volume (m ³)	Net Lateral Brineflow Through MB: MB 139, North
BRM38SNC	Brine Volume (m ³)	Net Lateral Brineflow Through MB: MB 138, South
BRAABSNC	Brine Volume (m ³)	Net Lateral Brineflow Through MB: Anhydrite A & B, South
BRM39SNC	Brine Volume (m ³)	Net Lateral Brineflow Through MB: MB 139, South
BRAALNC	Brine Volume (m ³)	Net Lateral Brineflow Into DRZ Through All Anhydrite Layers
GASBHUPC	Gas Volume (m ³)	Cumulative Gas Flow Up Borehole: Top Of Waste Panel
GASBHUDZ	Gas Volume (m ³)	Cumulative Gas Flow Up Borehole: Top Of Upper DRZ
GSSHUSCC	Gas Volume at Reference Conditions (m ³)	Gas flow up shaft (@element 1496 Santa Rosa)
GSSHRRUC	Gas Volume at Reference Conditions (m ³)	Gas Flow Up Shaft (@Element 1493 49er/Dewey Lake)
GSSHUCUC	Gas Volume at Reference Conditions (m ³)	Gas flow up shaft (@element 1489 unnamed/Culebra)
GSSHUDRZ	Gas Volume at Reference Conditions (m ³)	Gas flow up shaft (@element 1381 U_DRZ/Upper 138)
GASSHABC	Gas Volume at Reference Conditions (m ³)	Gas flow up shaft (@element 1315 Anhy AB/CONC_MON)
GSM38NOC	Gas Volume at Reference Conditions (m ³)	Total Gas Flow Through MB Away From Repository: MB 138, North
GSAABNOC	Gas Volume at Reference Conditions (m ³)	Total Gas Flow Through MB Away From Repository: Anhydrite A & B, North
GSM39NOC	Gas Volume at Reference Conditions (m ³)	Total Gas Flow Through MB Away From Repository: MB 139, North
GSM38SOC	Gas Volume at Reference Conditions	Total Gas Flow Through MB Away From Repository: MB 138, South

Name	Type/Units	Description
PVOLI_T	Permeability (m ²)	Total Frac Zone Pore Vol Increase: All Marker Beds
BRNVOL_B	Brine Volume (m ³)	Brine Vol: Castille Brine Pocket
BNBHDNUZ	Brine Volume (m ³)	Downward Brine Flow: Borehole At Top Of MB 138
BRNBHDNC	Brine Volume (m ³)	Downward Brine Flow: Borehole At Top Of Waste Panel
FEKG_W	Steel (kg)	Steel Mass Remaining: Waste Panel
CELLKG_W	Cellulose (kg)	Cellulose Mass Remaining: Waste Panel
FEREM_W	Fraction of Initial Iron & Steel	Fraction Steel Remaining: Waste Panel
CELREM_W	Fraction of Initial Cellulose	Fraction Cellulose Remaining: Waste Panel
GASMOL_W	Gas (moles)	Total Number Of Moles Of Gas Generated: Waste Panel
GASVOL_W	Gas at Reference Conditions (m ³) Total	Gas Volume Generated: Waste Panel
PORVOL_W	Pore volume (m ³)	Total Pore Volume: Waste Panel
BRNM38I	Brine Volume (m ³)	Total Brineflow Out Of MB, Towards Repository: MB 138
BRNAABI	Brine Volume (m ³)	Total Brineflow Out Of MB, Towards Repository: Anhydrite A & B
BRNM39I	Brine Volume (m ³)	Total Brineflow Out Of MB, Towards Repository: MB 139
BRNM38O	Brine Volume (m ³)	Total Brineflow Into MB, Away From Respository: MB 138
BRNAABO	Brine Volume (m ³)	Total Brineflow Into MB, Away From Respository: Anhydrite A & B
BRNM39O	Brine Volume (m ³)	Total Brineflow Into MB, Away From Respository: MB 139
BRN_RMVW	Brine Volume (m ³)	Brine Consumed: Waste Panel
BRN_RMSR	Brine Volume (m ³)	Brine Consumed: RoR South
BRN_RMNR	Brine Volume (m ³)	Brine Consumed: RoR North
BRN_RMVR	Brine Volume (m ³)	Brine Consumed: RoR (North + South)
FEREM_SR	Fraction of Initial Iron & Steel	Fraction Of Steel Remaining: RoR South
CELREM_S	Fraction of Initial Cellulose	Fraction Of Cellulose Remaining: RoR South
FEREM_NR	Fraction of Initial Iron & Steel	Fraction Of Steel Remaining: RoR North
CELREM_N	Fraction of Initial Cellulose	Fraction Of Cellulose Remaining: RoR North
FEREM_R	Fraction of Initial Iron & Steel	Fraction Of Steel Remaining: RoR (North + South)
CELREM_R	Fraction of Initial Cellulose	Fraction Of Cellulose Remaining: RoR (North + South)
GASMOL_S	Gas (moles)	Total Number Of Moles Of Gas Generated: RoR South
GASMOL_N	Gas (moles)	Total Number Of Moles Of Gas Generated: RoR North
GASMOL_R	Gas (moles)	Total Number Of Moles Of Gas Generated: RoR (North + South)
BRWI_XBH	Brine Volume (m ³)	Cumulative Brineflow Into Waste Panel, Excluding Borehole
SAL_BR_T	Fraction of Total Brine Inflow	(Salado Brine Inflow)/(Total Brine Inflow): DRZ
SAL_BR_U	Fraction of Unconsumed Brine Inflow	(Salado Brine Inflow)/(Unconsumed Brine Inflow): DRZ

Name	Type/Units	Description
SB_TB_WP	Fraction of Total Brine Inflow	(Salado Brine Inflow)/(Total Brine Inflow): Waste Panel
SB_UB_WP	Fraction of Unconsumed	Brine Inflow: (Salado Brine Inflow)/(Unconsumed Brine Inflow): Waste Panel
BRNBHUMC	Brine Volume (m ³)	Brineflow Up: Borehole At Magenta Dolomite
BRNSHUMC	Brine Volume (m ³)	Brineflow Up: Shaft At Magenta Dolomite
BRM38NLW	Brine Volume (m ³)	Total Outward Brineflow In MBs Across LWB: MB 138, North
BRAABNLW	Brine Volume (m ³)	Total Outward Brineflow In MBs Across LWB: Anhydrite A & B, North
BRM39NLW	Brine Volume (m ³)	Total Outward Brineflow In MBs Across LWB: MB 139, North
BRM38SLW	Brine Volume (m ³)	Total Outward Brineflow In MBs Across LWB: MB 138, South
BRAABSLW	Brine Volume (m ³)	Total Outward Brineflow In MBs Across LWB: Anhydrite A & B, South
BRM39SLW	Brine Volume (m ³)	Total Outward Brineflow In MBs Across LWB: MB 139, South
BRAALLWC	Brine Volume (m ³)	Total Outward Brineflow In MBs Across LWB: All Marker Beds
FR_TG_C	Fraction of Total Gas	Fraction Of Total Gas Due To Steel Corrosion: All Waste Regions
FR_TG_M	Fraction of Total Gas	Fraction Of Total Gas Due To Total Microbial Activity: All Waste Regions
FR_TG_H	Fraction of Total Gas	Fraction Of Total Gas Due To Humid Microbial Activity: All Waste Regions
FR_TG_I	Fraction of Total Gas	Fraction Of Total Gas Due To Inundated Microbial Activity: All Waste Regions
FR_MG_H	Fraction of Total Gas	Fraction Of Microbial Activity Gas From Humid Conditions: All Waste Regions
FR_MG_I	Fraction of Total Gas	Fraction Of Microbial Activity Gas From Inundated Conditions: All Waste Regions
PORVOL_S	Pore volume (m ³)	Total Pore Vol: RoR South
PORVOL_N	Pore volume (m ³)	Total Pore Vol: RoR North
PORVOL_R	Pore volume (m ³)	Total Pore Vol: RoR (North + South)

Caporuscio, F., J. Gibbons, et al. (2002). Waste Isolation Pilot Plant: Salado Flow Conceptual Models Peer Review Report. Carlsbad, NM, U.S. Department of Energy, Carlsbad Area Office, Office of Regulatory Compliance.

Caporuscio, F., J. Gibbons, et al. (2003). Waste Isolation Pilot Plant: Salado Flow Conceptual Models Final Peer Review Report. Carlsbad, NM, U.S. Department of Energy, Carlsbad Area Office, Office of Regulatory Compliance.

Clayton, D. J. (2008). AP-137, Analysis Plan for the Performance Assessment for the 2009 Compliance Recertification Application, Revision 1. Carlsbad, NM, Sandia National Laboratories.

Cotsworth, E. (2004). EPA's CRA completeness comments, 2nd set. Washington, DC, U.S. Environmental Protection Agency.

Cotsworth, E. (2004). EPA's CRA completeness comments, 3rd set. Washington, DC, U.S. Environmental Protection Agency.

Cotsworth, E. (2004). EPA received CRA on March 26, 2004. Washington, DC, U.S. Environmental Protection Agency.

Cotsworth, E. (2004). Fourth Set of CRA Comments (December 17, 2004 Letter to Lloyd Piper, Acting Manger. Carlsbad Field Office, U.S. Department of Energy). Washington, DC, U.S. Environmental Protection Agency.

Cotsworth, E. (2005). EPA letter on conducting the performance assessment baseline change (PABC) verification test. Washington, D.C., U.S. EPA, Office of Radiation and Indoor Air.

Detwiler, P. (2004). DOE Letter #4: Response to CRA Comments (September 29, 2004 Letter to E. Cotsworth, Director, Office of Radiation and Indoor Air, U.S. Environmental Protection Agency). Carlsbad, NM, U.S. Department of Energy.

Detwiler, P. (2004). DOE Letter #5: Response to CRA Comments (October 20, 2004 Letter to E. Cotsworth, Director, Office of Radiation and Indoor Air, U.S. Environmental Protection Agency). Carlsbad, NM, U.S. Department of Energy.

Detwiler, P. (2004). DOE Letter #6: Response to CRA Comments (November 1, 2004 Letter to E. Cotsworth, Director, Office of Radiation and Indoor Air, U.S. Environmental Protection Agency). Carlsbad, NM, U.S. Department of Energy.

Detwiler, P. (2004). Partial response to Environmental Protection Agency (EPA) May 20, 2004 letter on CRA. Carlsbad, NM, U.S. Department of Energy.

Detwiler, P. (2004). Partial response to Environmental Protection Agency (EPA) May 20, 2004 letter on CRA, [1st response submittal to EPA]. Carlsbad, NM, U.S. Department of Energy.

Detwiler, P. (2004). Response to Environmental Protection Agency (EPA) July 12, 2004 letter on CRA. Carlsbad, NM, U.S. Department of Energy.

DOE (2007). Transuranic Waste Acceptance Criteria for The Waste Isolation Pilot Plant, Revision 6.1. Carlsbad, NM.

Dotson, L. (1996). Memo to M. Tierney, Parameter Values for Forty-Niner, Tamarisk, and Unnamed Lower Members of the Rustler Formation (Addendum to Records # 21,22, 23, 24) Carlsbad, NM, Sandia National Laboratory.

EPA (2005). Notification of Compliance Application Completeness Determination. Washington, DC.

EPA (2006). "Criteria for the Certification and Recertification of the Waste Isolation Pilot Plant's Compliance With the Disposal Regulations: Recertification Decision." Federal Register 71(68): 18010-18021.

Gilkey, A. P. (1995). User's Manual for PCCSRC, Version 2.21, Document Version 1.00. Albuquerque, NM, Sandia National Laboratories.

Gilkey, A. P. (1996). User's Manual for Splat, Version 1.02. Carlsbad, NM, Sandia National Laboratories.

Gilkey, A. P. (1996). User's Manual for ALGEBRACDB, Version 2.35, Document Version 1.01. Albuquerque, NM, Sandia National Laboratories.

Gilkey, A. P. (2001). User's Manual and Criteria Form for MATSET, Version 9.10. Carlsbad, NM, Sandia National Laboratory.

Gilkey, A. P. (2002). User's Manual Criteria Form and User's Manual for PRELHS, Version 2.30. Carlsbad, NM, Sandia National Laboratories.

Gilkey, A. P. and D. K. Rudeen (2007). User's manual for PREBRAG version 8.00. Carlsbad, NM, Sandia National Laboratories.

Gitlin, B. (2005). Fifth Set of CRA Comments (February 3, 2005 Letter to Ines Triay, Acting Manger. Washington, DC, U.S. Environmental Protection Agency.

Hansen, C. W. and C. Leigh (2002). A Reconciliation of the CCA and PAVT Parameter Baselines, Revision 2. Carlsbad, NM, Sandia National Laboratories.

Hansen, C. W., C. Leigh, et al. (2002). BRAGFLO Results for the Technical Baseline Migration. Carlsbad, NM, Sandia National Laboratories.

Helton, J. C., J. E. Bean, et al. (1998). Uncertainty and Sensitivity Analysis Results Obtained in the 1996 Performance Assessment for the Waste Isolation Pilot Plant. Albuquerque, NM, Sandia National Laboratories.

Ismail, A. E. (2007). Parameter Problem Report (PPR), PPR-2007-002 for S_HALITE, DRZ_0. Carlsbad, NM, Sandia National Laboratories.

Kanney, J. F. and C. D. Leigh (2005). Analysis Plan for Post CRA PA Baseline Calculation AP-122. Carlsbad, NM, Sandia National Laboratory.

Kirchner, T. (2008). Generation of the LHS Samples for the AP-137 Revision 0 (CRA09) PA Calculations. Carlsbad, NM, Sandia National Laboratories.

Leigh, C., J. Kanney, et al. (2005). 2004 Compliance Recertification Application Performance Assessment Baseline Calculation. Carlsbad, NM, Sandia National Laboratories.

Long, J. J. (2008). Execution of Performance Assessment Codes for the 2009 Compliance Recertification Application Performance Assessment, Revision 0. Carlsbad, NM, Sandia National Laboratories.

Long, J. J. and J. F. Kanney (2005). Execution of Performance Assessment Codes for the CRA-2004 Performance Assessment Baseline Calculation. Carlsbad, NM, Sandia National Laboratory.

Nemer, M. B. (2006). Design Document for BRAGFLO Version 6.00. Carlsbad, NM, Sandia National Laboratories.

Nemer, M. B. (2006). Users Manual for BRAGFLO Version 6.00. Carlsbad, NM, Sandia National Laboratories.

Nemer, M. B. (2007). Effects of Not Including Emplacement Materials in CPR Inventory on Recent PA Results. Carlsbad, NM, Sandia National Laboratories.

Nemer, M. B. (2007). POSTBRAG, Version 4.00A. Carlsbad, NM, Sandia National Laboratories.

Nemer, M. B. (2007). Software Problem Report (SPR) 07-001 For POSTBRAG, Version 4.00. Carlsbad, NM, Sandia National Laboratories.

Nemer, M. B. and J. S. Stein (2005). Analysis Package for BRAGFLO: 2004 Compliance Recertification Application Performance Assessment Baseline Calculation. Carlsbad, NM, Sandia National Laboratories.

Nemer, M. B., J. S. Stein, et al. (2005). Analysis Report for BRAGFLO Preliminary Modeling Results With New Gas Generation Rates Based Upon Recent Experimental Results. Carlsbad, NM, Sandia National Laboratory.

Nemer, M. B. and W. Zelinski (2005). Analysis Report for BRAGFLO Modeling Results with the removal of Methanogenesis from the Microbial-Gas-Generation Model. Carlsbad, NM, Sandia National Laboratory.

Park, B. Y. and F. D. Hansen (2003). Analysis Report for Determination of the Porosity Surfaces of the Disposal Room Containing Various Waste Inventories for WIPP PA. Carlsbad, NM, Sandia National Laboratories.

Patterson, R. (2005). DOE Letter #9: Response to CRA Comments (March 18, 2005 Letter to E. Cotsworth, Director, Office of Radiation and Indoor Air, U.S. Environmental Protection Agency). Carlsbad, NM, U.S. Department of Energy.

Piper, L. (2004). DOE Letter #7: Response to CRA Comments (December 23, 2004 Letter to E. Cotsworth, Director, Office of Radiation and Indoor Air, U.S. Environmental Protection Agency). Carlsbad, NM, U.S. Department of Energy.

Rath, J. (1995). ICSET, Version 2.21ZO, Version Date 9/14/95, User's Manual. Albuquerque, NM, Sandia National Laboratories.

Rechard, R. P., A. P. Gilkey, et al. (1990). Programmer's Manual for CAMCON: Compliance Assessment Methodology Controller, SAND90-1984. Albuquerque, NM, Sandia National Laboratory.

Shuldberg, H. K. (1995). User's Manual for GENMESH, Version 6.07, Document Version 1.00. Albuquerque, NM, Sandia National Laboratories.

SNL (1996). Verification of 2-D Radial Flaring Using 3-D Geometry. Albuquerque, NM, Sandia National Laboratories.

SNL (1997). Final, Supplemental Summary of EPA-Mandated Performance Assessment Verification Test (All Replicates) and Comparison with the Compliance Certification Application Calculations.

Stein, J. S. (2002). Methodology Behind the TBM BRAGFLO Grid." Memorandum to M.K. Knowles, May 13, 2002. Carlsbad, NM, Sandia National Laboratories.

Stein, J. S. and W. Zelinski (2003). Analysis Package for BRAGFLO: Compliance Recertification Application. Carlsbad, NM, Sandia National Laboratories.

Stein, J. S. and W. P. Zelinski (2003). Analysis Report for: Testing of a Proposed BRAGFLO Grid to be used for the Compliance Recertification Application Performance Assessment Calculations. Carlsbad, NM, Sandia National Laboratories.

Stone, C. M. (1995). SANTOS - A Two-Dimensional Finite Element Program for the Quasistatic, Large Deformation, Inelastic Response of Solids. Albuquerque, NM, Sandia National Laboratories.

Triay, I. R. (2005). DOE Letter #8: Response to CRA Comments (January 19, 2005 Letter to E. Cotsworth, Director, Office of Radiation and Indoor Air, U.S. Environmental Protection Agency). Carlsbad, NM, U.S. Department of Energy, Carlsbad Field Office.

U. S. DOE (1980). Final Environmental Impact Statement: Waste Isolation Pilot Plant. Washington, D.C., U.S. Department of Energy, Assistant Secretary for Defense Programs, Vols. 1-2.

U. S. DOE (1990). Final Supplement: Environmental Impact Statement, Waste Isolation Pilot Plant. Washington, D.C., U.S. Department of Energy, Office of Environmental Restoration and Waste Management. Vols. 1-13.

U. S. DOE (1993). Waste Isolation Pilot Plant Strategic Plan. Washington, D.C., U.S. Department of Energy.

U.S. DOE (1996). Title 40 CFR Part 191 Compliance Certification Application for the Waste Isolation Pilot. Carlsbad, NM, U.S. Department of Energy Waste Isolation Pilot Plant, Carlsbad Area Office.

U.S. DOE (2004). Title 40 CFR Part 191 Compliance Recertification Application for the Waste Isolation Pilot. Carlsbad, NM, U.S. Department of Energy Waste Isolation Pilot Plant, Carlsbad Field Office.

U.S. EPA (1996). 40 CFR 194. Criteria for the Certification and Recertification of the Waste Isolation Pilot Plant's Compliance with the 40 CFR Part 191 Disposal Regulations; Final Rule. Washington, DC, U.S. Environmental Protection Agency.

Vaughn, P. (1996). WIPP Parameter Entry Form for SANTAROS: SAT_IBRN. Carlsbad, NM, Sandia National Laboratories.

Vugrin, E. (2005). POSTLHS, Version 4.07A. Carlsbad, NM, Sandia National Laboratories.

Vugrin, E., T. Kirchner, et al. (2005). Analysis Report for Modifying Parameter Distributions for S_MB139:COMP_RCK and S_MB139:SAT_RGAS. Carlsbad, NM, Sandia National Laboratory.

Vugrin, E. D. (2005). User's Manual for LHS Version 2.42 Document Version 2.42. Carlsbad, NM, Sandia National Laboratories.